

**DEVELOPMENT OF A GUIDE
FOR EVALUATION OF
EXISTING BRIDGES
PART I**

PROJECT 97-0245 DIR

**Report submitted to
the Michigan Department
of Transportation**

Andrzej S. Nowak and Sangjin Kim

Department of Civil and Environmental Engineering
University of Michigan
Ann Arbor, Michigan 48109-2125

**Testing and Research Section
Construction and Technology Division
Research Project No. RC-1362
Part I**

This report, authorized by the transportation director, has been prepared to provide technical information and guidance for personnel in the Michigan Department of Transportation, the FHWA, and other reciprocating agencies. The cost of publishing 40 copies of this report at \$7.57 per copy is \$302.84 and it is printed in accordance with Executive Directive 1991-6.

1. Report No. Research Report RC-1362	2. Government Accession No.	3. Recipient's Catalog No.	
4. Title and Subtitle Development of a Guide for Evaluation of Existing Bridges, Part I		5. Report Date May 1998	
7. Author(s) Andrzej S. Nowak and Sangjin Kim		6. Performing Organization Code	
9. Performing Organization Name and Address University of Michigan 2340 G. G. Brown Bldg. Ann Arbor, MI 48109-2125		8. Performing Org Report No. RC-1362	
12. Sponsoring Agency Name and Address Michigan Department of Transportation Construction and Technology Division P.O. Box 30049 Lansing, MI 48909		10. Work Unit No. (TRAIS)	
		11. Contract/Grant No. 97-0245 DIR	
15. Supplementary Notes		13. Type of Report & Period Covered Final Report, 5-97/5-98	
		14. Sponsoring Agency Code	
<p>16. Abstract</p> <p>The objective of this report is to present the results of the field tests carried out in 1997 by the team at the University of Michigan. The field tests were performed to determine the load distribution factors needed for evaluation of existing bridges. In some of the previous tests it was observed that the currently girder distribution factors can be conservative. However, the analytical study carried out in conjunction with the development of the AASHTO LRFD Code showed that for short spans and girder spacings, the current code provisions can be too permissive. Therefore, this study focused on short span steel girder bridges. The tests also included measurement of dynamic loads, and proof load testing. The research work involved formulation of the testing procedure, selection of structures, installation of equipment, measurements, and interpretation of the results. The work was based on experience gained in the previous study. Equipment included the data acquisition systems available at the University of Michigan. The measurements included strains and deflections. Five bridges were tested; including one proof load test. All selected structures are located in South Michigan. The results are summarized in the final chapter of this report.</p>			
17. Key Words bridges, field testing load distribution, proof load, dynamic load		18. Distribution Statement No restrictions. This document is available to the public through the Michigan Department of Transportation.	
19. Security Classification (report) Unclassified	20. Security Classification (Page) Unclassified	21. No of Pages	22. Price

DISCLAIMER

The contents of this report reflect the views of the authors, who are responsible for the facts and the accuracy of the information presented herein. This document is disseminated under the sponsorship of the Michigan Department of Transportation and Great Lakes Center for Truck Transportation Research at the University of Michigan Transportation Research Institute, in the interest of information exchange. The Michigan Department of Transportation assumes no liability for the contents or use thereof.

Executive Summary

The research work carried out as a part of this project is documented in two reports: Part I and Part II. This report presents the results of the field tests carried out in 1997. The other report, Part II, provides a guide for field testing. The field tests were performed to determine the load distribution factors needed for evaluation of existing bridges. Prior analytical studies showed that in most cases the current code provisions are too conservative, however, for short spans and girder spacings, they can be too permissive. There are many short span steel girder bridges in Michigan. Therefore, this study focused on these structures to verify the validity of the code specified distribution factor.

The research work involved formulation of the testing procedure, selection of structures, installation of equipment, measurements, and interpretation of the results. The work was based on experience gained in the previous study. Equipment included the data acquisition systems available at the University of Michigan. The measurements included strains and deflections. An important part of this project was further development of practical procedure for the proof load tests. The proof load was applied in form of military tanks (M-60) provided by the Michigan National Guard. Application of proof load required traffic control.

Bridges were selected for tests based of the following criteria: structural type (steel girder bridges), span length (less than 18 m), accessibility for testing equipment (unacceptable because of deep water or height), traffic volume (requirement for traffic control), and future repair/replacement schedule (bridges scheduled for major repairs/replacements in the near future were excluded). The five bridges selected for field tests are: Bridge B02-46032, M-156 over Silver Creek in Morenci, Bridge B05-46041, M-34 over Raisin River in Adrian, Bridge

B02-12021, US-12 over Swan Creek near Bronson, Bridge B02-38051, M-106 over Portage River Drain near Munith, and Bridge B01-70041, M-45 over Bass River near Grand Rapids.

For all tested bridges, the strains were measured under a single truck in various transverse positions within the roadway width, and under two trucks side-by-side. The measurements were taken for a crawling speed and a normal traffic speed. The observed girder distribution factors were compared to analytical values obtained using the formulas specified in the AASHTO specifications (1996) and AASHTO LRFD Code (1994).

The test results confirmed that the response is linear. The comparison of strain values for a single truck indicates that for two trucks side-by-side tests, the results are equal to superposition of single truck results. The absolute value of measured strains is lower than expected. The main reasons for low strains are: unintended composite action, partial fixity of supports and increased actual stiffness due to sidewalks, parapets and railings. For a single truck, girder distribution factors observed in the tests are lower than those specified by AASHTO. For two trucks side-by-side, the girder distribution factors are equal to those specified in AASHTO.

Dynamic load were measured in terms of the ratio of dynamic and static strains. It was observed that dynamic load is lower than specified and the dynamic load factor decreases with increasing static load effect. For two trucks side-by-side it is about 0.10.

Proof load test performed on bridge B02-12021 confirmed that it is adequate to carry the normal truck traffic. The measured deflections and strains were relatively low, and considerably lower than expected.

TABLE OF CONTENTS

Executive Summary	iii
Acknowledgments	vii
1. Introduction	1
2. Selected Bridges	4
3. Load Testing Procedures	7
4. Specified Load Distribution Factors and Impact Factors.....	21
5. Bridge on M-156 over Silver Creek in Morenci (B02-46032, M156/SC)	23
6. Bridge on M-34 over South Branch of Raisin River in Adrian (B05-46041, M34/RR)	43
7. Bridge on US-12 over Swan Creek near Bronson (B02-12021, US12/SC)	57
8. Bridge on M-106 over Portage River Drain near Munith in Jackson County (B02-38051, M106/PR)	101
9. Bridge on M-45 over Bass River west of Grand Rapids (B01-70041, M45/BR)	115
10. Summary and Conclusions	129
11. References	147

Note:

Intentionally left blank

Acknowledgments

The presented research has been sponsored by the Michigan Department of Transportation, and the Great Lakes Center for Truck and Transit Research (GLCTTR) at the University of Michigan which is gratefully acknowledged. The authors thank the technical staff of the Michigan DOT, Roger Till, Sonny Jadun, Sudhakar Kulkarni, and David Juntunen, for their useful comments, discussions and support, and Thomas Gillespie, of the University of Michigan Transportation Research Institute (UMTRI) for his support.

The project team received help from other researchers, current and former students and staff of the University of Michigan. In particular, thanks are due to Dr. Vijay Saraf, Junsik Eom, Chris Eamon, Chan-Hee Park, Tom Murphy, Dr. Ahmet Sanli, Dr. Maria Szerszen, Manu Puri, and Angela Campbell. They were involved in field instrumentation, measurements, and processing of the results.

Thanks are due to the Michigan State Police for their cooperation. Traffic control was provided by the Michigan DOT and several counties. Proof load test was carried out using military tanks provided by the Michigan National Guard which is gratefully acknowledged.

The realization of the research program would not be possible without in kind support of the Michigan DOT and the University of Michigan. Measurements were taken using equipment purchased by the University of Michigan.

Thanks are due to Junsik Eom who served as a technical editor of this Report. He was assisted by Dr. Ahmet Sanli and Chris Eamon.

Note:
Intentionally left blank

1. Introduction

A rational bridge management requires a good knowledge of the actual loads, load distribution, load effects and structural condition (load carrying capacity). Therefore, evaluation of existing structures is very important. However, there is a considerable number of bridges that are very difficult, if not impossible, to evaluate using traditional inspection methods and analysis. For example, this applies to many deteriorated structures (severe corrosion, cracking), and those for which the documentation is missing. It also may apply to structures showing difficult to explain behavior (excessive vibration, deflection, accelerated deterioration).

A considerable number of Michigan bridges show signs of deterioration. In particular, there is a severe corrosion on many steel and concrete structures. By analytical methods, many of these bridges are not adequate to carry the normal highway traffic. However, the actual load carrying capacity is often much higher than what can be determined by analysis, due to more favorable load sharing, effect of non-structural components (parapets, railing, sidewalks), composite deck action without shear developers, and other difficult to quantify factors. Field testing can reveal the hidden strength reserve and thus verify the adequacy of the bridge.

The research work carried out as a part of this project is documented in two reports: Part I and Part II. The objective Part I is to present the results of the field tests carried out in 1997. The other report, Part II, provides a guide for field testing, including weigh-in-motion truck measurement, measurement of dynamic loads, measurement of fatigue loads, verification of girder distribution factors, and proof load testing.

The field tests were performed to determine the load distribution factors needed for evaluation of existing bridges. In some of the previous tests it was observed that the currently used $S/4.27$ (S = girder spacing in meters; or $S/14$ where S = girder spacing in feet, and in both expressions, the resulting load distribution factor is a fraction of the entire truck weight) can be conservative. However, the analytical study carried out in conjunction with the development of the AASHTO LRFD Code (1994) showed that for short spans and girder spacings, $S/4.27$ or even $S/3.36$ ($=S/11$, where S is girder spacing in feet) can be too permissive. There are many such bridges in Michigan, in particular with steel girders. Therefore, the study focused on short span steel girder bridges to verify the validity of this distribution factor.

The research work involved formulation of the testing procedure, selection of structures, installation of equipment, measurements, and interpretation of the results. The work was based on experience gained in the previous study. Equipment included the data acquisition systems available at the University of Michigan. The measurements included strains and deflections. An attempt was made towards the development of an approach to difficult to access spans, spans over water, and spans over busy roads. Therefore, a special reach-all truck was used. Equipment for wireless transfer of the signal was purchased for this project. However, the system did not work and was sent back to the manufacturer for repairs and adjustments.

An important part of this project is further development of practical procedure for the proof load tests. The parameters which determine the proof load level include a live load factor, dynamic factor, number of lanes, and traffic volume and weight. The proof load was applied in form of military tanks (M-60) provided by the Michigan National Guard. The Project Team had an experience of using these

tanks for bridge testing. Application of proof load required traffic control.

Five bridges were tested, including one proof load test. All selected structures are located in South Michigan. The results are summarized in the final chapter of this report.

2. Selected Bridges

Bridges were selected for tests based of the following criteria:

- Structural type; it was decided to focus on steel girder bridges.
- Span length; the verification of distribution factors is needed mostly for shorter spans, less than 18 m.
- Accessibility; not all the structures can be accessed to install the testing equipment because of deep water, heavy traffic, or height.
- Traffic volume; very busy bridges can be difficult from the traffic control point of view.
- Future repair/replacement schedule; it was decided to exclude bridges scheduled for major repairs/replacements in the near future.

The five bridges selected for field tests are listed in Table 2.1.

Table 2.1. List of selected bridges.

MDOT ID Number	Location	Span (m)	Number of Girders	Girder Spacing (m)	Year of Construction	Skew
B02-46032	Morenci (M-156)	13.7	10	1.32	1935	30°
B05-46041	Adrian (M-34)	16.8	11	1.44	1932	0°
B02-12021	Bronson (US-12)	9.9	12	1.36	1922	10°
B02-38051	Munith (M-106)	13.7	9	1.46	1939	20°
B01-70041	Grand Rapids (M-45)	11.7	10	1.42	1929	0°

Bridges in Table 2.1 were selected from two lists prepared by the Michigan DOT. The first list includes 28 structures, Table 2.2, and the other one - 36 bridges, Table 2.3.

Table 2.2. List of Bridges Provided by MDOT, April 1997.

Bridge ID	Facility	Feature	Location	Yr Bld	Br Type	Max Span	Condition Rigs				Beam Spacing		District				
							Deck	Surface	Super	Paint	Subs	Load Rig		Feet	Inches		
1	12021-B03	US-12	COLDWATER R	W LT OF COLDWATER	1979	3	75	3	5	3	0	5	9	73	5	1	7
2	13032-B02	M-66	WANONDAGER CR	3.2 MI SW OF BARRY COL LN	1940	3	50	4	4	5	0	8	9	88	4	9	7
3	13061-R01	I-94BL	CONRAIL	1.0 MI E OF BATTLE CREEK	1937	3	40	3	5	4	1	5	9	82	4	6	7
4	38051-B02	M-106	PORTAGE R DRAIN	4.7 MI S&W OF INGHAM CO	1939	3	45	5	6	5	0	6	9	89	4	9	8
5	46032-B02	M-156	SILVER CR	IN MORENCI	1935	3	45	5	6	5	0	7	9	89	4	4	8
6	46041-B05	M-34	BEAN CR	IN HUDSON	1930	3	65	4	7	4	0	4	9	82	4	4	8
7	47014-S04	M-34	S BR RAISIN R	IN ADRIAN (BEECHER ST)	1932	3	55	4	7	4	5	6	9	78	4	8	8
8	47061-B03	CROUSE RD	US-23	1.6 MI N OF M-59	1961	3	60	6	6	5	0	7	9	81	6	0	8
9	47065-S09	I-96 BL	S BR SHIWASSE R	1.9 MI OF HOWEL	1918	3	40	5	7	4	0	6	9	80	4	5	8
10	50011-S04	DORR RD	I-96	1.6 MI SE OF I-96 BL	1961	3	91	6	6	4	0	6	9	78	6	0	8
11	58032-B01	CLINTON R RD	M-53	1.2 MI S OF M-59	1966	3	88	6	6	4	0	7	9	81	6	0	9
12	58053-B04	M-50	RAISIN R	IN DUDEE MONKOE ST	1937	3	60	3	5	3	0	4	9	82	4	11	8
13	63022-S03	US-24	HURON R	@WAYNE CO LINE	1933	3	81	4	8	3	0	4	9	55	4	11	8
14	63022-S04	SOUTH HILL RD	I-96	4.0 MI E OF LIVINGSTON CO	1957	3	71	6	6	5	5	7	9	80	4	5	9
15	63022-S06	OLD PLANK RD	I-96	5.1 MI OF LIVINGSTON CO	1957	3	71	6	7	5	1	6	9	82	4	5	9
16	63022-S09	BECK RD	I-96	IN NOV1	1957	3	72	4	5	4	0	6	9	82	4	11	9
17	63022-S10	HAGGERTY RD	M-102	ELTS OF NOV1	1957	3	73	4	5	4	0	7	9	87	4	5	9
18	63022-S11	10 MI RD(GD.R)	M-102	2 MI W OF FARMINGTON	1957	3	68	5	6	5	1	6	9	89	6	2	9
19	63081-B02	DRAKE RD	M-102	4.0 MI NW OF WAYNE CO LN	1957	3	69	4	5	4	0	6	9	80	4	7	9
20	63081-S112	M-10 NB	ROUGE R	IN SOUTHFIELD	1929	3	60	5	6	5	0	5	9	88	4	8	9
21	63081-S12	EVERGREEN RD S.H	M-10	IN SOUTHFIELD	1963	3	88	6	7	4	0	6	9	86	5	1	9
22	63172-S13	10 MI RD	M-10	IN SOUTHFIELD	1963	3	84	4	5	4	0	4	9	82	5	3	9
23	63172-S13	WALDON RD	I-75	2.5 MI SE OF M-15	1962	3	119	4	6	4	0	7	9	77	6	0	9
24	63172-S14	SASHABAW RD	I-75	2.2 MI SE OF M-15	1962	3	111	6	8	4	0	6	9	77	6	0	9
25	77091-B01	M-25	BLACK R SPILLWA	IN PORT HUKON	1932	3	55	4	5	4	0	5	9	83	4	8	9
26	78011-B01	M-103	WHITE PIGEON R	0.5 MI N OF INDIANA STATE	1931	3	50	3	4	3	0	4	9	80	4	8	7
27	80024-S02	PAW PAW RD	I-94	1.2 MI W OF M-40	1960	3	92	6	7	4	0	7	9	82	4	2	7
28	81074-S05	EARHART RD	US-23	3.0 MI N OF M-17 & US-23	1962	3	109	5	6	4	0	7	9	83	5	2	8

Table 2.3. List of Bridges Provided by MDOT, June 1997.

Bridge ID	Facility	Feature	Location	Yr Bld	Yr Reconst	Bridge Type	Condition Rigs		Oper Rigs	Max Span	Bridge Length	Deck Width	Beam Spacing	Skews	
							Deck	Supst							
1 03072-B03	M-40	S BRANCH CR	4.0 MI SE OF OTTAWA CO LI	1935	0	3 02	3	3	6	77.0	10.6	11.7	4'-6"	0	
2 03072-B04	M-40	N BRANCH CR	2.4 MI SE OF OTTAWA CO LI	1935	0	3 02	3	3	6	77.0	10.6	11.7	4'-6"	0	
3 06071-B01	M-13	SAGANING CR	4.0 MI S OF STANDISH	1937	1952	3 02	4	2	7	90.0	10.0	25.3	22.0	4'-11"	0
4 06071-B02	M-13	S BR PINE R	3.0 MI S OF STANDISH	1935	1952	3 02	4	4	2	80.0	9.7	29.2	22.0	4'-11"	0
5 06072-B01	US-23 (WDN MAIN)	N BR PINE RIVER	1.8 MI NE OF STANDISH	1930	0	3 02	5	6	7	89.0	10.6	10.6	14.3	4'-8"	0
6 09011-B01	M-84	DUTCH CREEK	5.7 MI SW OF BAY CITY PO	1927	0	3 02	5	4	4	97.0	13.7	13.7	14.1	4'-8"	0
7 09012-B01	M-247	KAWKAWLIN R	4.4 MI NW OF BAY CITY PO	1935	0	3 02	4	5	4	85.0	13.7	41.1	12.6	4'-4"	0
8 12021-B02	US-12	SWAN CR	2.7 MI NE OF BRONSON	1922	1974	3 02	5	6	0	77.0	12.2	12.2	14.8	4'-6"	10
9 19031-B01	US-27	LOOKING GLASS RIVER	5.3 MI N OF INGHAM CO LIN	1941	1947	3 02	5	4	7	87.0	13.7	27.1	21.1	4'-7"	0
10 19062-B01	M-21	LITTLE MAPLE R	2.0 MI W OF OVID	1929	0	3 02	4	4	8	77.0	12.2	12.2	14.2	4'-8"	0
11 23052-B01	M-50	LITTLE THORNAPPLE R	6.4 MI N W OF CHARLOTTE	1931	0	3 02	6	8	7	80.0	10.6	10.6	14.1	4'-8"	38
12 25051-B01	M-54BR	THREAD CR	IN FLINT 2000 BLK S SAGIN	1941	0	3 02	4	4	4	90.0	12.2	12.2	28.8	5'-6"	24
13 26022-B02	M-81	MOLASSE R	4.5 MI E OF M-30	1931	0	3 02	3	3	3	94.0	10.6	20.4	10.9	4'-9"	25
14 29021-B01	M-57	PINE CRK	5.8 MI W OF US 27	1939	0	3 02	5	4	4	89.0	12.2	33.5	12.3		
15 29022-B01	M-57	BEAR CRK	3.5 MI E OF US 27	1941	0	3 02	5	7	8	85.0	13.7	13.7	13.9	4'-10"	30
16 29031-B01	US-27BR	PINE RIVER	IN CITY OF ALMA	1928	1977	2 04	4	4	7	75.0	9.7	28.6	15.1	6'-0"	0
17 32012-B02	M-25	PIGEON R	IN CASEVILLE	1930	0	3 02	3	4	6	81.0	12.2	24.3	17.0	4'-8"	15
18 34021-B01	M-50	DUCK CREEK	3.5 MI E OF KENT CO	1923	0	1 21	4	5	8	85.0	10.6	10.6	7.2		0
19 38051-B02	M-106	PORTAGER DRAIN	4.7 MI SW OF INGHAM CO	1939	0	3 02	5	5	6	89.0	13.7	13.7	12.3	4'-10"	20
20 38101-S03	SANDSTONE RD	I-94	2.2 MI W OF M-80	1958	0	3 32	5	6	7	85.0	14.9	46.7	14.3	6'-3"	0
21 38101-S04	BLACKMAN RD	I-94	5 MI W OF M-60	1958	0	3 32	6	6	7	85.0	14.9	49.0	10.1	6'-3"	0
22 44061-B03	M-90	FLINT R	1.0 MI W OF NORTH BRANCH	1948	0	3 32	4	4	4	90.0	12.2	33.8	10.1	5'-3"	0
23 46011-B02	US-127	BEAN CREEK	0.6 MI NE OF HILLDALE CO	1925	0	3 42	6	4	3	80.0	10.6	10.6	10.5		0
24 54012-B02	US-131	PARIS CR	IN PARIS	1929	0	3 02	5	8	6	98.0	10.3	10.3	24.2	4'-5"	0
25 54032-B02	M-66	N BR CHIPPEWA R	IN BARRYTON	1927	0	3 02	4	5	4	90.0	12.2	24.3	11.1	4'-8"	0
26 61153-B04	US-31 BR EB	MUSKEGON R	IN MUSKEGON	1944	0	2 01	6	6	6	78.0	12.2	32.0	14.3	4'-8"	15
27 70041-B01	M-45	BASS R	7.7 MI E OF US-31	1929	0	3 02	4	4	6	83.0	12.2	12.2	13.7	4'-8"	0
28 70041-B03	M-45	SAN CR	2.7 MI W OF KENT CO L	1929	0	3 02	3	4	6	84.0	13.7	13.7	14.3	4'-8"	0
29 73051-B05	M-13	BIRCH RUN OUTLET DR	7.1 MI S OF M-46	1941	0	3 02	6	7	7	83.0	12.2	33.5	11.7	4'-7"	0
30 74061-B02	M-46	S BR CASS RIVER	2.0 MI W OF M-19	1930	0	3 02	4	6	4	80.0	12.2	24.3	11.2	4'-8"	40
31 76021-B013	TEMP I-69	S BR LOOKING CLASS N	1.3 MI NE OF CLINTON CO L	1931	0	3 02	2	5	7	80.0	12.2	12.2	18.7	4'-4"	15
32 78042-B05	M-60 & M-66	NOTTAWA CR	1.2 MI E OF JCT M-66	1931	0	3 02	5	8	6	92.0	10.6	21.3	14.1		22
33 78062-B01	M-86	SWAN CR	IN COLON	1932	0	3 02	3	4	4	84.0	10.0	30.1	12.9	4'-8"	0
34 79081-B06	M-25	WISCOGGIN CR	0.1 MI S OF HURON CO LINE	1941	0	3 02	4	5	6	88.0	13.7	13.7	13.8	4'-10"	0
35 81062-S06	STONE SCHOOL RD	I-94	IN ANN ARBOR	1954	0	2 04	4	6	5	89.0	14.9	52.7	9.5	4'-11"	0
36 82072-R01	M-3 (GRATIOT AVE)	I-84 GTW RR	IN DETROIT	1929	1970	3 42	5	6	5	91.0	13.4	25.9	36.5		34

3. Load Testing Procedures

3.1 Instrumentation and Data Acquisition

The strain transducers were attached to the lower surface of the bottom flange of the steel girders at midspan (Figure 3.1). In addition, they were installed in selected girders at supports to measure the moment restraint provided by supports. The transducers were also installed at quarter points on Bridge B02-12021 to determine longitudinal load distribution. LVDTs were used to measure deflections and to monitor the global response of the structure during proof load testing of Bridge B02-12021. Each LVDT was placed on a tripod and connected to the bottom of the girder by a wire. Figure 3.2 shows the setup of an LVDT for the measurement of a girder deflection. Strain transducers and LVDTs were connected to the SCXI data acquisition system from the National Instruments. The data acquisition mode is controlled from the external PC notebook computer, and acquired data are processed and directly saved in PC's hard drive (Figure 3.3).

The system consists of a four slot SCXI-1000 chassis, one SCXI-1200 data acquisition module and two SCXI-1100 multiplexers. Each multiplexer can handle up to 32 channels of input data. The current system is capable of handling 64 channels of strain or deflection inputs. Up to 32 additional channels can be added if required. A portable field computer is used to store, process and display the data on site. A typical data acquisition setup is shown in Figure 3.3. The data from all instruments is collected after placing the trucks in desired positions or while trucks are passing on the bridge. The real time responses of all transducers are displayed on the monitor during all stages of testing.

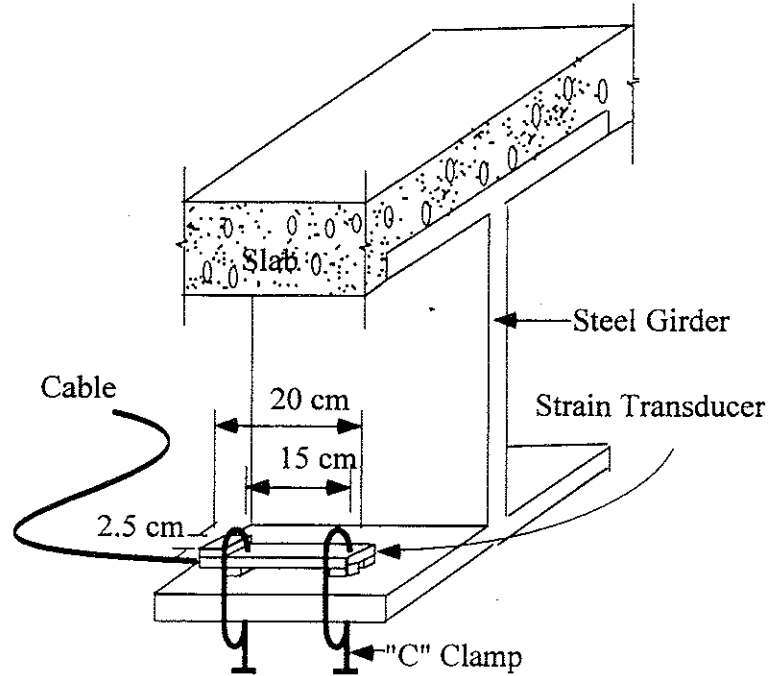


Figure 3.1 Demountable Strain Transducer Mounted to the Lower Flange.

3.2 Test Loads for Load Distribution Tests

Strain data necessary to calculate girder distribution and impact factors were taken from bottom-flanges of girders in the middle of a span. Strain data were obtained under passes of three-unit 10-axle and 11-axle trucks with known weight and configuration for all bridges except bridge B01-70041. Configurations of test trucks are shown in Table 3.1 for all bridges except bridge B01-70041. The same two trucks were used for all bridges except bridge B01-70041. Two three-unit 11-axle trucks were used in bridge B01-70041 and the test truck configurations are shown in Table 3.2. Two trucks have the same axle spacings. Strain data obtained from side-by-side truck tests were used to calculate load distribution and impact factors. Superposition of strain data from each truck provided the verification of the obtained data and the linear-elastic behavior of the bridge.

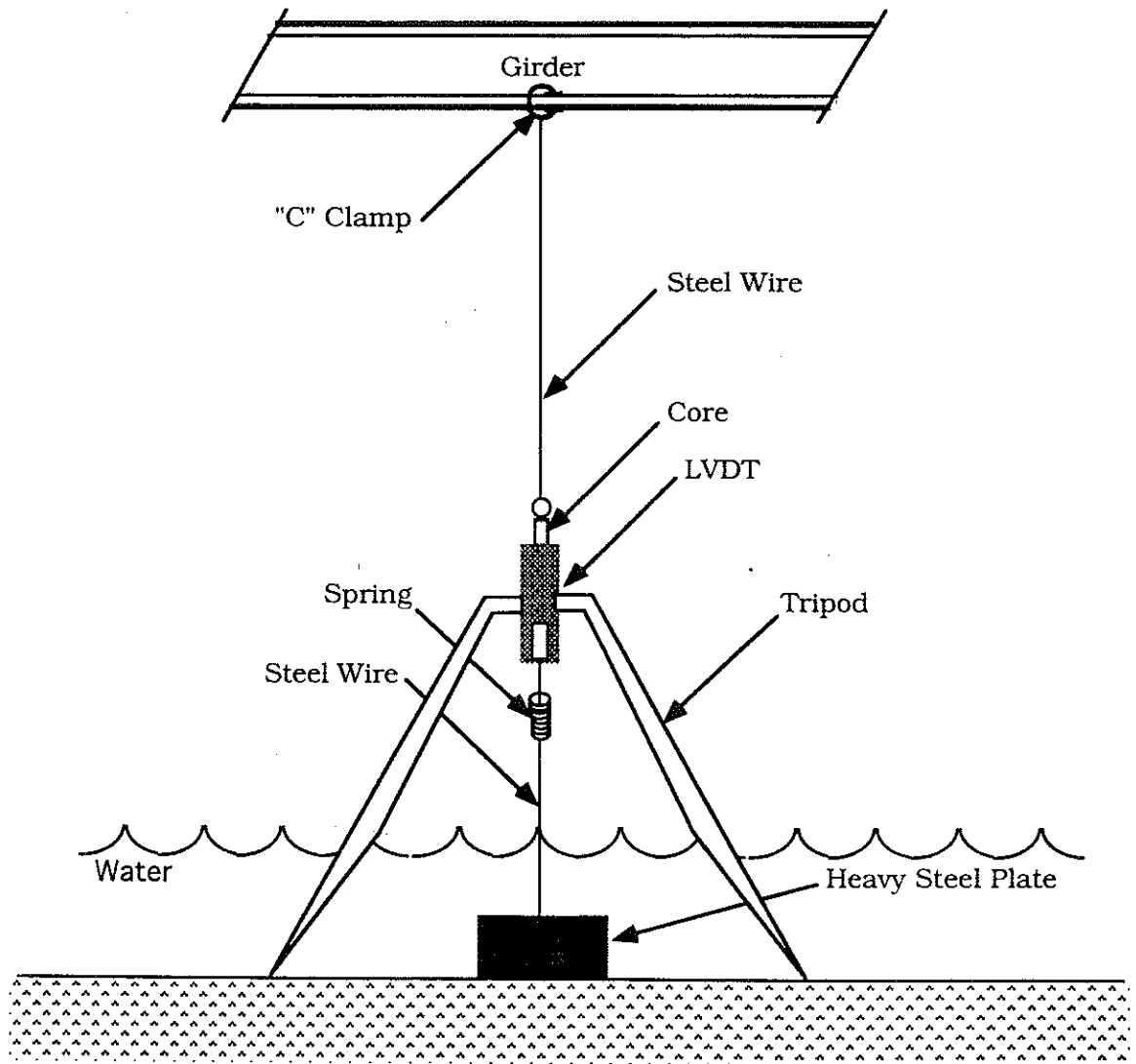


Figure 3.2 Typical LVDT setup.

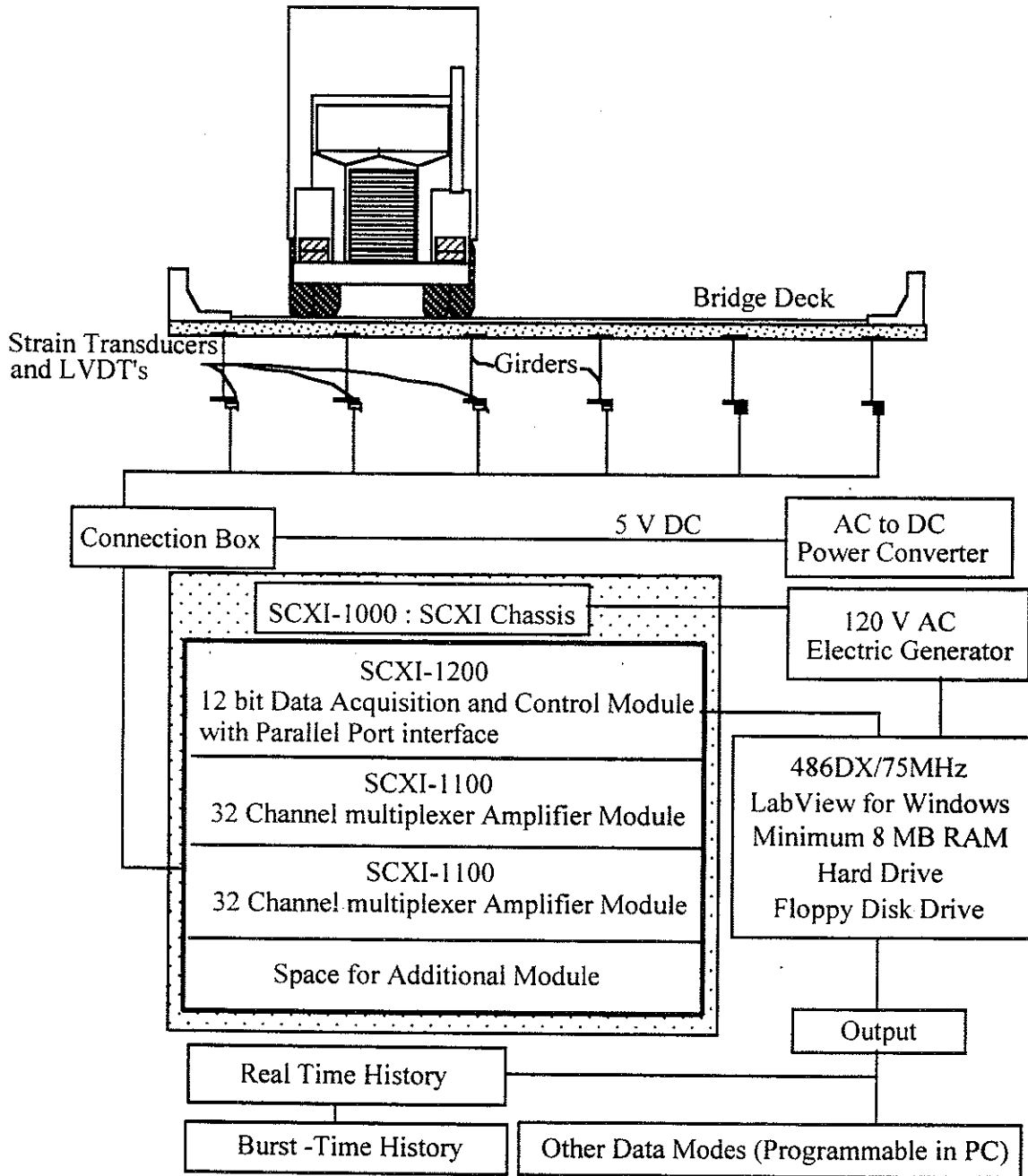


Figure 3.3 SCXI Data Acquisition System Setup.

In addition to static loading at predetermined positions, trucks were driven over the bridge at crawling speed to simulate static loads and at high speed to obtain dynamic effect on the bridge. For the bridge carrying M-156 over Silver Creek in Morenci, the locations causing maximum bending moment were analytically calculated before tests and trucks were statically placed at the analytical maximum bending position. However, the strains obtained from crawling speed tests were always greater than those from the analytical maximum bending position. Therefore, bridges except Bridge B02-46032 (M-156 over Silver Creek in Morenci) were tested under crawling speed and the maximum speed obtained by a test truck at a bridge site (high speed).

In general, the following load cases were applied for bridges with two lanes. Truck 1 is 11-axle truck or truck A for bridge B01-70041. Truck 2 is 10-axle truck or truck B for bridge B01-70041. Lane 1 and lane 2 indicate east and west lane for bridge B02-46032 and north and south lane for all other bridges.

(a) at crawling speed,

- truck 1 in the center of lane 1
- truck 1 close to the curb of lane 1
- truck 2 in the center of lane 1
- truck 2 close to the curb of lane 1
- truck 1 in the center of lane 2
- truck 1 close to the curb of lane 2
- truck 2 in the center of lane 2
- truck 2 close to the curb of lane 2
- truck 1 in the center of lane 1 and truck 2 in the center of lane 2
- truck 2 in the center of lane 1 and truck 1 in the center of lane 2

(b) at high speed,

- truck 1 in the center of lane 1
- truck 2 in the center of lane 1
- truck 1 in the center of lane 2
- truck 2 in the center of lane 2
- truck 1 in the center of lane 1 and truck 2 in the center of lane 2
- truck 2 in the center of lane 1 and truck 1 in the center of lane 2

Table 3.1 Test Truck Configurations for All Bridges except B01-70041

Ten-Axle Truck												
Axle Spacing (m)												
	Front Axle	1	2	3	4	5	6	7	8	9	10	
Bridge ID Number	GVW (kN)	Each Axle Weight (kN)										
B02-46032	582	82	59	54	52	60	57	55	44	55	64	
B05-46041	580	74	66	56	54	58	47	40	58	63	64	
B02-12021	573	74	67	54	51	58	46	39	63	60	61	
B02-38051	585	73	65	56	54	56	50	41	64	62	64	
Eleven-Axle Truck												
Axle Spacing (m)												
	Front Axle	1	2	3	4	5	6	7	8	9	10	11
Bridge ID Number	GVW (kN)	Each Axle Weight (kN)										
B02-46032	637	85	60	53	51	58	55	61	68	44	48	54
B05-46041	637	80	58	56	55	62	52	58	65	45	49	57
B02-12021	640	77	59	58	57	59	52	56	65	49	51	57
B02-38051	644	84	55	58	57	57	51	53	63	49	57	60

Table 3.2 Test Truck Configuration for Bridge B01-70041

Axle Spacing (m)	Front Axle											
Truck ID	GVW	Each Axle Weight (kN)										
Number	(kN)	1	2	3	4	5	6	7	8	9	10	11
Truck A	696	71	71	67	57	53	80	49	64	61	57	66
Truck B	682	72	71	67	65	55	59	52	72	41	52	76

3.3 Test Loads for Proof Load Tests

3.3.1 Proof Load Level

Proof load tests were carried out to verify if the bridge can safely carry the maximum allowable legal load. In Michigan, the maximum mid-span moment in medium span bridges is caused by 11-axle two unit trucks with the wheel configuration shown in Figure 3.4. For an 11-axle truck, the gross vehicle weight (GVW) can be up to 730 kN, which is almost twice the allowable legal load in other states. Most states allow a maximum GVW of 356 kN only. It is more than twice the MS18 design load (AASHTO 1996). The proof load testing was designed to verify the moment capacity of steel girders close to mid-span. Before the proof load tests, the target proof load has to be calculated. If the test load safely reaches the target proof load level, then the operating rating factor for 11-axle two unit truck would be 1.0.

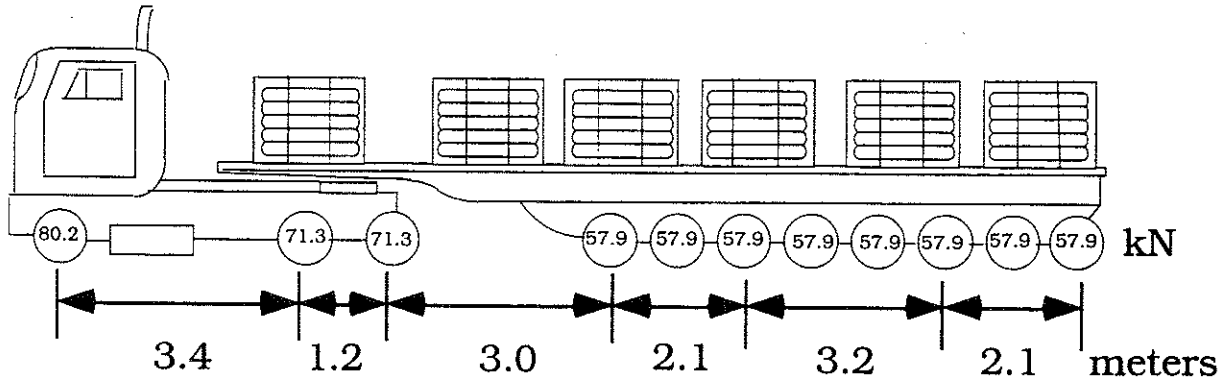


Figure 3.4 11-Axle Two-Unit Truck.

The proof load level should be sufficiently higher than that from 11-axle truck, to ensure the desired safety level. The final draft NCHRP Report 12-28(13)A titled "Bridge Rating Through Load Testing" by A.G. Lichtenstein (1993) provides guidelines for calculating the target proof load level. It suggests that the maximum allowable legal load should be multiplied by a factor X_p , which represents the live load factor needed to bring the bridge to an operating rating factor of 1.0. The guide recommends that X_p should be 1.4 before any adjustments are made. It also recommends the following adjustments to X_p , that should be considered in selecting a target live load magnitude.

- Increase X_p by 15 percent for one lane structures or for other spans in which the single lane loading augmented by an additional 15 percent would govern.
- Increase X_p by 10 percent for spans with fracture critical details.
- Increase X_p by 10 percent for structures without redundant load paths.
- Reduce X_p by 5 percent if the structure is ratable.
- Additional factors including traffic intensity and bridge condition may also be incorporated in the selection of the live load factor X_p .

Application of the recommended adjustment factors, leads to the target live load factor X_{pa} . The net percent increase in X_p (Σ) is found by summing the appropriate adjustments given above. Then

$$X_{pa} = X_p (1 + \Sigma/100) \quad (3-1)$$

The target proof load (L_t) is then:

$$L_t = X_{pa} (1 + I) L_r \quad (3-2)$$

$$1.3 \leq X_{pa} \leq 2.2 \quad (3-3)$$

where,

L_r = the comparable live load due to the rating vehicle for the loaded lanes.

I = impact factor

X_{pa} = the target live load factor.

Based on the span length, the AASHTO Standard Specifications (1996) specifies the impact factors of less than 0.3. However, previous studies by several researchers have indicated that the dynamic amplification is much smaller for heavy loads (Hwang and Nowak 1991, Nassif and Nowak 1995, Nowak, Laman and Nassif 1994). Therefore, for this study, an impact factor of 0.1 was selected.

3.3.2 Load Selection

The M-60 military tanks were selected. Each tank weighs 504 kN (obtained from tank weight information from the Michigan National Guard) and the load is distributed over a track length of 4.5 m. Hence, these tanks cause very high moments at mid-span. The tanks were provided by the Michigan National Guard. The front and side views of the M-60 tanks are shown in Figures 3.5 and 3.6.

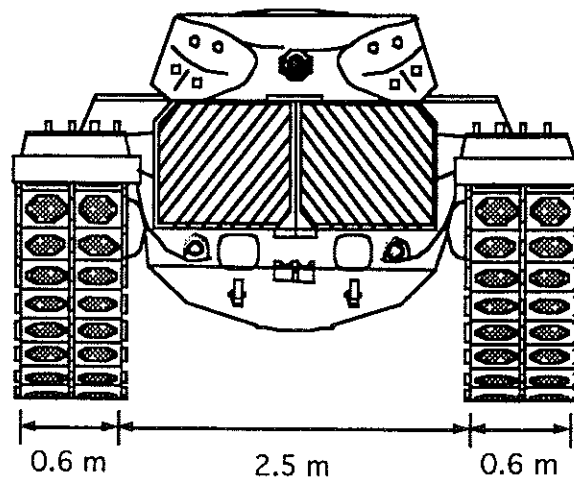


Figure 3.5 Cross-Section of M-60 Tank.

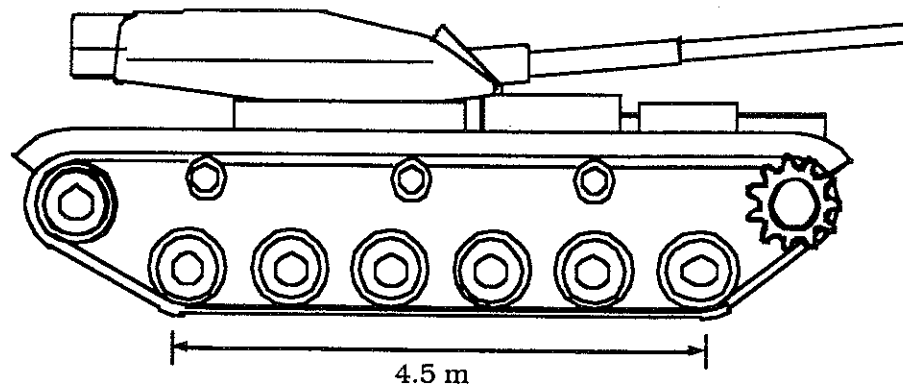


Figure 3.6 Side Elevation of M-60 Tank.

The following proof load cases were applied for Bridge US12/SC:

- one tank close to the curb of north lane
 - in the middle of span
 - 0.61 m east from the middle of span
 - 0.61 m west from the middle of span
- one tank at the center of north lane
 - in the middle of span
 - 0.61 m east from the middle of span
 - 0.61 m west from the middle of span
- one tank close to the curb of south lane
 - in the middle of span
 - 0.61 m east from the middle of span
 - 0.61 m west from the middle of span
- one tank at the center of south lane
 - in the middle of span
 - 0.61 m east from the middle of span
 - 0.61 m west from the middle of span
- two side-by-side tanks at the center of bridge width
 - both tanks 0.61 m east from the middle of span
 - one tank 0.61 m east from the middle of span, the other tank in the middle of span
 - both tanks in the middle of span
 - one tank 0.61 m west from the middle of span, the other tank in the middle of span
 - both tanks 0.61 m west from the middle of span

Detailed proof load positions are shown in chapter 7.

3.4 Load Distribution and Impact Factor Calculation from Test Results

Collected strain data from the tests were processed to identify impact and girder distribution factors. Girder Distribution Factors (GDF) are calculated from the maximum static strain obtained from the static loading at each girder at the same section along the length of the bridge. Ghosn *et al.* (1986) assumed that GDF was equal to the ratio of the static strain at the girder to the sum of all the static strains. Stallings and Yoo (1993) used the weighted strains to account for the different section moduli of the girders. Accordingly, GDF for the *i*th girder, GDF_i , can be derived as follows:

$$GDF_i = \frac{M_i}{\sum_{j=1}^k M_j} = \frac{ES_i \varepsilon_i}{\sum_{j=1}^k ES_j \varepsilon_j} = \frac{\frac{S_i}{S_j} \varepsilon_i}{\sum_{j=1}^k \frac{S_j}{S_i} \varepsilon_j} = \frac{\varepsilon_i w_i}{\sum_{j=1}^k \varepsilon_j w_j} \quad (3-4)$$

where M_i = bending moment at the *i*th girder; E = modulus of elasticity; S_i = section modulus of the *i*th girder; S_j = typical interior section modulus; ε_i = maximum bottom-flange static strain at the *i*th girder; w_i = ratio of the section modulus of the *i*th girder to that of a typical interior girder; and k = number of girders. When all girders have the same section modulus (that is, when weight factors, w_i , are equal to one for all girders), Eq. (3-4) is the equivalent to that of Ghosn *et al.* (1986). Because of edge stiffening effect due to curbs and barrier walls, the section modulus in exterior girders is slightly greater than in interior girders. In other words, the weight factors, w_i , for exterior girders are greater than one. Therefore, from Eq. (3-4), the assumption of the weight factors, w_i , equal to one will cause slightly overestimated girder distribution factors in interior girders and underestimated girder distribution factors in exterior girders. In this study, the weight factors, w_i , are assumed to be one.

Impact factors are defined in several ways, as discussed in previous studies (Paultre *et al.* 1992; Bakht and Pinjarkar 1989). In this study, the impact factor was taken as the ratio of the maximum dynamic strain and the maximum static strain (Figure 3.7):

$$I = \frac{\epsilon_{dyn}}{\epsilon_{stat}} \tag{3-5}$$

where ϵ_{dyn} = absolute maximum dynamic strain under the vehicle traveling at normal speed; and ϵ_{stat} = maximum static strain obtained by filtering the dynamic response. A numerical procedure is applied to filter collected data.

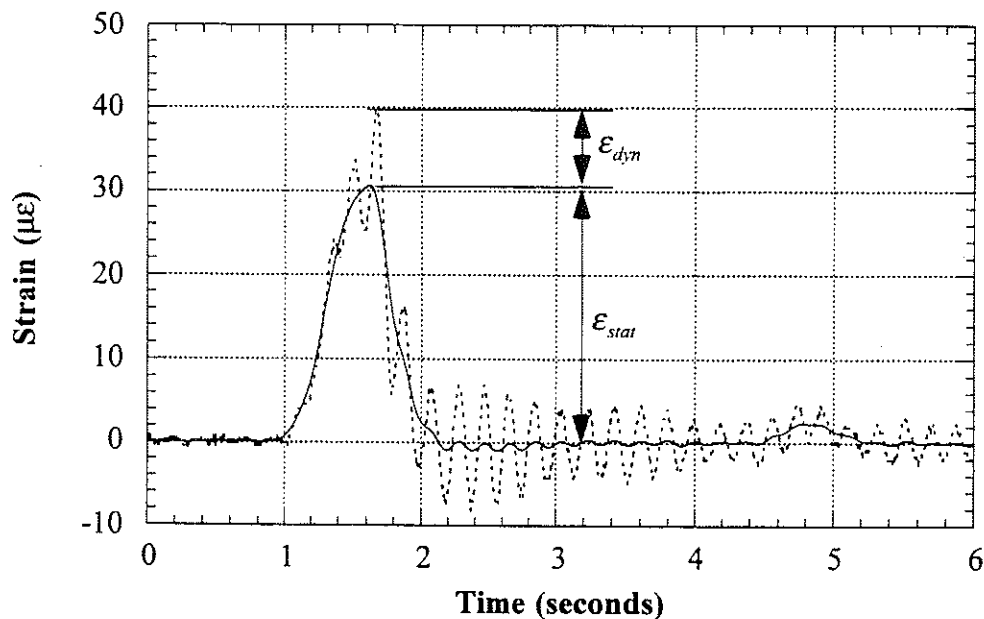


Figure 3.7 Dynamic and Static Strain under a Truck at Highway Speed.

Two additional considerations are associated with calculation of impact factors: strain magnitude and girder selection. First, the level of strain for each girder should be considered to calculate impact factors.

Impact factors corresponding to light vehicles, being relatively on the high side, tend to bias the data. It is, therefore, necessary that the data considered for developing the statistics of the impact factor correspond to the weight class of the design or evaluation vehicle. Strain data collected under passes of side-by-side trucks provided the reference strain value to obtain impact factors.

Second, impact factors should be calculated from the girder with maximum strain to be compatible with current design codes. Otherwise it will result in overestimated values. This is because the distribution factors in current design codes provide maximum static load effect in any girder from any possible static load combinations and the distribution factor is multiplied by an impact factor.

4. Specified Load Distribution Factors and Impact Factors

Measured girder distribution factors (GDF) and impact factors are compared in tables and figures with the values calculated according to the current design codes. Throughout the report, distribution factors are expressed in terms of axle load or full truck rather than a line of wheel loads or half truck. For moment in interior girders, the American Association of State Highway and Transportation Officials (AASHTO) standard specifications (1996) specifies GDF's as follows. For one lane steel girder and prestressed concrete girder bridges, GDF is:

$$GDF = \frac{S}{4.27} \quad (4-1)$$

and for multi lane steel and prestressed concrete girder bridges,

$$GDF = \frac{S}{3.36} \quad (4-2)$$

where S = girder spacing (m).

The AASHTO Load and Resistant Factor Design (LRFD) Code (1994) specifies GDF as a function of girder spacing, span length, stiffness parameters, and bridge skew. For moment in interior girders with one lane loading, GDF is:

$$GDF = \left\{ 0.075 + \left(\frac{S}{2900} \right)^{0.6} \left(\frac{S}{L} \right)^{0.2} \left(\frac{K_g}{Lt_s^3} \right)^{0.1} \right\} \left\{ 1 - c_1 (\tan \theta)^{1.5} \right\} \quad (4-3)$$

and in multi lane loading:

$$GDF = \left\{ 0.06 + \left(\frac{S}{4300} \right)^{0.4} \left(\frac{S}{L} \right)^{0.3} \left(\frac{K_g}{Lt_s^3} \right)^{0.1} \right\} \left\{ 1 - c_1 (\tan \theta)^{1.5} \right\} \quad (4-4)$$

$$c_1 = 0.25 \left(\frac{K_g}{Lt_s^3} \right)^{0.25} \left(\frac{S}{L} \right)^{0.5} \quad \text{for } 30^\circ < \theta < 60^\circ \quad (4-5)$$

$$c_1 = 0 \quad \text{for } \theta < 30^\circ \quad (4-6)$$

where S = girder spacing (mm); L = span length (mm); $K_g = n(I + Ae_g^2)$; t_s = depth of concrete slab (mm); n = modular ratio between girder and slab materials; I = moment of inertia of the girder (mm^4); A = area of the girder (mm^2); e_g = distance between the center of gravity of the girder and slab (mm); and θ = skew angle in degrees. Because the term $K_g / (Lt_s^3)$ implies more accuracy than exists for bridge evaluation, it is recommended that they be taken as 1.0. In this report, however, actual values of the term $K_g / (Lt_s^3)$ are used in calculation of girder distribution factors. The AASHTO LRFD (1994) formulas have been developed based on a National Cooperative Highway Research Program (NCHRP) Project 12-26 (Zokaie *et al.* 1991). This method includes the longitudinal stiffness parameter, K_g , and the span length, L , in addition to the girder spacing, S . AASHTO Guide for Load Distribution (1994) specifies similar load factors to those of AASHTO LRFD (1994).

Most bridge design codes specify the dynamic load as an additional static live load. In the current AASHTO (1996), impact factors are specified as a function of span length only:

$$I = \frac{50}{3.28L + 125} \quad (4-7)$$

where I = impact factor (maximum 30 percent); and L = span length (m). This empirical equation has been in effect since 1944. In the AASHTO LRFD (1994), live load is specified as a combination of MS18 truck (AASHTO 1996) and a uniformly distributed load of 9.3 kN/m. The impact factor is equal to 0.33 of the truck effect, with no dynamic load applied to the uniform loading.

5. Bridge on M-156 over Silver Creek in Morenci (B02-46032, M156/SC)

5.1 Description

This bridge was built in 1935 and is located on state highway M-156 over Silver Creek in Morenci, Michigan. This bridge is designated as M156/SC, and can be identified by the road carried by the bridge and the creek under the bridge. It has one lane in each direction. As shown in Figure 5.1, the superstructure is composed of ten steel girders spaced at 1.32 m and a 190 mm thick concrete slab with a 76 mm asphalt overlay. It is a simply supported single span structure and was designed to be noncomposite. The total span length is 13.7 m with a skew of 30 degrees. The legal speed limit is 48 km/h. The deck slab and approach to the bridge were in good condition, and the bridge has a load rating of 792 kN.

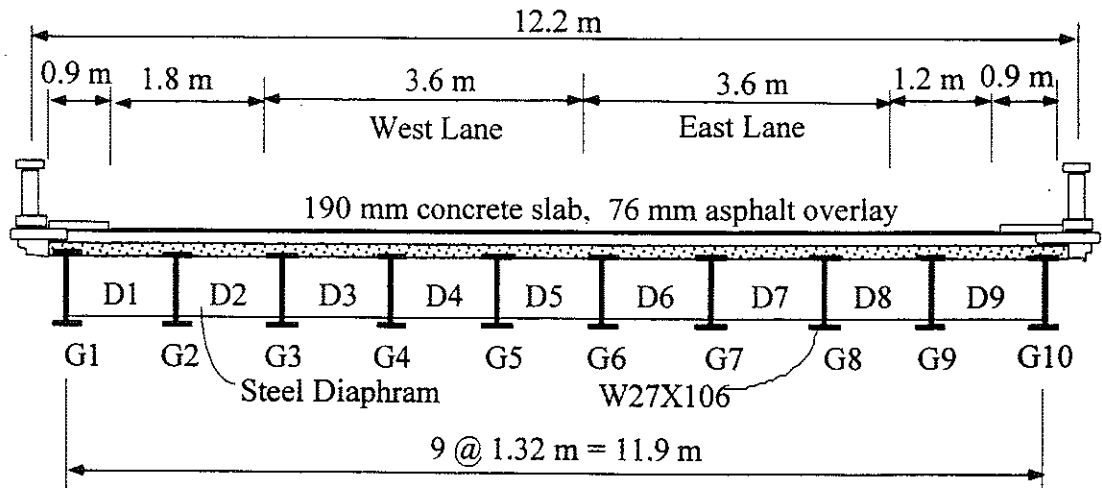


Figure 5.1 Cross-Section of Bridge M156/SC in Morenci.

5.2 Instrumentation

Strain transducers were installed on the bottom flanges of girders in the middle of the span and close to the support (Figure 5.2). The bridge test was performed on June 26, 1997.

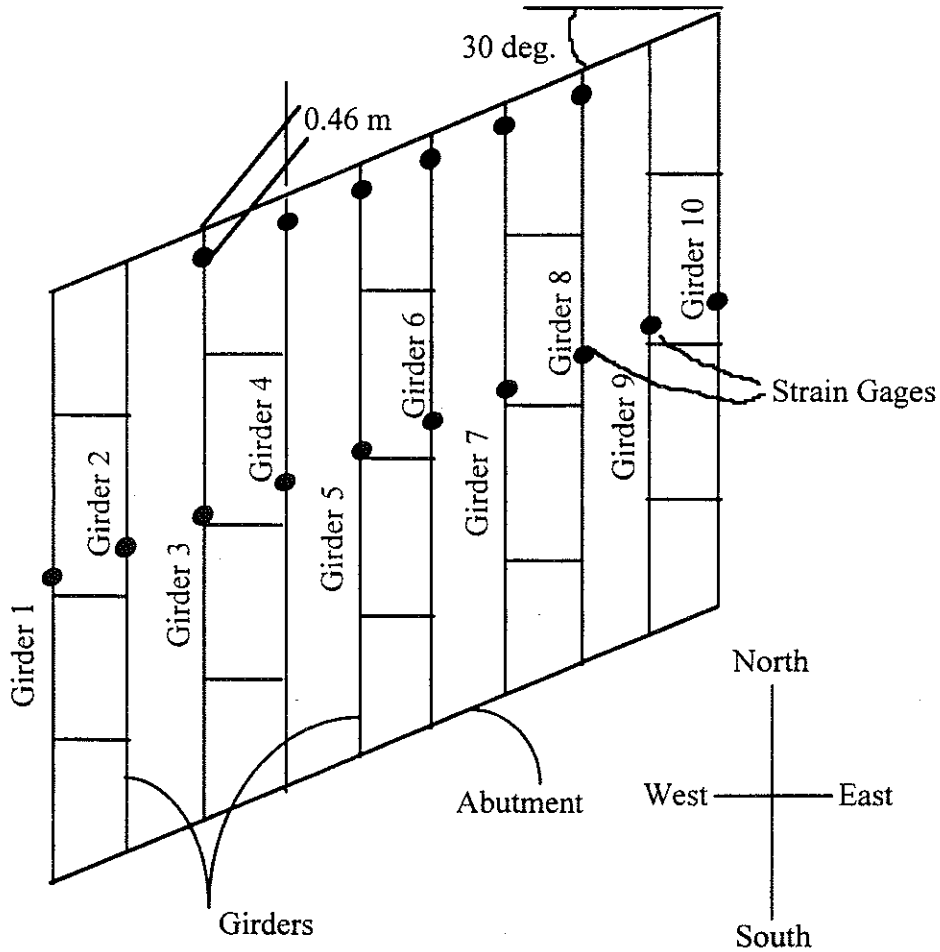


Figure 5.2 Strain Transducer Locations in Bridge M156/SC in Morenci.

5.3 Truck Loads

The strain data necessary to calculate girder distribution and impact factors were taken from the midspan transducers. The bridge was loaded with three-unit 10-axle and 11-axle trucks. The 10 and 11-axle trucks have gross weights of 582 kN and 637 kN, with wheelbases of 14.3 m and 15.6 m, respectively. Truck configurations are shown in Figures 5.3 and 5.4.

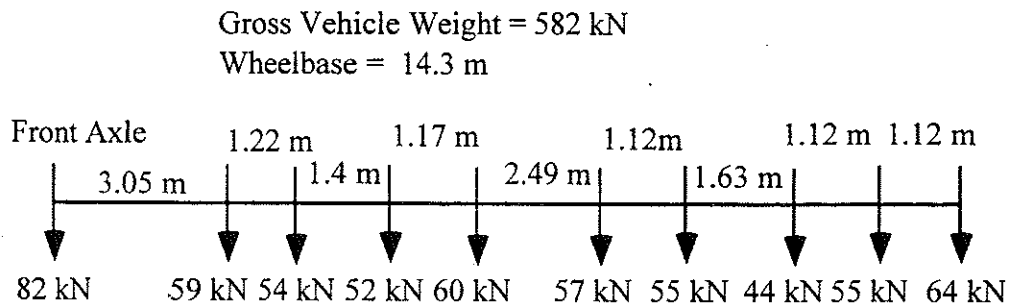


Figure 5.3 Ten-Axle Truck Configuration, Bridge M156/SC in Morenci.

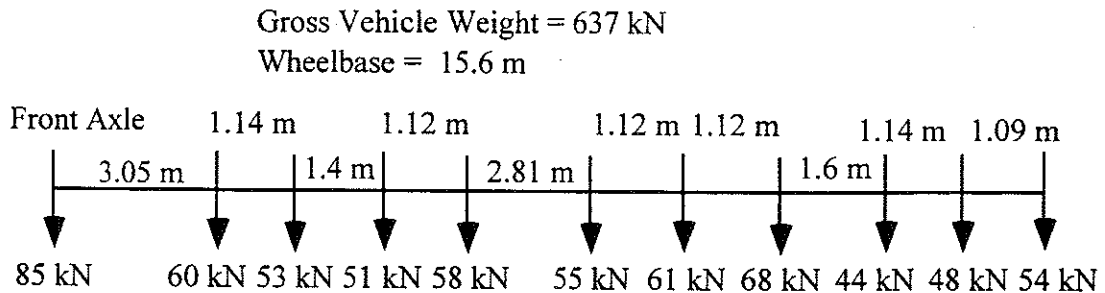


Figure 5.4 Eleven-Axle Truck Configuration, Bridge M156/SC in Morenci.

The following load cases were applied during the tests:

Static positions (trucks were stopped completely):

- 11-axle truck at near analytical maximum bending moment location in the center of west lane
- 11-axle truck at analytical maximum bending moment location in the center of west lane
- 11-axle truck at analytical maximum bending moment location contact with curb of west lane
- 11-axle truck at near analytical maximum bending moment location in the center of east lane
- 11-axle truck at analytical maximum bending moment location in the center of east lane
- 11-axle truck at analytical maximum bending moment location contact with the curb of east lane
- 10-axle truck at analytical maximum bending moment location in the center of east lane
- 10-axle truck at near analytical maximum bending moment location in the center of west lane
- 10-axle truck at analytical maximum bending moment location in the center of west lane

Crawling speed positions:

- 11-axle truck in the center of west lane
- 11-axle truck close to curb of west lane
- 11-axle truck in the center of east lane
- 10-axle truck in the center of west lane
- 10-axle truck in the center of east lane
- 10-axle truck in the center of west lane and 11-axle truck in the center of east lane

At high speed, the maximum speed obtained by the test trucks were:

- 11-axle truck in the center of east lane, 48 km/h
- 10-axle truck in the center of west lane, 64 km/h
- 10-axle truck in the center of east lane, 64 km/h
- 11-axle truck in the center of west lane, 56 km/h
- 11-axle truck in the center of west lane and 10-axle truck in the center of east lane, 48 km/h

5.4 Load Test Results

Strains resulting from both the static and crawling-speed tests are considered non-dynamic. For a given truck and lane position, the maximum strains from a non-dynamic test can be compared with its high-speed counterpart. By subtracting out non-dynamic strain, the strains caused by dynamic effects can then be determined. Girder distribution factors were determined from static strains using Eq. (3-4) and the impact factor was calculated using dynamic strains.

Figures 5.5 to 5.9 present all static load cases including static positioning and crawling-speed tests. Strains from a crawling-speed test were always greater than those from static positioning at the analytical maximum bending position. This likely indicates a combination of actual bridge behavior differing from simplified theory and a truck positioning error. Each figure presents all load cases of one truck type in the same lane for all longitudinal and lateral positions. Figure 5.13 shows dynamic strains from all high speed tests.

Figures 5.5 to 5.8 present static strains and girder distribution factors (GDF's) for one truck on the bridge. Figure 5.9 shows static strains and GDF's for a side-by-side static load test. GDF's are calculated from corresponding static strains using Eq. (3-4).

Figures 5.5 to 5.8 show the static strains and resulting GDF's on each girder for several different load cases, as described on the diagrams. Figure 5.10 shows the maximum effect from all cases in Figures 5.5 to 5.8. Because the AASHTO Code specifies GDF's for both lanes loaded, the results in Figure 5.10, which represent the effect of a single truck, are not directly comparable to code values. By superimposing the results of one loaded lane with the other, however, the GDF's for two loaded lanes can be determined. The results are shown in Figure 5.11, together with those of a side-by-side crawling-speed truck test. For the purpose of comparison, code specified distribution factors are also plotted. In calculation of AASHTO LRFD Girder distribution factors, actual value of the term $K_g / (L t_s^3)$ is used.

Notice that in Figure 5.11, the results are taken as the maximum effect caused by the combination of two transverse truck positions in each lane (see Figs. 5.5 to 5.8); in the center of the lane, and near the curb. In contrast, Figure 5.9 shows the results when both trucks were in the same transverse position in their respective lanes.

As expected, as the trucks are placed closer to the curbs, the GDF increases on the outside girders. The interior girders still experience a higher load effect, however. The maximum value obtained from the tests is very close to AASHTO Standard (S/3.36) GDF. However, this does not indicate that the bridge behaves as assumed when designed. Comparing design stresses and stresses found from the tests, it was found that the bridge has a significant extra live load carrying capacity, despite the fact that the maximum GDF is close to design values.

Figure 5.12 compares static strains obtained by superposing strains under one truck loading with those from simultaneous side-by-side truck loading. They have practically the same values, verifying the superposition method used.

Figure 5.13 presents the dynamic strains obtained from high speed tests. The girder distribution factors calculated from those dynamic

strains are plotted in Figure 5.14 and 5.15 and compared with Code specified distribution factors.

Figure 5.16 presents the corresponding strains from static tests used to calculate impact factors. Only the static load cases in which the trucks have the same lateral positions as in the high-speed tests are shown in Figure 5.16. Impact factors are calculated from Eq. (3-5) and presented in Figure 5.17. Impact factors for exterior girders are high because the static strains in these girders are very low. Because of these low static strains, the addition of dynamic effects still results in a low overall value. Therefore, large impact factors in exterior girders are not of concern. It is clear in Figure 5.18, which shows the relationship between strain magnitude and impact factors, that large impact factors correspond to low static strains. Dynamic strains remain nearly constant, while static strains increase with truck loading. This results in large impact factors for low static strains. For side-by-side truck loading, the impact factor is approximately 10%.

Figures 5.19 to 5.23 show the strains taken from transducers installed close to the abutment. They correspond to Figures 5.5 to 5.9. It is not surprising that there are negative strains at the support, which indicates partial fixity of the joints. These values are significant when compared with those in the middle of span. Support strains vary from one third to one half of the strain values in the middle of the span.

The measured static strains were compared to static strains calculated using the design stiffness and GDF's determined by tests in this study. The maximum observed static strain for this bridge is $67.5 \mu\epsilon$ for a single truck and $102.4 \mu\epsilon$ for two trucks side-by-side. The corresponding calculated static strain for a single truck in a composite section is $180 \mu\epsilon$ and for a non-composite section it is $260 \mu\epsilon$. For two trucks side-by-side, the calculated static strains are $262 \mu\epsilon$ and $379 \mu\epsilon$ for a composite section and a non-composite section, respectively.

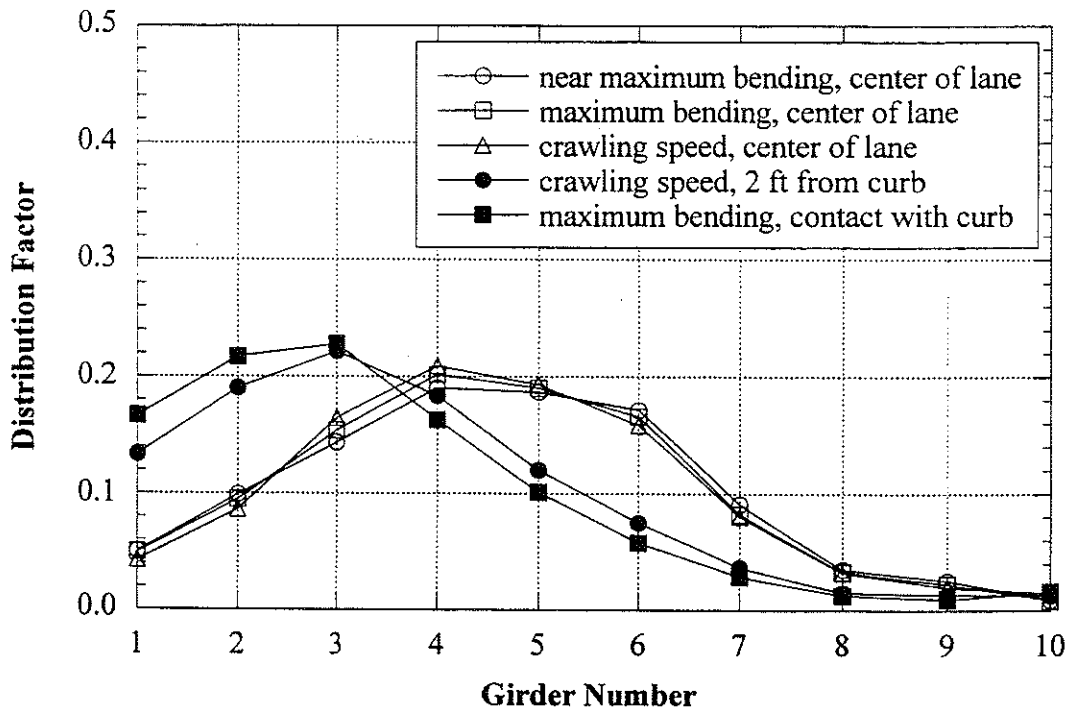
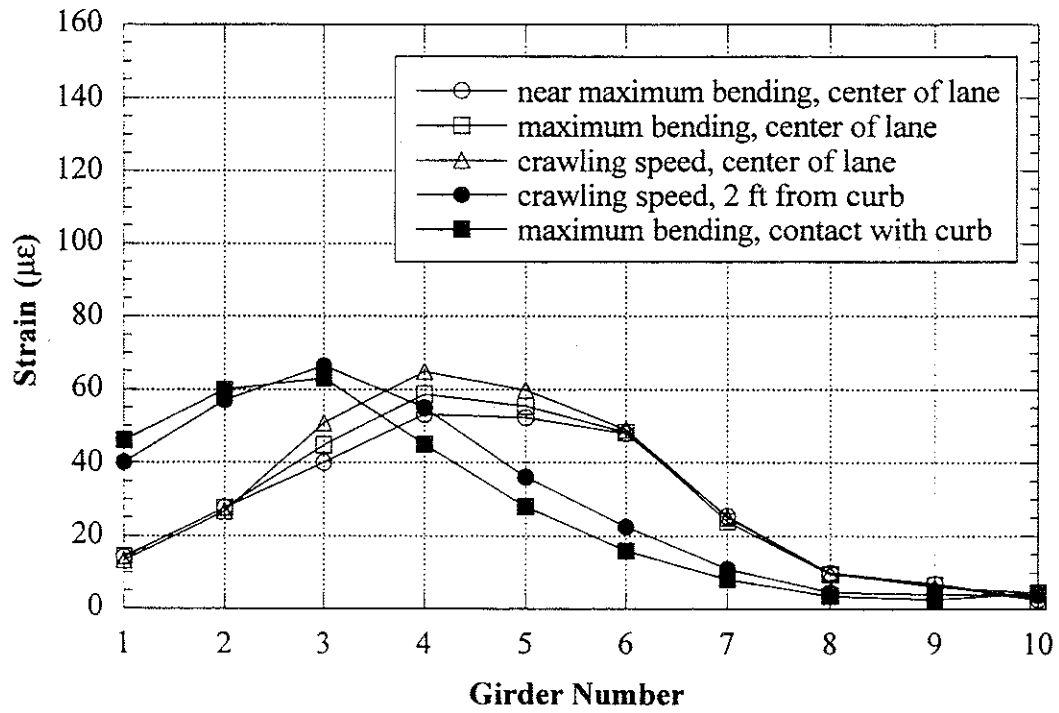


Figure 5.5 West Lane, 11-Axle Truck, Static Loading, Midspan.

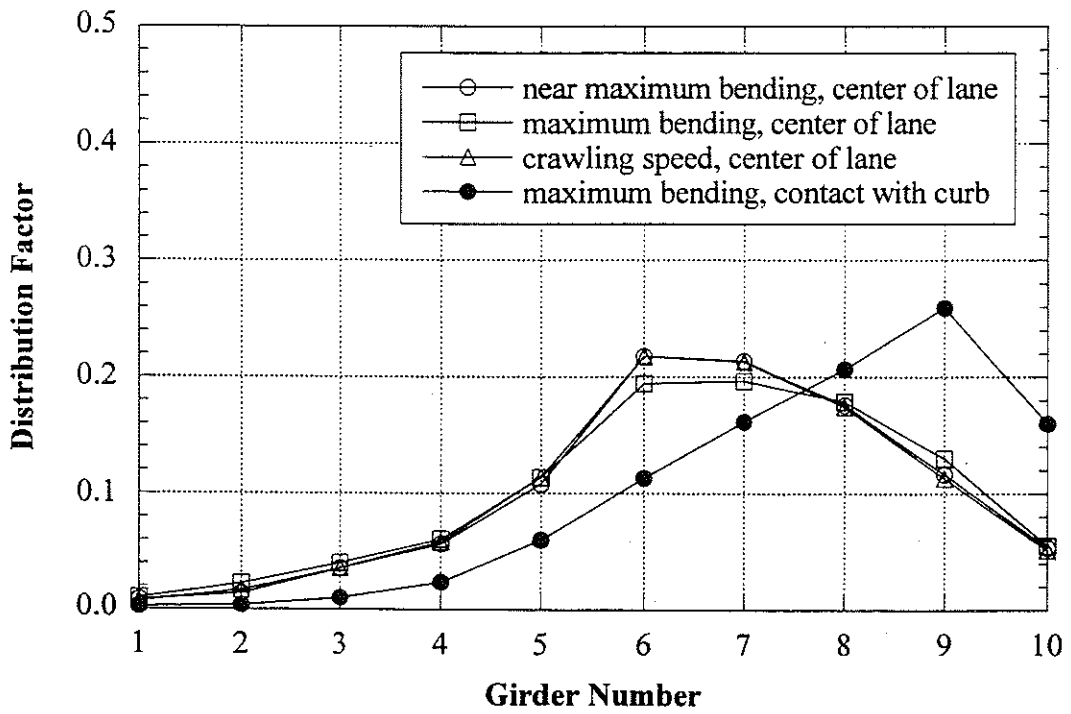
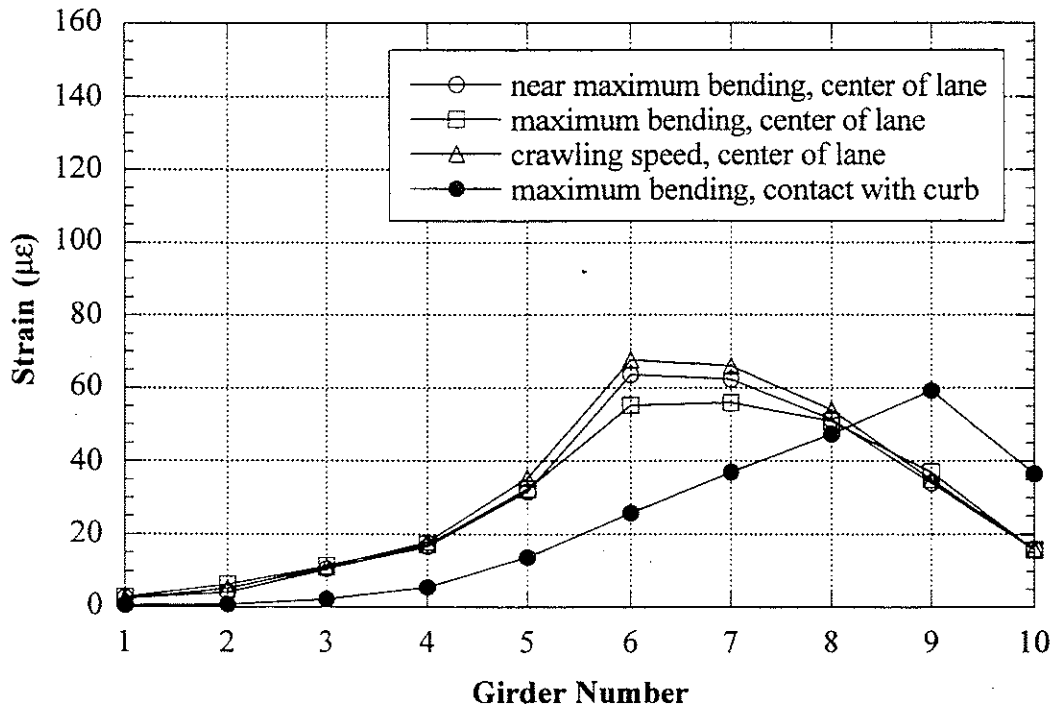


Figure 5.6 East Lane, 11-Axle Truck, Static Loading, Midspan.

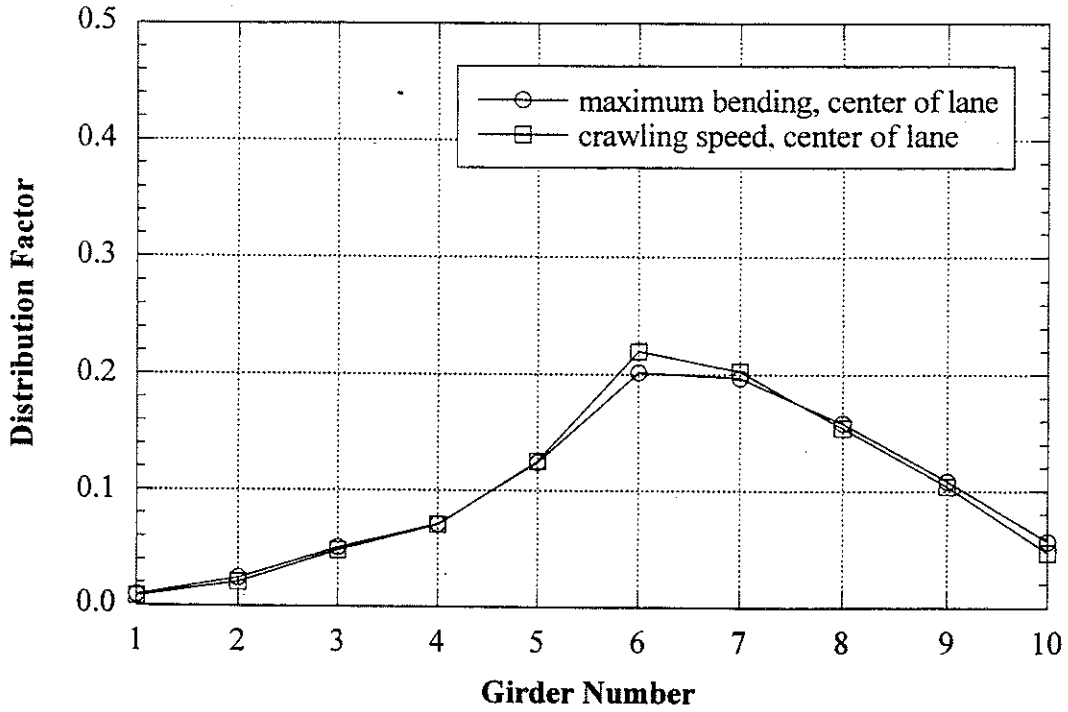
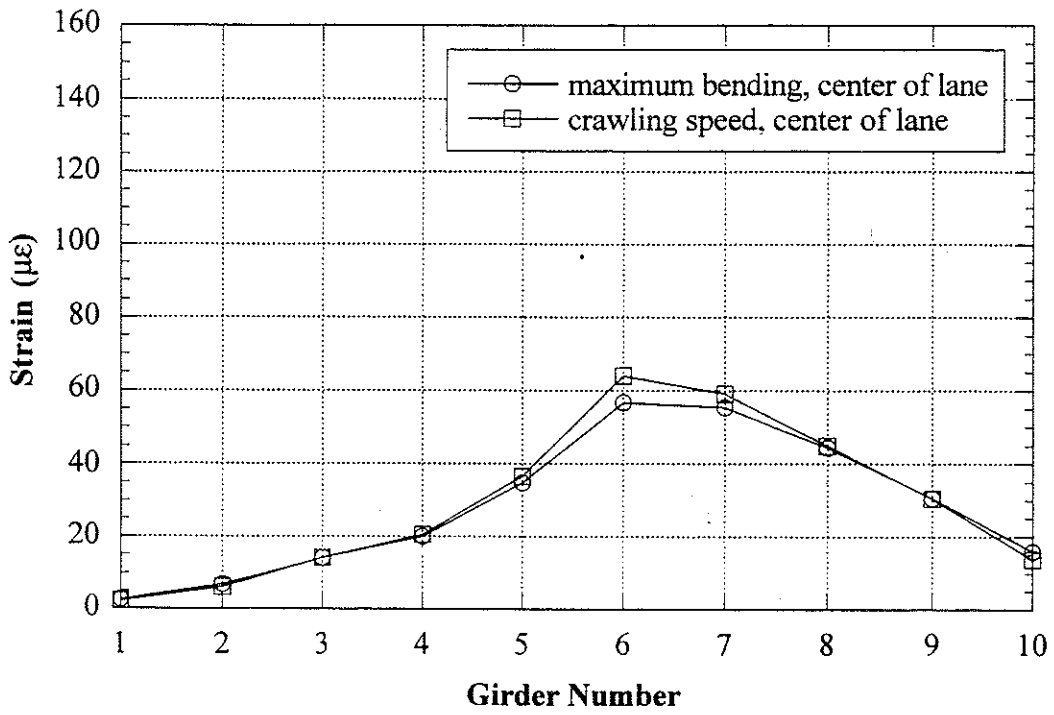


Figure 5.7 East Lane, 10-Axle Truck, Static Loading, Midspan.

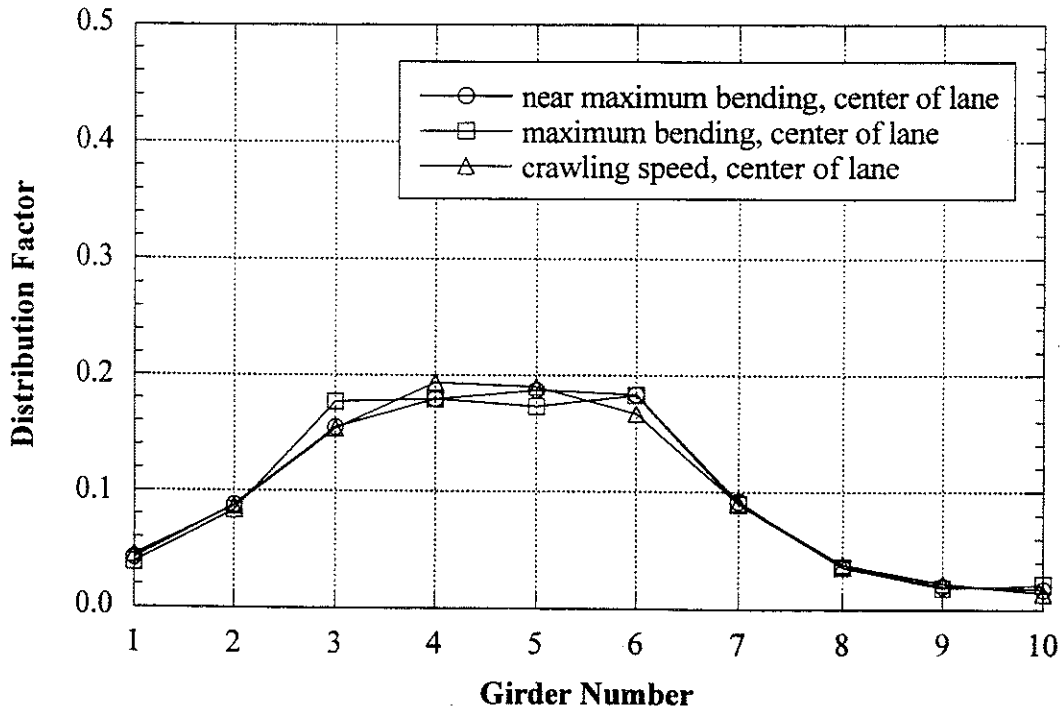
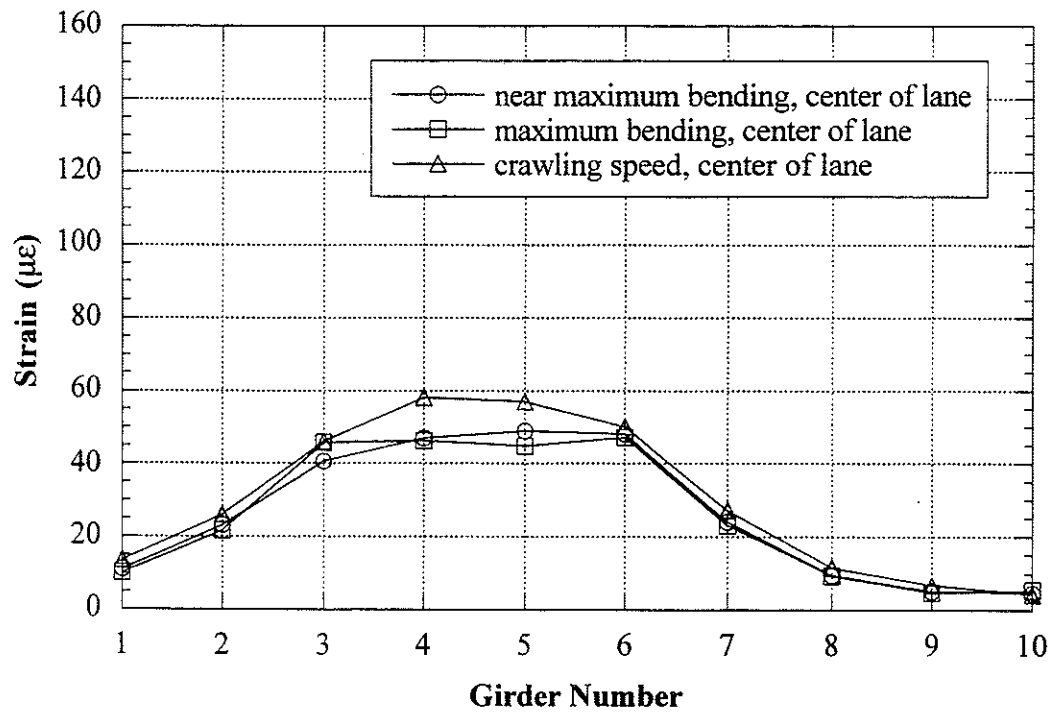


Figure 5.8 West Lane, 10-Axle Truck, Static Loading, Midspan.

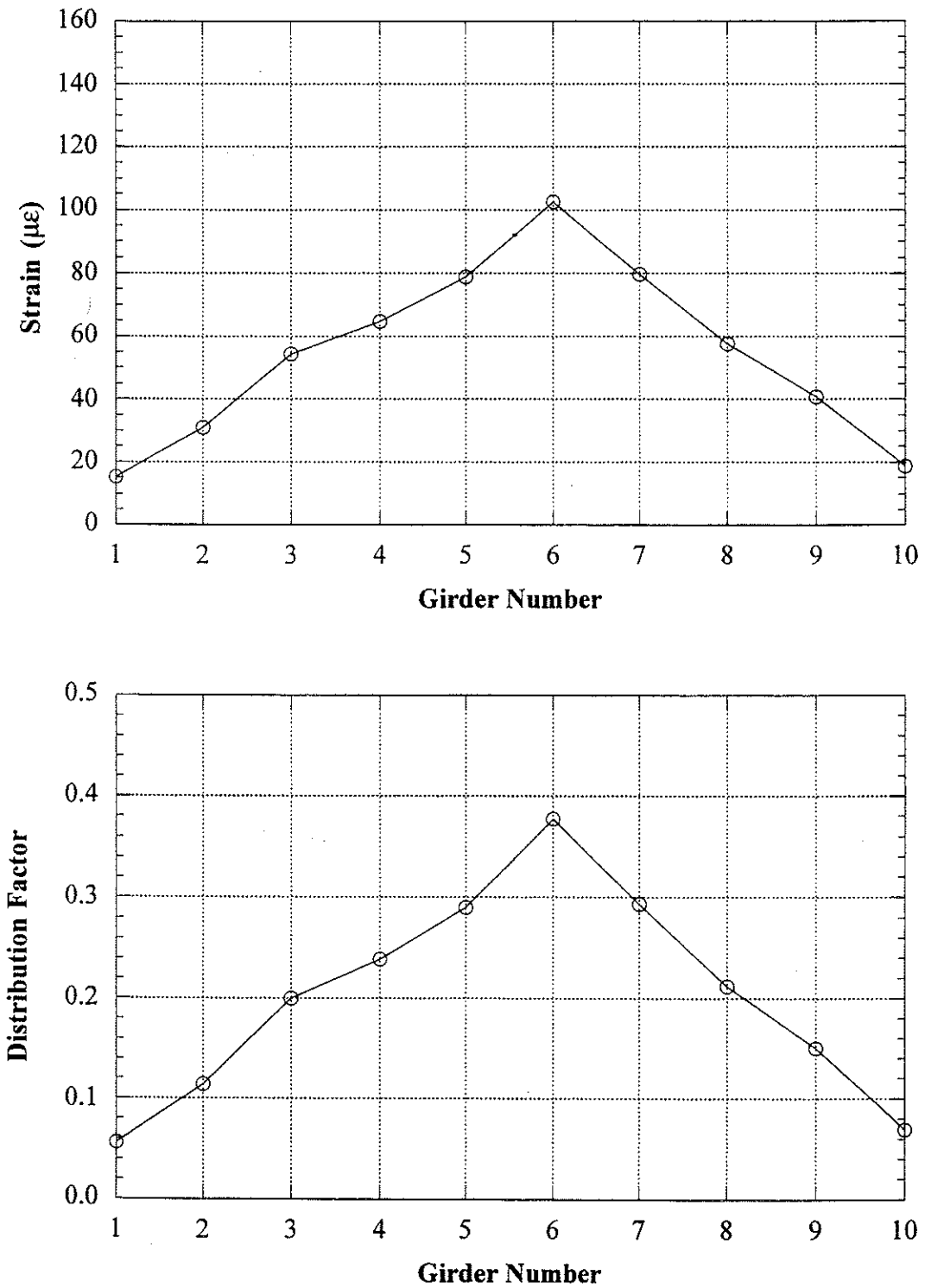


Figure 5.9 Side-by-Side Crawling Speed, Center of Lane, 10-Axle in West Lane, 11-Axle in East Lane, Midspan.

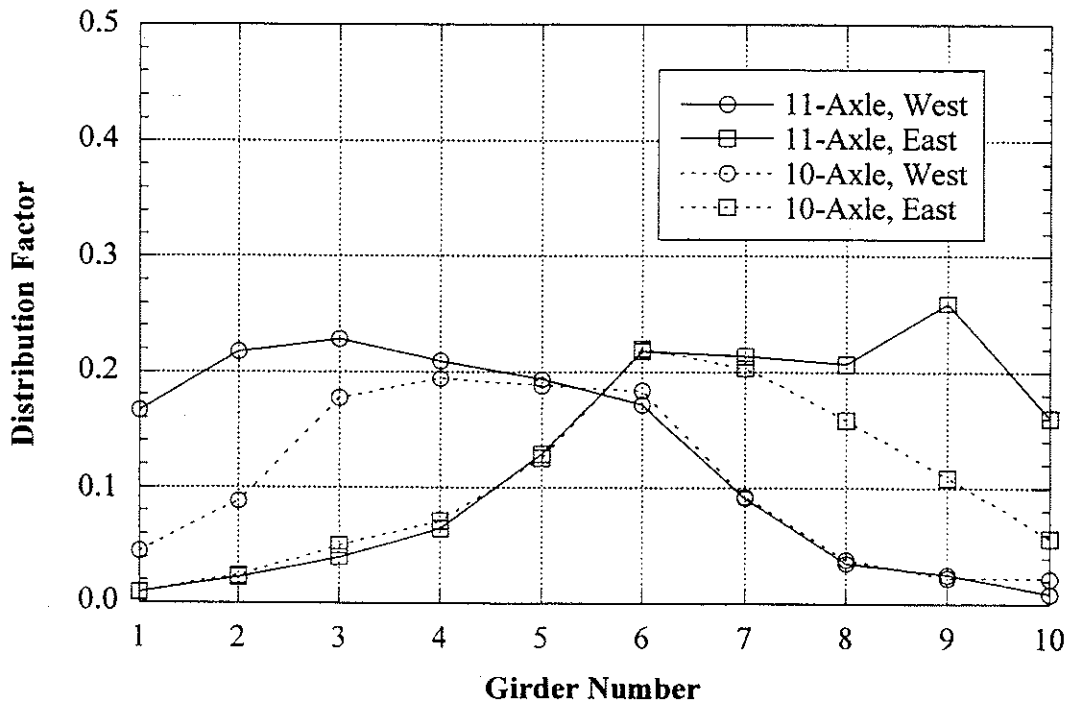


Figure 5.10 Maximum Girder Distribution Factor For One Truck at Crawling Speed.

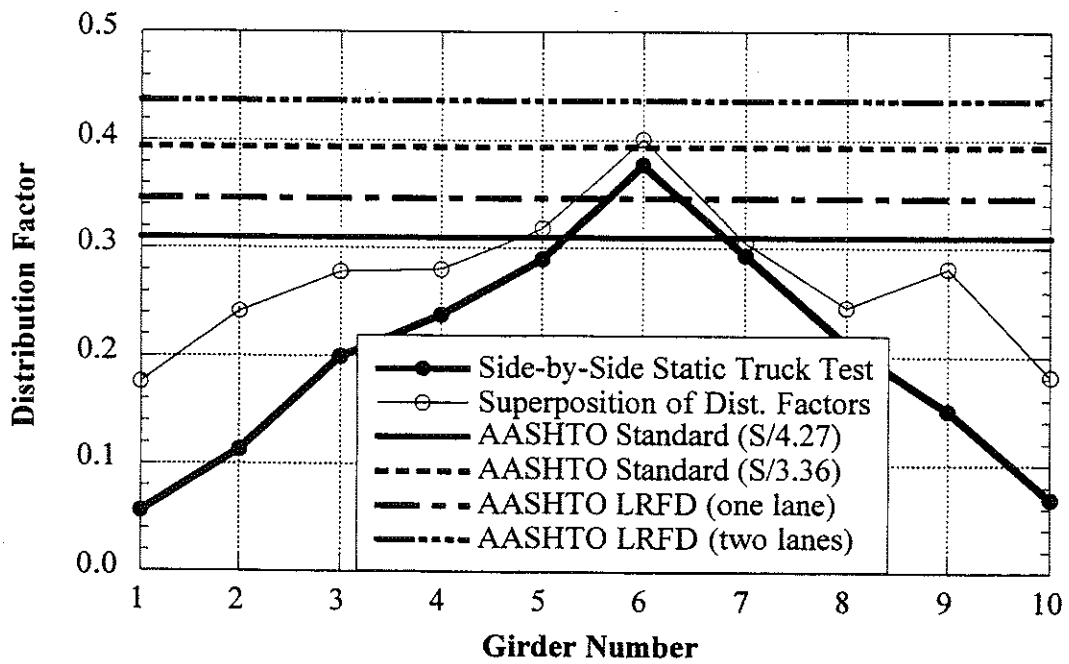


Figure 5.11 Comparison with Code Specified Distribution Factors at Crawling Speed

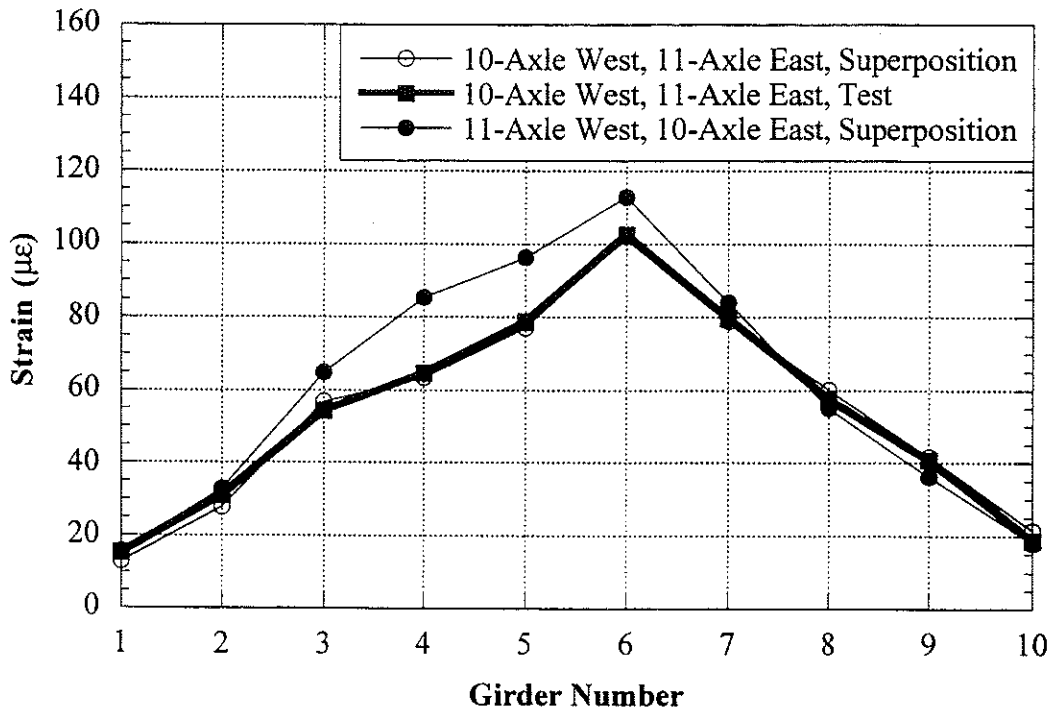


Figure 5.12 Strain Superposition and Comparison with Static Test.

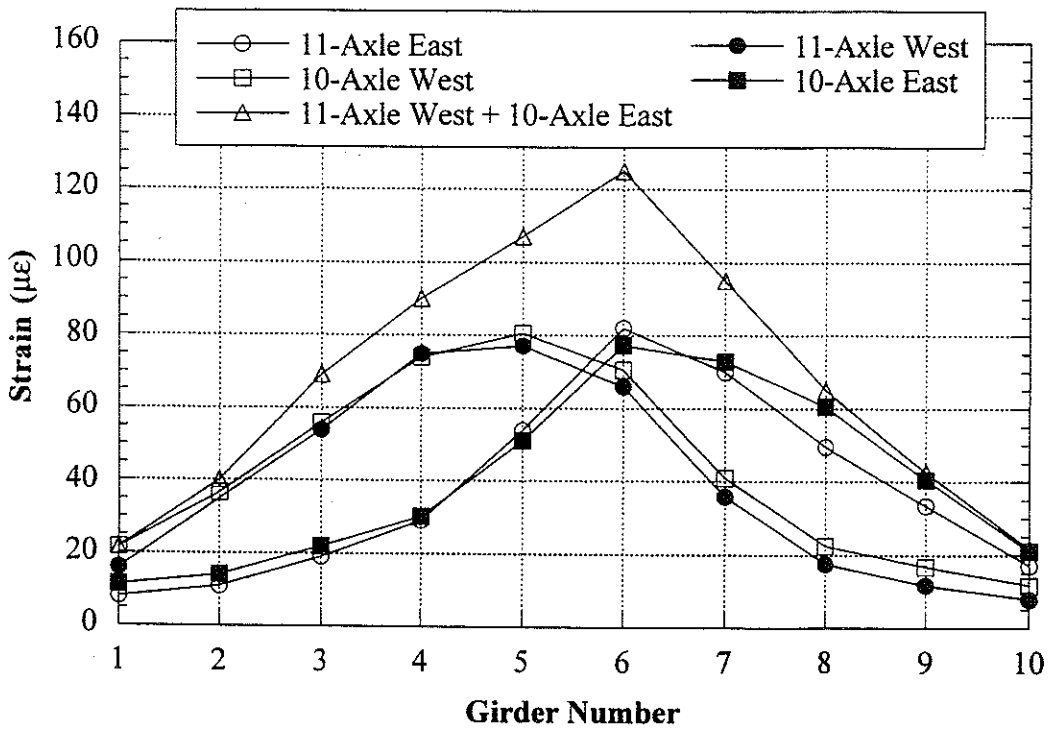


Figure 5.13 Strains under High Speed Trucks.

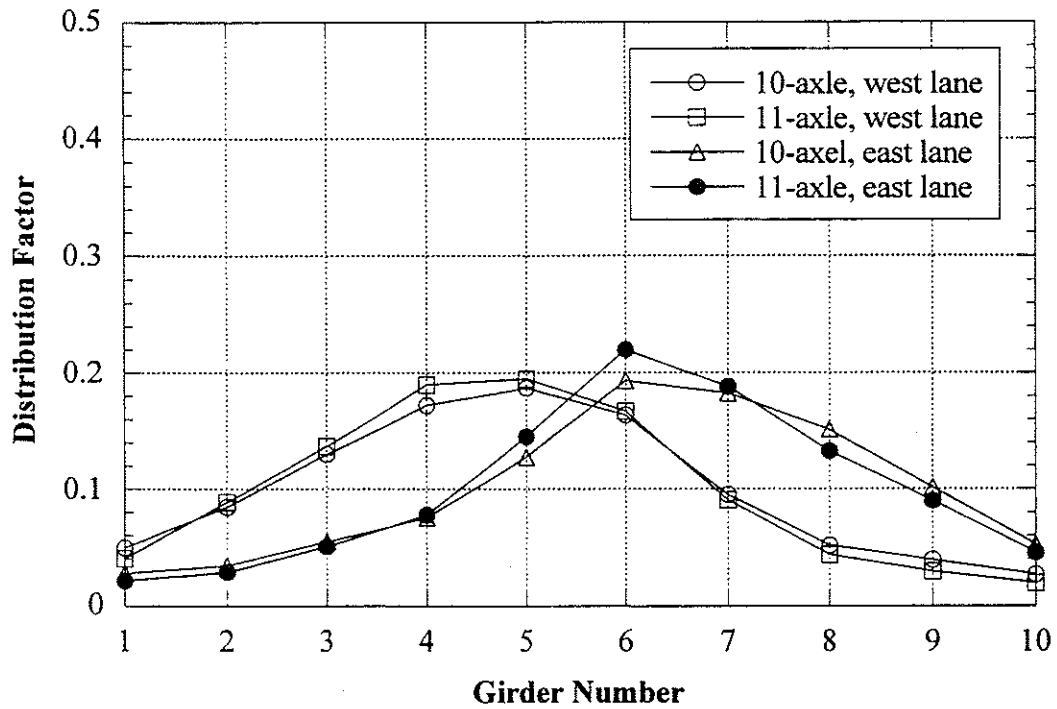


Figure 5.14 Distribution Factors for One Truck Loading at High Speed.

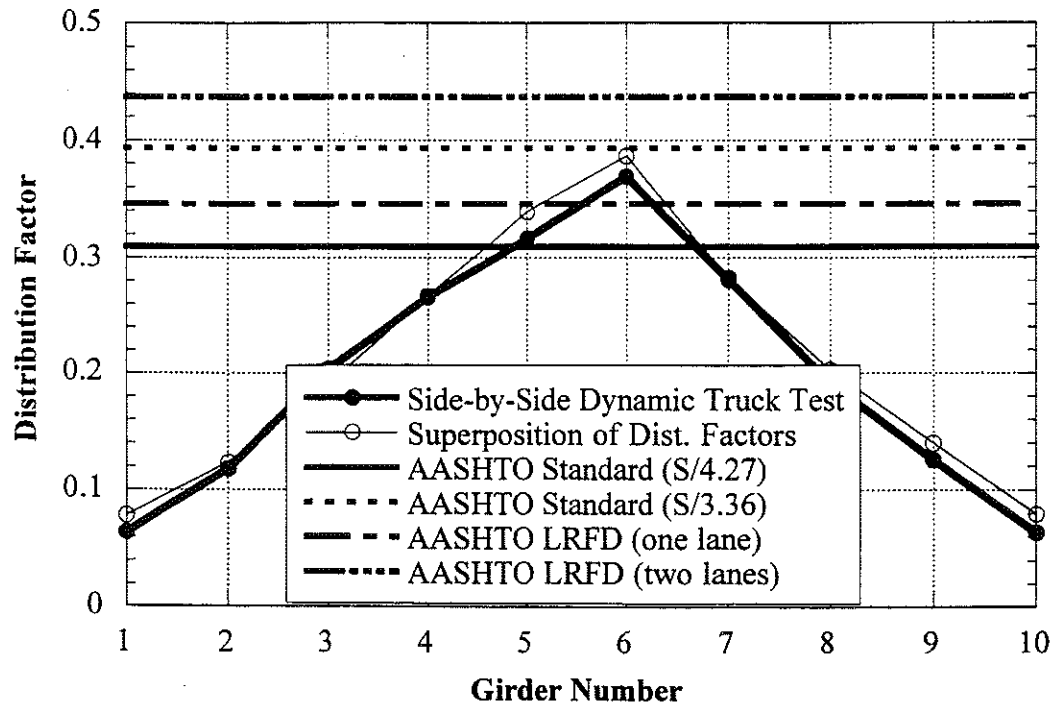


Figure 5.15 Comparison with Code Specified Distribution Factors at High Speed.

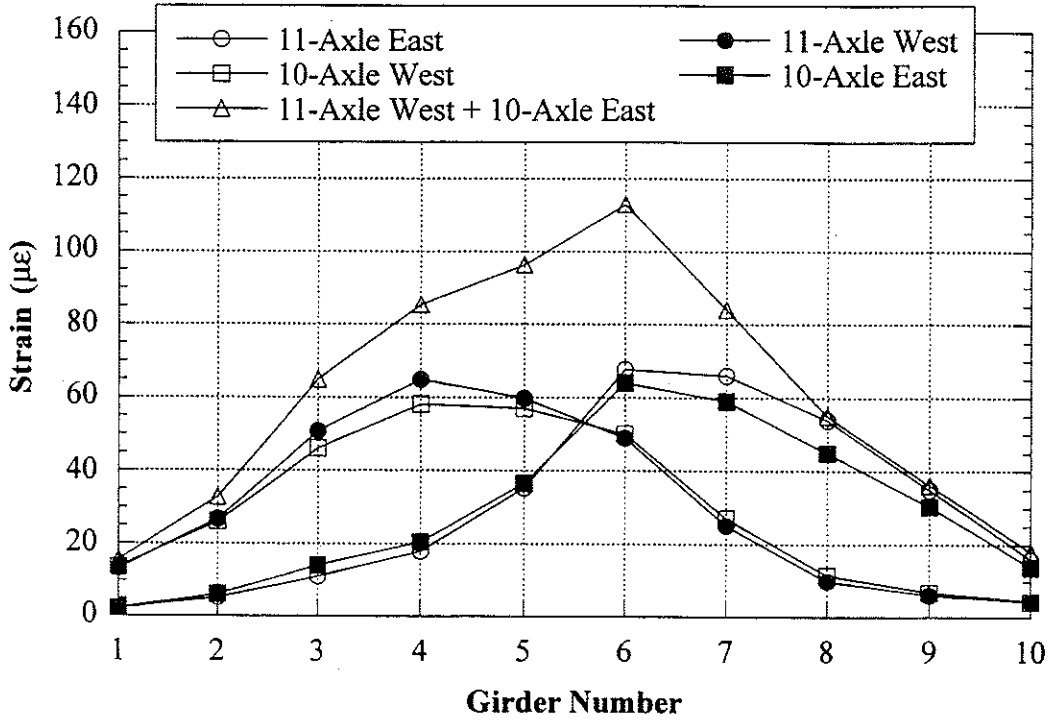


Figure 5.16 Static Strains for Impact Factors.

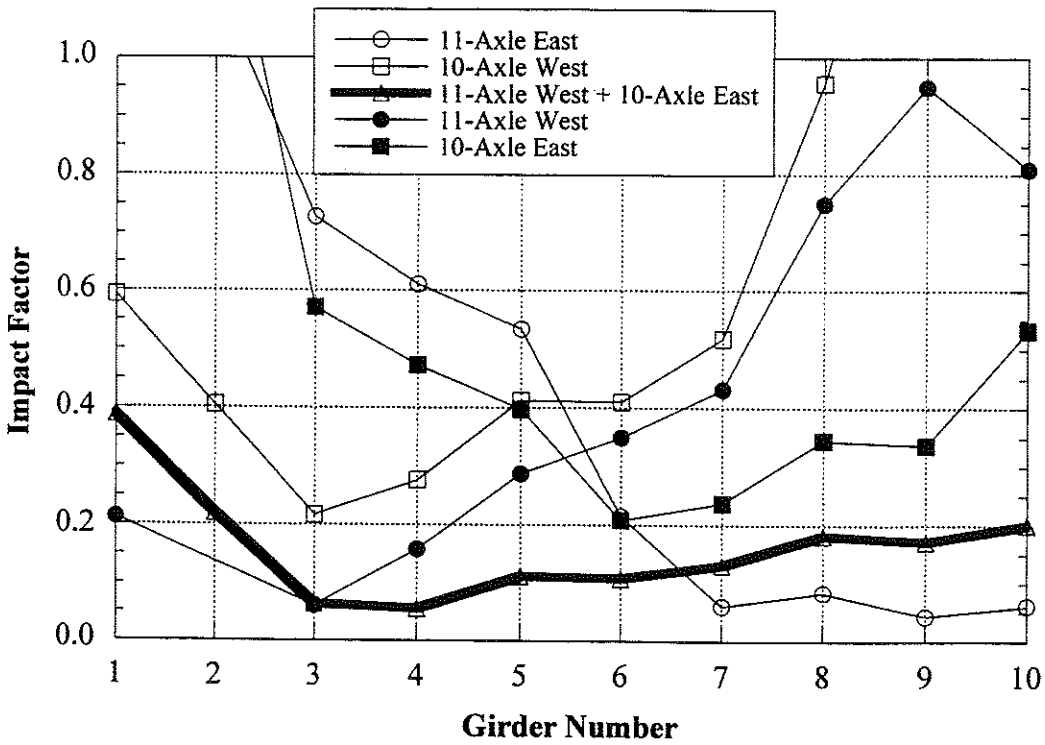


Figure 5.17 Impact Factors.

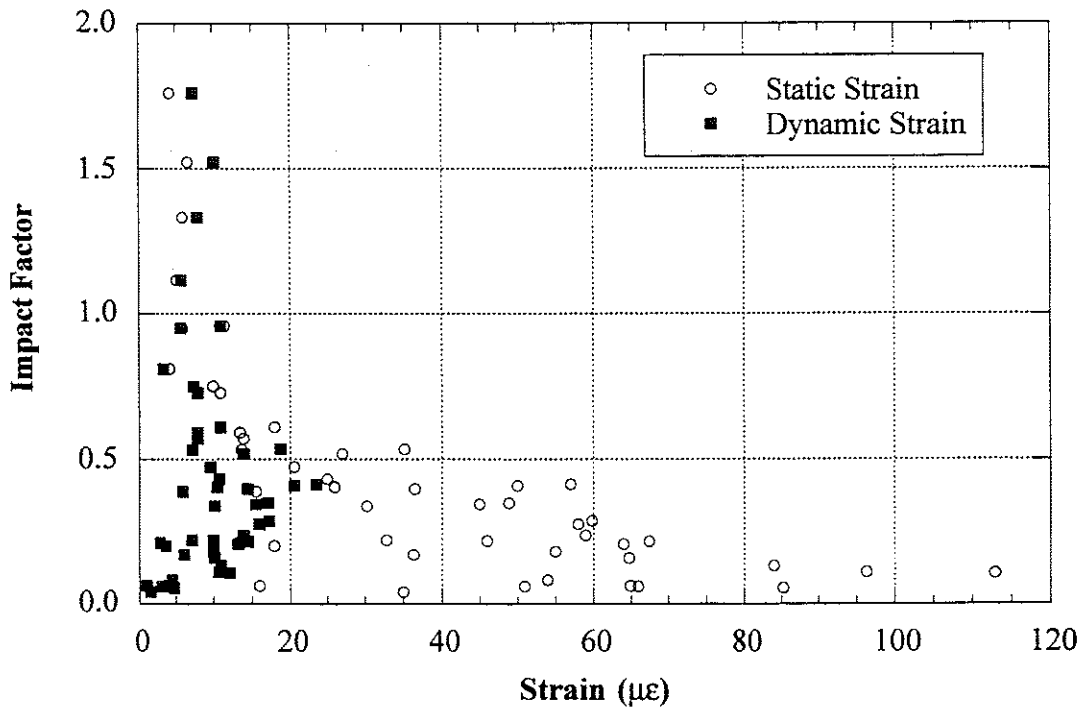


Figure 5.18 Strain versus Impact Factors.

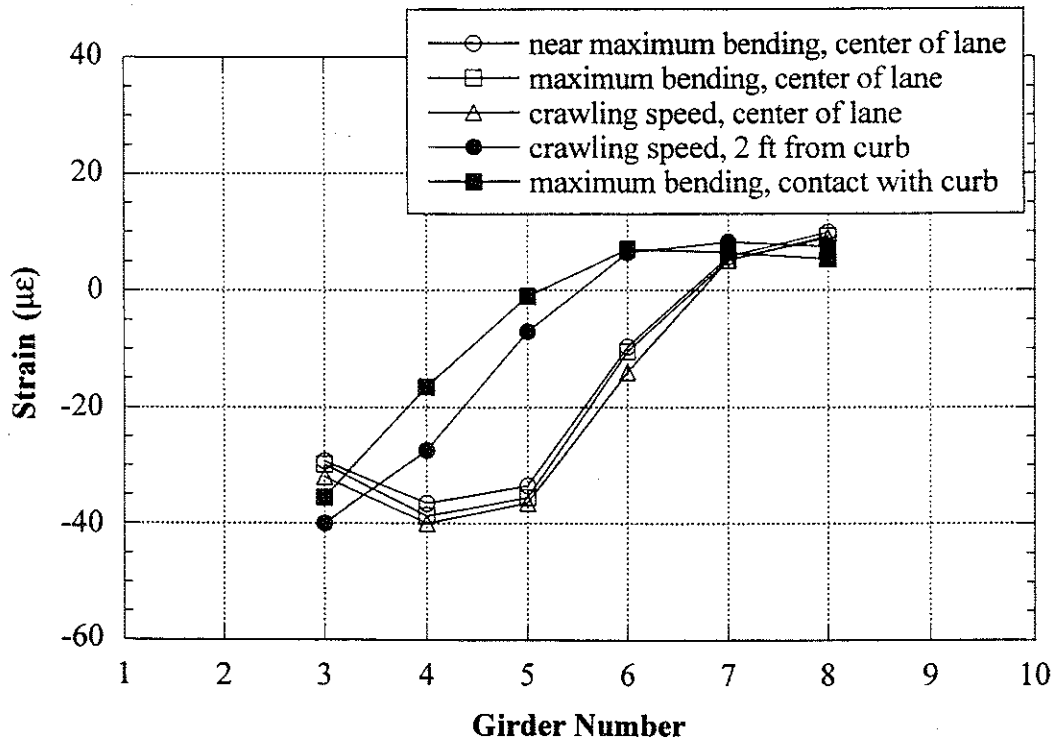


Figure 5.19 West Lane, 11-Axle Truck, Static Loading, Support.

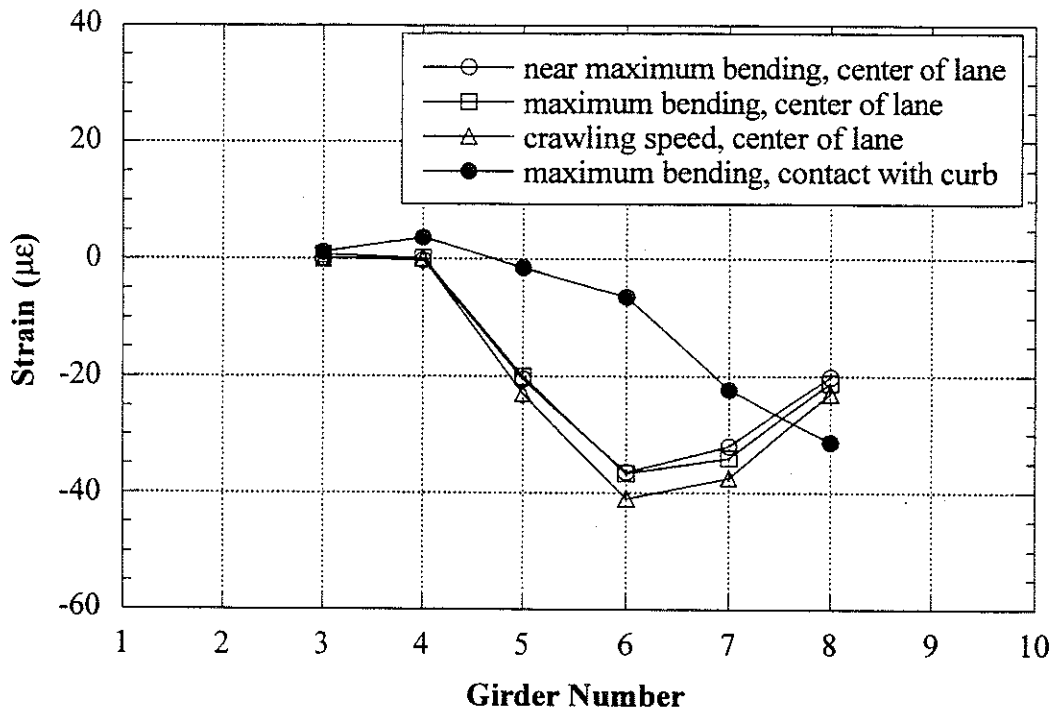


Figure 5.20 East Lane, 11-Axle Truck, Static Loading, Support.

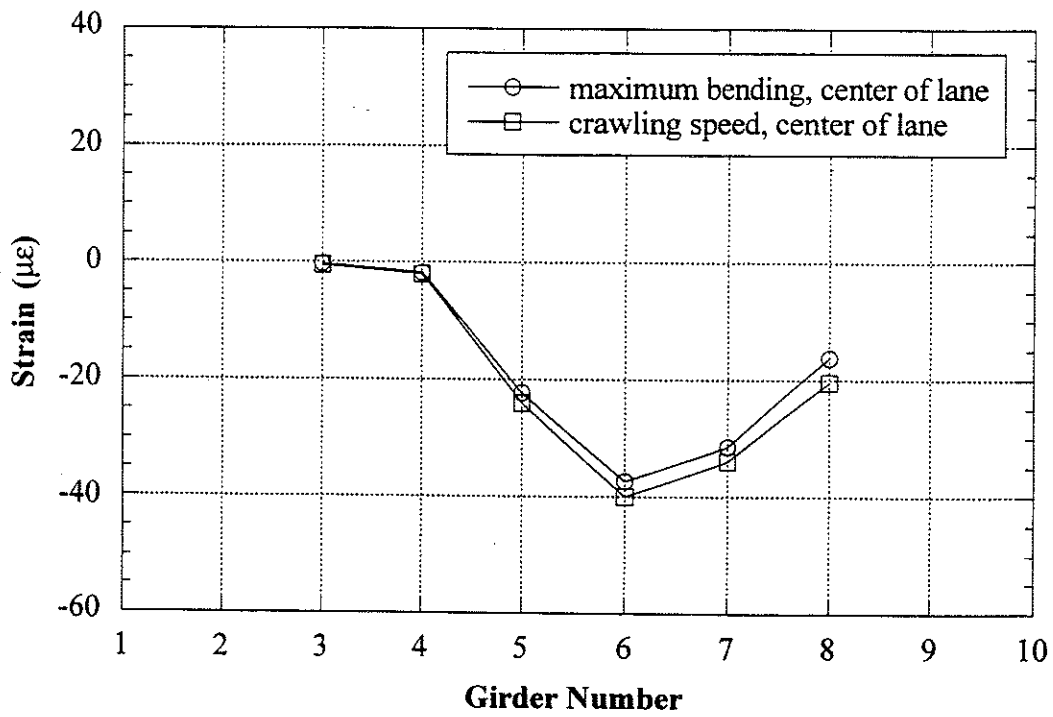


Figure 5.21 East Lane, 10-Axle Truck, Static Loading, Support.

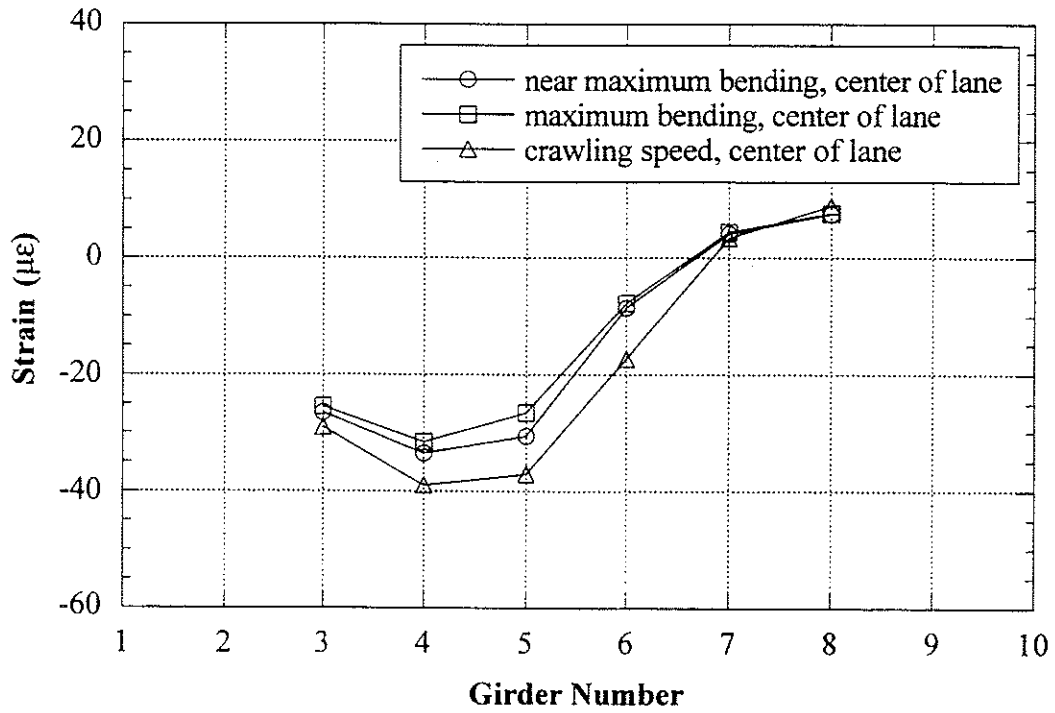


Figure 5.22 West Lane, 10-Axle Truck, Static Loading, Support.

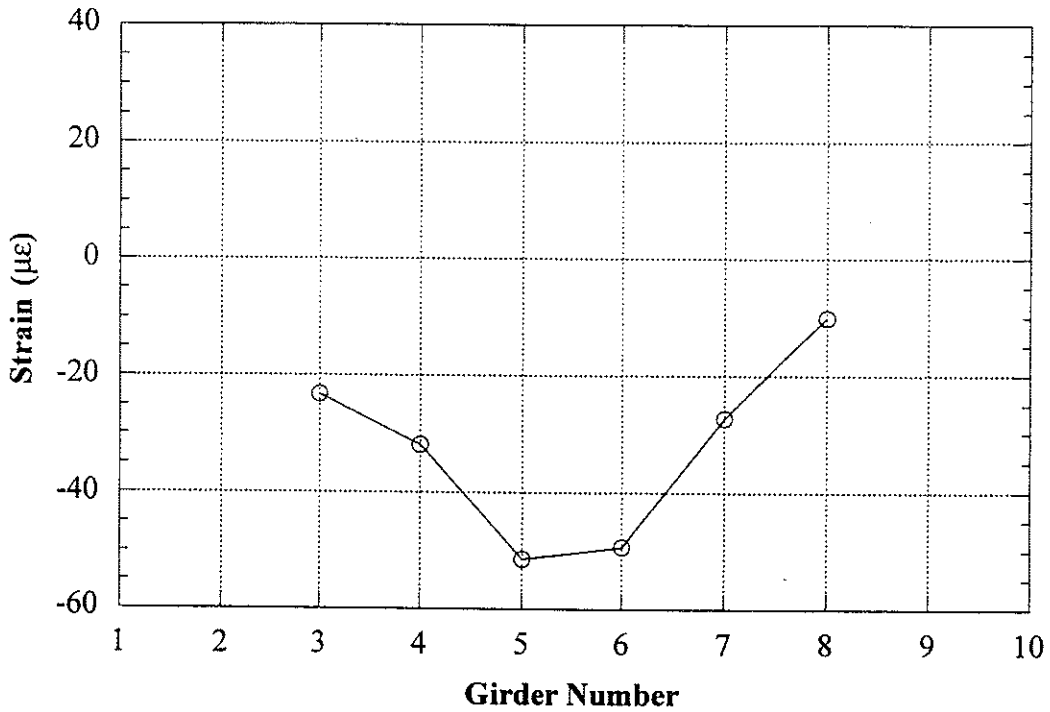


Figure 5.23 Side-by-Side Static Loading, Center of Lane, 10-Axle in West Lane, 11-Axle in East Lane, Support.

Note:

Intentionally left blank

6. Bridge on M-34 over South Branch of Raisin River in Adrian (B05-46041, M34/RR)

6.1 Description

This bridge was built in 1932 and is located over South Branch of Raisin River in Adrian, Michigan. This bridge is designated as M34/RR and was identified by the road over the bridge and the river under the bridge. It has one lane in each direction and carries state highway M-34. As shown in Figure 6.1, it has eleven steel girders spaced at 1.41 m to 1.46 m. It is a simply supported single span structure and was designed to be noncomposite. The total span length is 16.8 m without skew. The bridge is near traffic lights and the speed limit is 48 km/h. Although the approach to the bridge showed slight cracks, both the deck slab and the approach to the bridge were in good condition. The bridge has a load rating of 694 kN. The thickness of slab is 152 mm, with a 76 mm concrete wearing surface.

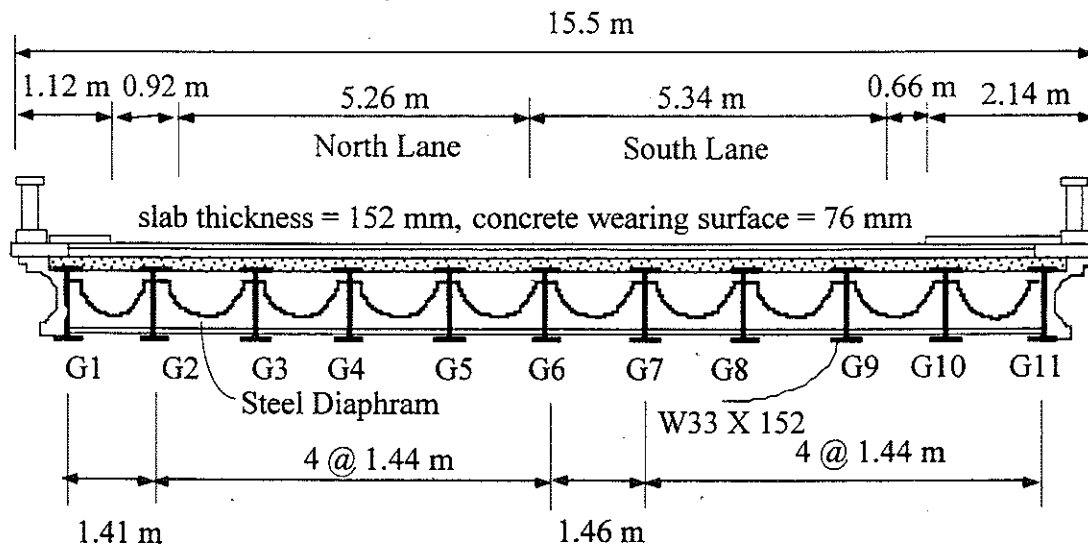


Figure 6.1 Cross-Section of Bridge M34/RR in Adrian.

6.2 Instrumentation

Strain transducers were installed on the bottom flanges of girders in the middle of the span and close to the support (Figure 6.2). The bridge test was performed on July 22, 1997.

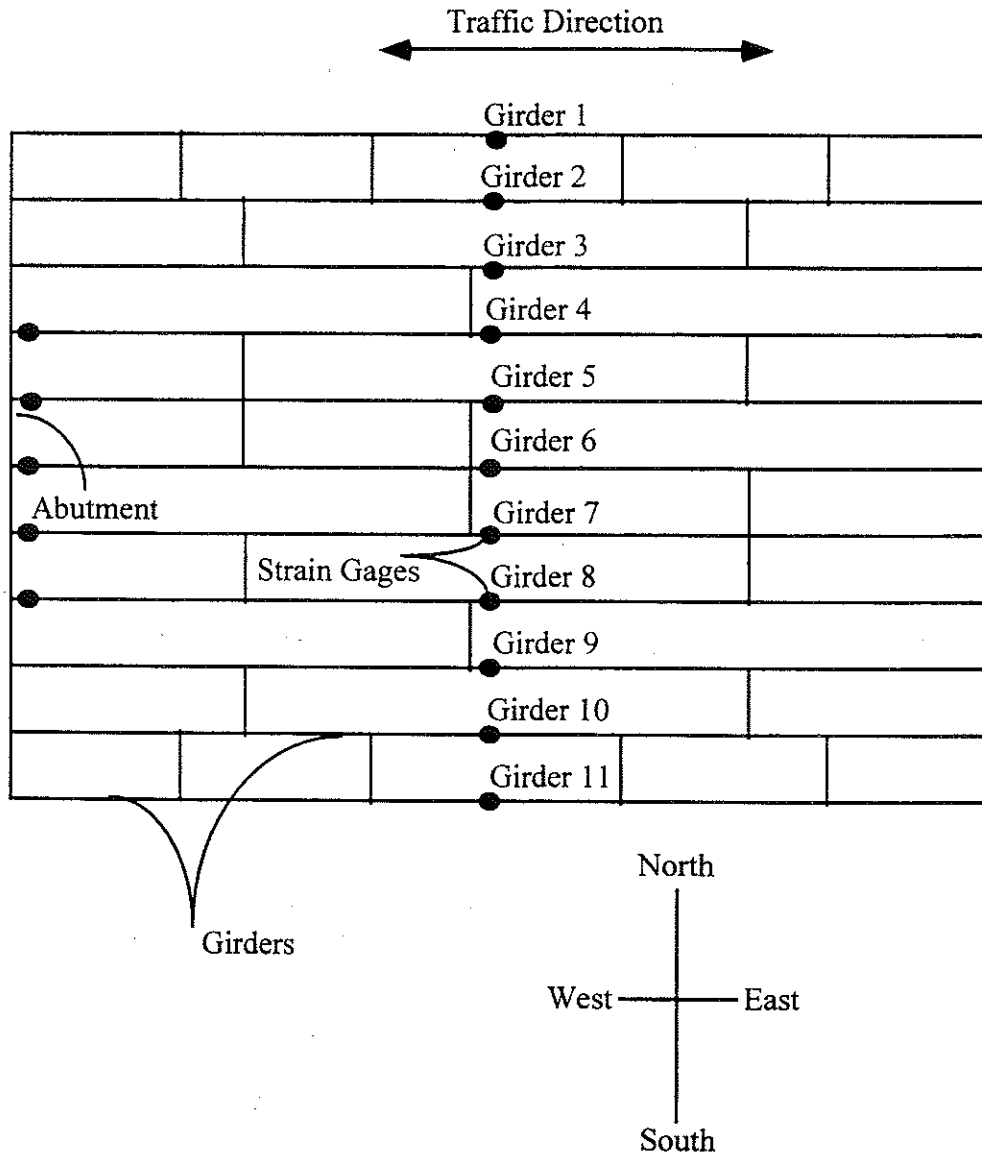


Figure 6.2 Strain Transducer Locations in Bridge M34/RR in Adrian.

6.3 Truck Loads

Strain data necessary to calculate girder distribution and impact factors were taken from the mid-span transducers. The data were obtained under passes of 10-axle and 11-axle three-unit trucks with known weights and configurations. The ten-axle and 11-axle trucks have gross weights of 580 kN and 637 kN, with wheelbases of 14.3 m and 15.6 m respectively. Truck configurations are shown in Figures 6.3 and 6.4.

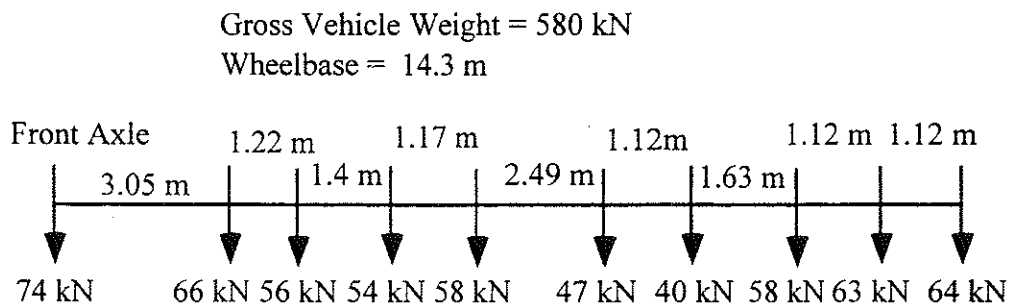


Figure 6.3 Ten-Axle Truck Configuration, Bridge M34/RR in Adrian.

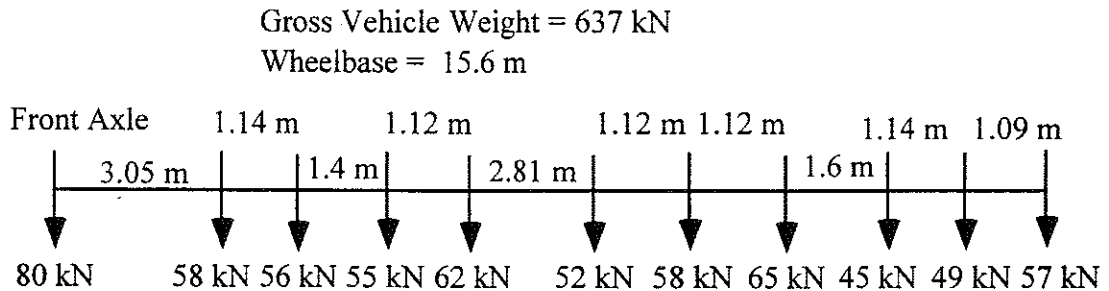


Figure 6.4 Eleven-Axle Truck Configuration, Bridge M34/RR in Adrian.

For the bridge carrying M-156 over Silver Creek in Morenci, the locations causing the analytical maximum bending moments were calculated and the trucks were statically placed at these positions. Because the strains obtained from the crawling speed tests were always greater than those which resulted from placing the trucks at the

calculated positions of maximum moment, bridge M34/RR was tested only under crawling speed and high speed. The following load combinations were performed during the tests:

at crawling speed,

- 11-axle truck along the center of north lane
- 11-axle truck close to the curb of north lane
- 10-axle truck along the center of north lane
- 10-axle truck close to the curb of north lane
- 11-axle truck along the center of south lane
- 11-axle truck close to the curb of south lane
- 10-axle truck along the center of south lane
- 10-axle truck close to the curb of south lane
- 10-axle truck along the center of south lane and 11-axle truck along the center of north lane
- 11-axle truck along the center of south lane and 10-axle truck along the center of north lane

at high speed, the maximum speed obtained by a test truck at a bridge site,

- 10-axle truck along the center of north lane, 48 km/h
- 11-axle truck along the center of north lane, 40 km/h
- 10-axle truck along the center of south lane, 56 km/h
- 11-axle truck along the center of south lane, 40 km/h
- 10-axle truck along the center of south lane and 11-axle truck along the center of north lane, 40 km/h
- 11-axle truck along the center of south lane and 10-axle truck along the center of north lane, 40 km/h

6.4 Load Test Results

As with the Morenci (M156/SC) bridge, strains from crawling-speed tests are considered static, and these were used to calculate girder distribution factors. Additional strains above the static values that were caused by high-speed tests are considered dynamic, and these were used to compute impact factors.

Figures 6.5 to 6.7 present the results of all crawling-speed (static) tests. Figures 6.5 to 6.6 present static strains and GDF's for one truck on the bridge. Figure 6.7 shows static strains and GDF's from side-by-side static load tests. GDF's are calculated from static strains using Eq. (3-4). Figure 6.7 also compares static strains obtained by superposing strains under one truck loading with those from side-by-side truck loading. They have practically the same values and again verify the superposition method used.

The maximum distribution factors from all cases in Figure 6.5 to 6.6 are presented in Figure 6.8, which represents the envelope of GDF's for one truck static loading. The maximum GDF's for one loaded lane were superimposed with the other to obtain GDF's for two-lane loading. The results are shown in Figure 6.9 together with the distribution factors from a side-by-side crawling-speed truck test.

In Figure 6.8, the results are taken as the maximum effect caused by the combination of two transverse truck positions in each lane; in the center of the lane, and near the curb. In contrast, Figure 6.9 shows the results when both trucks were in the same transverse position in their respective lanes. As expected, as the trucks are placed closer to the curbs, the GDF increases on the outside girders. The interior girders still experience a higher load effect, however. All measured GDF's are well below all AASHTO Code specified GDF's. Actual values of the term $K_g / (L_t^3)$ are used in calculation of Code specified GDF values.

Figures 6.10 and 6.11 present the dynamic strains obtained from high-speed tests. The distribution factors calculated from the dynamic strains using Eq. (3-4) are plotted and compared with Code specified GDF's in Figures 6.12 and 6.13.

From the corresponding static and dynamic strains from Figures 6.10 and 6.11, impact factors are calculated using Eq. (3-5) and presented in Figure 6.14. Similar to the Morenci bridge, the impact factors for exterior girders are large, due to a low static strain versus dynamic strain. But again, the absolute magnitude of dynamic strain at the exterior girders is low and is not significant. Figure 6.15 shows the relationship between strain magnitude and impact factors. For side-by-side truck loading, the impact factors do not exceed 10% at interior girders.

No significant strains at the supports were found, but a qualitative description of the results is as follows: At the beginning of the loading (when a truck begins to drive upon the span), small negative strains are induced, which indicates partial fixity of the supports. As the truck continues across the bridge, the negative strain values suddenly drop. This may indicate that the support fixity is released under heavy loads.

The measured static strains were compared to static strains calculated using the design stiffness and GDF's determined by tests in this study. The maximum observed static strain for this bridge is $64 \mu\epsilon$ for a single truck and $87 \mu\epsilon$ for two trucks side-by-side. The corresponding calculated strain for a single truck in a composite section is $148 \mu\epsilon$ and for a non-composite section it is $242 \mu\epsilon$. For two trucks side-by-side loading, the calculated strains are $201 \mu\epsilon$ and $328 \mu\epsilon$ for a composite section and a non-composite section, respectively.

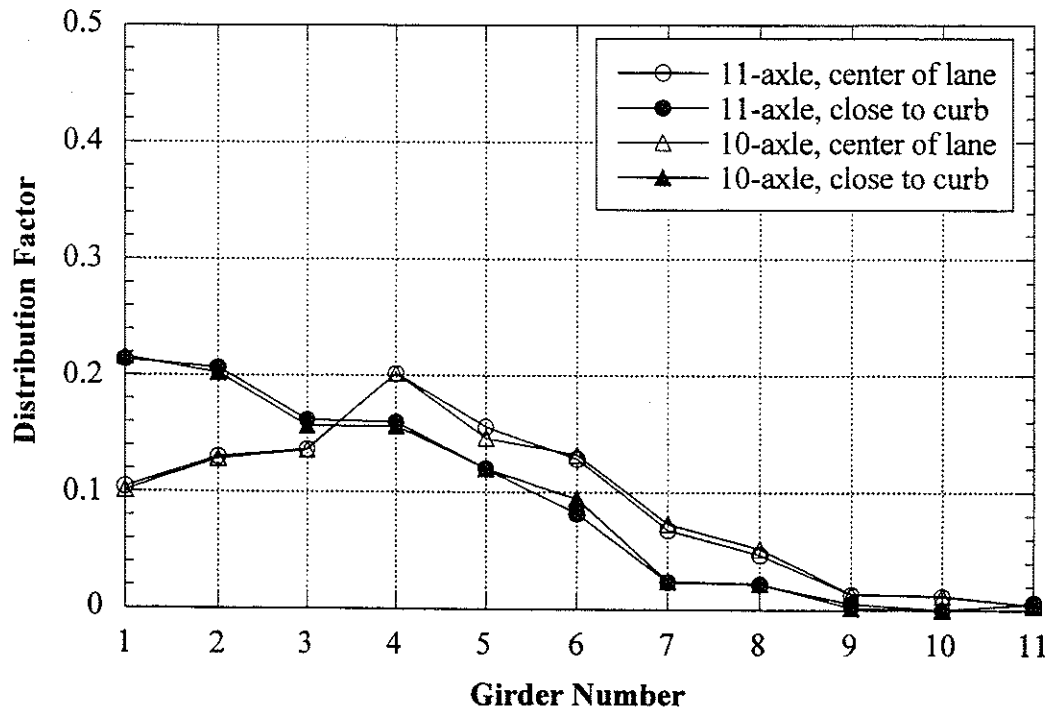
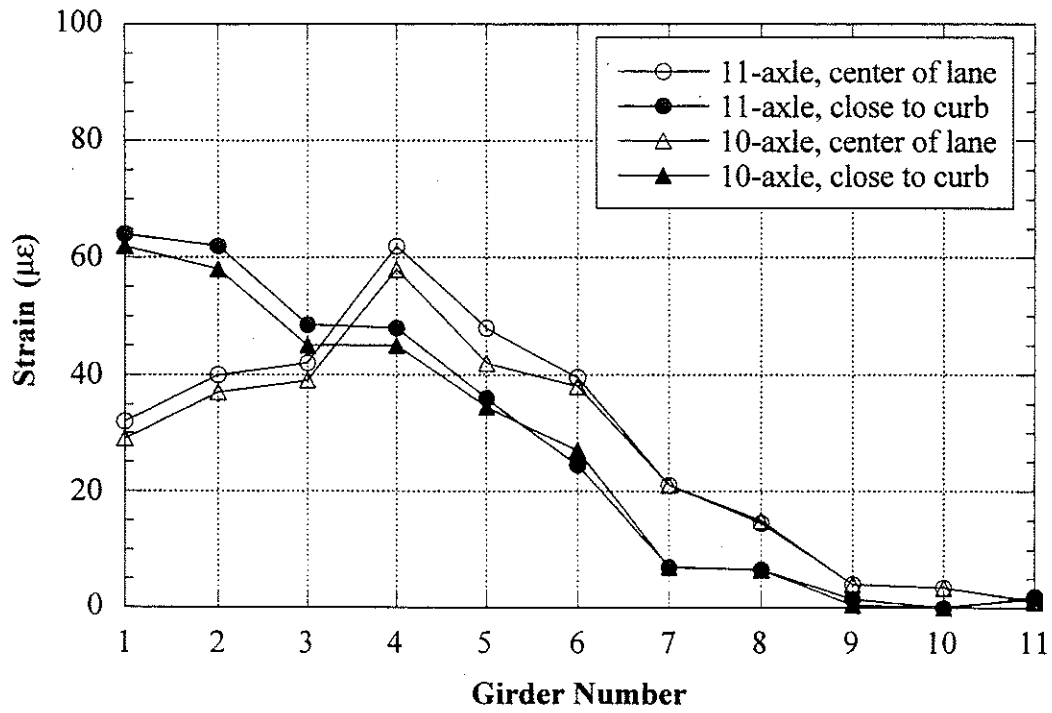


Figure 6.5 North Lane, Crawling Speed, Midspan.

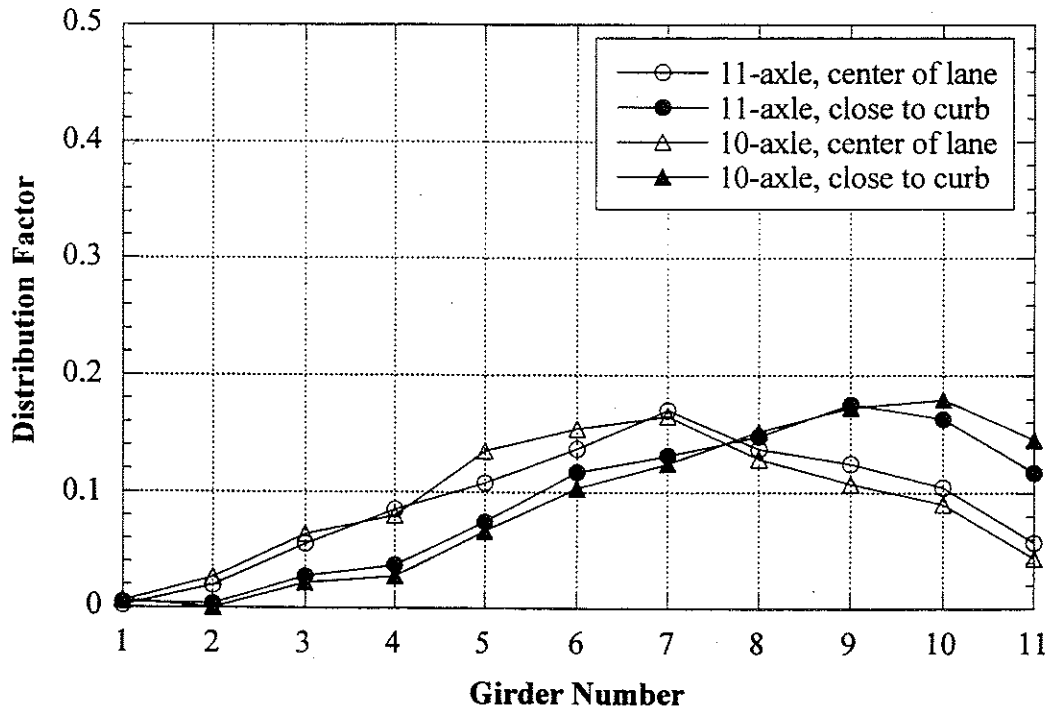
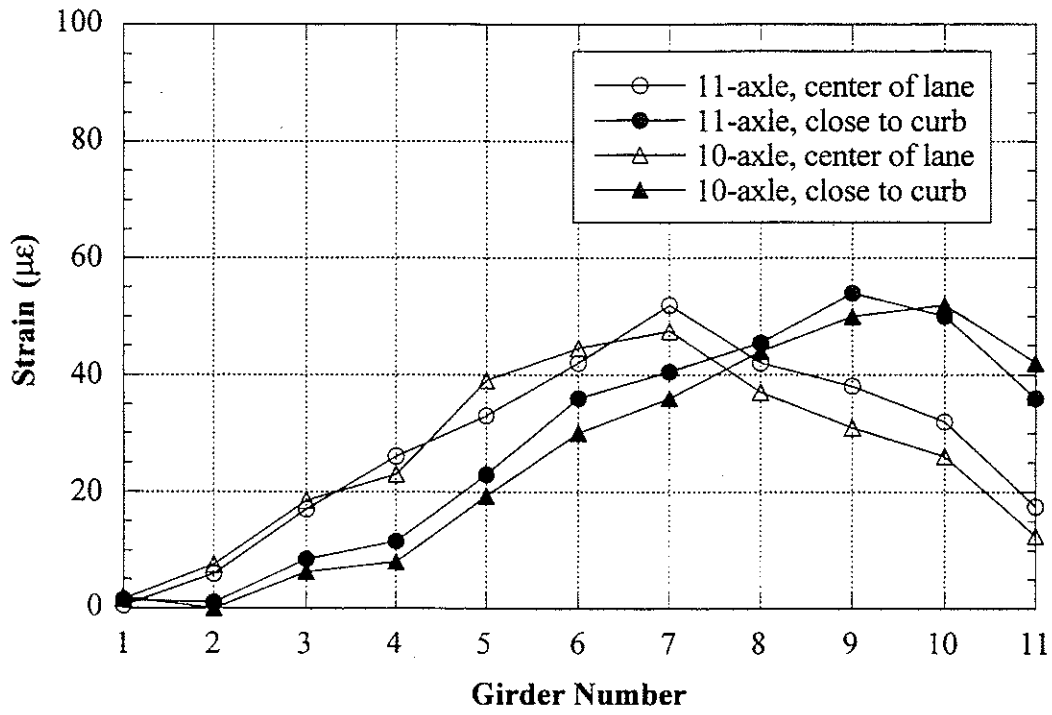


Figure 6.6 South Lane, Crawling Speed, Midspan.

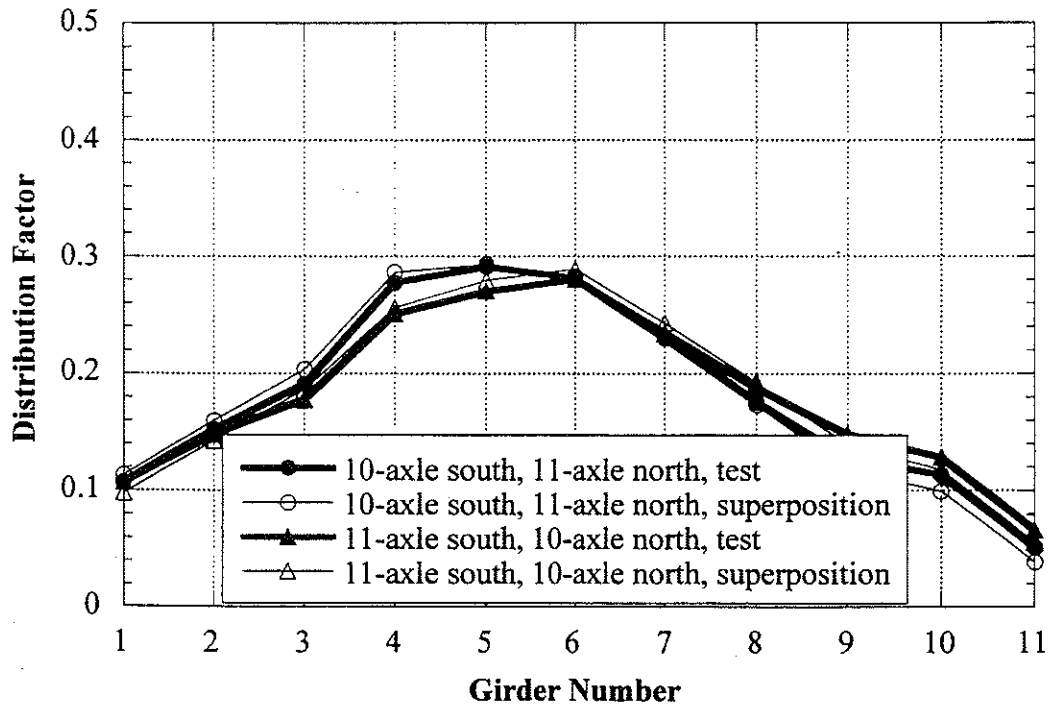
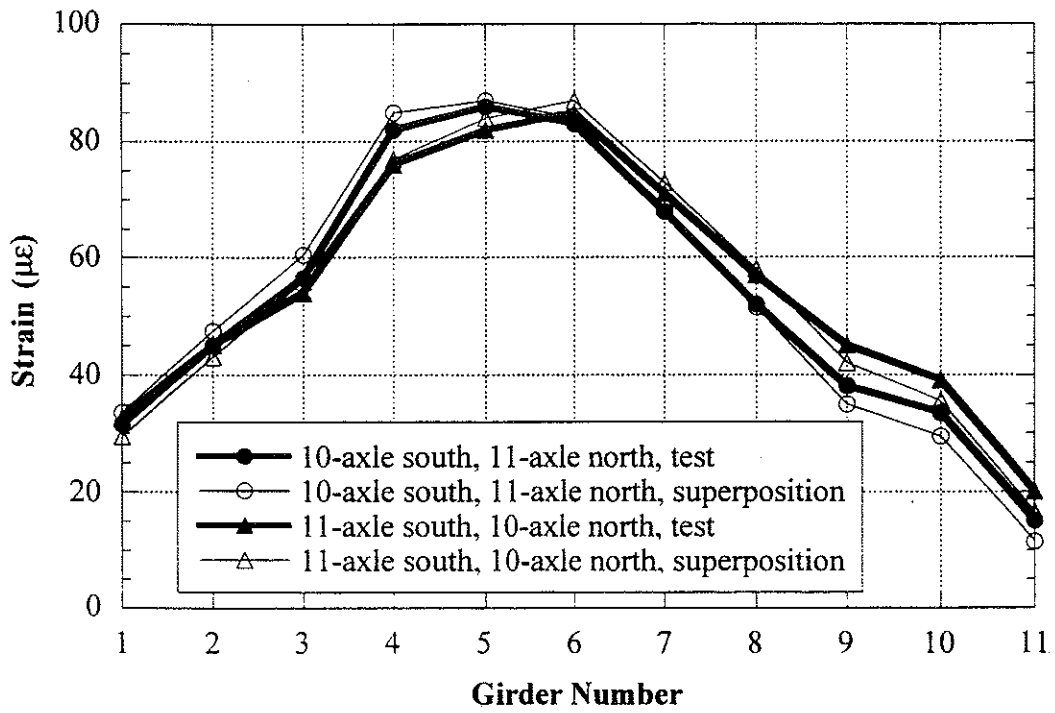


Figure 6.7 Side-by-Side Static Loading, Center of Lane, Midspan at Crawling Speed.

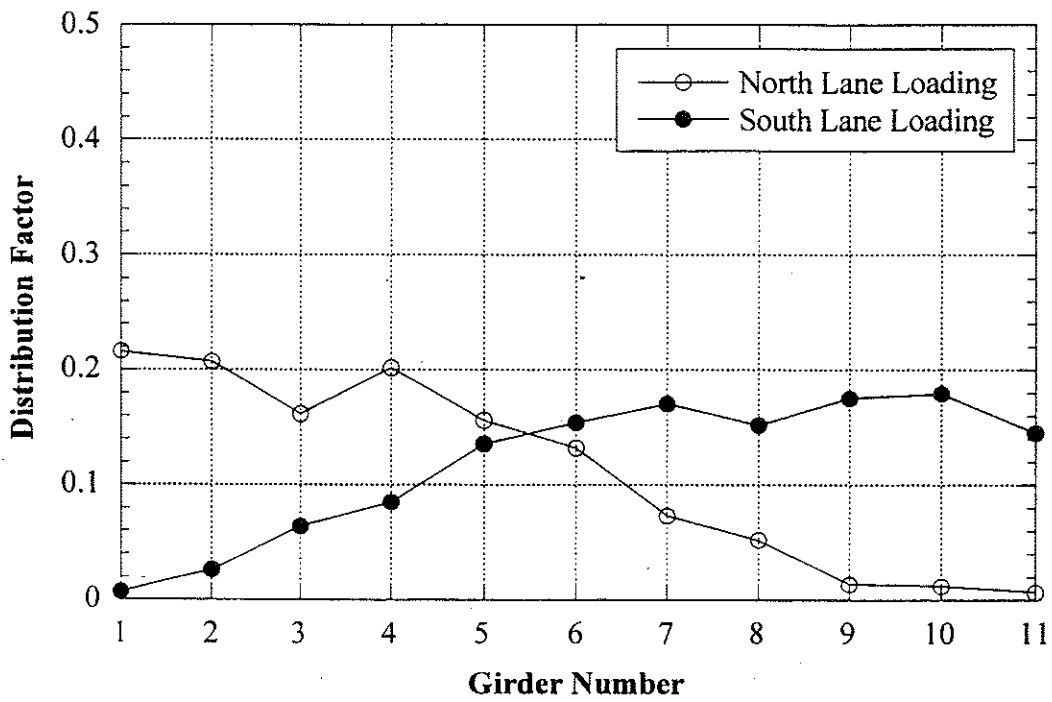


Figure 6.8 Envelope of Girder Distribution Factor For One Truck Static Loading, Crawling Speed.

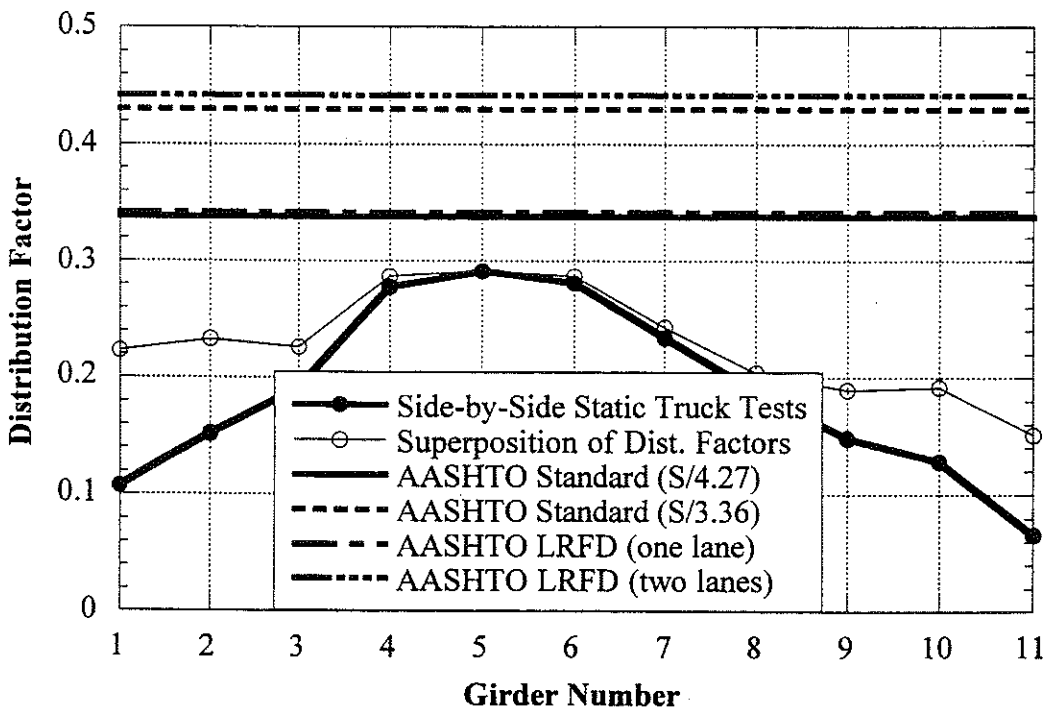


Figure 6.9 Comparison with Code Specified Distribution Factor at Crawling Speed.

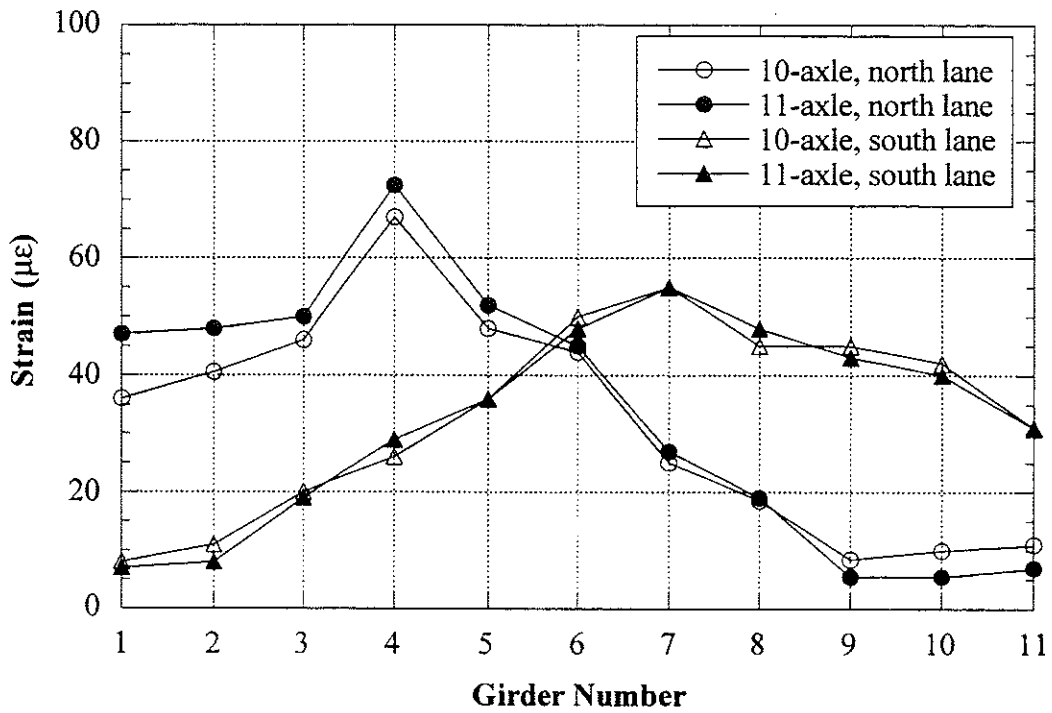


Figure 6.10 Strains under One Truck Loading at High Speed.

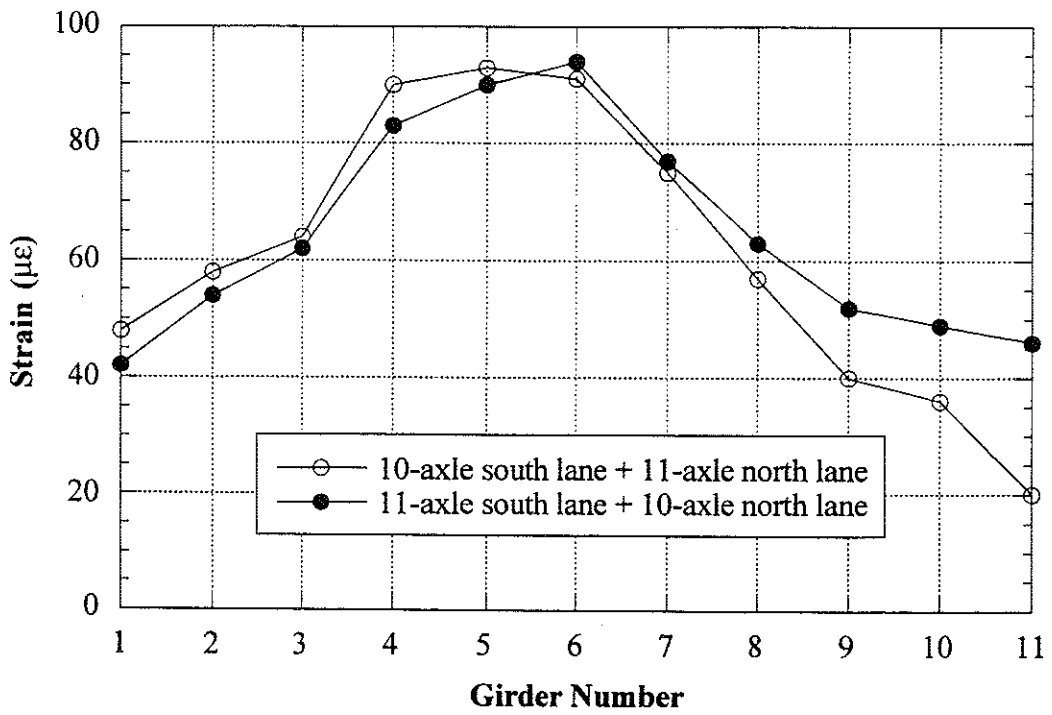


Figure 6.11 Strains under Side-by-Side Truck Loading at High Speed.

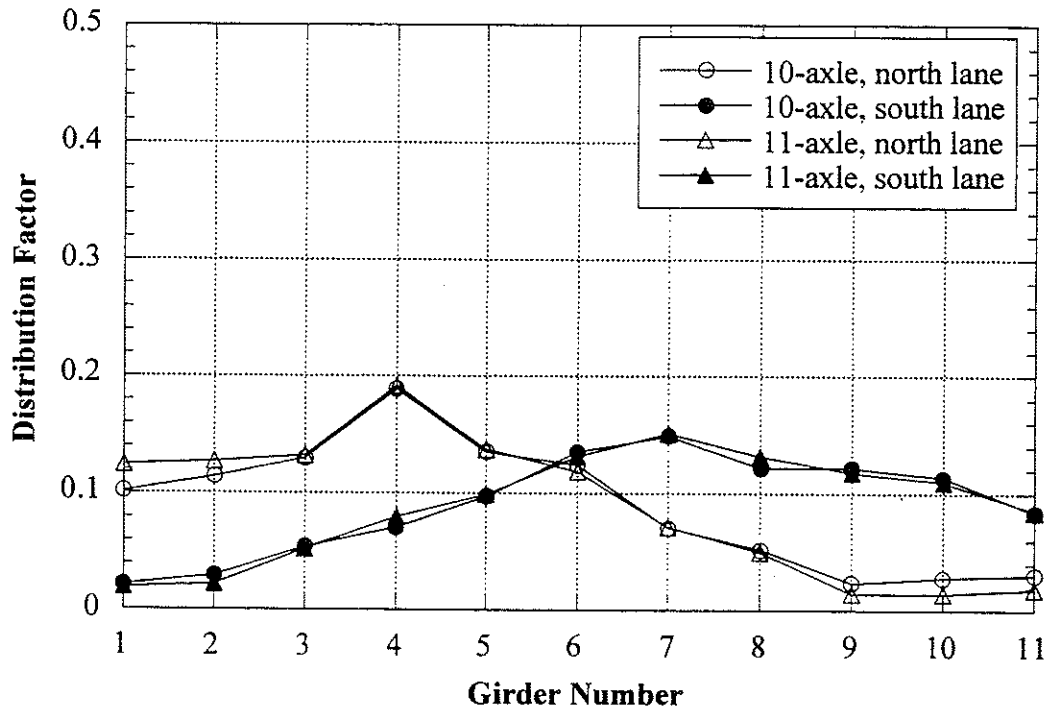


Figure 6.12 Distribution Factors for One Truck Loading at High Speed.

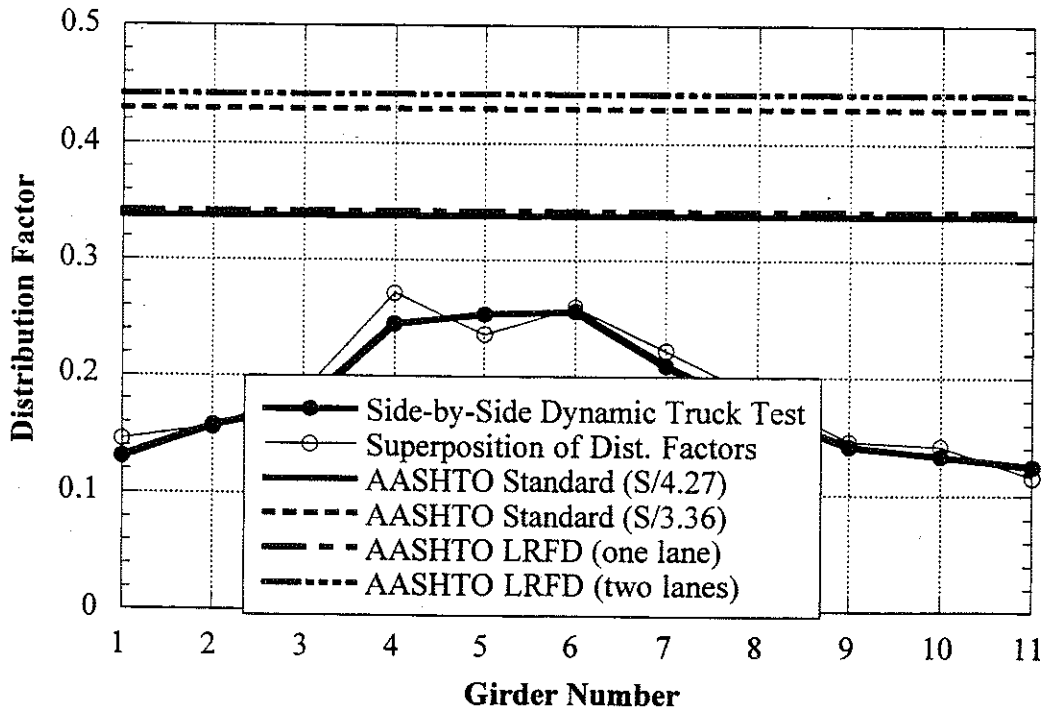


Figure 6.13 Comparison with Code Specified Distribution Factors at High Speed.

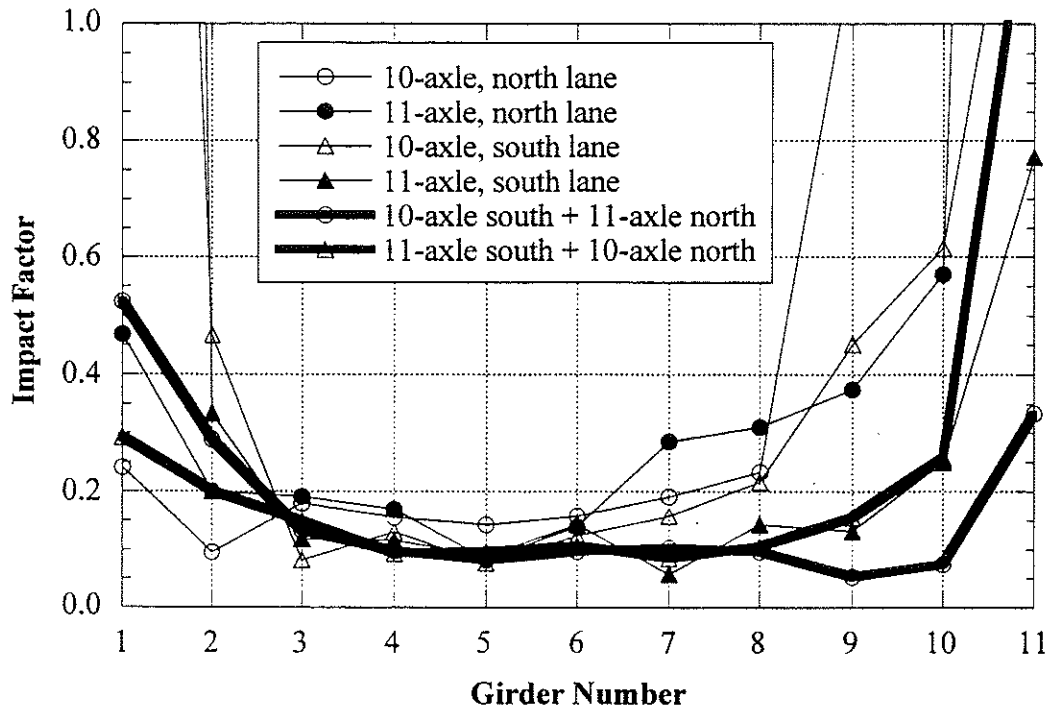


Figure 6.12 Impact Factors.

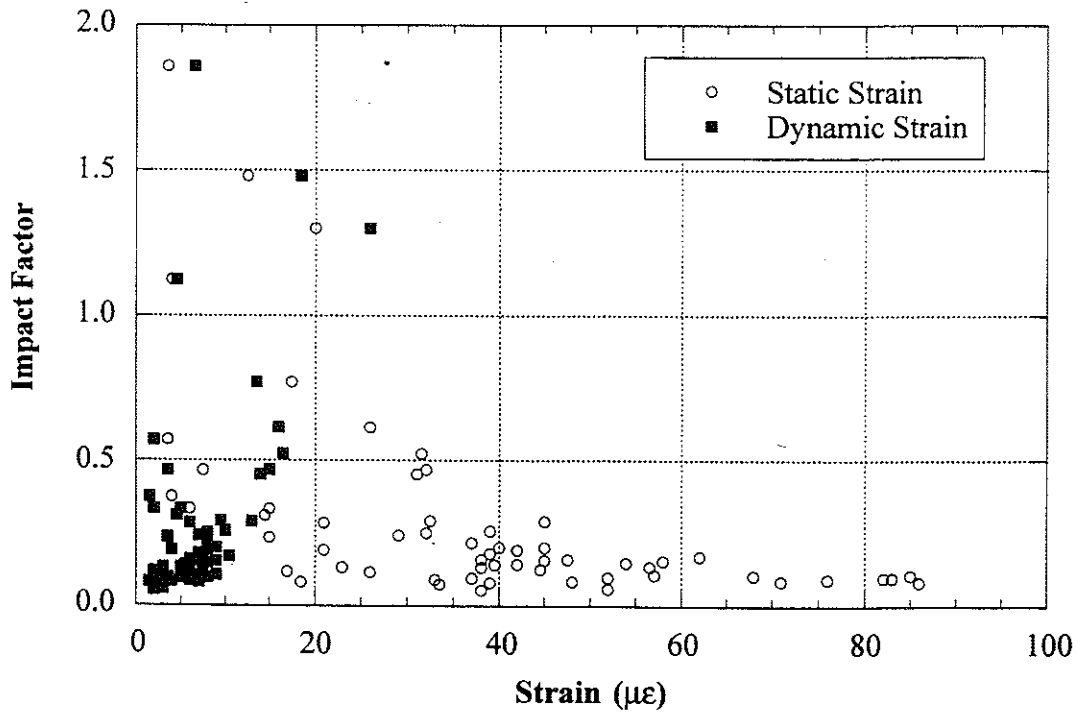


Figure 6.15 Strain versus Impact Factors.

Note:

Intentionally left blank

7. Bridge on US-12 over Swan Creek near Bronson (B02-12021, US12/SC)

7.1 Description

This bridge was built in 1922 and is located on US-12 over Swan Creek near Bronson, Branch County, Michigan. This bridge is designated as US12/SC and can be identified by the road carried by the bridge and the creek under the bridge. It has one lane in each direction. As shown in Figure 7.1, it has twelve steel girders spaced at 0.91 m to 1.39 m. The middle 6 girders were built in 1922. The remaining girders were added in 1932, along with additional abutments to support them. With these abutments, a large transverse beam was added that helps support the original girders near the bearings (see Figures. 7.1 and 7.2). The bridge is a simply supported single span structure and was designed to be noncomposite. The total span length is 11.7 m between the outside abutments (original abutments) with a skew of 10 degrees. The span length between the added abutments is 9.9 m. The supporting beam practically reduces the total span length from 11.7 m to 9.9 m. With the addition of the transverse beam, the middle six girders act as a three span continuous structure with a long main span (9.9 m) and very short end spans (see Figure 7.2). For structural calculations, a 9.9 m span length was used. The speed limit on the bridge is 72 km/h. Although the approach to the bridge showed slight cracks, both the deck slab and approach to the bridge were in good condition. The bridge has a load rating of 685 kN. The bridge has a 190 mm thick concrete slab, a 105 mm concrete wearing surface and a 50 mm asphalt overlay.

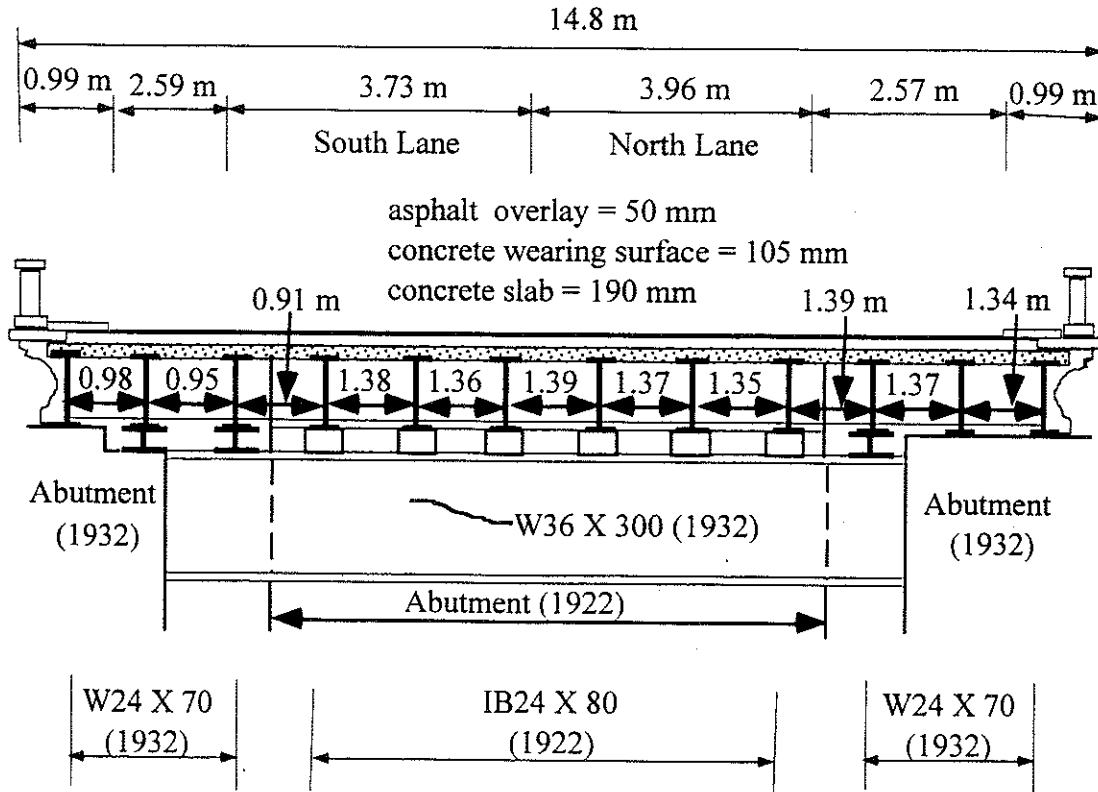


Figure 7.1 Cross-Section of Bridge US12/SC near Bronson, East Abutment View from West to East or West Abutment View from East to West.

7.2 Instrumentation

Strain transducers were installed on the bottom flanges of all girders in the middle of the span, and at the quarter points and close to the supports for girder 6 (Figure 7.2). LVDTs were installed on girders 2 to 11. The bridge test was performed on August 21, 1997.

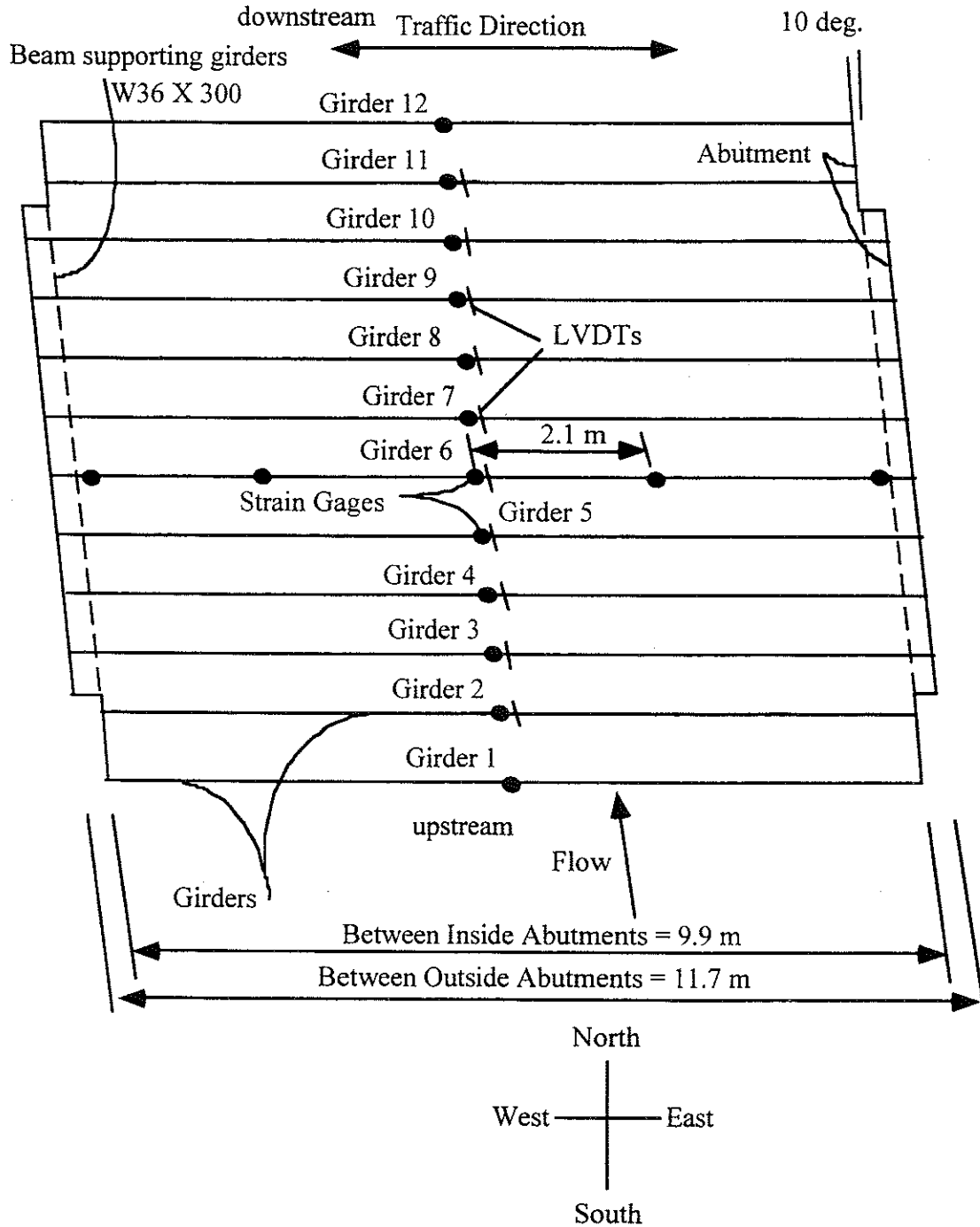


Figure 7.2 Strain and LVDT Transducer Locations in Bridge US12/SC near Bronson.

7.3 Truck Loads for Load Distribution Test

Both load distribution and proof load tests were performed on Bridge US12/SC. For the load distribution test, 10 and 11-axle trucks were used. For the proof load test, two M-60 military tanks were used.

Strain data necessary to calculate girder distribution and impact factors were taken from midspan transducers. The bridge was loaded with three-unit 10-axle and 11-axle trucks. The 10 and 11-axle trucks have gross weights of 573 kN and 640 kN, with wheelbases of 14.3 m and 15.6 m, respectively. Truck configurations are shown in Figures 7.3 and 7.4.

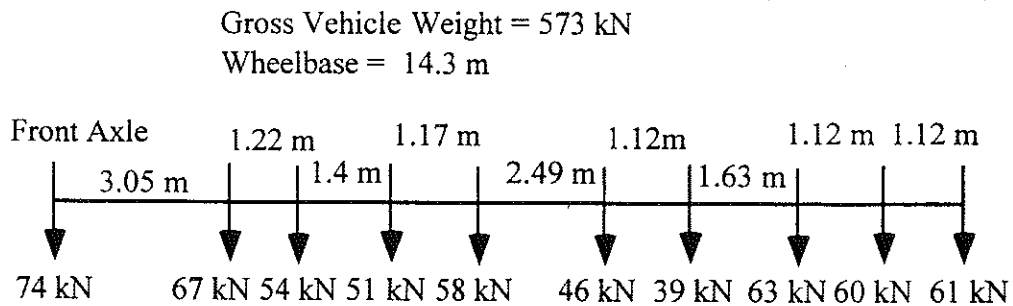


Figure 7.3 Ten-Axle Truck Configuration, Bridge US12/SC near Bronson

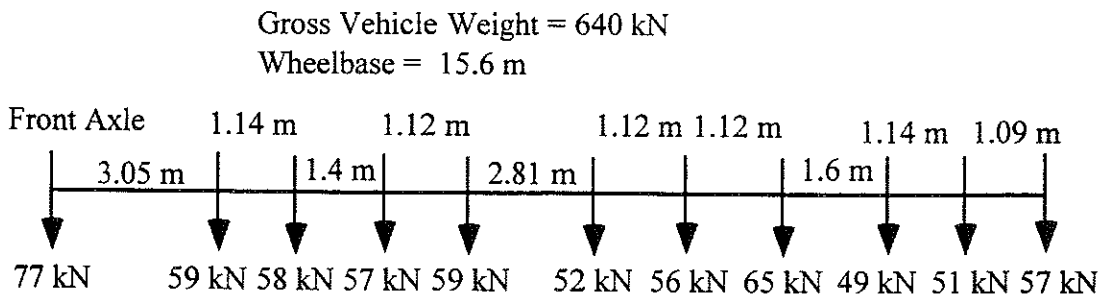


Figure 7.4 Eleven-Axle Truck Configuration, Bridge US12/SC near Bronson

This bridge was tested under crawling speed and full speed for the experimental derivation of load distribution and impact factors. The following load combinations were performed during the tests:

At crawling speed:

- 11-axle truck along the center of north lane
- 11-axle truck close to the curb of north lane
- 10-axle truck along the center of north lane
- 10-axle truck close to the curb of north lane
- 11-axle truck along the center of south lane
- 11-axle truck close to the curb of south lane
- 10-axle truck along the center of south lane
- 10-axle truck close to the curb of south lane
- 10-axle truck along the center of south lane and 11-axle truck along the center of north lane
- 11-axle truck along the center of south lane and 10-axle truck along the center of north lane

At high speed, the maximum speed obtained by the test trucks were:

- 10-axle truck along the center of north lane, 48 km/h
- 11-axle truck along the center of north lane, 48 km/h
- 10-axle truck along the center of south lane, 48 km/h
- 11-axle truck along the center of south lane, 45 km/h
- 10-axle truck along the center of south lane and 11-axle truck along the center of north lane, 42 km/h
- 11-axle truck along the center of south lane and 10-axle truck along the center of north lane, 42 km/h

7.4 Load Distribution Test Results

Strains from crawling-speed tests are considered static, and these were used to calculate girder distribution factors. Additional strains above the static values that were caused by high-speed tests are considered dynamic, and these were used to compute impact factors.

Figures 7.5 to 7.7 present the results of all crawling-speed (static) tests. Figures 7.5 to 7.6 present static strains and GDF's for one truck on the bridge. Figure 7.7 shows static strains and GDF's from side-by-side static load tests. GDF's are calculated from corresponding static strains using Eq. (3-4). Figure 7.7 also compares static strains obtained by superposing strains under one truck loading with those from side-by-side truck loading. They have practically the same values and again verify the superposition method used.

The maximum distribution factors from all cases in Figure 7.5 to 7.6 are presented in Figure 7.8, which represents the envelope of GDF's for one truck static loading. The maximum GDF's for one loaded lane were superimposed with the other to obtain GDF's for two-lane loading. The results are shown in Figure 7.9 together with the distribution factors from a side-by-side crawling-speed truck test.

In Figure 7.8, the results are taken as the maximum effect caused by the combination of two transverse truck positions in each lane; in the center of the lane, and near the curb. In contrast, Figure 7.9 shows the results when both trucks were in the same transverse position in their respective lanes. As expected, as the trucks are placed closer to the curbs, the GDF increases on the outside girders. The interior girders still experience a higher load effect, however. All measured GDF's are well below the AASHTO Code specified values. Actual value of the term $K_g / (L t_s^3)$ is used in calculation of AASHTO LRFD GDF values.

Figures 7.10 to 7.12 show the static strain profile of girder 6 along the bridge length. Not all gages were working during the test, however,

so some data points are missing. Readings at the west supports show small negative strains, indicating partial support fixity in the case of north lane and side-by-side truck loading. For south lane loading, strain at the support is practically zero. In addition, the east supports seem to have less fixity than the west supports.

Figures 7.13 and 7.14 present the strains obtained from high-speed tests. The distribution factors calculated from the dynamic strains are plotted and compared with Code specified GDF's in Figures 7.15 and 7.16.

From the corresponding static and dynamic strains, impact factors are calculated using Eq. (3-5) and presented in Figure 7.17. As in previous tests, this bridge also shows large impact factors for exterior girders, due to a low static strain versus dynamic strain. And again, the absolute magnitude of dynamic strain at the exterior girders is low and is not significant. Figure 7.18 shows the relationship between strain magnitude and impact factors. For side-by-side truck loading, the impact factors do not exceed 10% at interior girders.

The measured static strains were compared to static strains calculated using the design stiffness and GDF's determined by tests in this study. The maximum observed static strain for this bridge is 42 $\mu\epsilon$ for a single truck and 71 $\mu\epsilon$ for two trucks side-by-side. The corresponding calculated strain for a single truck in a composite section is 94 $\mu\epsilon$ and for a non-composite section it is 181 $\mu\epsilon$. For two trucks side-by-side loading, the calculated strains are 124 $\mu\epsilon$ and 240 $\mu\epsilon$ for a composite section and a non-composite section, respectively.

For truck loading, only strains were measured during the test. However, deflections caused by the proof load tests were measured by LVDT's.

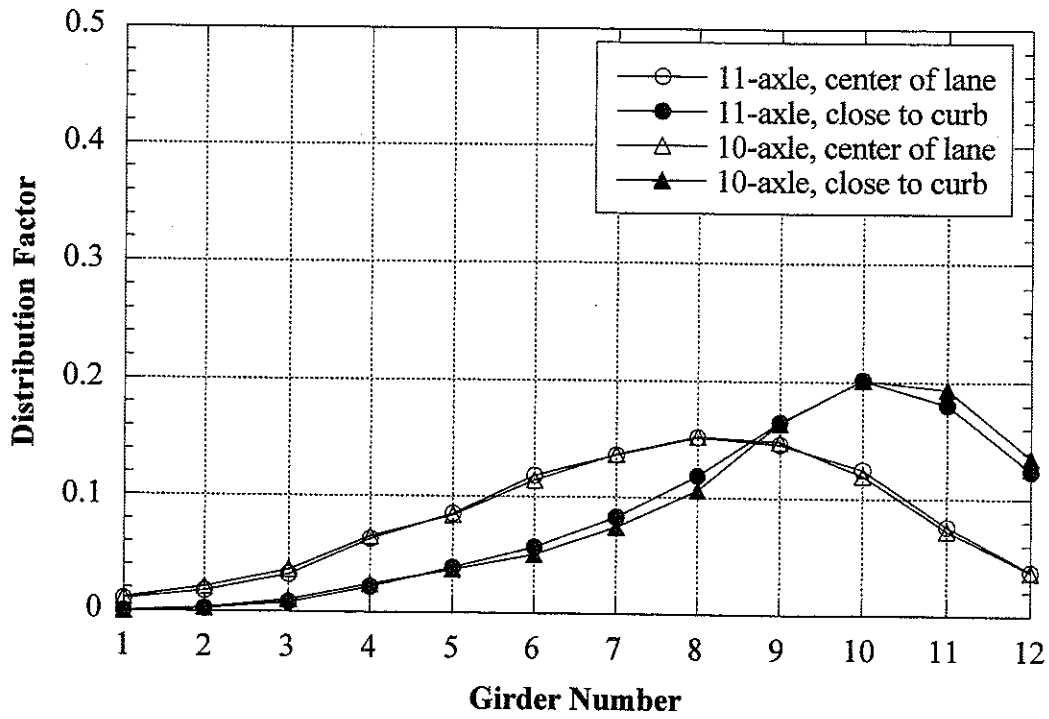
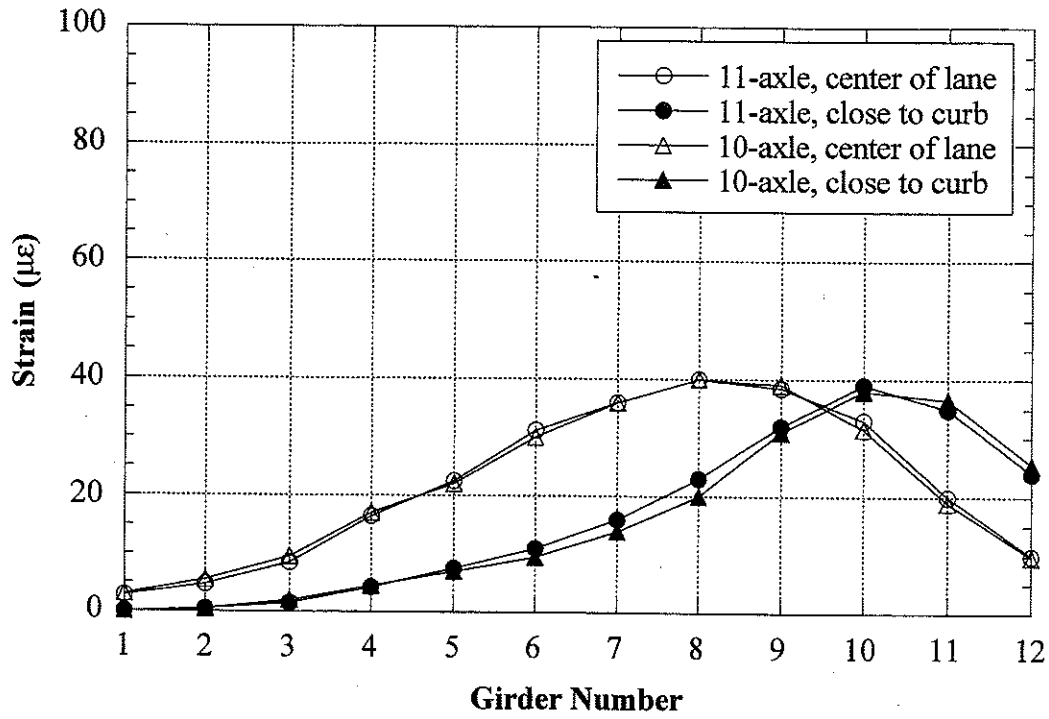


Figure 7.5 North Lane, Crawling Speed, Midspan.

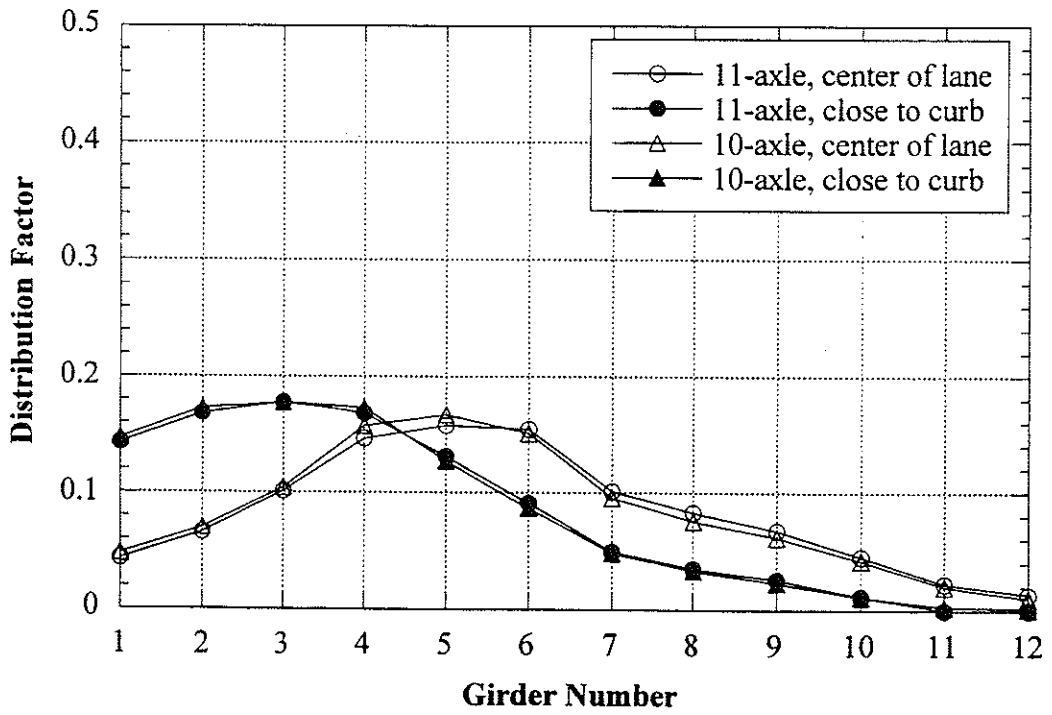
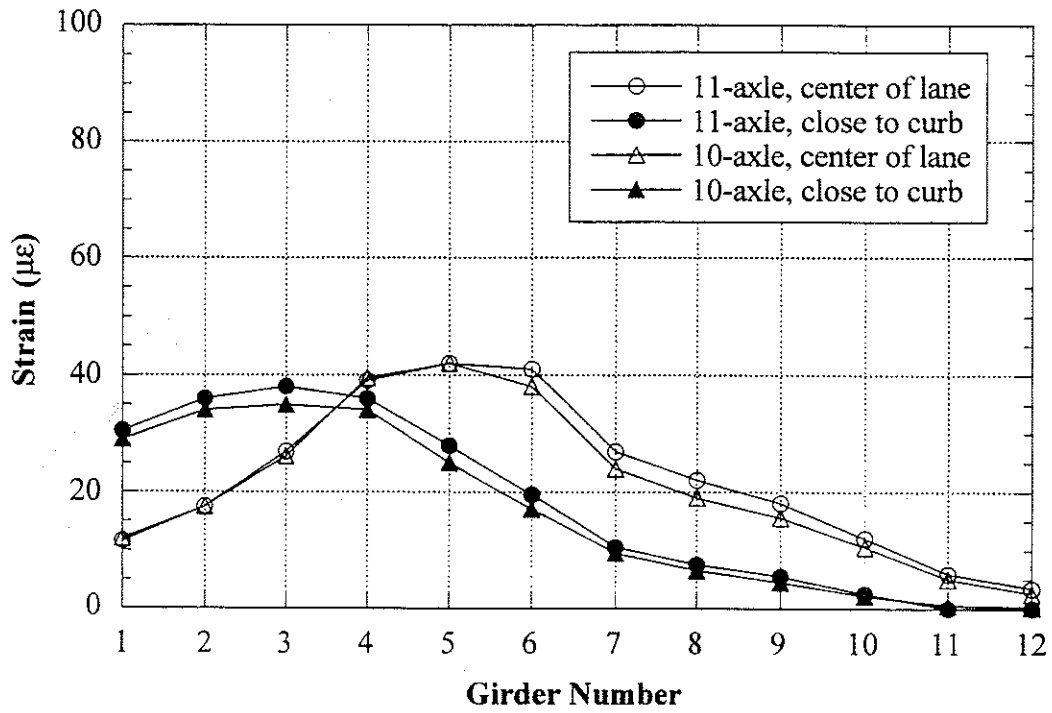


Figure 7.6 South Lane, Crawling Speed, Midspan.

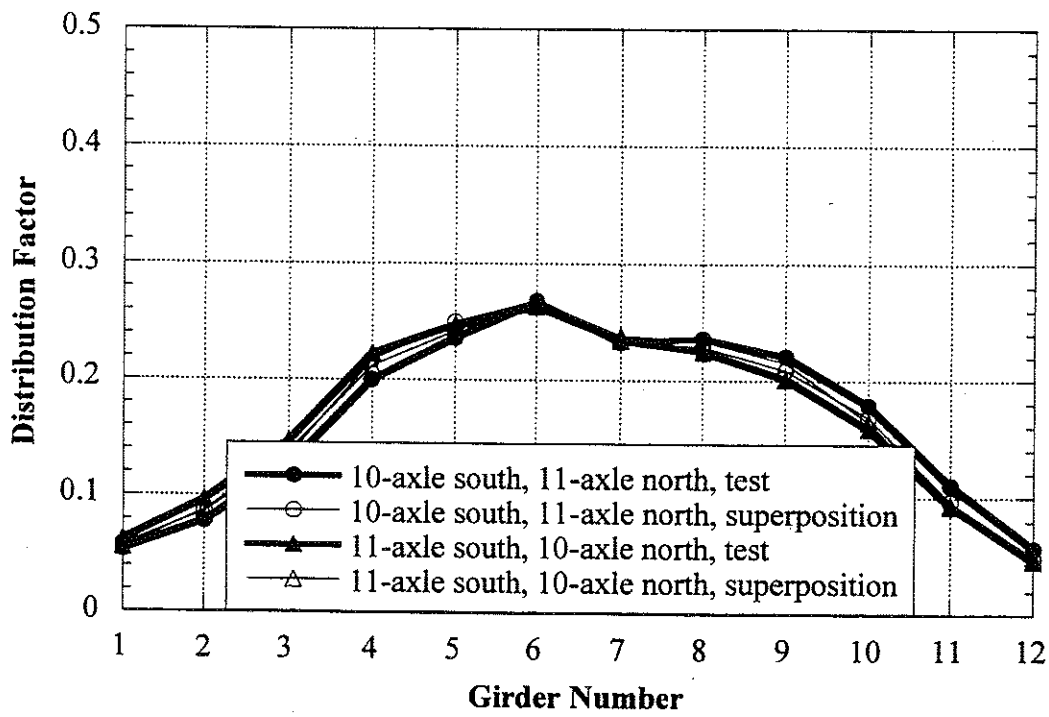
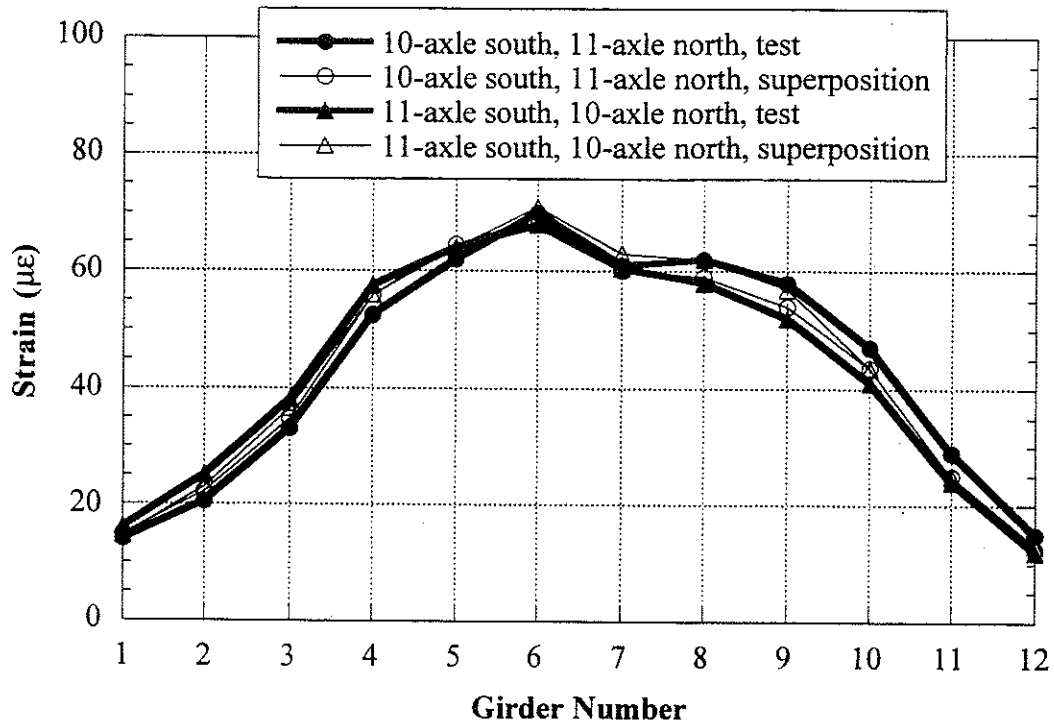


Figure 7.7 Side-by-Side Loading, Center of Lane, Crawling Speed Midspan.

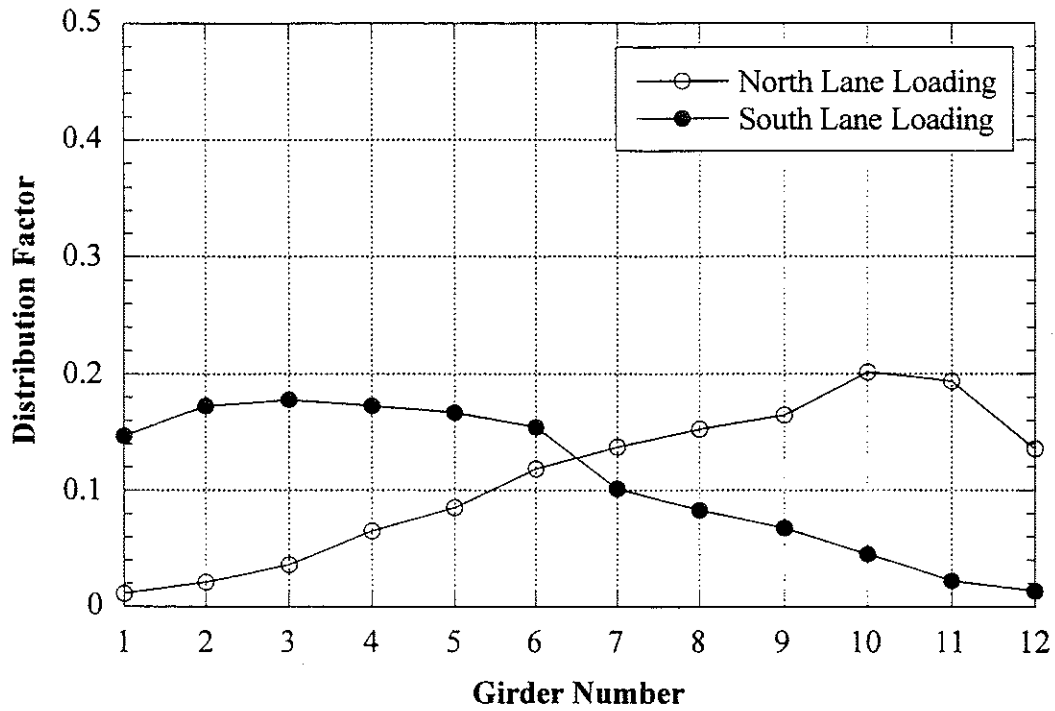


Figure 7.8 Envelope of Girder Distribution Factor For One Truck Static Loading, Crawling Speed.

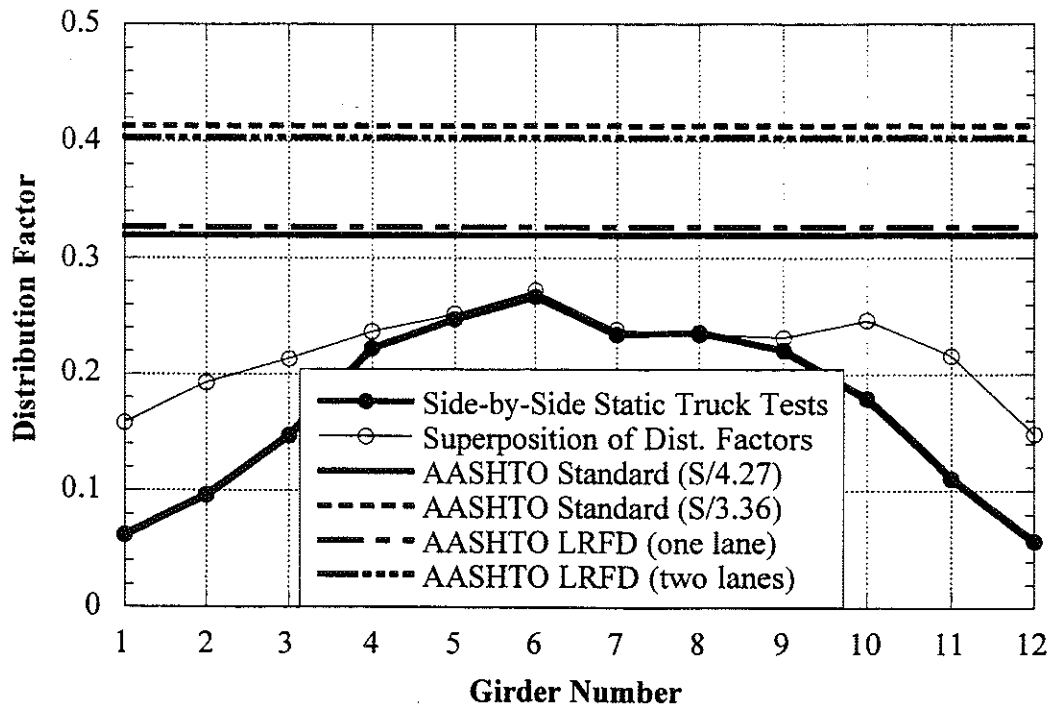


Figure 7.9 Comparison with Code Specified Distribution Factors, Crawling Speed

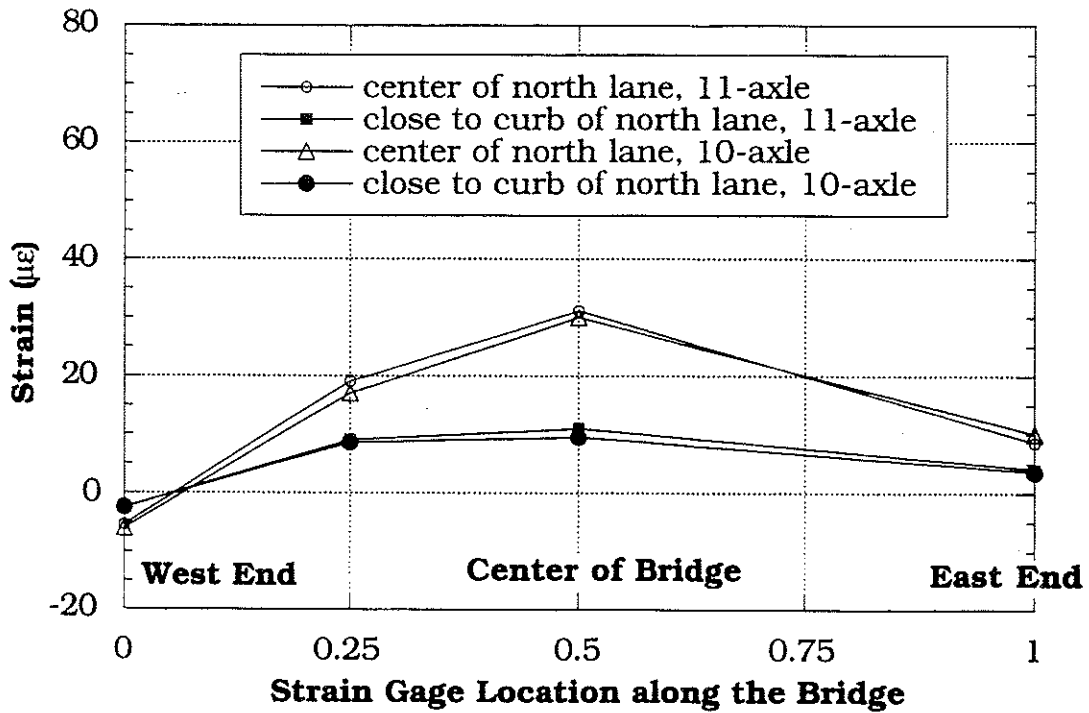


Figure 7.10 Strain Profile on Girder 6 along the Bridge, North Lane, Crawling Speed.

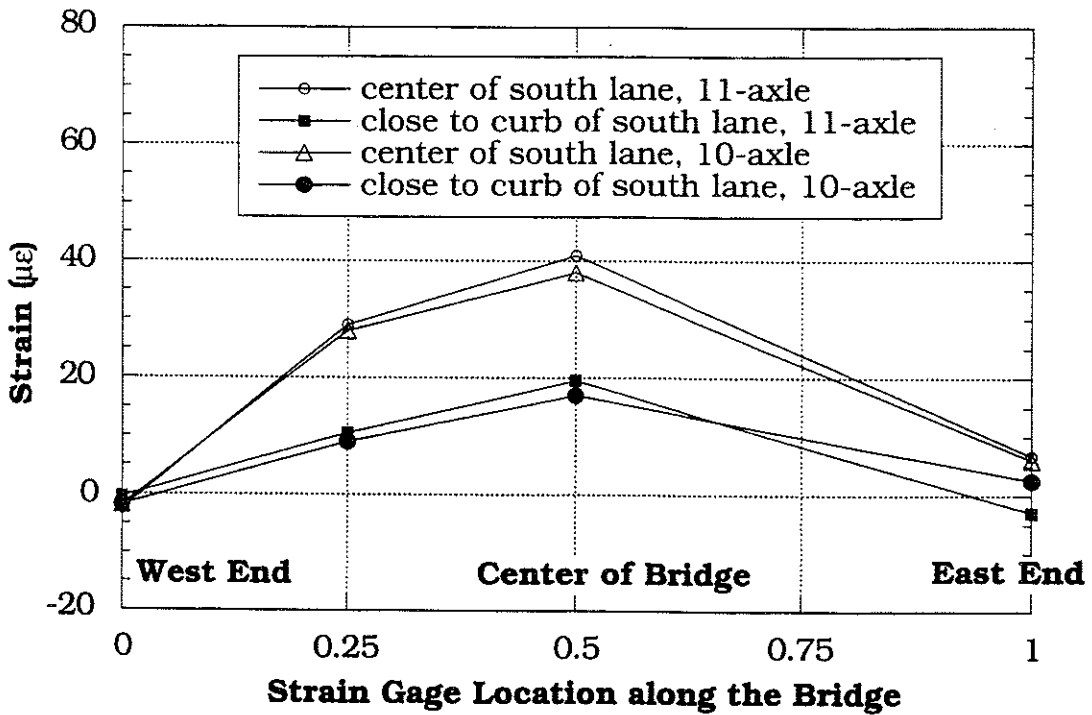


Figure 7.11 Strain Profile on Girder 6 along the Bridge, South Lane, Crawling Speed.

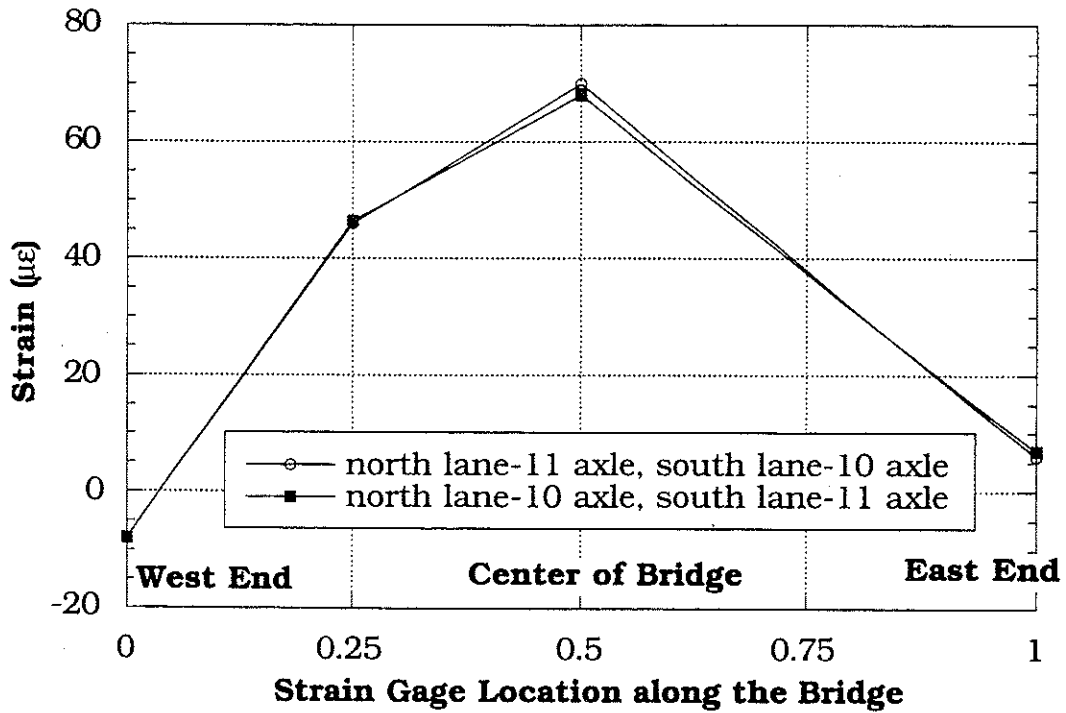


Figure 7.12 Strain Profile on Girder 6 along the Bridge, Side-by-Side, Crawling Speed.

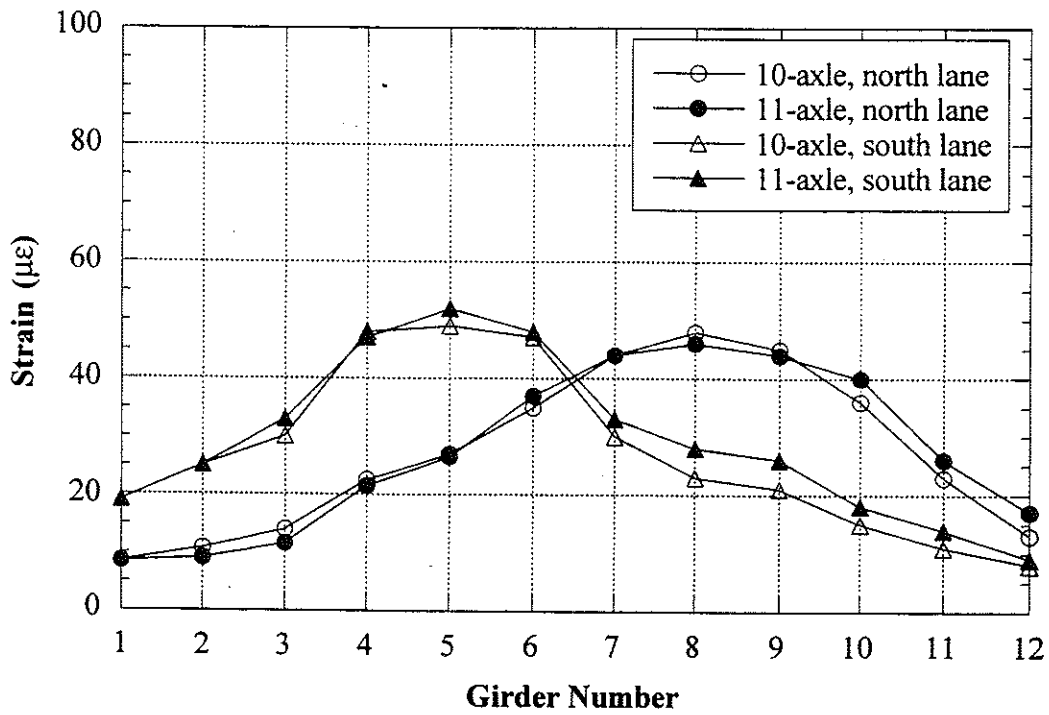


Figure 7.13 Strains under One Truck Loading at High Speed.

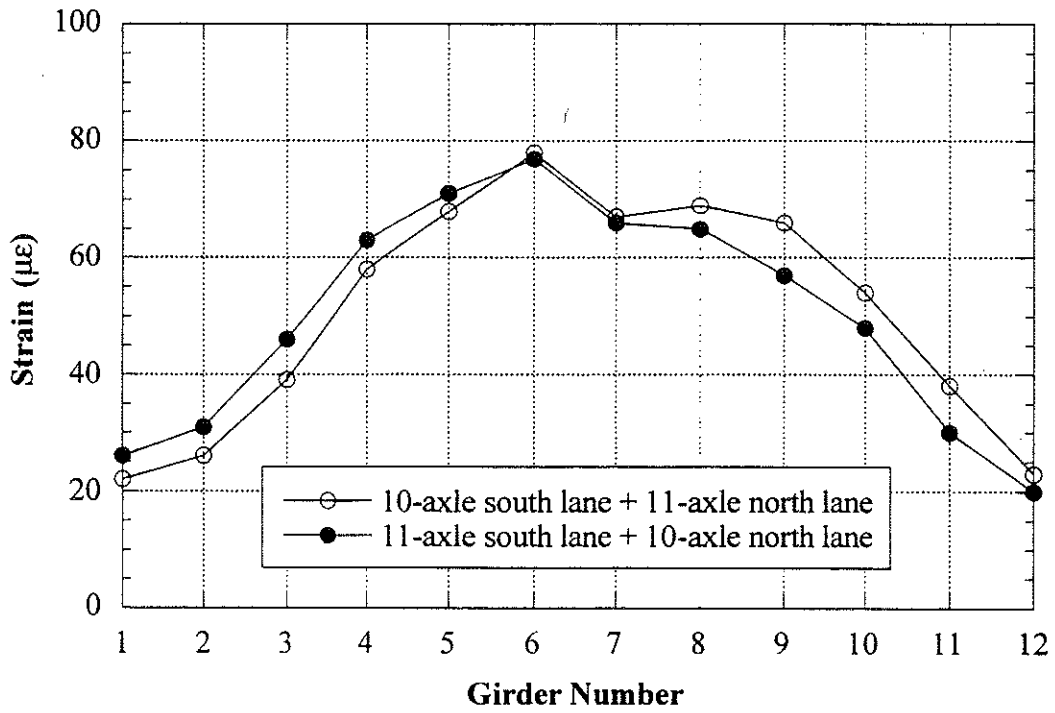


Figure 7.14 Strains under Side-by-Side Truck Loading at High Speed.

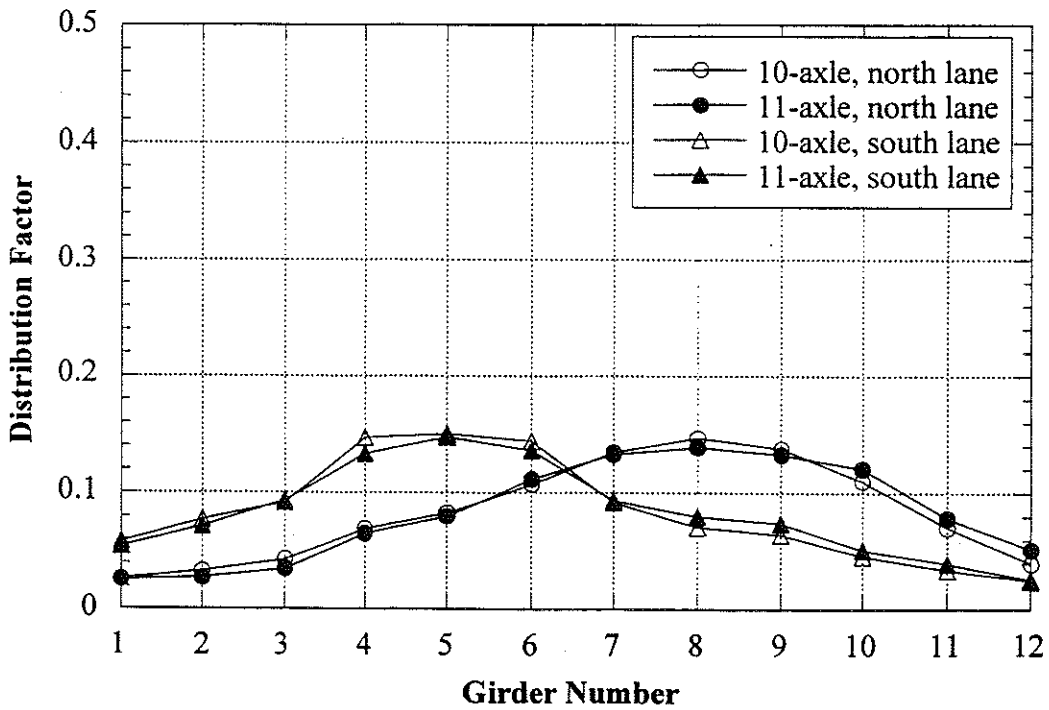


Figure 7.15 Distribution Factors under One Truck Loading at High Speed

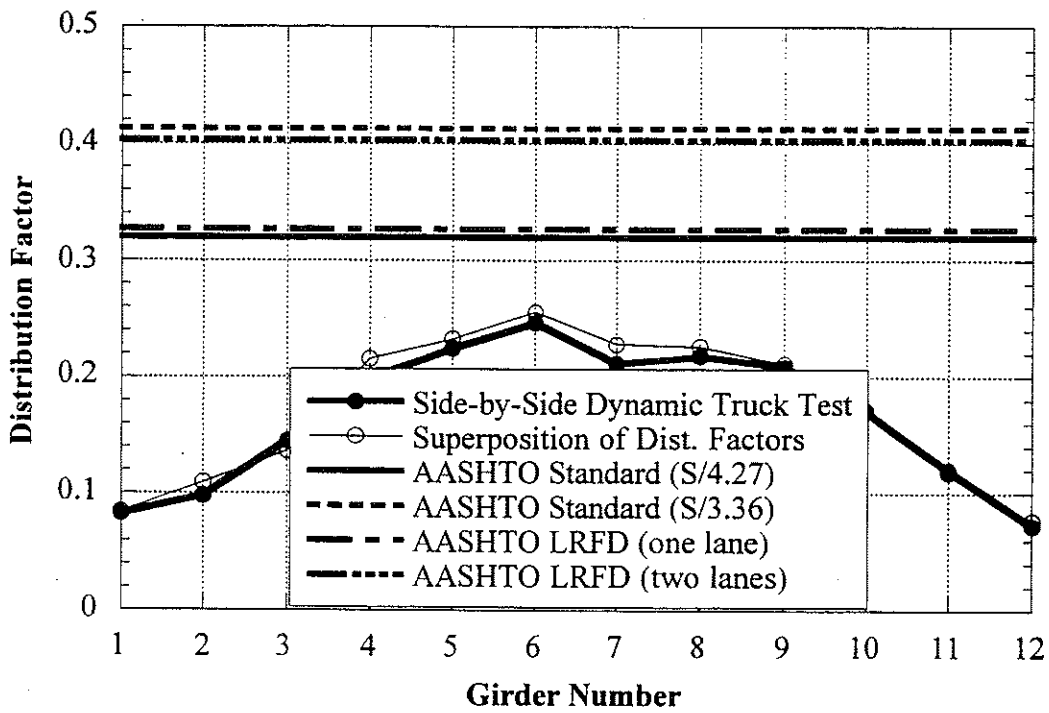


Figure 7.16 Comparison with Code Specified Distribution Factors at High Speed

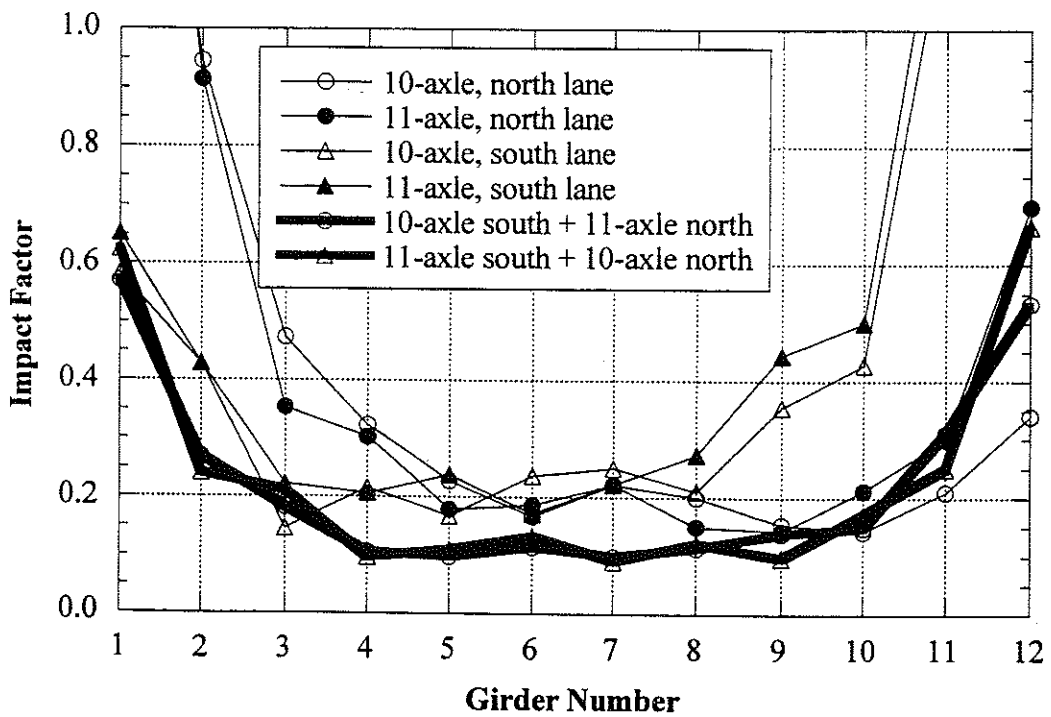


Figure 7.17 Impact Factors.

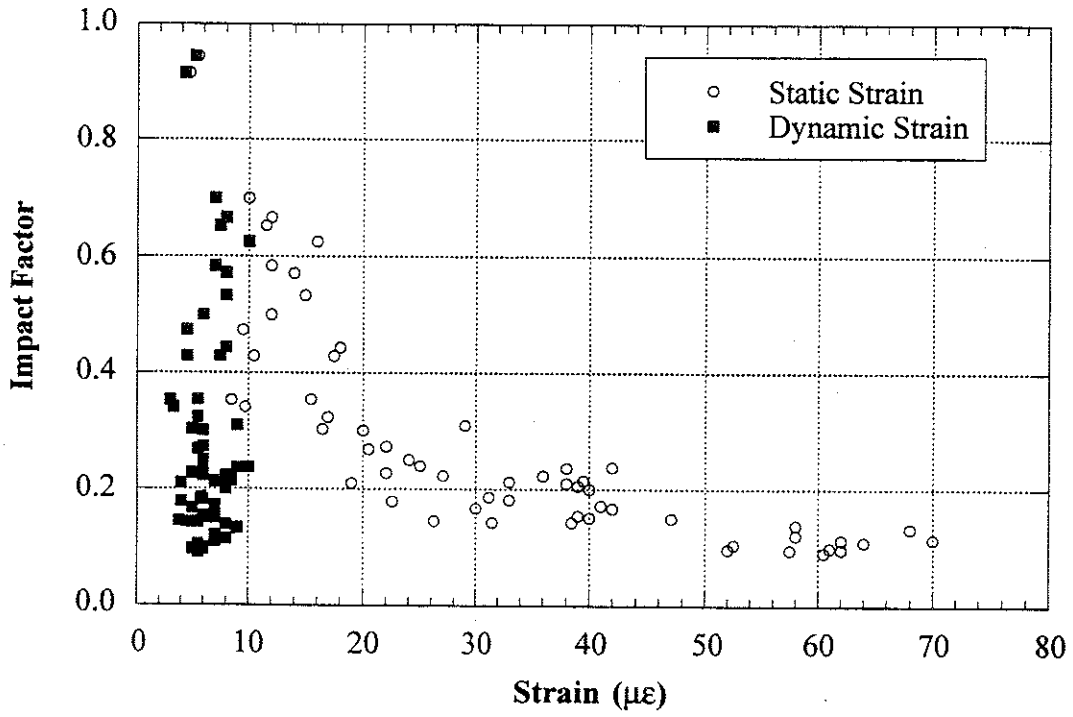


Figure 7.18 Strain versus Impact Factors.

7.5 Loads for Proof Load Test

Two M-60 tanks were used for the proof load test. The tanks were placed adjacent to each other in three different longitudinal and three different transverse positions, and rested directly on the pavement. Traffic was allowed over a partial width of the bridge during the test, and it was fully stopped only at critical times of maximum load placement.

Maximum lane moment on the 9.9m span due to the legal load is 638 kN-m. The target proof load lane moment was obtained from Section 3.3.1. The bridge is ratable and has no hidden details. Therefore, the target proof load was reduced by 5 percent. No other adjustment was applicable to the bridge. The required proof load level of 933 kN was determined as follows:

$$X_p = 1.4 \quad \text{basic target load factor}$$

$$\Sigma = -5 \% \quad \text{because the bridge is ratable and has no hidden details}$$

$$X_{pa} = 1.4(1+(\Sigma/100)) = 1.33 \quad \text{from Eq. (3-1)}$$

Above X_{pa} satisfies Eq. (3-3).

The target proof load (L_t) is

$$L_t = 1.33 \times 1.10 L_r = 1.46 L_r \quad \text{from Eq. (3-2)}$$

$$L_r = 638 \text{ kN from Michigan Bridge Analysis Guide}$$

$$L_t = 1.46 \times 638 = 933 \text{ kN}$$

Table 7.1 shows the maximum lane moments caused by the trucks and tanks. The applied proof load lane moment was 964 kN-m.

Table 7.1 Moment due to Trucks and Tanks.

Load Type	Maximum Lane Moment
Ten-axle test truck	469 kN-m
Eleven-axle test truck	514 kN-m
Tank at 0.61 m from middle of span	943 kN-m
Tank in the middle of span	964 kN-m

The testing sequence was as follows: First, one tank per lane was applied to the bridge with two different lateral positions: center of lane and close to the curb. Then, side-by-side tanks were placed in the middle of the bridge width to obtain the maximum proof load level. When placed side-by-side, the tanks are nearly in contact with each other. The following proof load cases were applied for Bridge US12/SC:

- one tank close to the curb of north lane in the middle of span
- one tank close to the curb of north lane 0.61 m east from the middle of span
- one tank close to the curb of north lane 0.61 m west from the middle of span
- one tank at the center of north lane in the middle of span
- one tank at the center of north lane 0.61 m east from the middle of span
- one tank at the center of north lane 0.61 m west from the middle of span
- one tank close to the curb of south lane in the middle of span
- one tank close to the curb of south lane 0.61 m east from the middle of span

- one tank close to the curb of south lane 0.61 m west from the middle of span
- one tank at the center of south lane in the middle of span
- one tank at the center of south lane 0.61 m east from the middle of span
- one tank at the center of south lane 0.61 m west from the middle of span
- two side-by-side tanks at the center of bridge width, both tanks 0.61 m east from the middle of span
- two side-by-side tanks at the center of bridge width, one tank 0.61 m east from the middle of span, the other tank in the middle of span
- two side-by-side tanks at the center of bridge width, both tanks in the middle of span
- two side-by-side tanks at the center of bridge width, one tank 0.61 m west from the middle of span, the other tank in the middle of span
- two side-by-side tanks at the center of bridge width, both tanks 0.61 m west from the middle of span

Detailed proof load positions are shown in Figures 7.19 to 7.23.

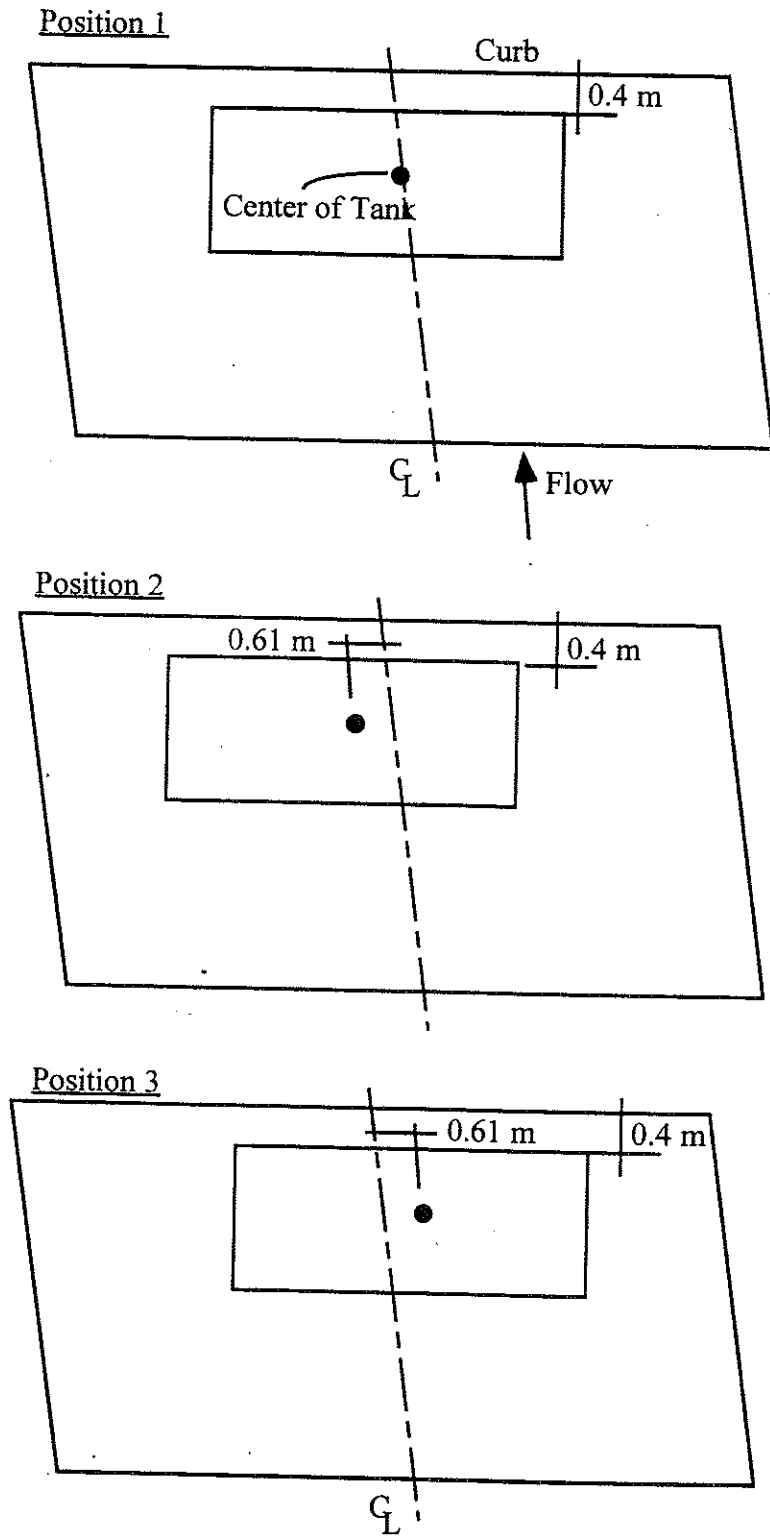


Figure 7.19 Proof Load, North Lane Loading, Close to Curb.

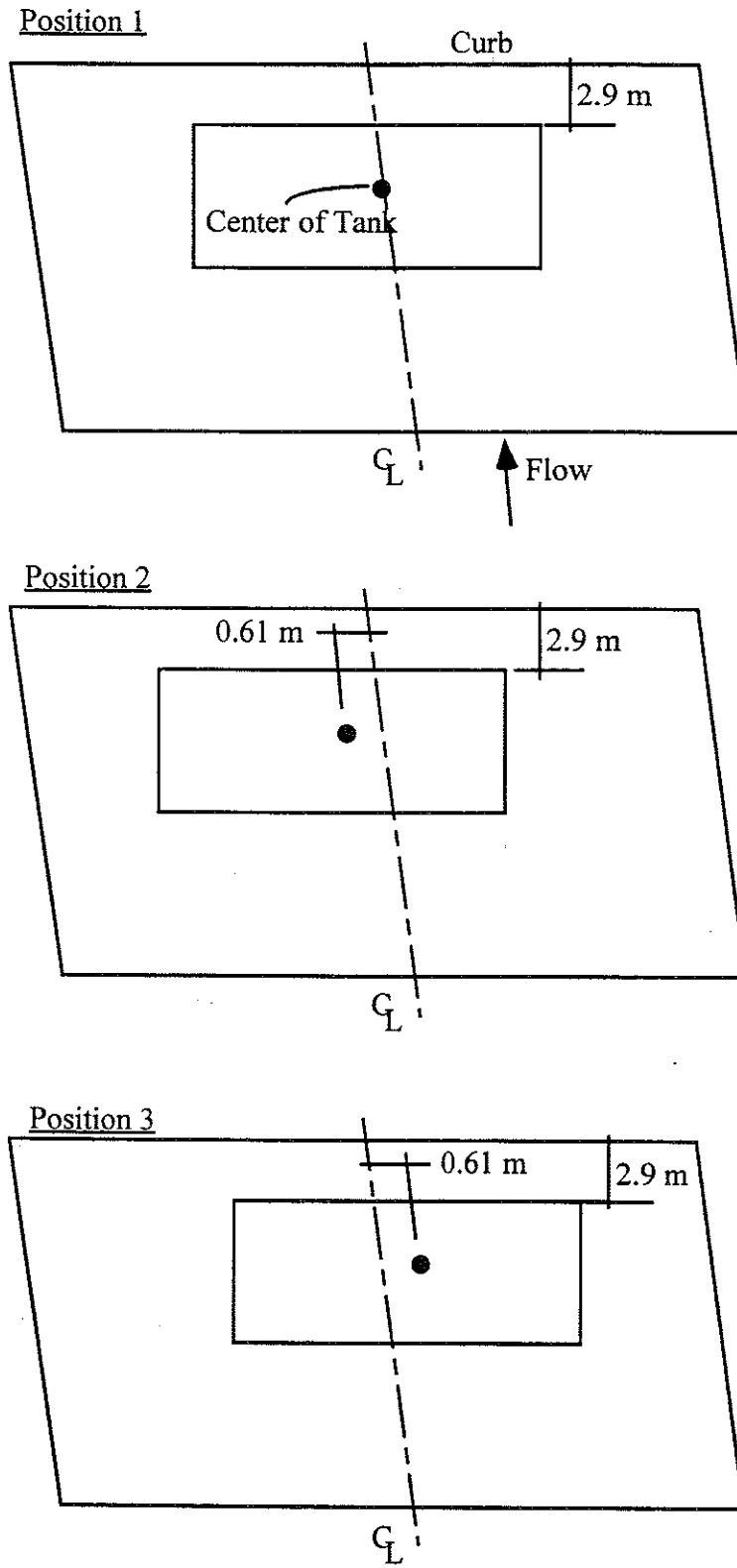


Figure 7.20 Proof Load, North Lane Loading, Center of Lane.

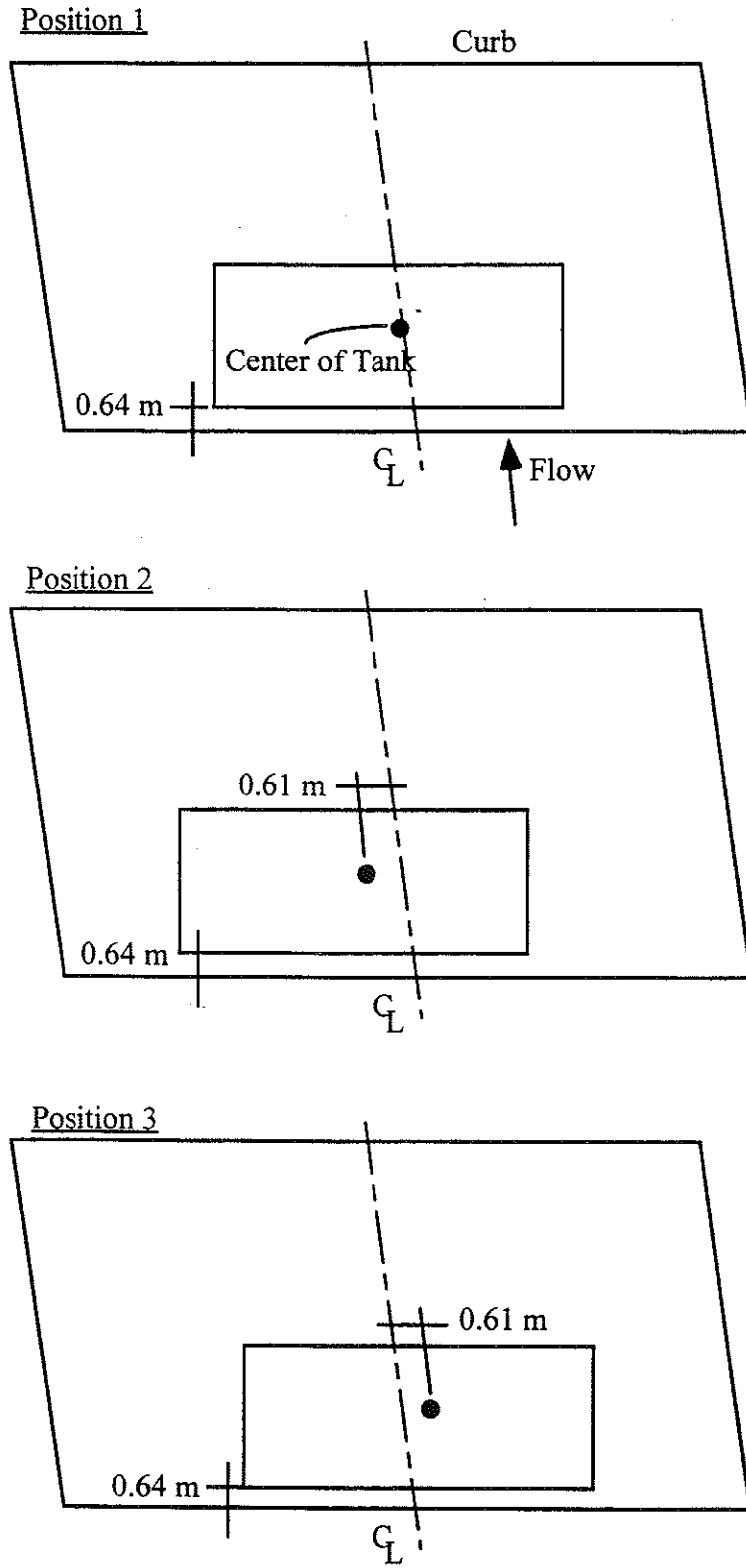


Figure 7.21 Proof Load, South Lane Loading, Close to Curb.

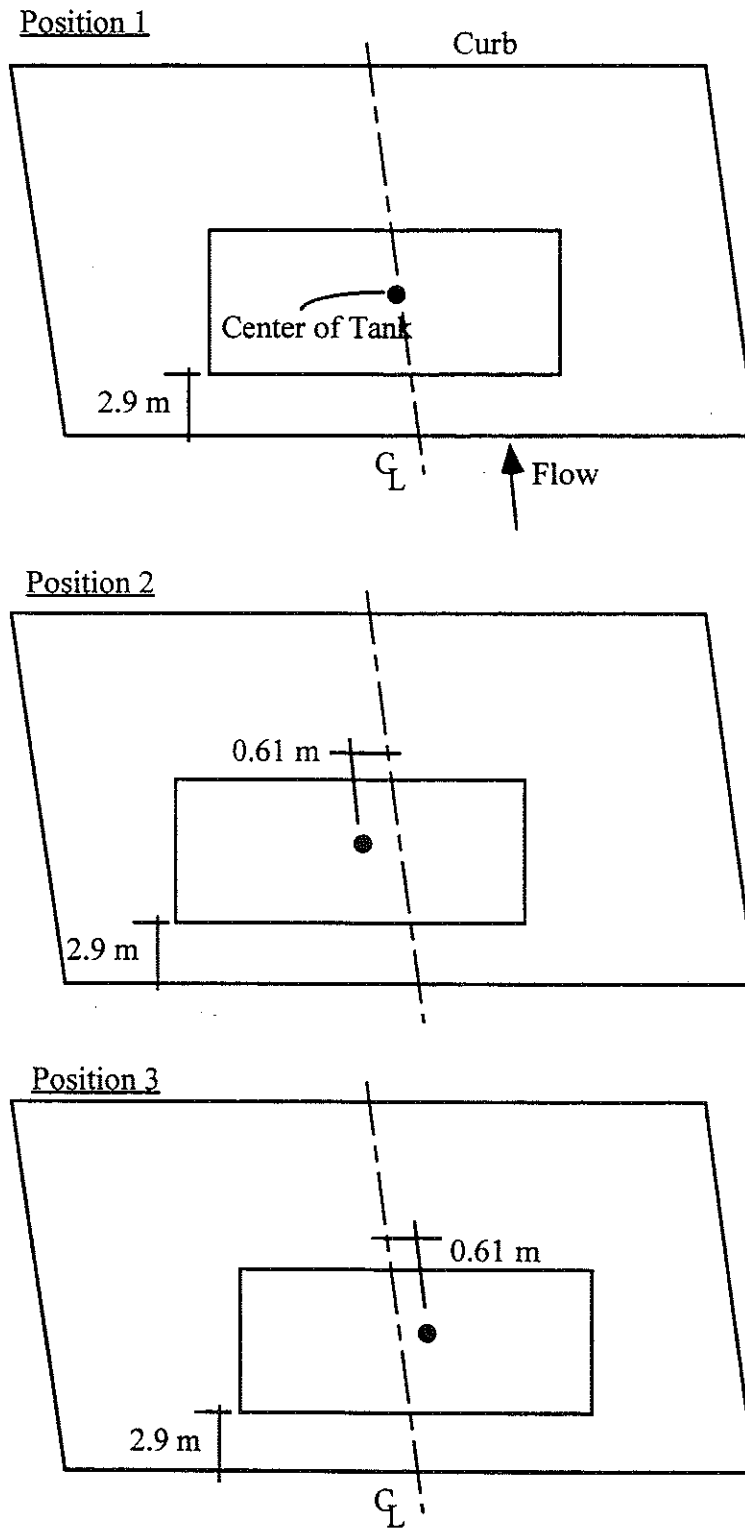


Figure 7.22 Proof Load, South Lane Loading, Center of Lane.

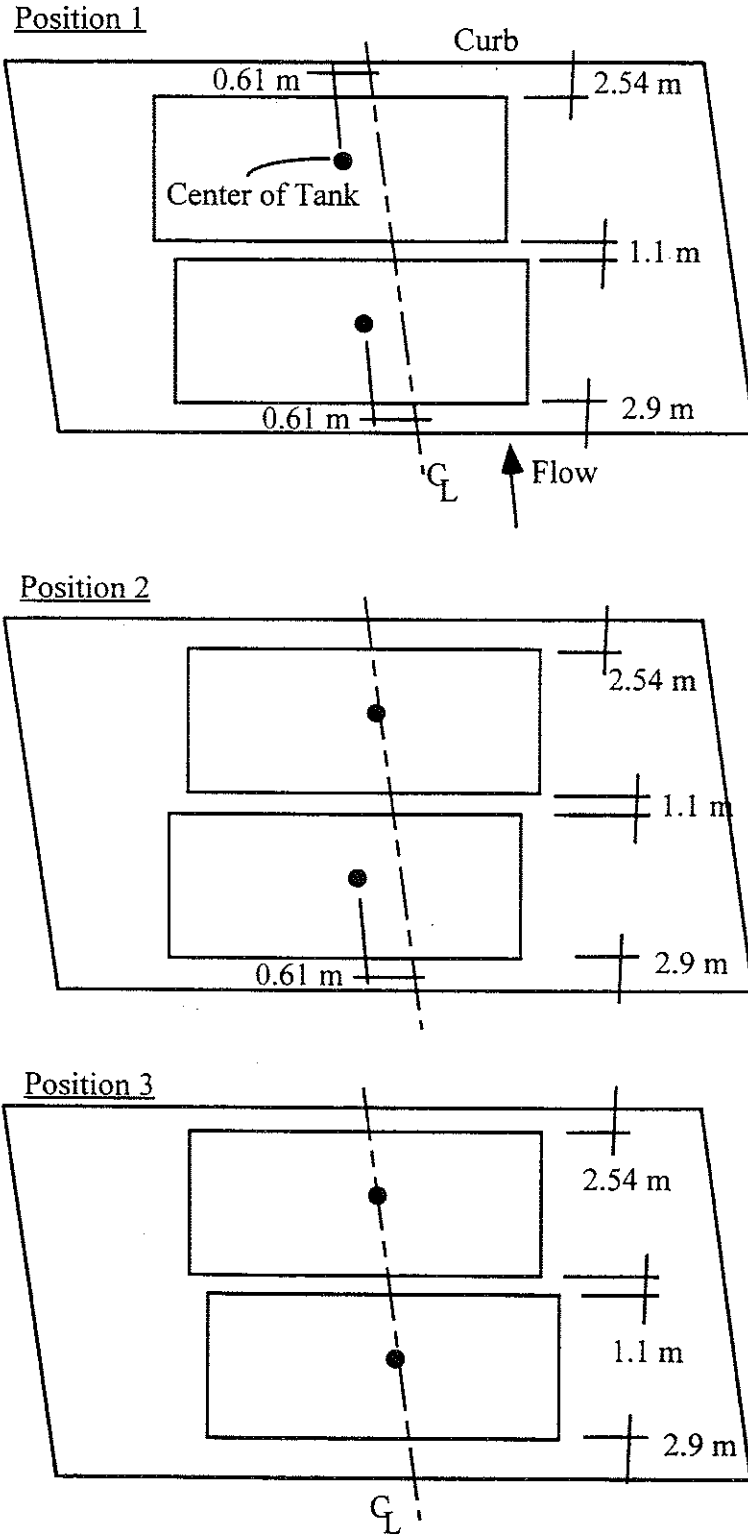
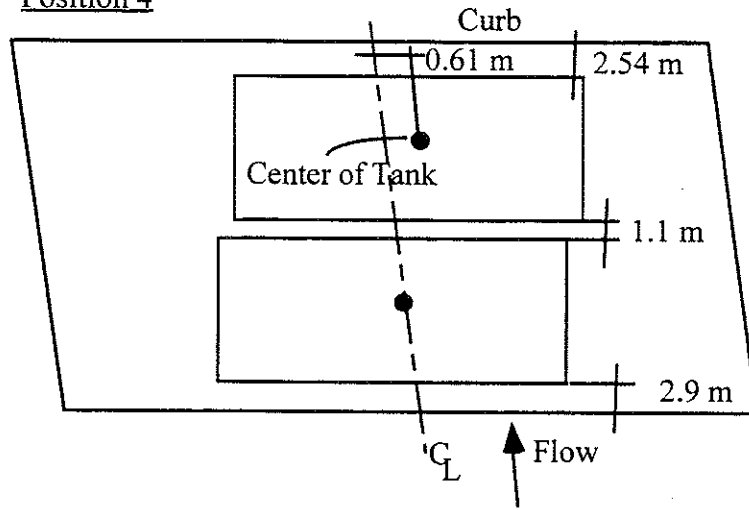


Figure 7.23 Proof Load, Side-by-Side Loading, Center of Bridge Width.

Position 4



Position 5

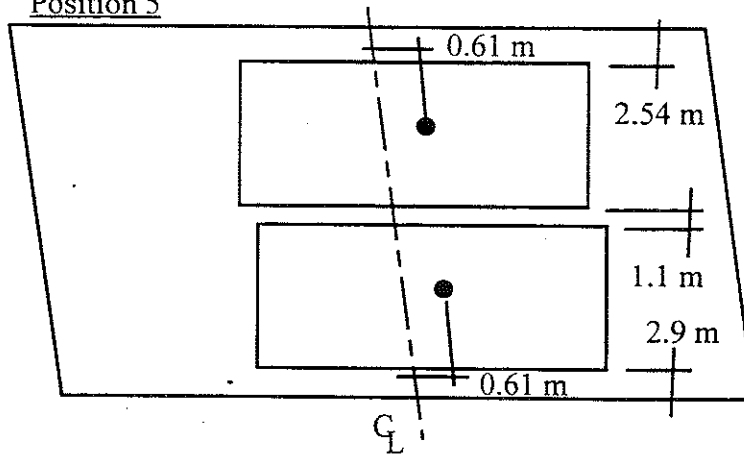


Figure 7.23 Proof Load, Side-by-Side Loading, Center of Road, Continued.

7.6 Results for Proof Load Test

The proof load test was successfully completed without any sign of distress to the structure. The maximum deflection due to the applied load was only 2.4 mm. The maximum strain was about 130 micro-strain, which is approximately a stress of 26 MPa. The load versus response curve indicated that the structure behaved linearly.

Figure 7.24 shows strains and girder distribution factors for a tank in the north lane. The load positions for Figure 7.24 are shown in Figures 7.19 and 7.20. Figure 7.25 shows strains and GDF's for a tank in the south lane. The load positions for Figure 7.25 are shown in Figures 7.21 and 7.22. The results from one tank (Figure 7.24 and 7.25) indicate a slightly more uniform load distribution than that of one truck (Figures 7.5 and 7.6). The better distribution may be caused by the tank's larger width. Figure 7.26 shows strains and GDF's for side-by-side tanks. The load positions for Figure 7.26 are shown in Figure 7.23. The load distribution factors for side-by-side tanks (Figure 7.26) are slightly larger than those for side-by-side trucks (Figure 7.7). This was probably caused by the closer adjacent positioning of the tanks compared with that of the trucks. Figure 7.27 shows the envelope of GDF's for one tank loading. It is very similar to that for a single truck (Figure 7.8). Figure 7.28 shows load distribution comparison with AASHTO Code specified values. Actual value of the term $K_r / (L_t^3)$ is used in calculation of Code specified GDF values.

Figures 7.29 to 7.31 show strain profiles on girder 6 along the bridge length. Because some strain gages were not working, not all expected data values could be plotted on the figures. The strain reading at the west supports shows small negative values. However, the readings at the east end show less fixity than at the west end.

Figure 7.32 shows deflections for a tank in the north lane. The load positions are shown in Figures 7.19 and 7.20. A total of 10 LVDTs were installed, one each on girders 2 to 11. LVDTs on girders 5 and 6

were not working and thus these data values are missing. Figure 7.33 shows deflections for a tank in the south lane. The load positions are shown in Figures 7.21 and 7.22. Figure 7.34 shows deflections for side-by-side tanks on the bridge. The load positions are shown in Figure 7.23.

Figures 7.35 to 7.46 plot applied moment per girder versus measured strain, for girders 1 to 12. The applied moment per girder was obtained by multiplying, for each load case, the total applied moment due to the load by the GDF measured for that load case. Included in the figures are not only the measured strains from tanks but also those from trucks. All girders showed reasonably linear behavior.

Figures 7.47 to 7.54 present the applied moment per girder versus measured deflection, for girders 2, 3, 4, 7, 8, 9, 10, and 11, respectively. Again, all girders showed reasonably linear behavior.

The measured static strains were compared to static strains calculated using the design stiffness and GDF's determined by tests in this study. The maximum observed static strain for this bridge is $72 \mu\epsilon$ for a single tank and $137 \mu\epsilon$ for two tanks side-by-side. The corresponding calculated strain for a single tank in a composite section is $156 \mu\epsilon$ and for a non-composite section it is $302 \mu\epsilon$. For two tanks side-by-side loading, the calculated strains are $260 \mu\epsilon$ and $504 \mu\epsilon$ for a composite section and a non-composite section, respectively.

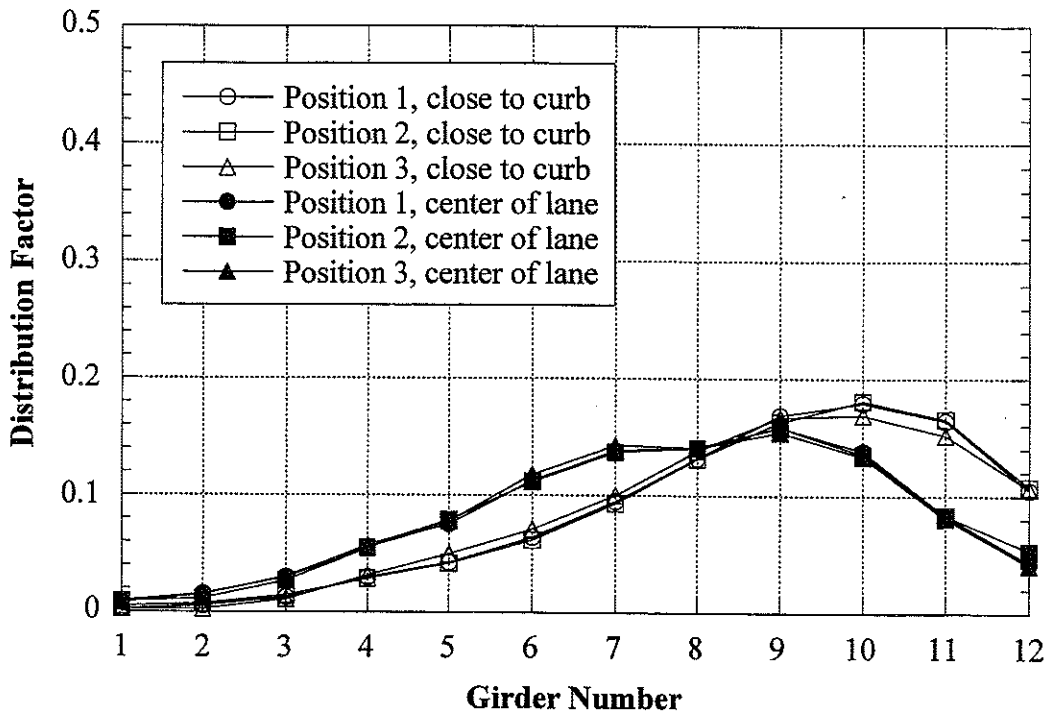
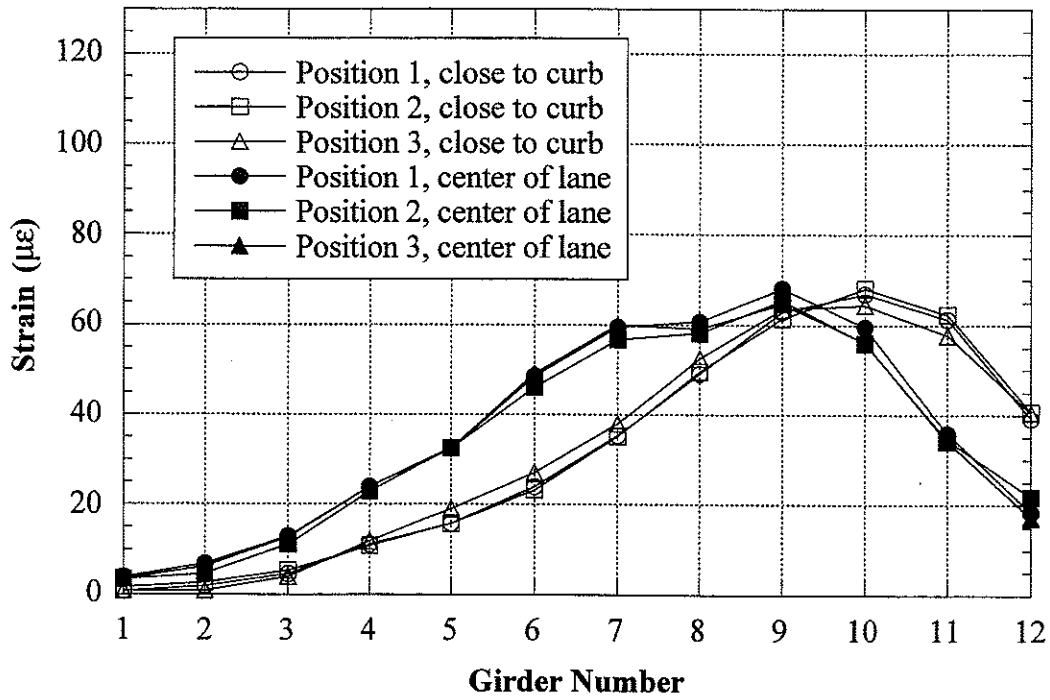


Figure 7.24 Proof Load, North Lane Loading.

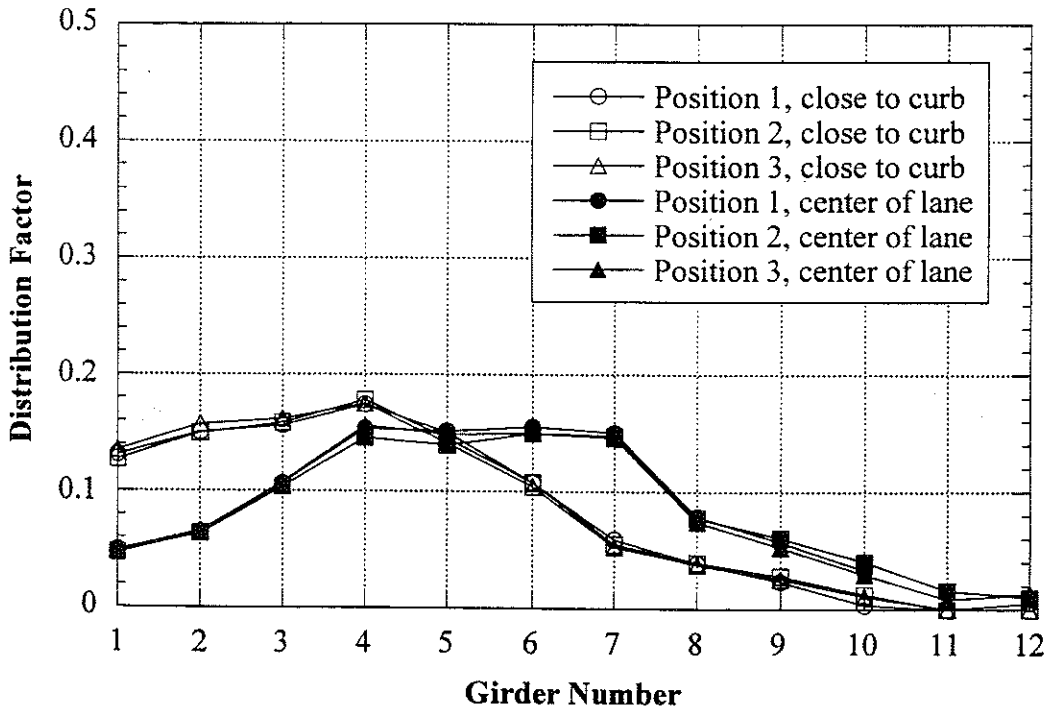
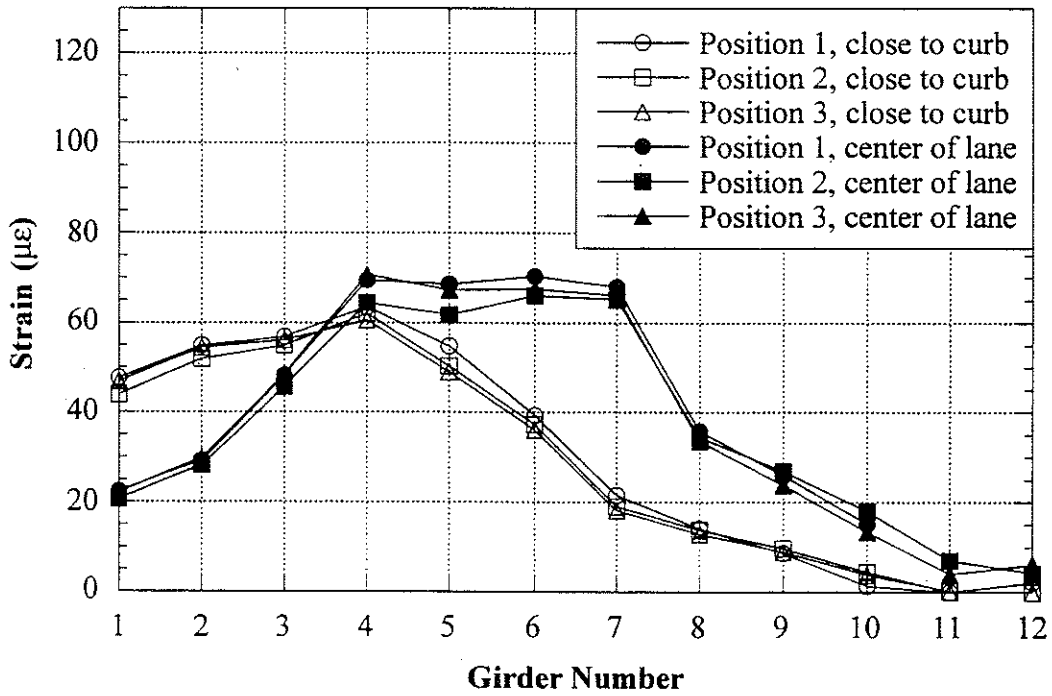


Figure 7.25 Proof Load, South Lane Loading.

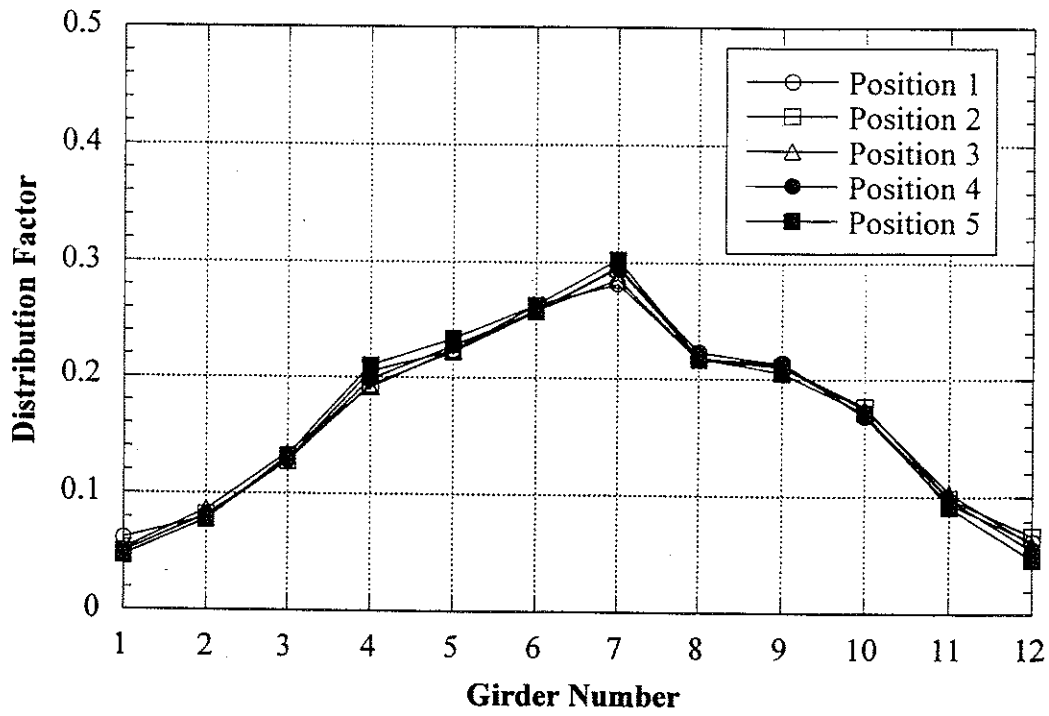
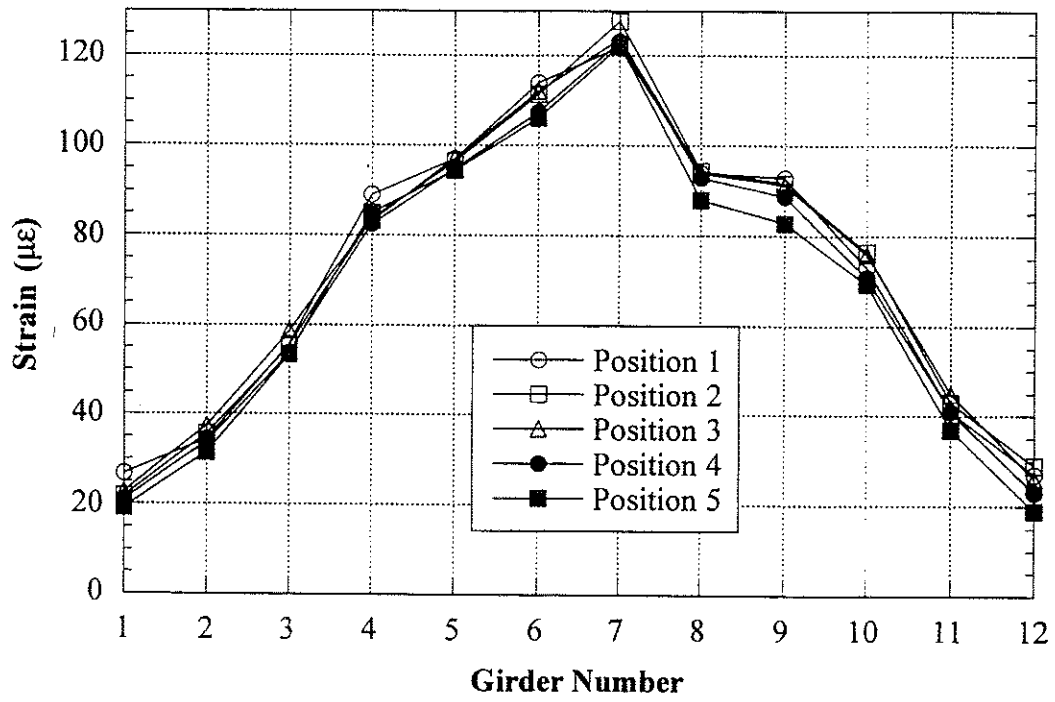


Figure 7.26 Proof Load, Side-by-Side Loading.

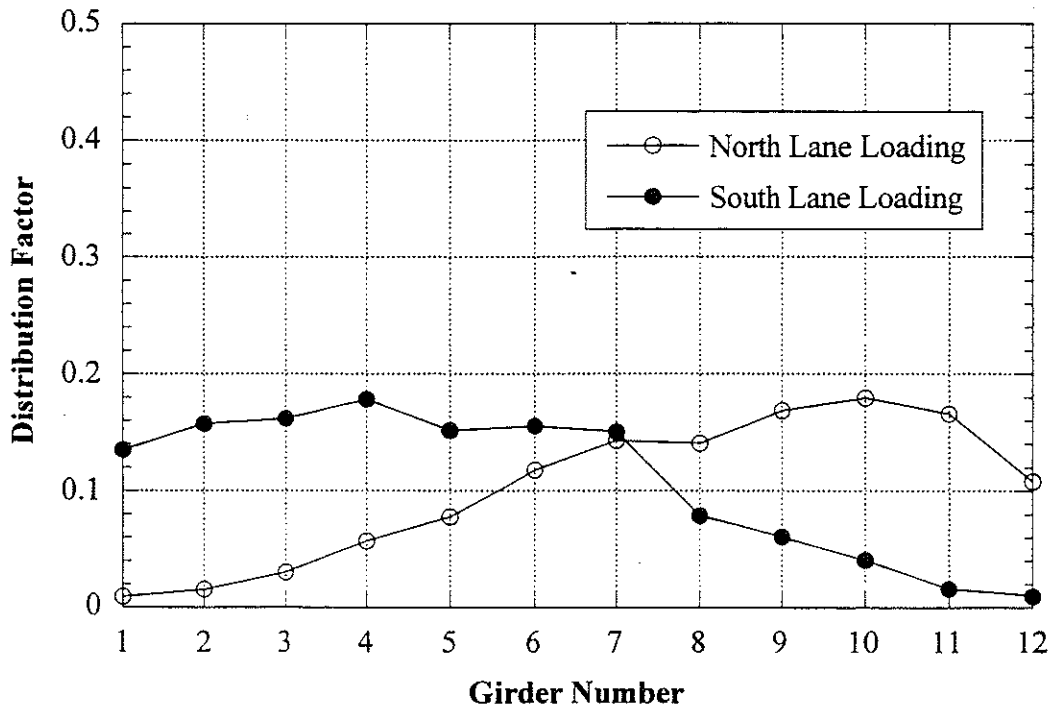


Figure 7.27 Envelope of Girder Distribution Factors For One Tank Loading.

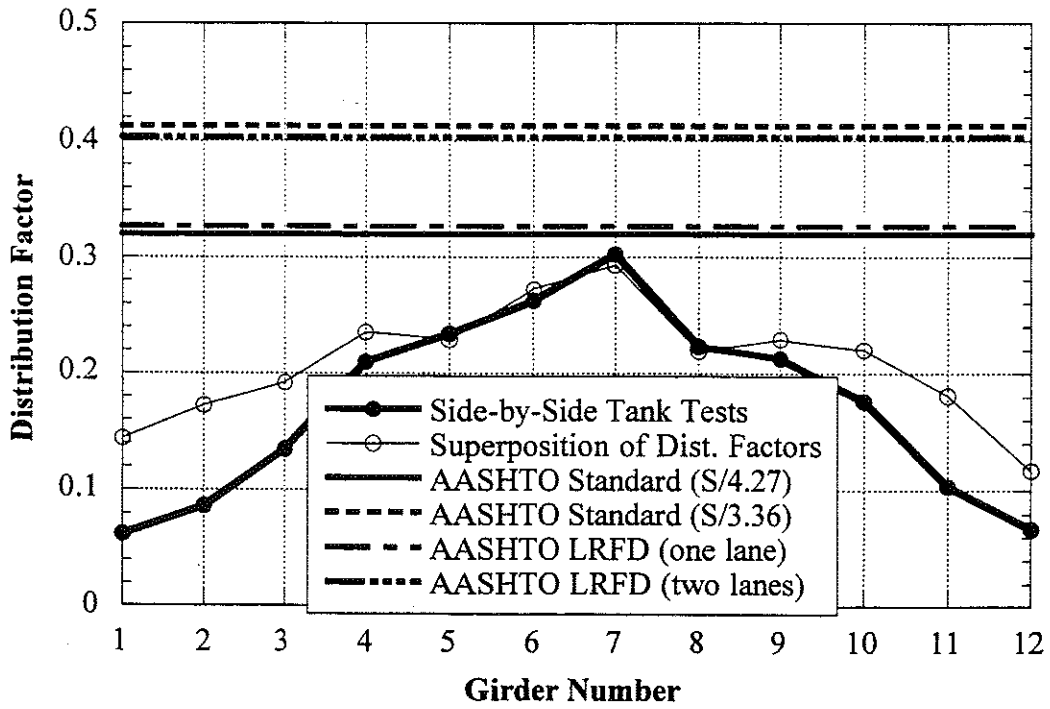


Figure 7.28 Proof Load Test, Comparison with Code Specified Distribution Factor.

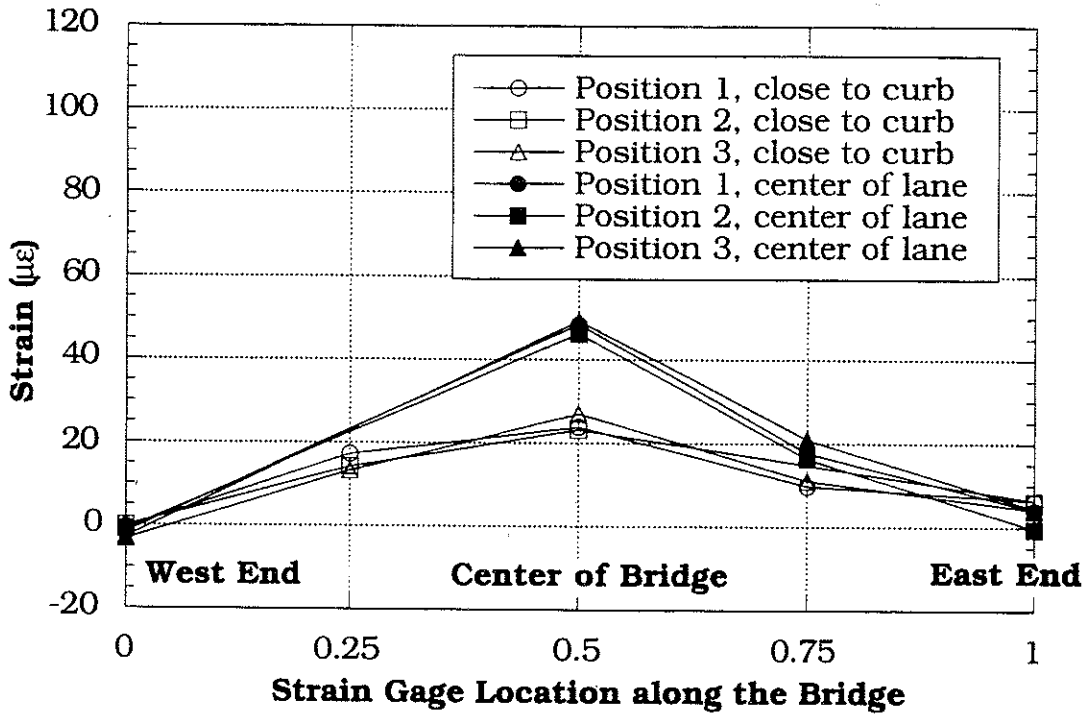


Figure 7.29 Proof Load Test, Strain Profile on Girder 6 along the Bridge, North Lane Loading.

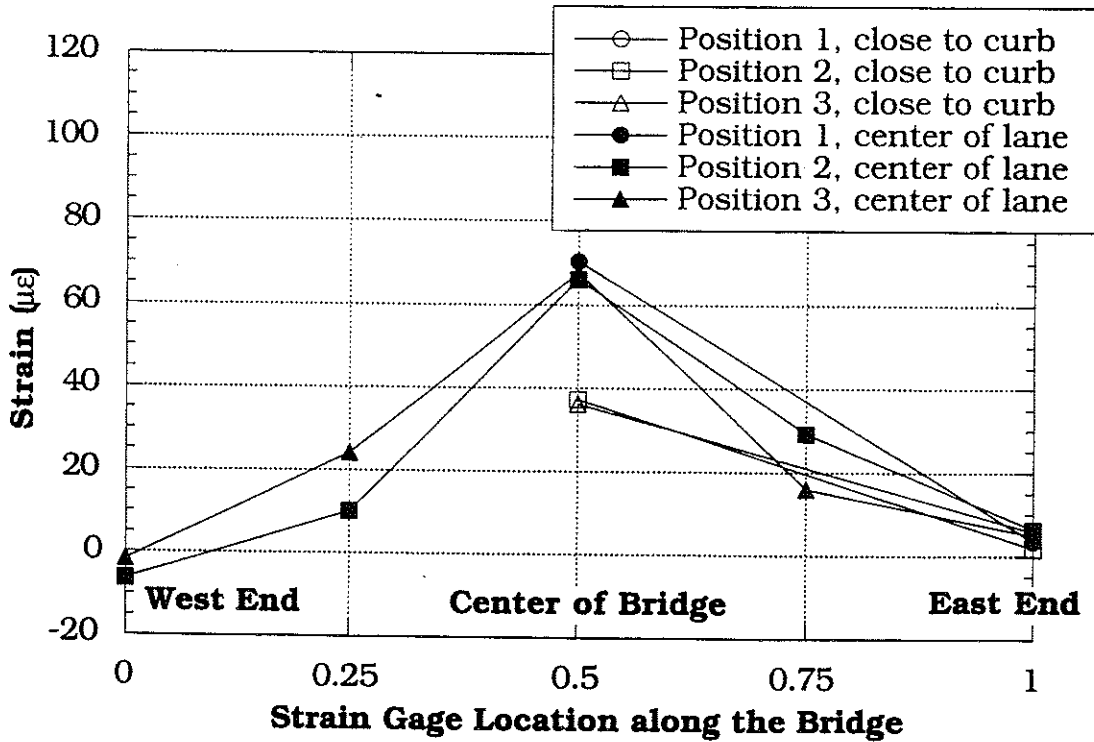


Figure 7.30 Proof Load Test, Strain Profile on Girder 6 along the Bridge, South Lane Loading.

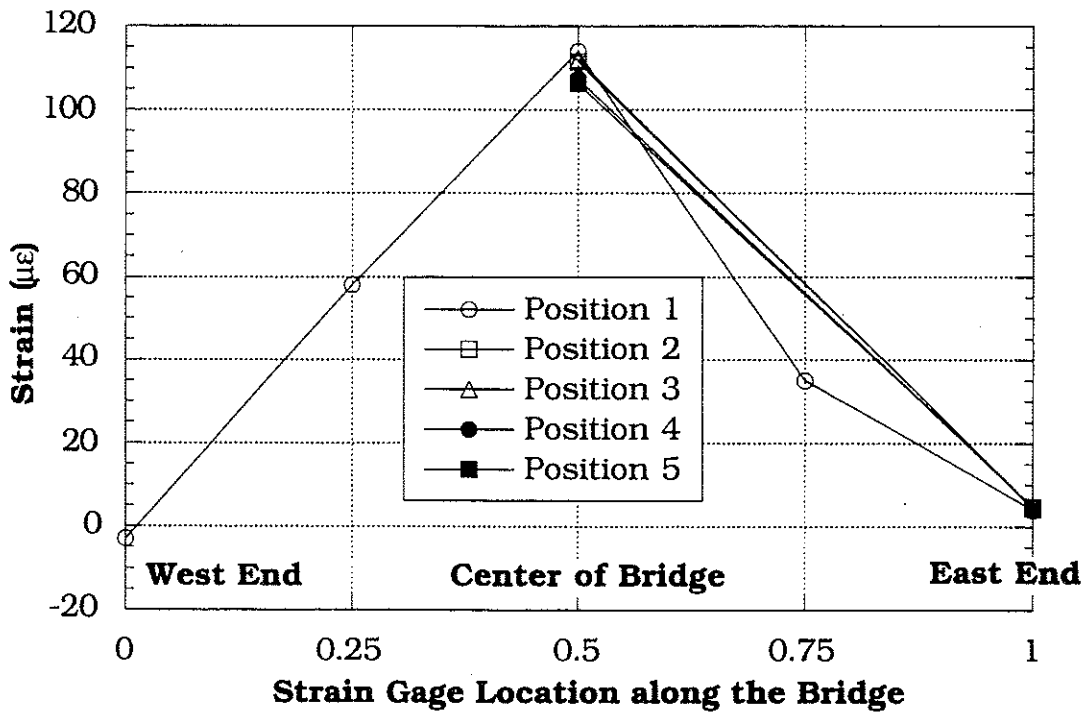


Figure 7.31 Strain Profile on Girder 6 along the Bridge, Side-by-Side Proof Load Test.

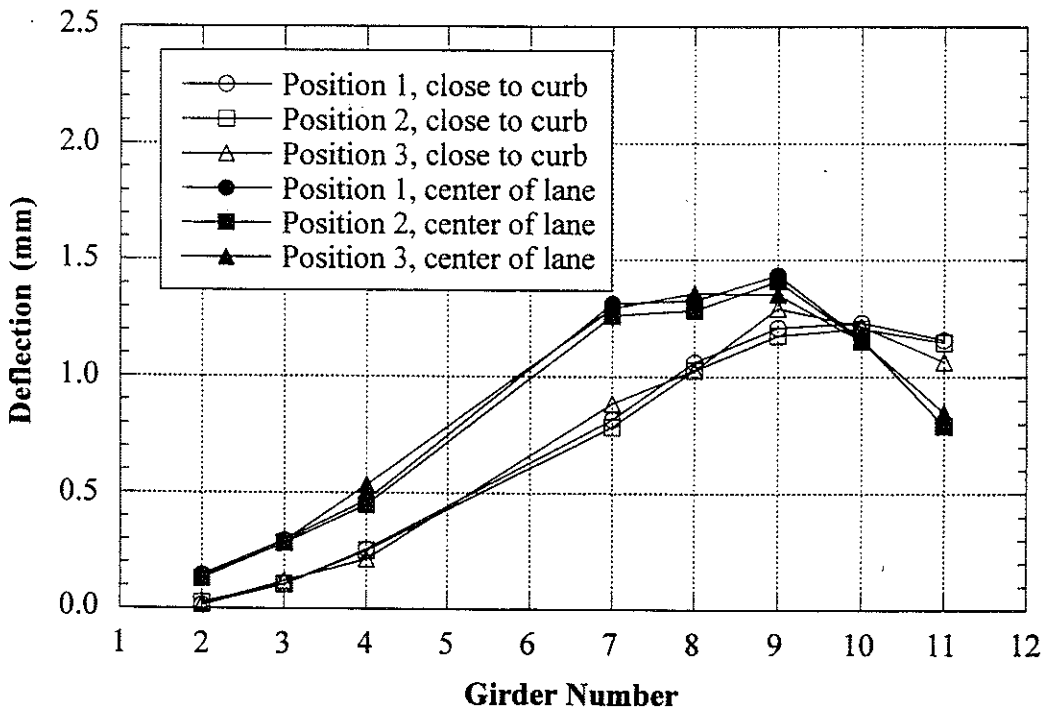


Figure 7.32 Deflections due to Proof Load, North Lane Loading.

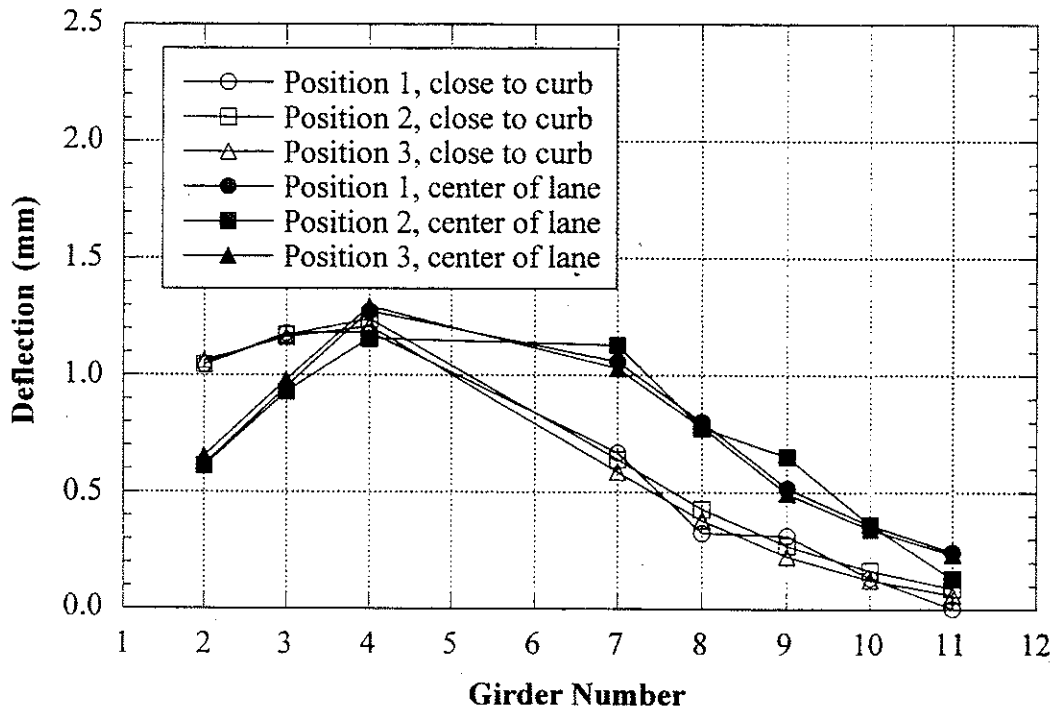


Figure 7.33 Deflections due to Proof Load, South Lane Loading.

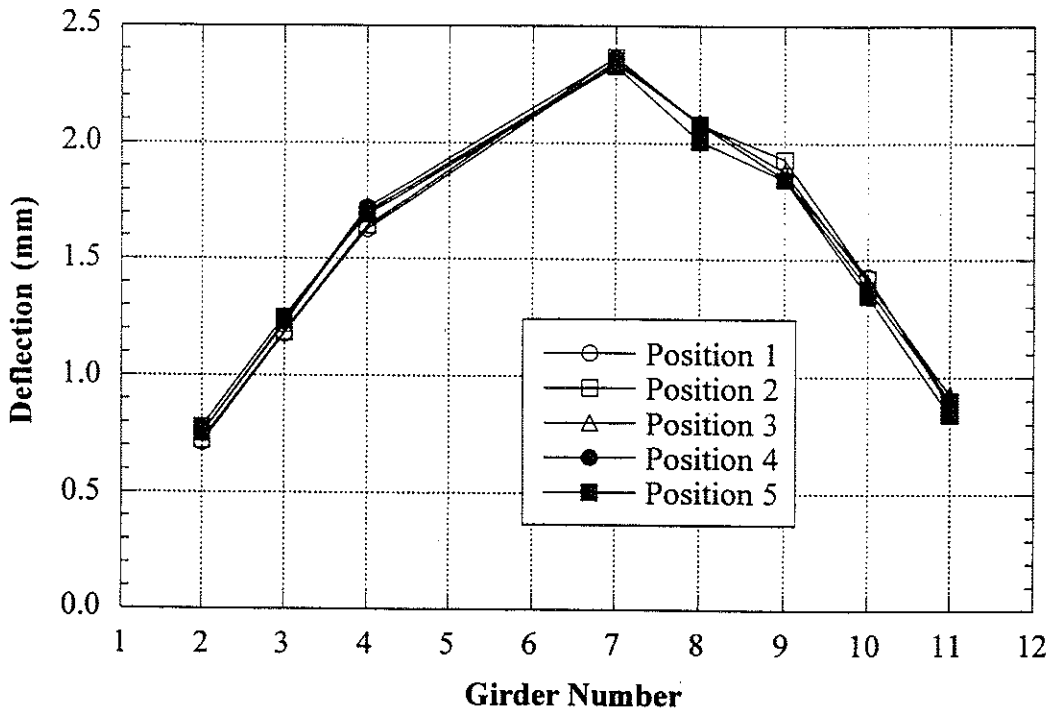


Figure 7.34 Deflections due to Proof Load, Side-by-Side Loading.

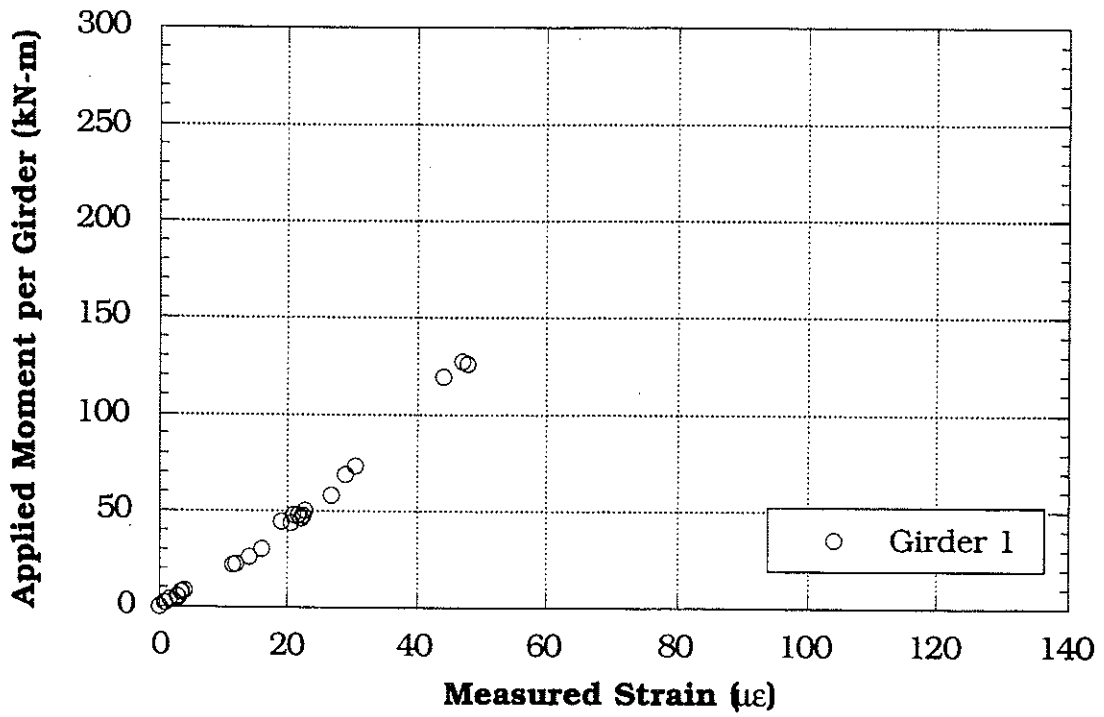


Figure 7.35 Moment per Girder vs Measured Strain, Girder 1.

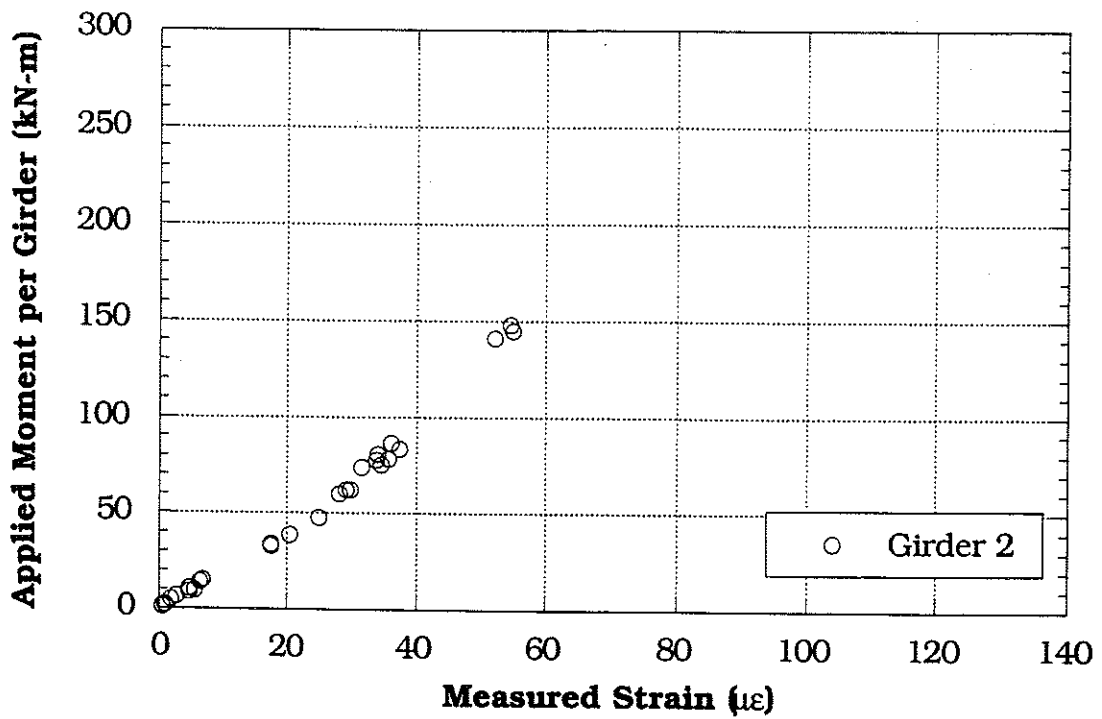


Figure 7.36 Moment per Girder vs Measured Strain, Girder 2.

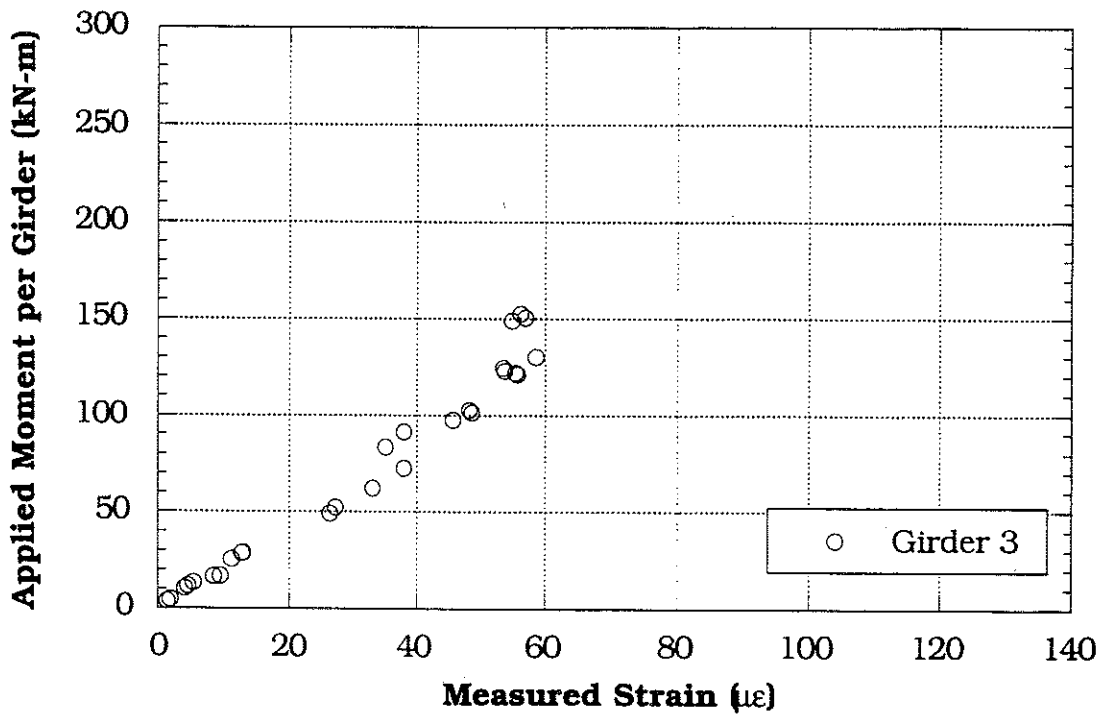


Figure 7.37 Moment per Girder vs Measured Strain, Girder 3.

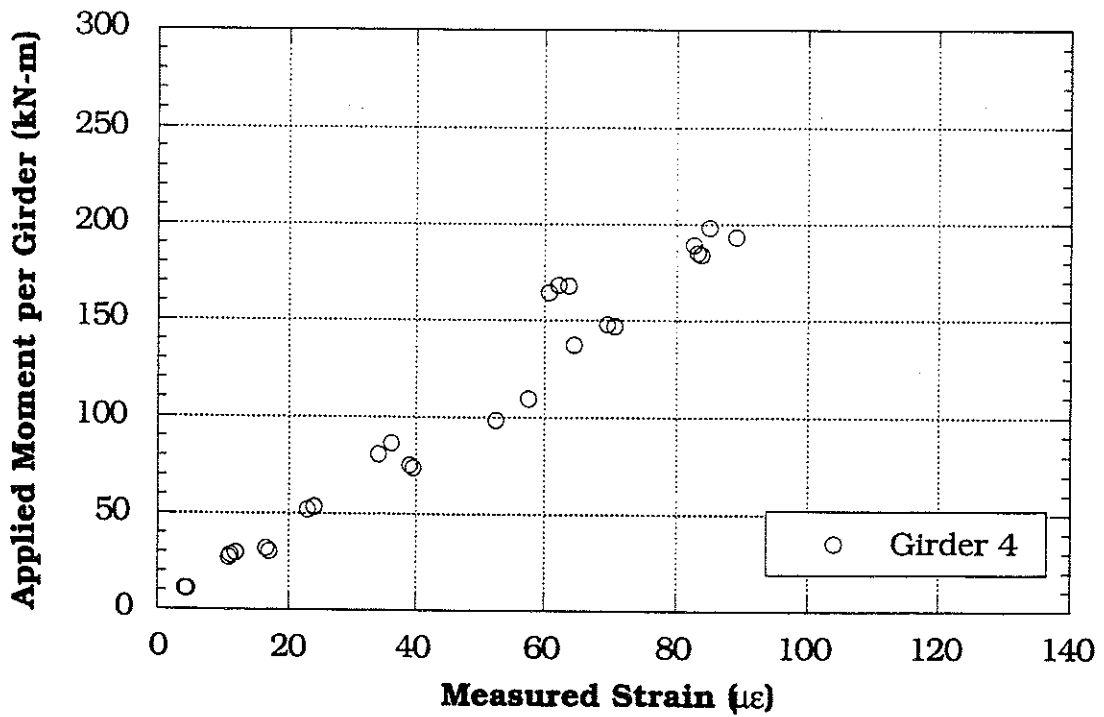


Figure 7.38 Moment per Girder vs Measured Strain, Girder 4.

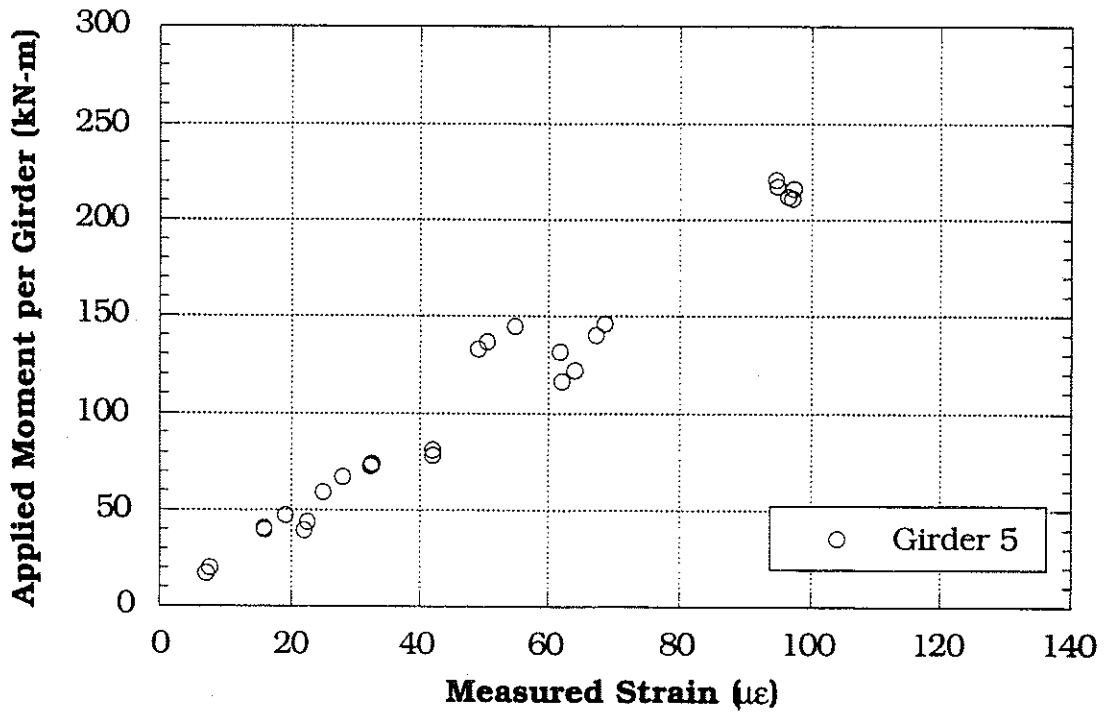


Figure 7.39 Moment per Girder vs Measured Strain, Girder 5.

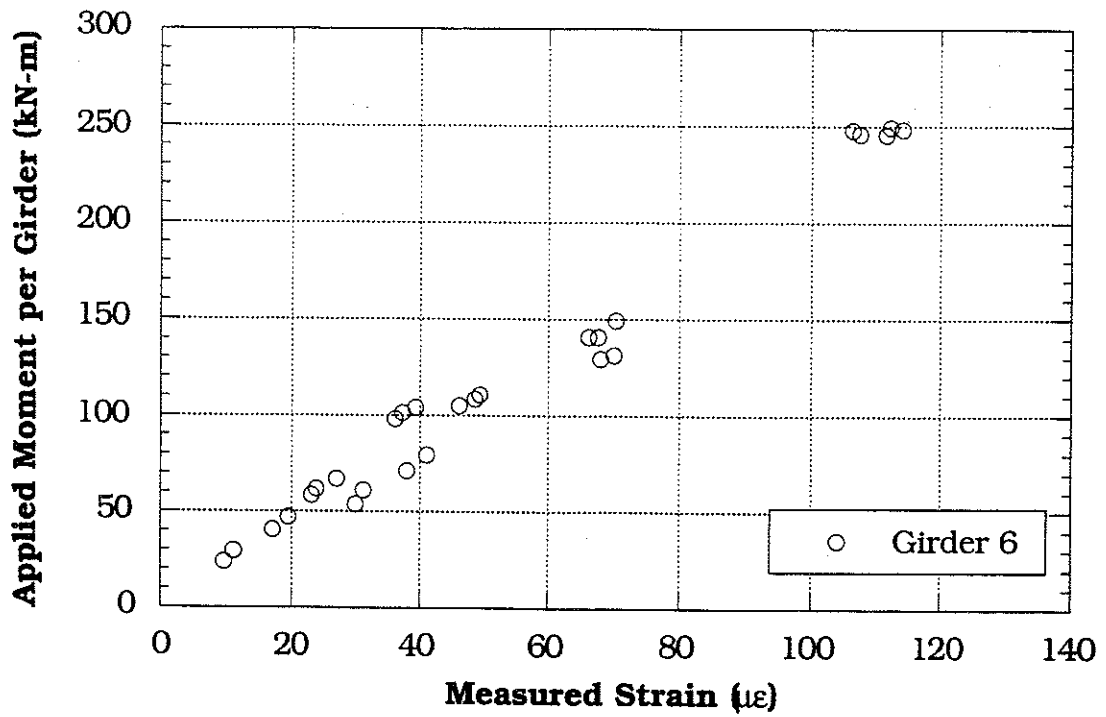


Figure 7.40 Moment per Girder vs Measured Strain, Girder 6.

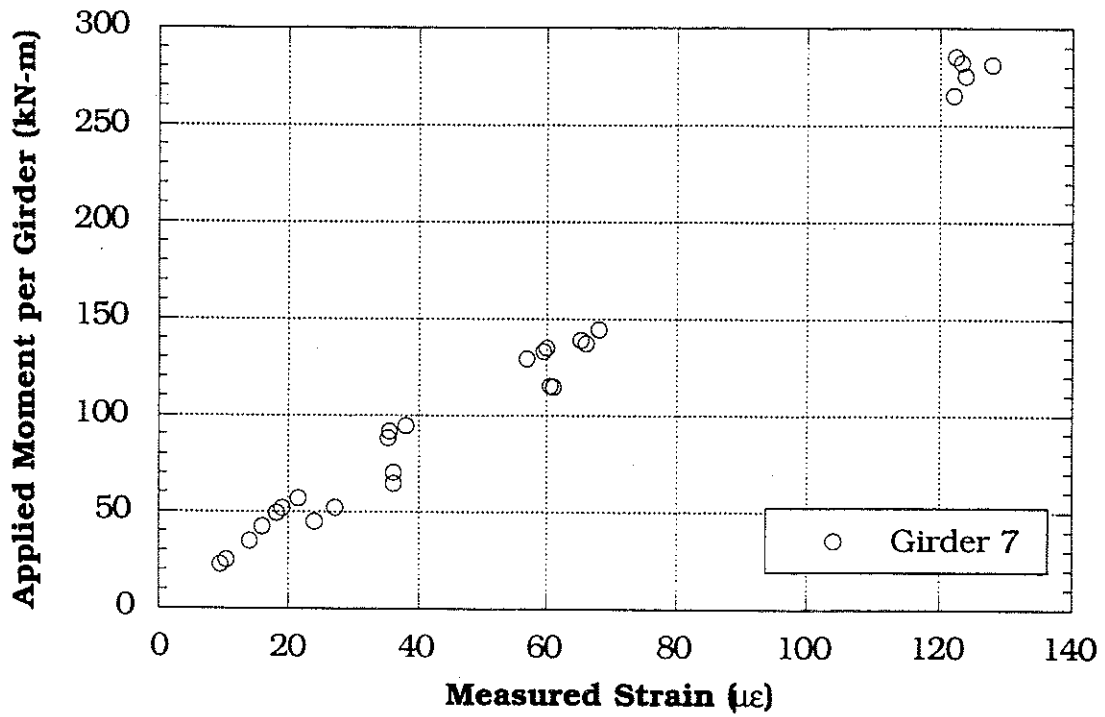


Figure 7.41 Moment per Girder vs Measured Strain, Girder 7.

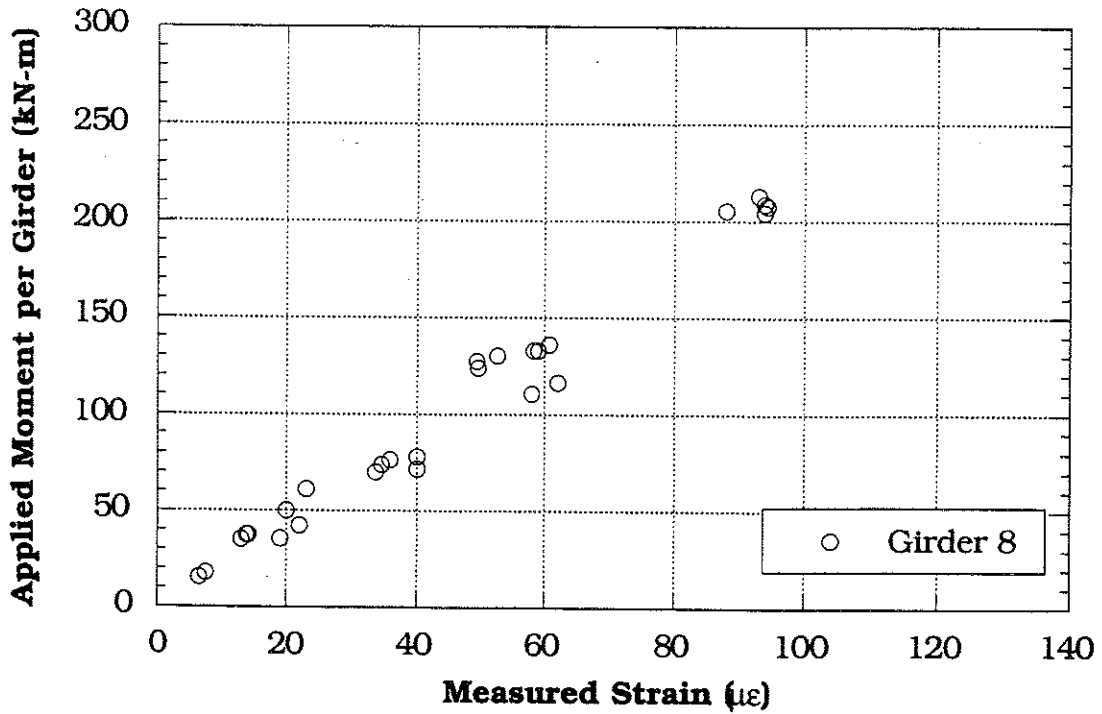


Figure 7.42 Moment per Girder vs Measured Strain, Girder 8.

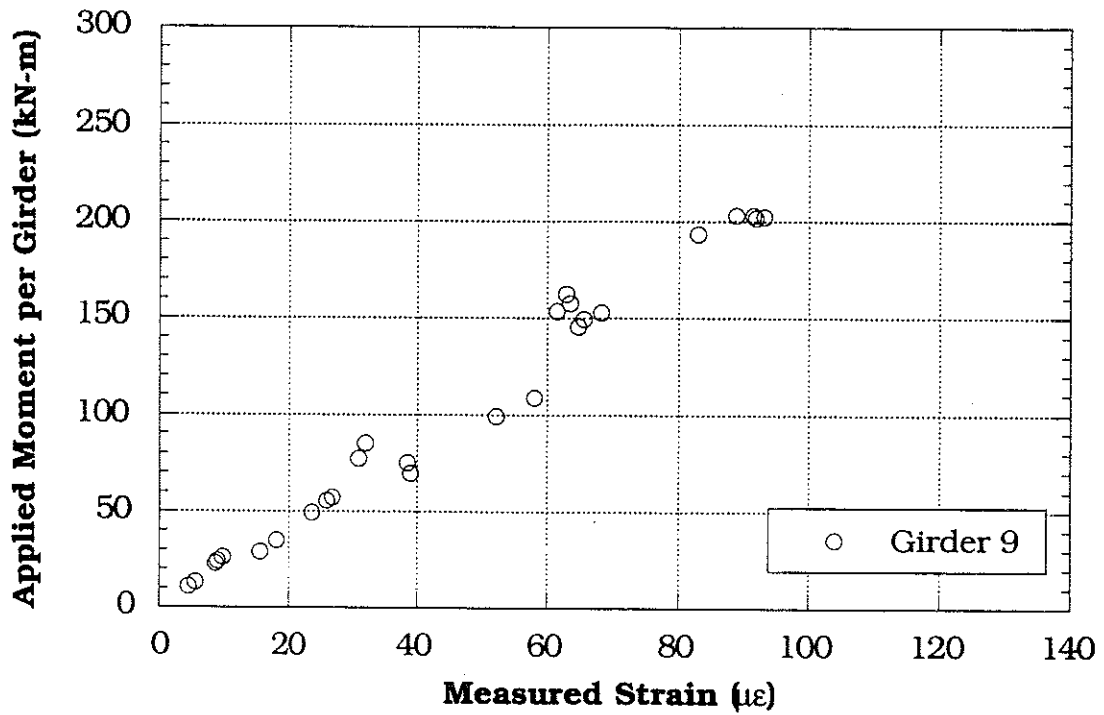


Figure 7.43 Moment per Girder vs Measured Strain, Girder 9.

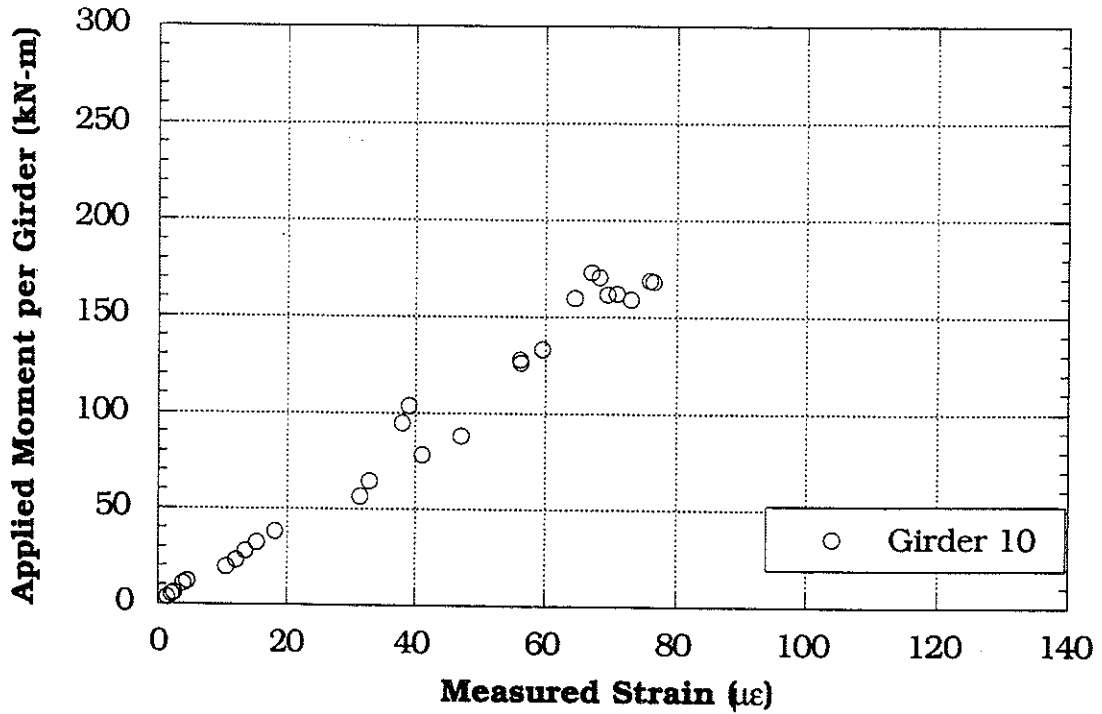


Figure 7.44 Moment per Girder vs Measured Strain, Girder 10.

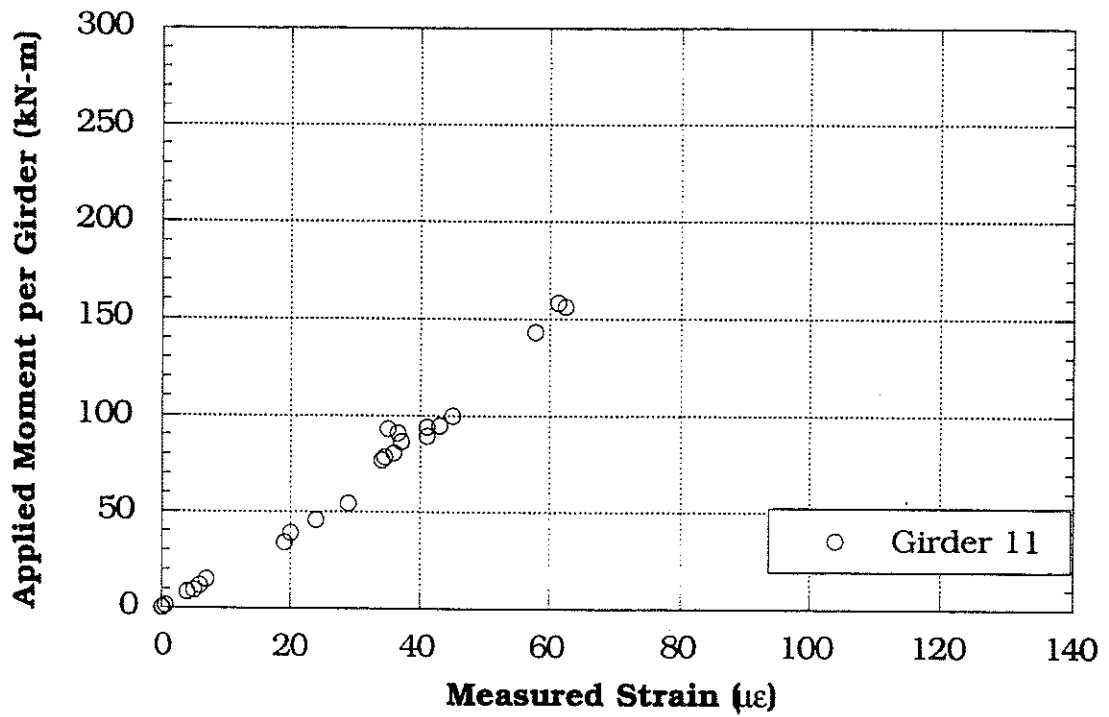


Figure 7.45 Moment per Girder vs Measured Strain, Girder 11.

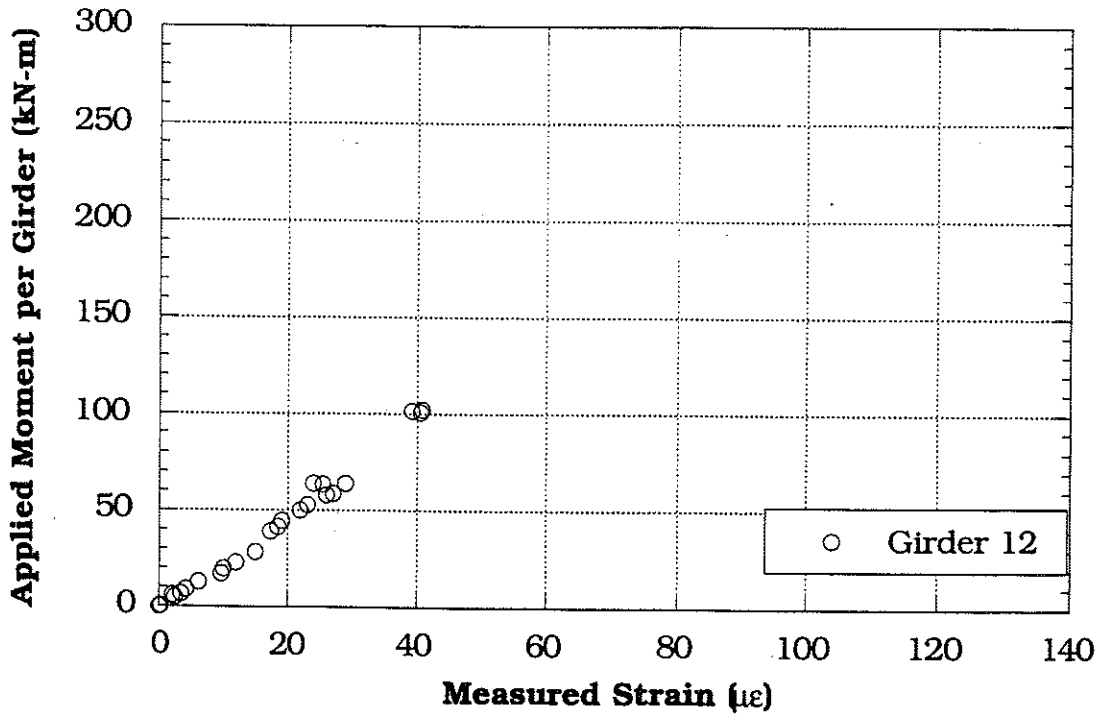


Figure 7.46 Moment per Girder vs Measured Strain, Girder 12.

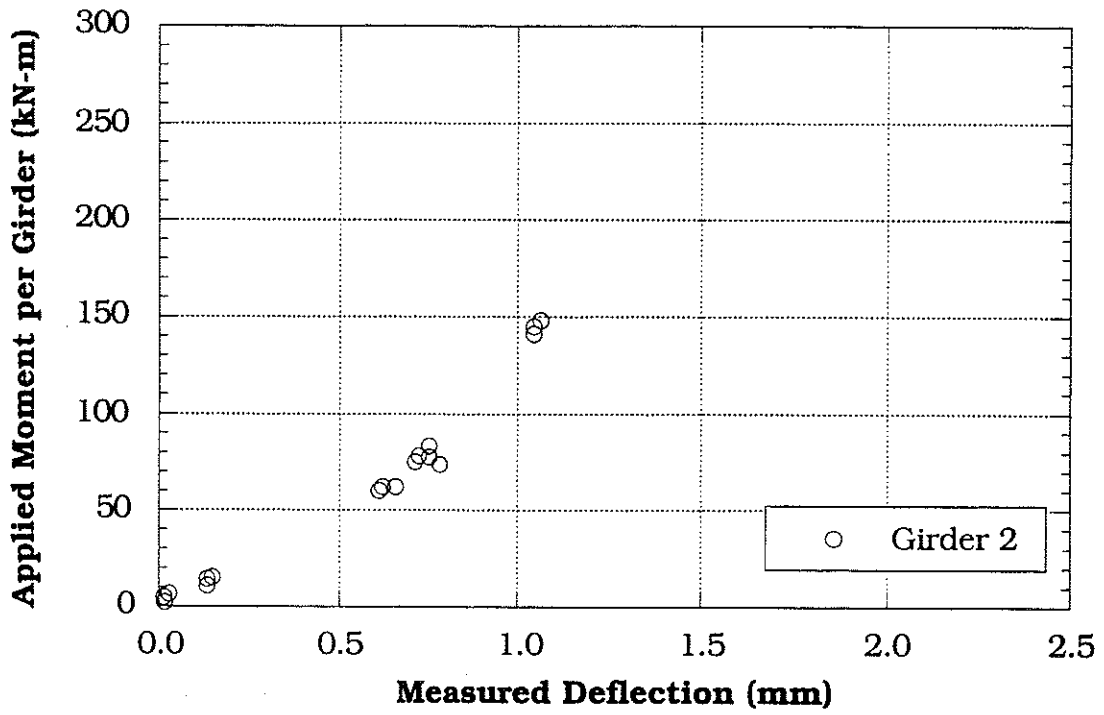


Figure 7.47 Moment per Girder vs Measured Deflection, Girder 2.

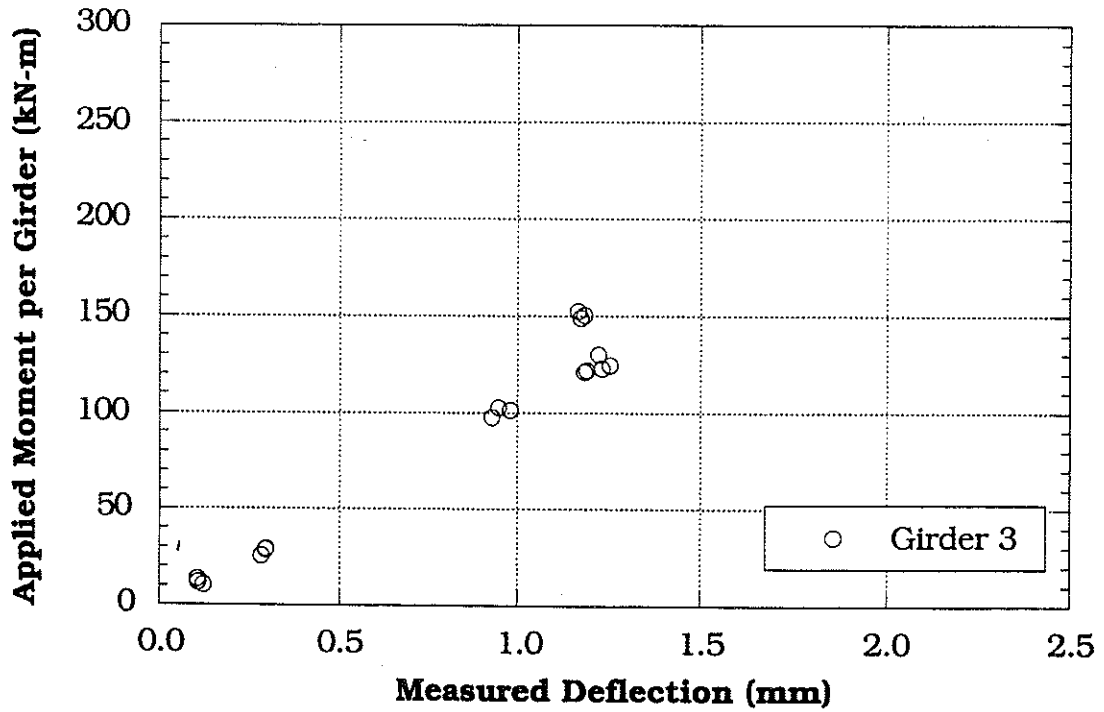


Figure 7.48 Moment per Girder vs Measured Deflection, Girder 3.

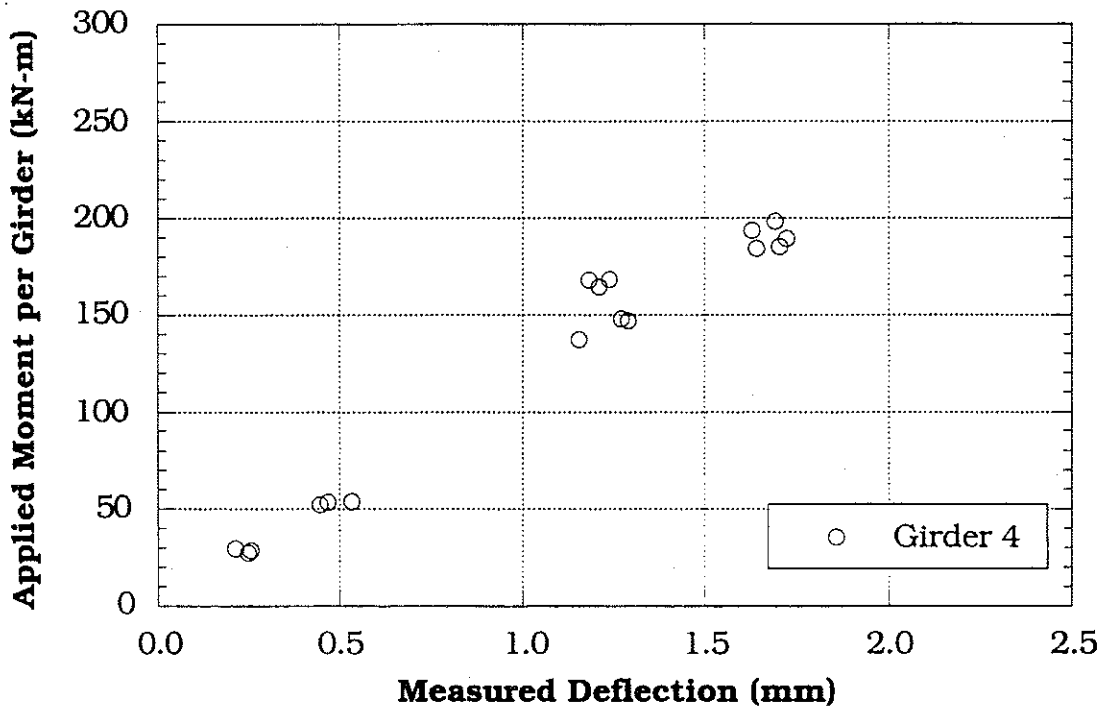


Figure 7.49 Moment per Girder vs Measured Deflection, Girder 4.

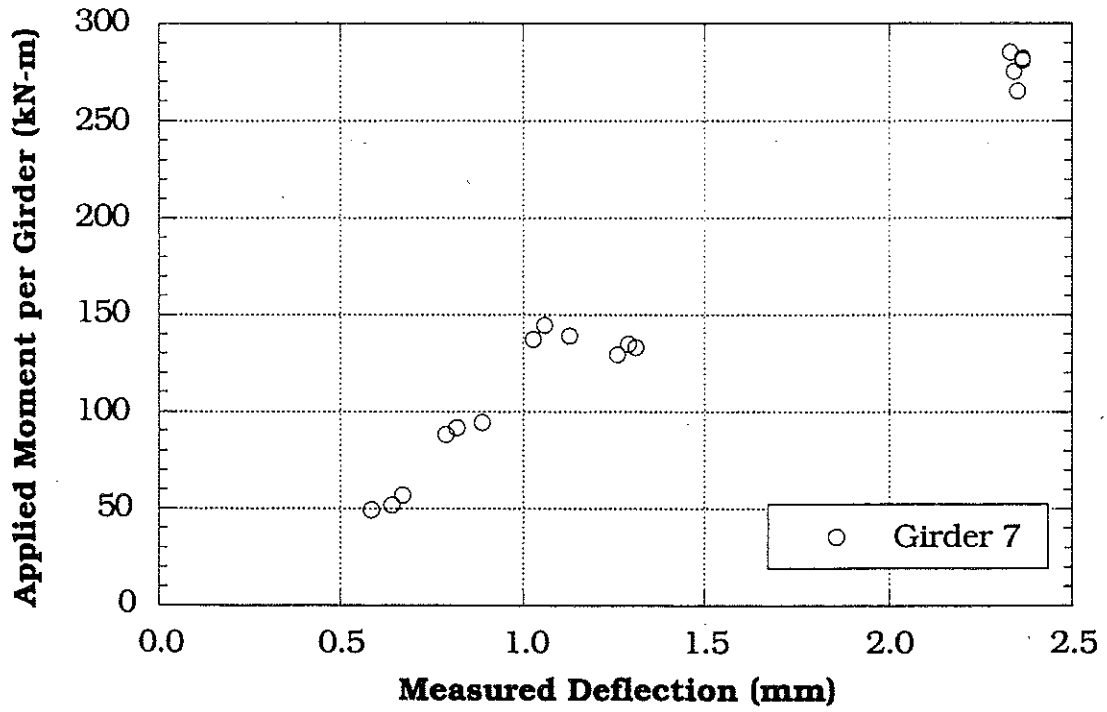


Figure 7.50 Moment per Girder vs Measured Deflection, Girder 7.

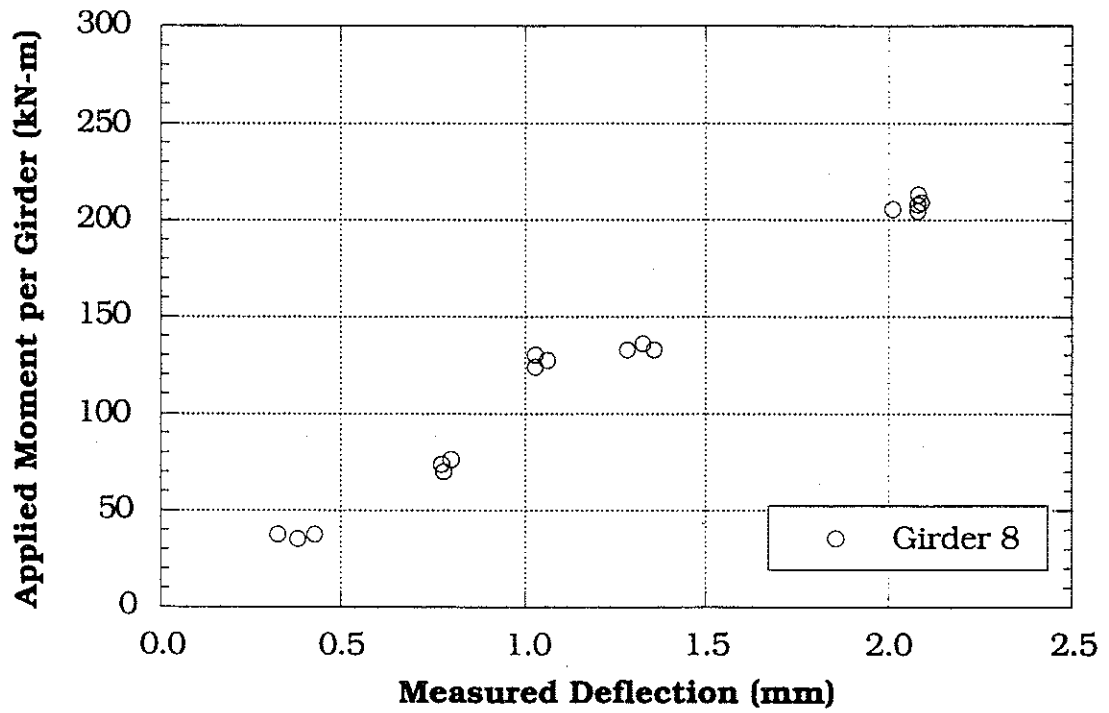


Figure 7.51 Moment per Girder vs Measured Deflection, Girder 8.

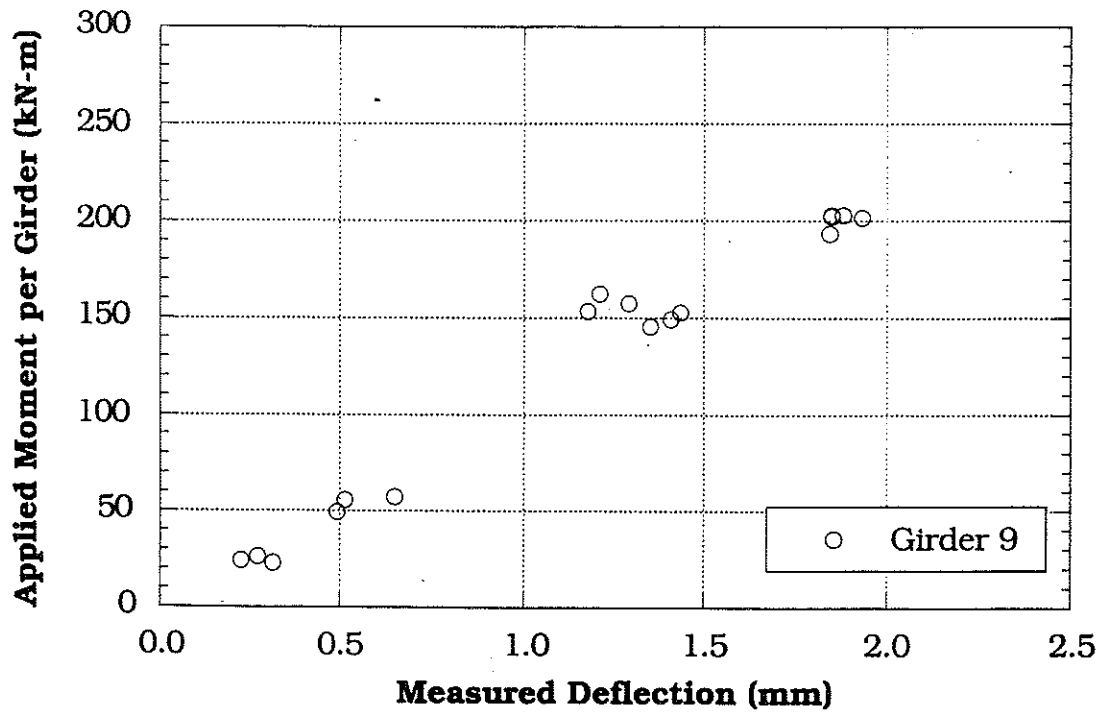


Figure 7.52 Moment per Girder vs Measured Deflection, Girder 9.

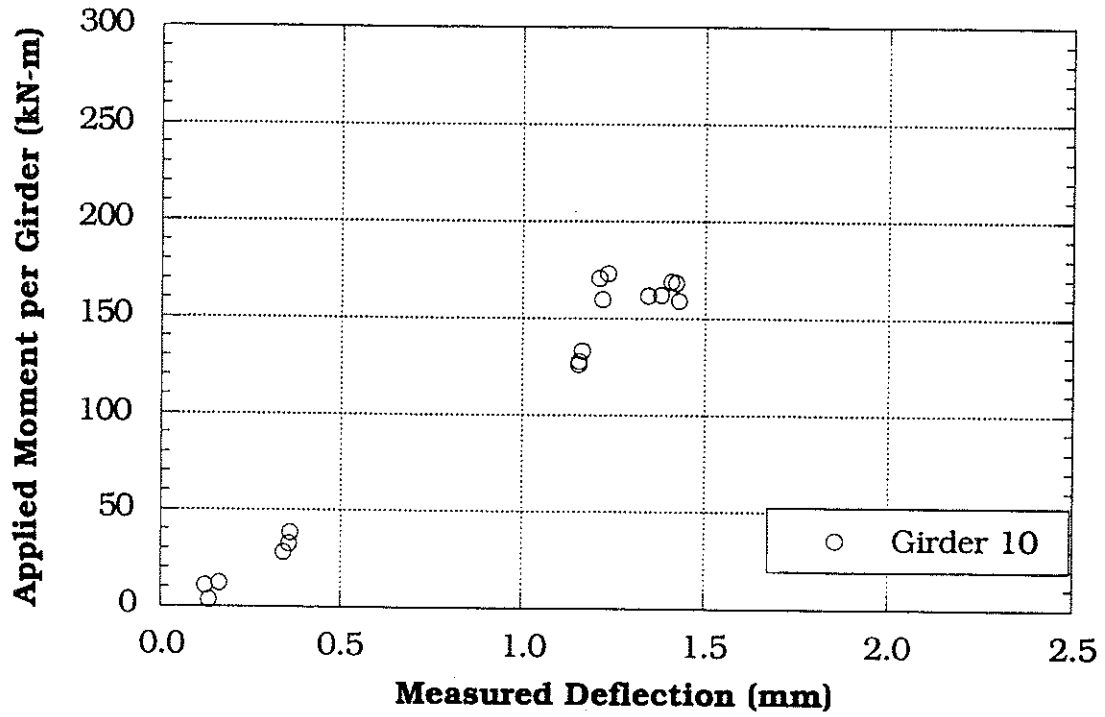


Figure 7.53 Moment per Girder vs Measured Deflection, Girder 10.

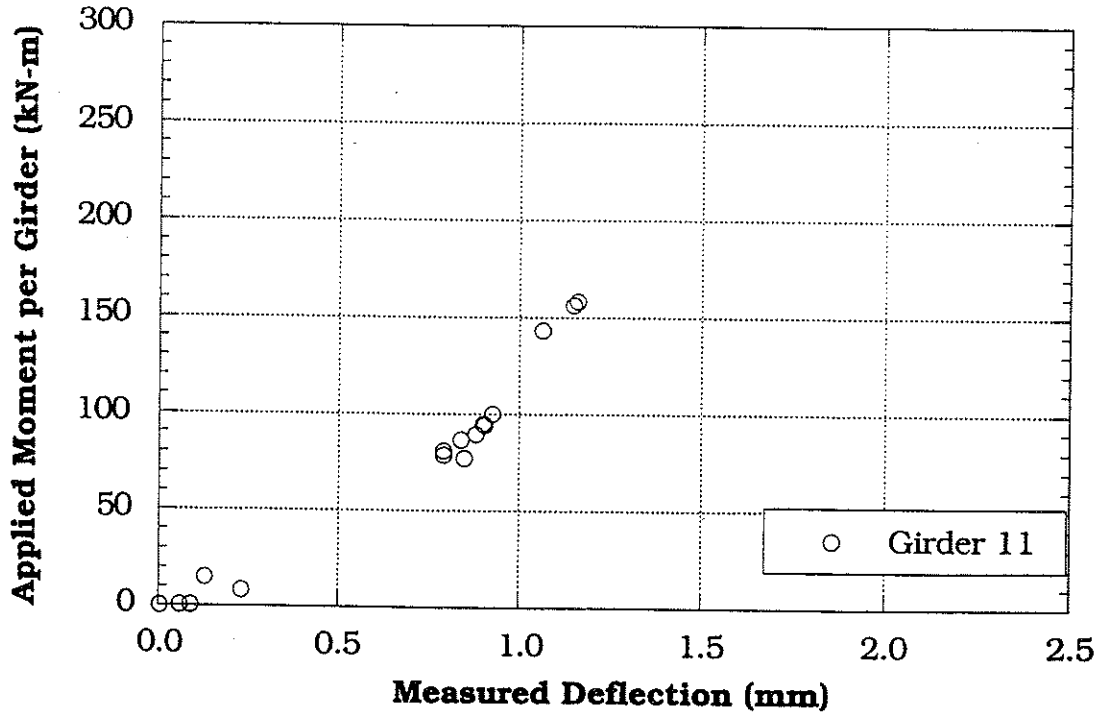


Figure 7.54 Moment per Girder vs Measured Deflection, Girder 11.

8. Bridge on M-106 over Portage River Drain near Munith (B02-38051, M106/PRD)

8.1 Description

This bridge was built in 1939 and is located on M-106 over Portage River Drain near Munith, Michigan. This bridge is designated as M106/PRD and can be identified by the road carried by the bridge and the river under the bridge. It has one lane in each direction. As shown in Figure 8.1, it has nine steel girders spaced at 1.46 m. It is a simply supported single span structure, designed as a noncomposite section. The total span length is 13.7 m with a skew of 20 degrees. The speed limit on this bridge is 89 km/h. Both the deck slab and the approach of the bridge were in good condition. The bridge has a load rating of 792 kN. The thickness of slab is 235 mm, with 61 mm of asphalt overlay.

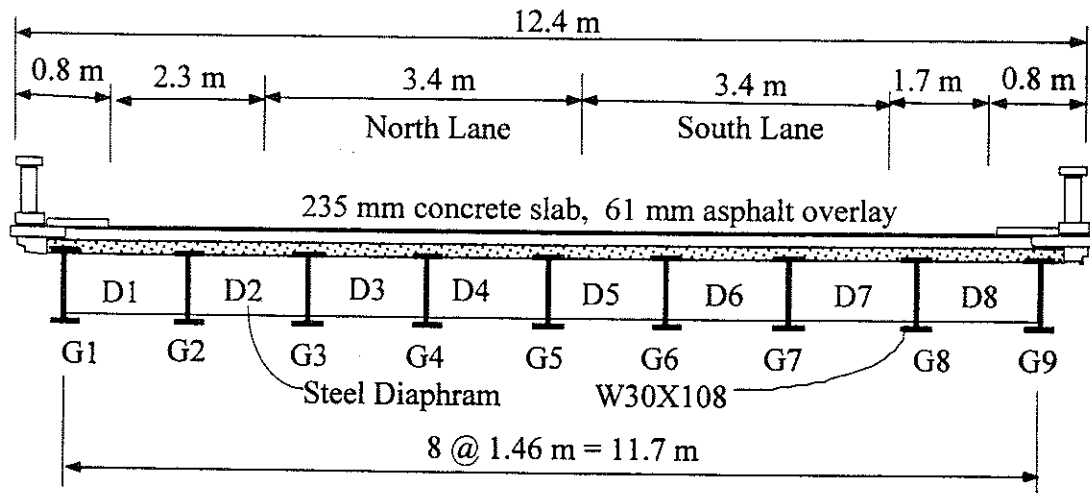


Figure 8.1 Cross-Section of Bridge M106/PRD near Munith.

8.2 Instrumentation

Strain transducers were installed on the bottom flanges of girders at mid-span (Figure 8.2). The bridge test was performed on September 25, 1997.

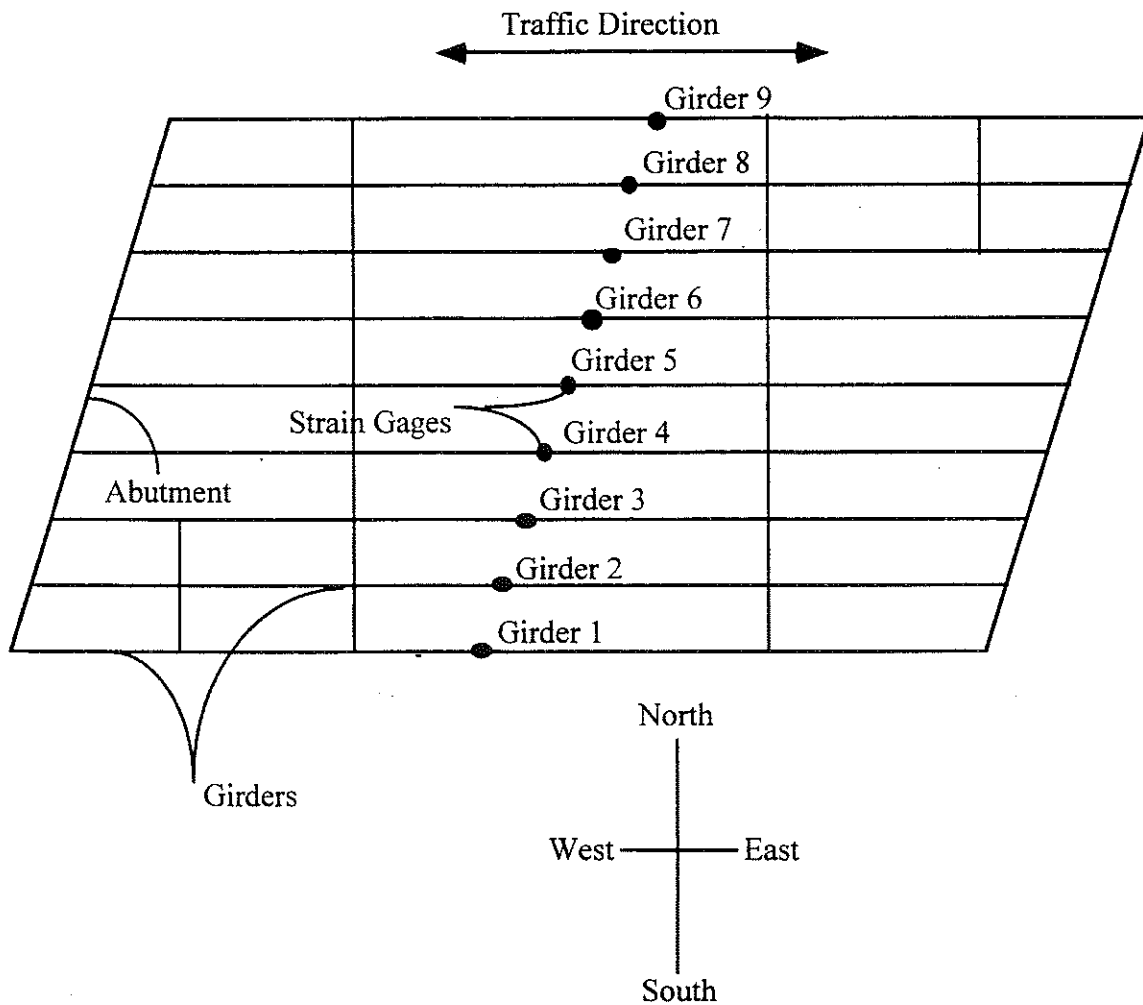


Figure 8.2 Strain Transducer Locations in Bridge M106/PRD near Bronson.

8.3 Truck Loads

Strain data necessary to calculate girder distribution and impact factors were taken from the mid-span transducers. The bridge was loaded with three-unit 10-axle and 11-axle trucks. The 10 and 11-axle trucks have gross weights of 585 kN and 644 kN, with wheelbases of 14.3 m and 15.6 m, respectively. Truck configurations are shown in Figures 8.3 and 8.4.

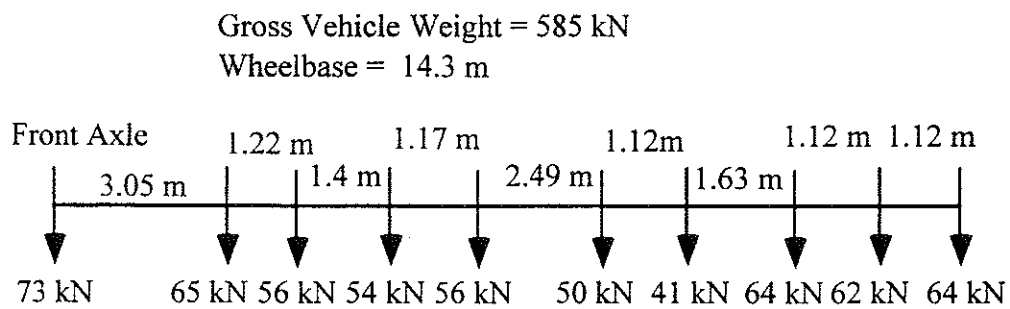


Figure 8.3 Ten-Axle Truck Configuration, Bridge M106/PRD near Munith.

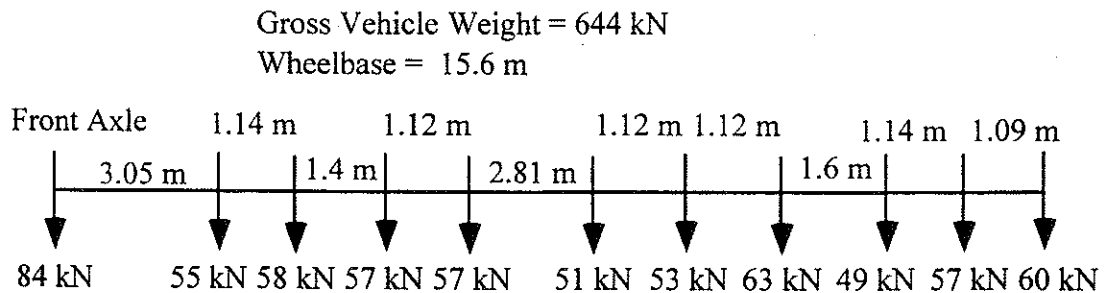


Figure 8.4 Eleven-Axle Truck Configuration, Bridge M106/PRD near Munith.

This bridge was tested only under crawling speed and full speed for the experimental derivation of load distribution and impact factors. The following load combinations were performed during the tests:

At crawling speed:

- 11-axle truck along the center of north lane
- 11-axle truck close to the curb of north lane
- 10-axle truck along the center of north lane
- 10-axle truck close to the curb of north lane
- 11-axle truck along the center of south lane
- 11-axle truck close to the curb of south lane
- 10-axle truck along the center of south lane
- 10-axle truck close to the curb of south lane
- 10-axle truck along the center of south lane and 11-axle truck along the center of north lane
- 11-axle truck along the center of south lane and 10-axle truck along the center of north lane

At high speed, the maximum speed obtained by the test trucks were:

- 10-axle truck along the center of north lane, 48 km/h
- 11-axle truck along the center of north lane, 40 km/h
- 10-axle truck along the center of south lane, 56 km/h
- 11-axle truck along the center of south lane, 40 km/h
- 10-axle truck along the center of south lane and 11-axle truck along the center of north lane, 40 km/h
- 11-axle truck along the center of south lane and 10-axle truck along the center of north lane, 40 km/h

8.4 Load Test Results

Strains from crawling-speed tests are considered static, and these were used to calculate girder distribution factors. Additional strains above the static values that were caused by high-speed tests are considered dynamic, and these were used to compute impact factors.

Figures 8.5 to 8.7 present the results of all crawling-speed (static) tests. Figures 8.5 to 8.6 present static strains and GDF's for one truck on the bridge. Figure 8.7 shows static strains and GDF's from side-by-side static load tests. GDF's are calculated from static strains using Eq. (3-4). Figure 8.7 also compares static strains obtained by superposing strains under one truck loading with those from side-by-side truck loading. They have practically the same values and again verify the superposition method used.

The maximum distribution factors from all cases in Figure 8.5 to 8.6 are presented in Figure 8.8, which represents the envelope of GDF's for one truck static loading. The maximum GDF's for one loaded lane were superimposed with the other to obtain GDF's for two-lane loading. The results are shown in Figure 8.9 together with the distribution factors from a side-by-side crawling-speed truck test.

In Figure 8.8, the results are taken as the maximum effect caused by the combination of two transverse truck positions in each lane; in the center of the lane, and near the curb. In contrast, Figure 8.9 shows the results when both trucks were in the same transverse position in their respective lanes. As expected, as the trucks are placed closer to the curbs, the GDF increases on the outside girders. The interior girders still experience a higher load effect, however. All measured GDF's are below the AASHTO Standard (S/3.36) and LRFD (two lanes) distribution factors. Actual value of the term $K_g / (L t_s^3)$ is used in calculation of Code specified GDF values.

Figures 8.10 and 8.11 present the dynamic strains obtained from high-speed tests. The distribution factors calculated from the dynamic

strains are plotted in Figures 8.12 and 8.13 and compared to Code specified values.

From the corresponding static and dynamic strains, impact factors are calculated using Eq. (3-5) and presented in Figure 8.14. As in previous tests, this bridge also shows large impact factors for exterior girders, due to a low static strain versus dynamic strain. And again, the absolute magnitude of dynamic strain at the exterior girders is low and is not significant. Figure 8.15 shows the relationship between strain magnitude and impact factors. For side-by-side truck loading, the impact factors do not exceed 10% at interior girders.

The measured static strains were compared to static strains calculated using the design stiffness and GDF's determined by tests in this study. The maximum observed strain for this bridge is $78 \mu\epsilon$ for a single truck and $112 \mu\epsilon$ for two trucks side-by-side. The corresponding calculated static strain for a single truck in a composite section is $151 \mu\epsilon$ and for a non-composite section it is $235 \mu\epsilon$. For two trucks side-by-side loading, the calculated strains are $236 \mu\epsilon$ and $369 \mu\epsilon$ for a composite section and a non-composite section, respectively.

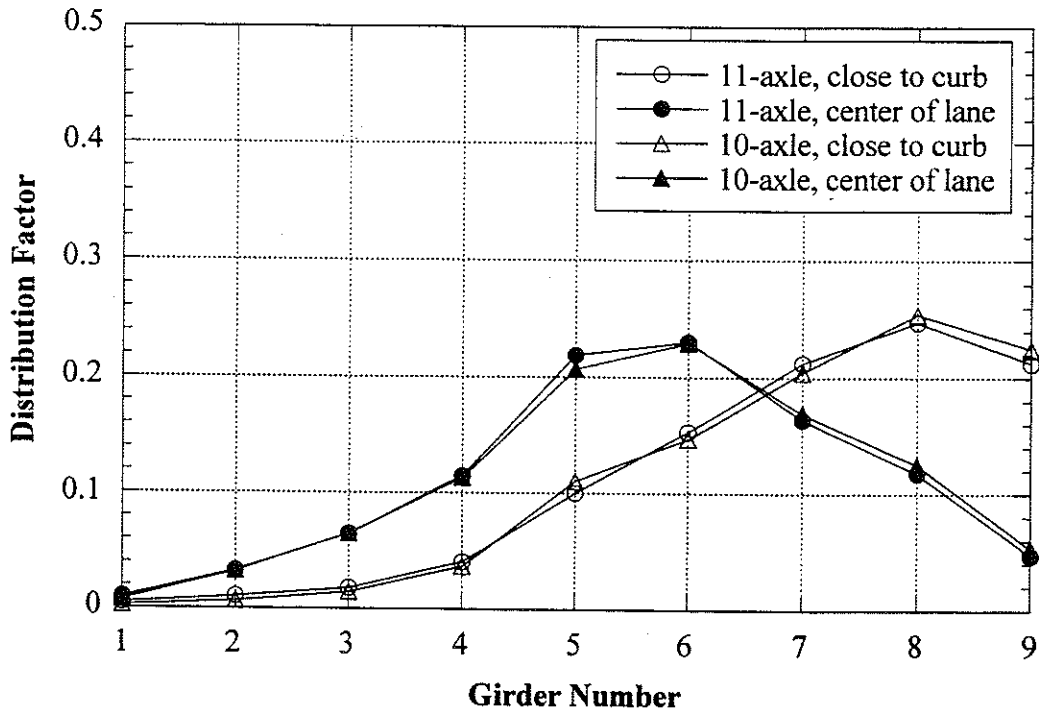
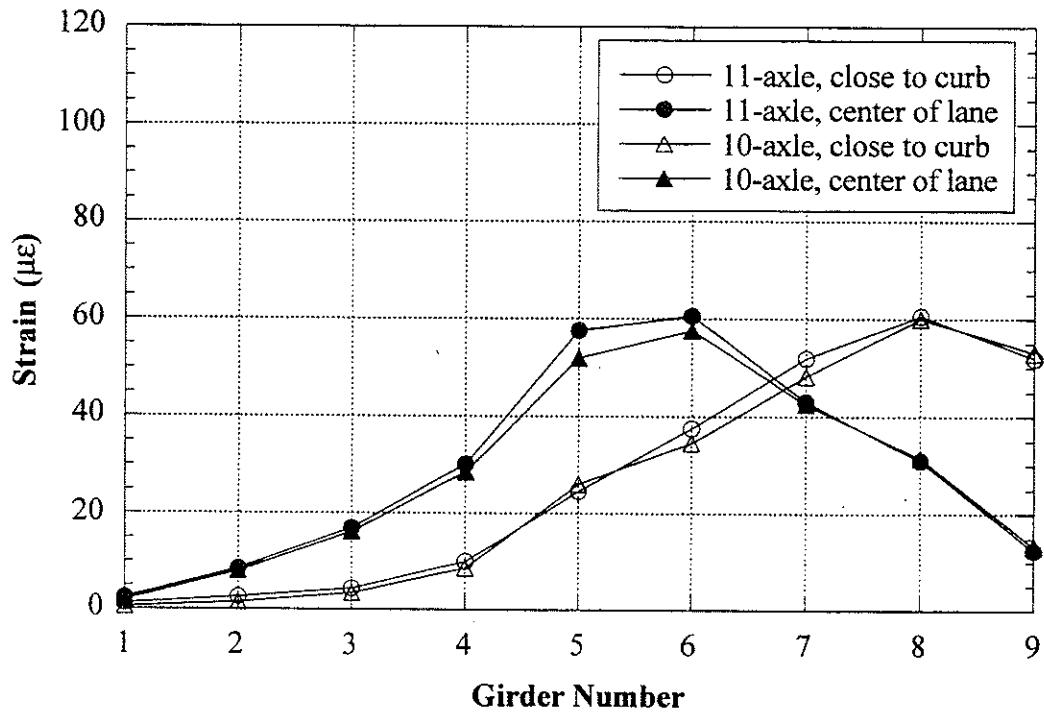


Figure 8.5 North Lane, Crawling Speed, Midspan.

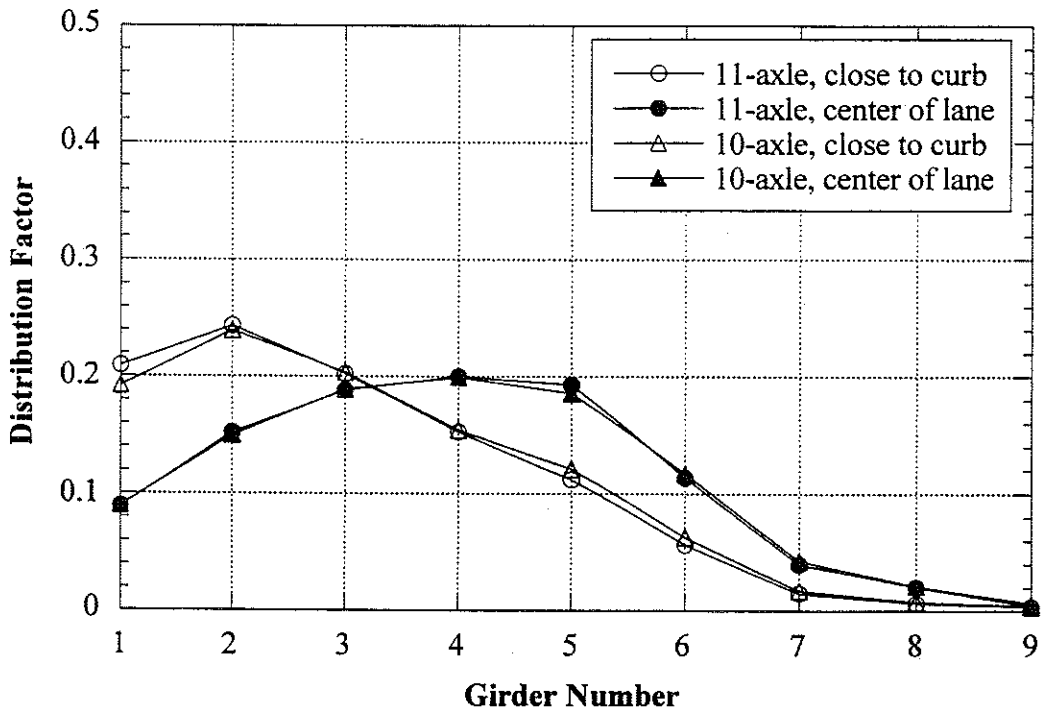
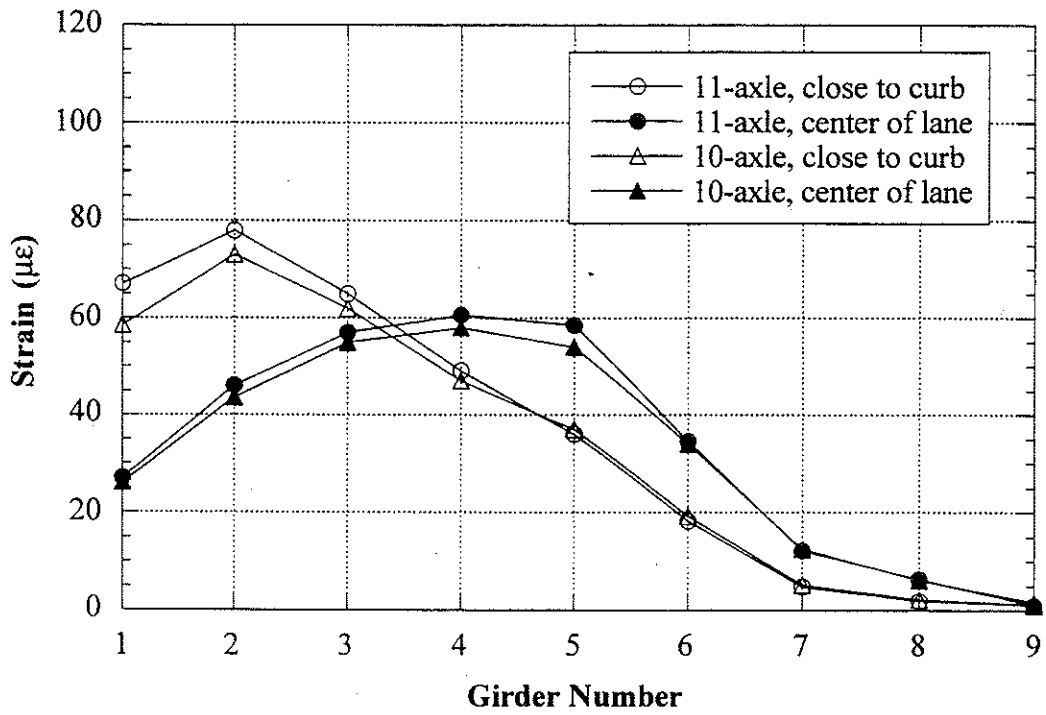


Figure 8.6 South Lane, Crawling Speed, Midspan.

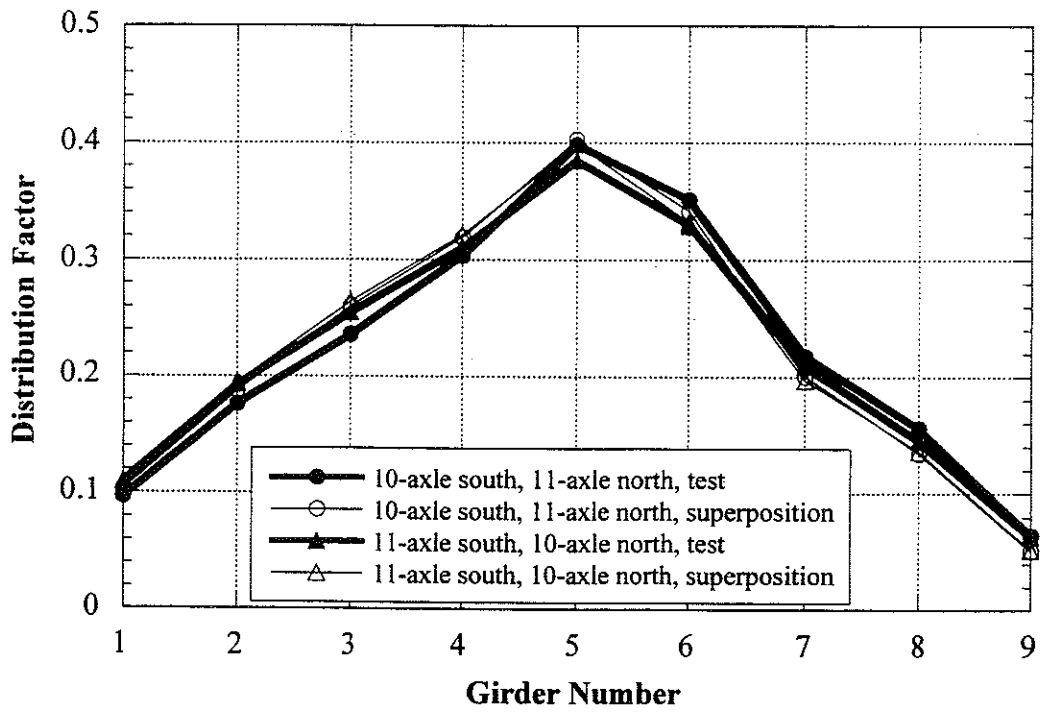
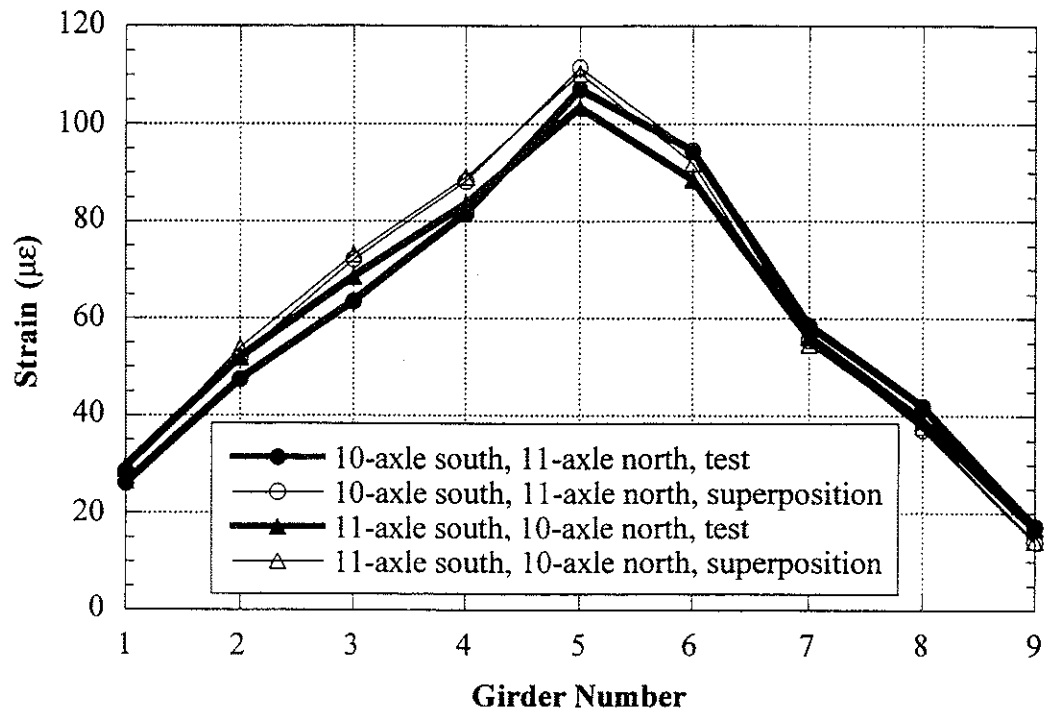


Figure 8.7 Side-by-Side Static Loading, Center of Lane, Midspan, Crawling Speed.

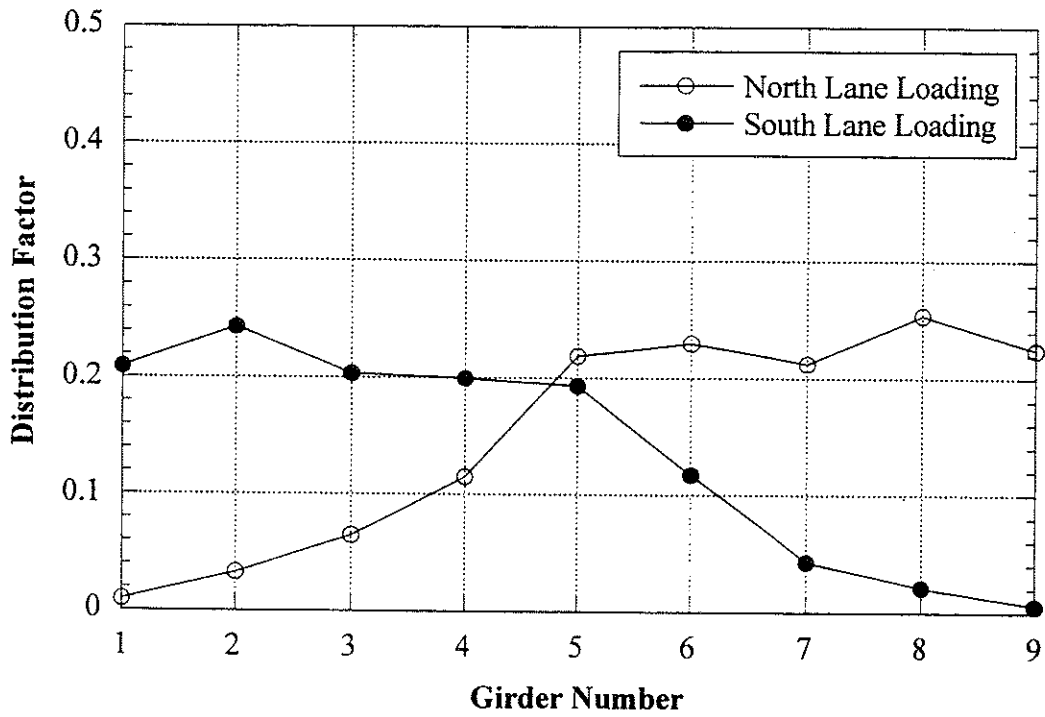


Figure 8.8 Envelope of Girder Distribution Factor For One Truck Static Loading, Crawling Speed.

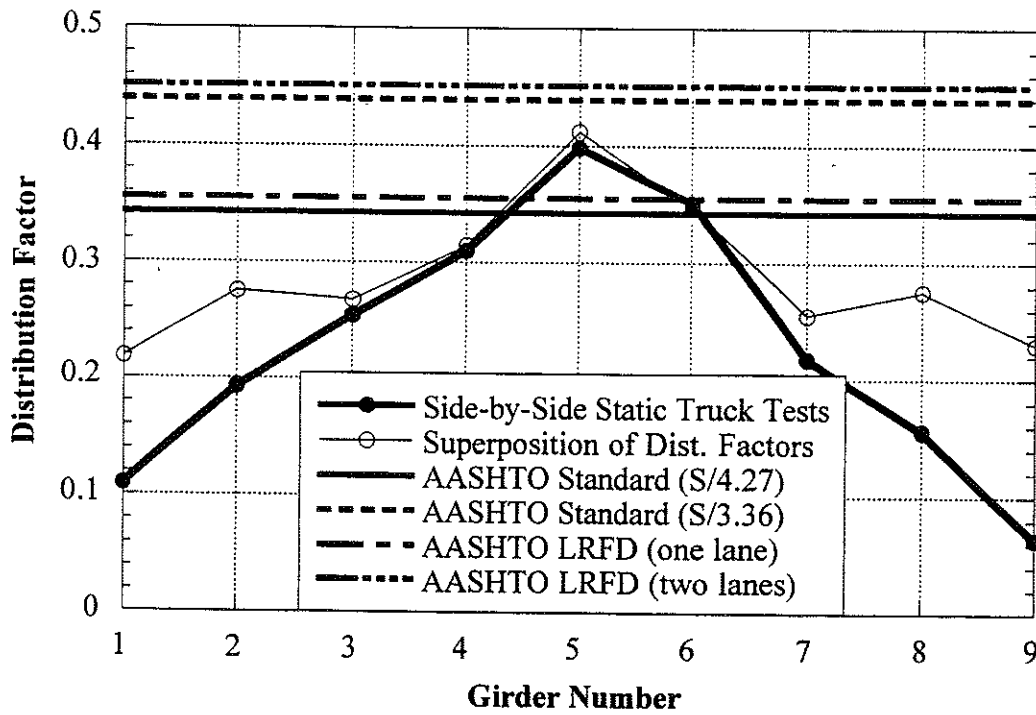


Figure 8.9 Comparison with Code Specified Distribution Factor, Crawling Speed.

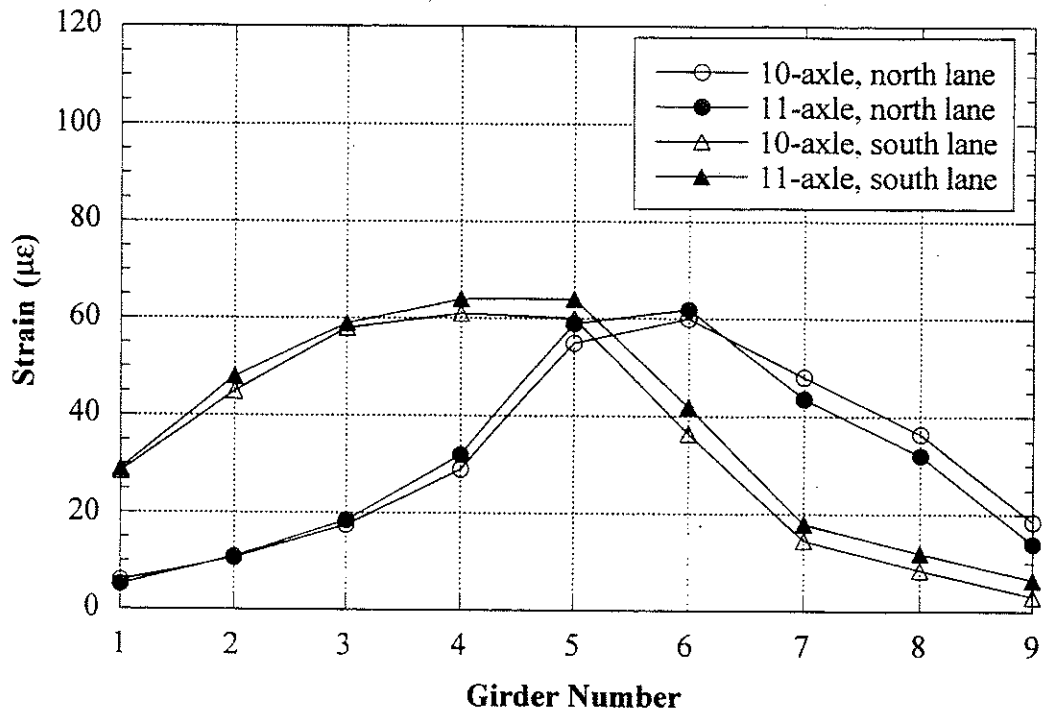


Figure 8.10 Strains under One Truck Loading at High Speed.

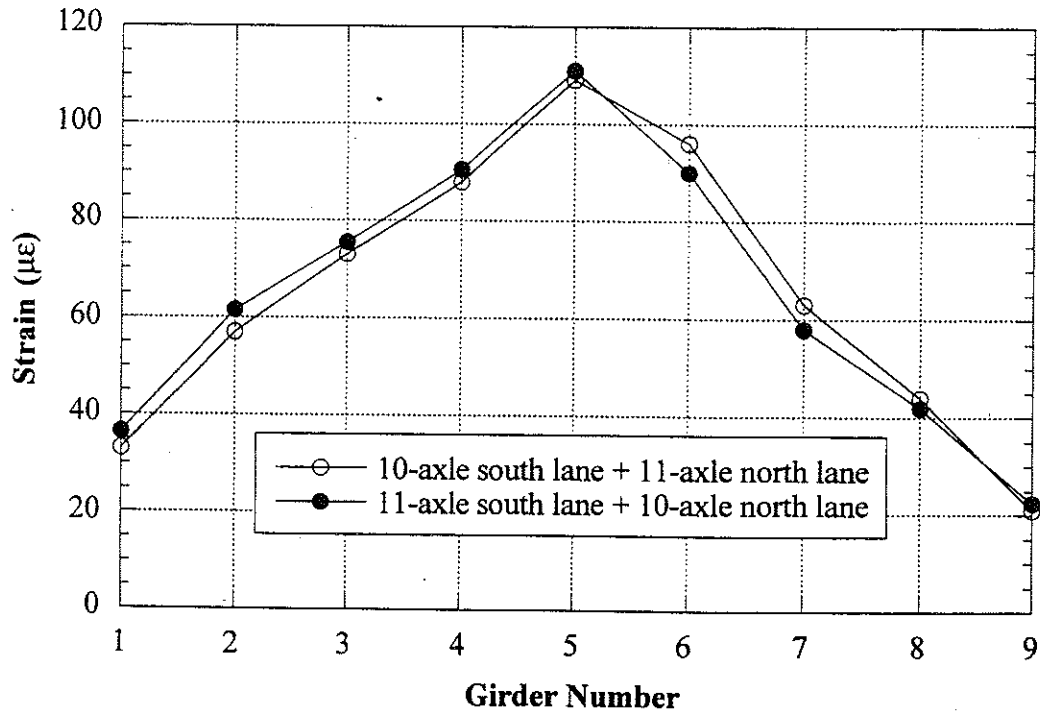


Figure 8.11 Strains under Side-by-Side Truck Loading at High Speed.

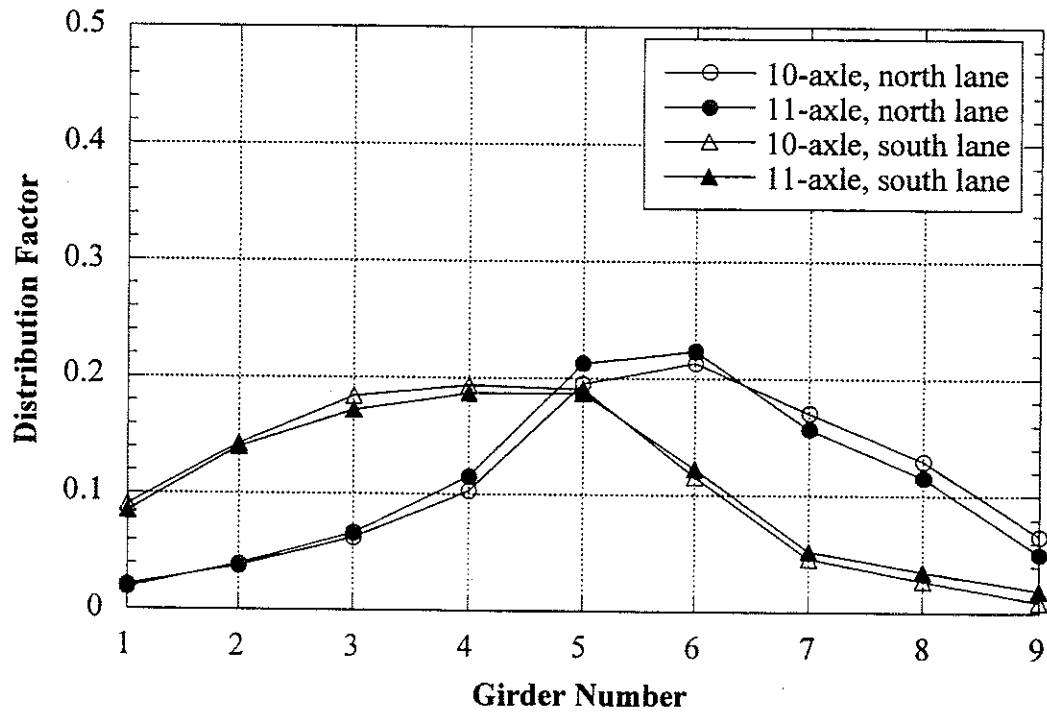


Figure 8.12 Distribution Factors for One Truck Loading at High Speed

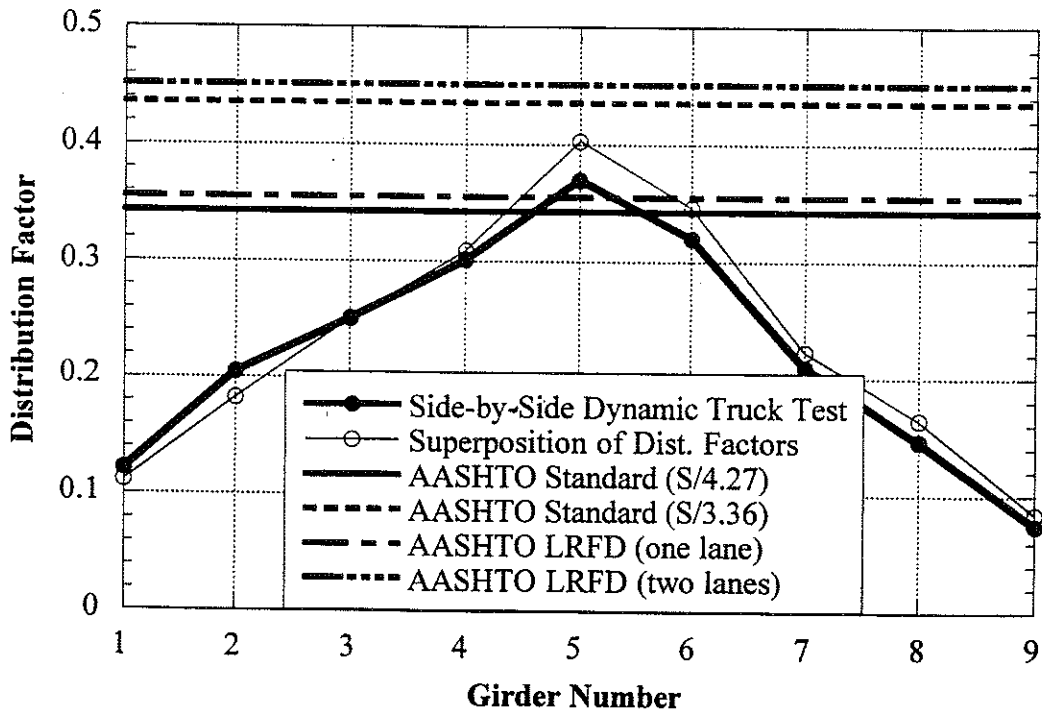


Figure 8.13 Comparison with Code Specified Distribution Factors at High Speed

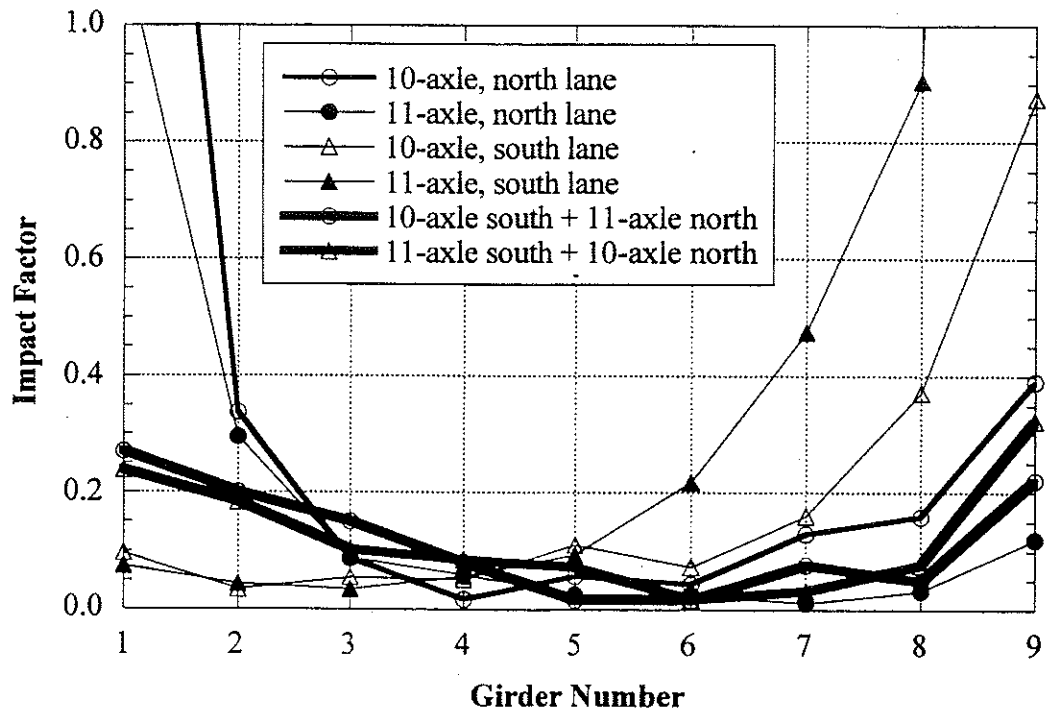


Figure 8.14 Impact Factors.

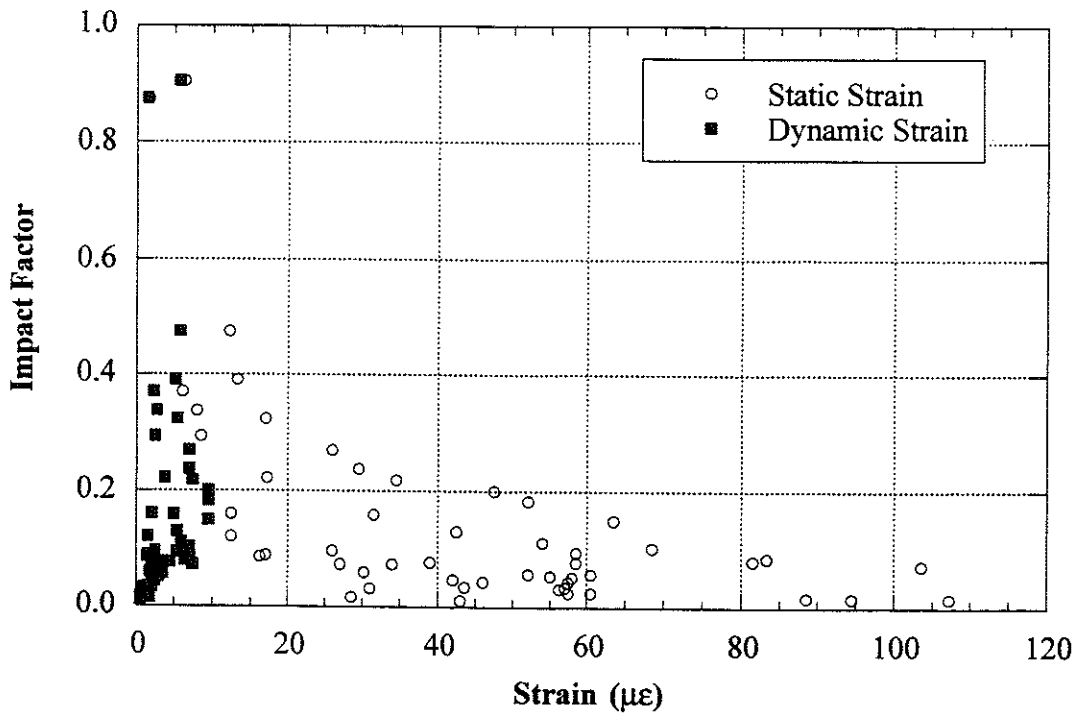


Figure 8.15 Strain versus Impact Factors.

Note:

Intentionally left blank

9. Bridge on M-45 over Bass River, West of Grand Rapids (B01-70041, M45/BR)

9.1 Description

This bridge was built in 1929 and is located on M-45 over Bass River west of Grand Rapids, Michigan. This bridge is designated as M45/BR and can be identified by the road carried by the bridge and the river under the bridge. It has one lane in each direction. As shown in Figure 9.1, it has ten steel girders spaced at 1.42 m. The total span length is 11.7 m without skew. The bridge has a slightly wider south lane than north lane. It is a simply supported single span structure and was designed to be noncomposite. The speed limit on this bridge is 88 km/h. Both the deck slab and the approach slab of the bridge were in good condition. The bridge has a load rating of 738 kN. The thickness of the slab is 317 mm, with a 38 mm asphalt overlay. The slab thickness and asphalt overlay depth were obtained from MDOT's rating sheet of the bridge.

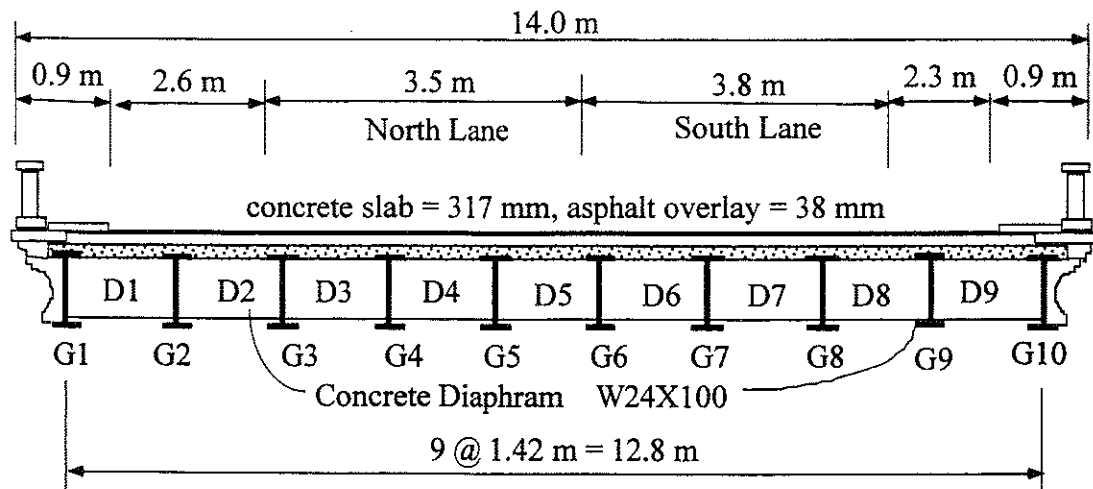


Figure 9.1 Cross-Section of Bridge M45/BR, West of Grand Rapids.

9.2 Instrumentation

Strain transducers were installed on the bottom flanges of girders at midspan (Figure 9.2). The bridge test was performed on October 30, 1997.

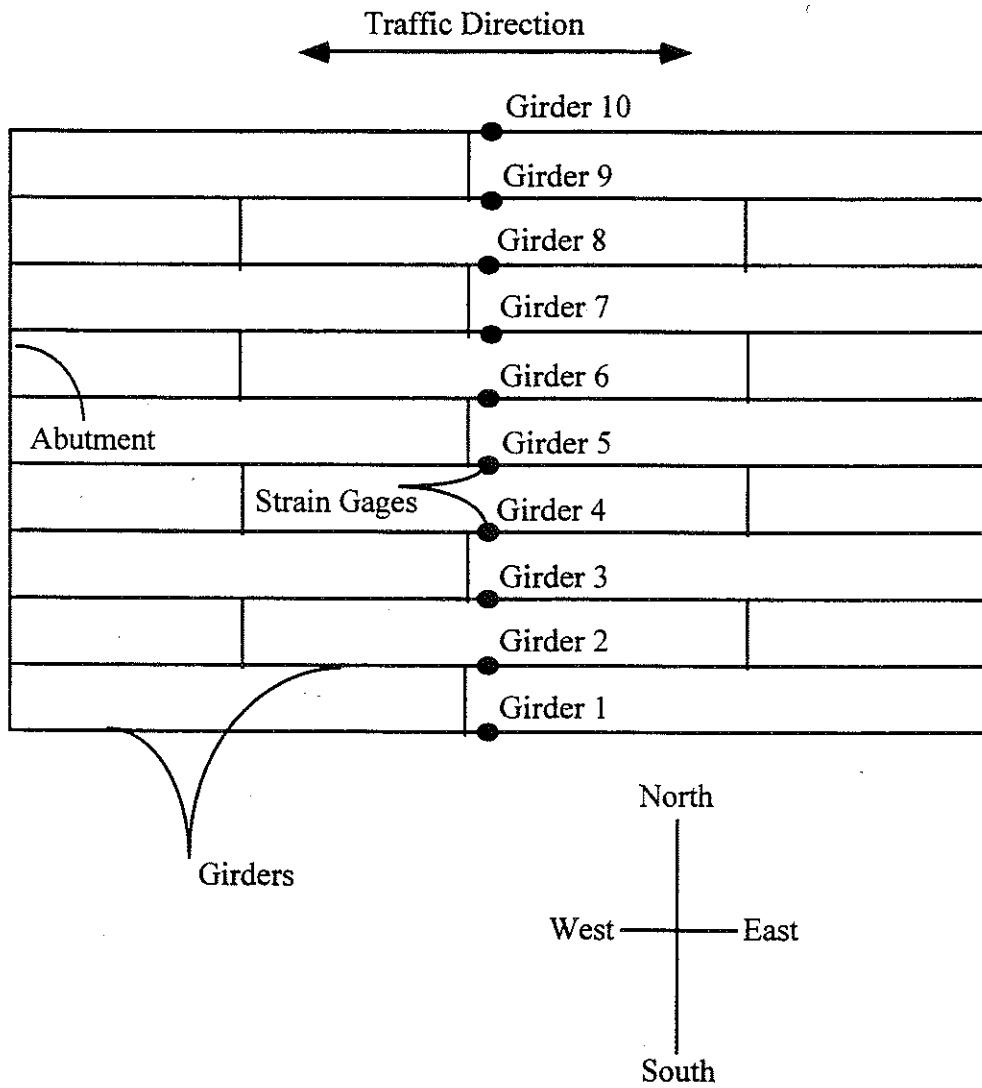


Figure 9.2 Strain Transducer Locations in Bridge M45/BR, West of Grand Rapids.

9.3 Truck Loads

Strain data necessary to calculate girder distribution and impact factors were taken from midspan transducers. The bridge was loaded with 2 three-unit 11-axle trucks. The trucks have gross weights of 696 kN and 682 kN, and both have a wheelbase of 18.2 m. Truck configurations are shown in Figures 9.3 and 9.4.

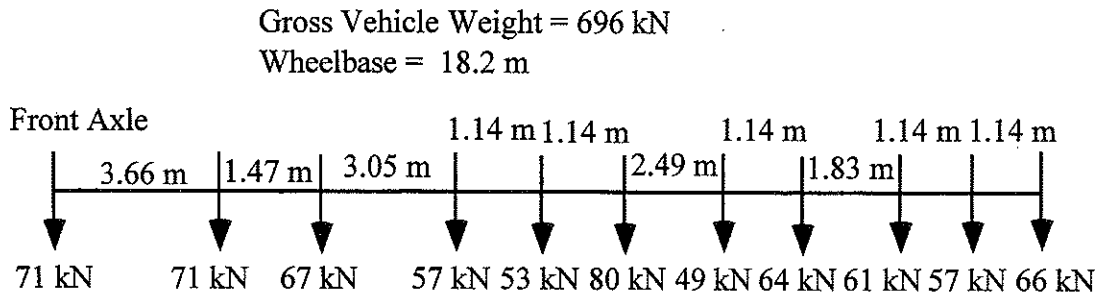


Figure 9.3 Configuration of Truck A, Bridge M45/BR, West of Grand Rapids.

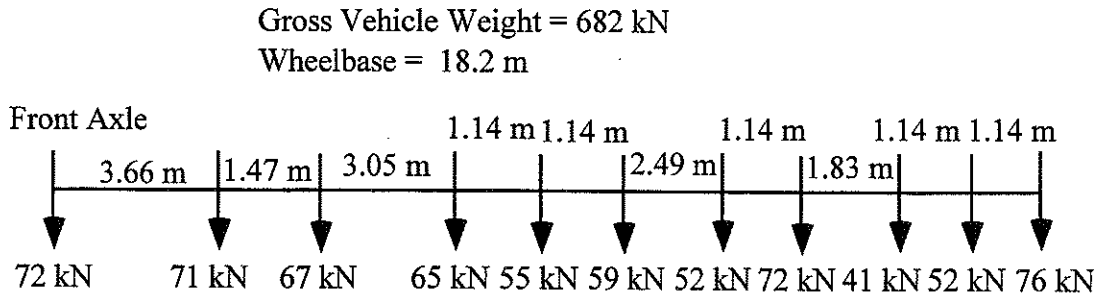


Figure 9.4 Configuration of Truck B, Bridge M45/BR, West of Grand Rapids.

This bridge was tested under crawling speed and full speed for the experimental derivation of load distribution and impact factors. The following load combinations were performed during the tests:

At crawling speed:

- truck A along the center of north lane
- truck A close to the curb of north lane

- truck B along the center of north lane
- truck B close to the curb of north lane
- truck A along the center of south lane
- truck A close to the curb of south lane
- truck B along the center of south lane
- truck B close to the curb of south lane
- truck A along the center of south lane and truck B along the center of north lane

At high speed, the maximum speed obtained by the test trucks were:

- truck A along the center of north lane, 48 km/h
- truck B along the center of north lane, 56 km/h
- truck A along the center of south lane, 56 km/h
- truck B along the center of south lane, 56km/h
- truck A along the center of south lane and truck B along the center of north lane, 58km/h

9.4 Load Test Results

Strains from crawling-speed tests were used to obtain static strains to calculate girder distribution factors and to calculate impact factors by comparing with strains from high-speed tests. In other words, strains from crawling-speed tests are considered as static strain, while strains from high speed tests provide dynamic strains.

Figures 9.5 to 9.7 present the results of all crawling-speed (static) tests. Figures 9.5 to 9.6 present static strains and GDF's for one truck on the bridge. Figure 9.7 shows static strains and GDF's from side-by-side static load tests. GDF's are calculated from static strains using Eq. (3-4). Figure 9.7 also compares static strains obtained by superposing

strains under one truck loading with those from side-by-side truck loading. They have practically the same values and again verify the superposition method used.

The maximum distribution factors from all cases in Figure 9.5 to 9.6 are presented in Figure 9.8, which represents the envelope of GDF's for one truck static loading. The maximum GDF's for one loaded lane were superimposed with the other to obtain GDF's for two-lane loading. The results are shown in Figure 9.9 together with the distribution factors from a side-by-side crawling-speed truck test.

In Figure 9.8, the results are taken as the maximum effect caused by the combination of two transverse truck positions in each lane; in the center of the lane, and near the curb. In contrast, Figure 9.9 shows the results when both trucks were in the same transverse position in their respective lanes. As expected, as the trucks are placed closer to the curbs, the GDF increases on the outside girders. The interior girders still experience a higher load effect. Measured GDF's are close to the specified AASHTO LRFD Code GDF (two lanes) but less than Standard GDF (S/3.36). AASHTO Standard (S/4.27) and LRFD (one lane) GDF's are also plotted in Figure 9.9. Actual value of the term $K_g / (L t_s^3)$ is used in calculation of Code specified GDF values.

Figures 9.10 and 9.11 present the dynamic strains obtained from high-speed tests. Girder distribution factors calculated from dynamic strains are plotted and compared with Code specified GDF's in Figure 9.13.

From the corresponding static and dynamic strains, impact factors are calculated using Eq. (3-5) and presented in Figure 9.14. As in previous tests, this bridge also shows large impact factors for exterior girders, due to a low static strain versus dynamic strain. And again, the absolute magnitude of dynamic strain at the exterior girders is low and is not significant. Figure 9.15 shows the relationship between strain magnitude and impact factors. For side-by-side truck loading, the impact factors do not exceed 10% at interior girders.

The measured static strains were compared to static strains calculated using the design stiffness and GDF's determined by tests in this study. The maximum observed static strain for this bridge is 64 $\mu\epsilon$ for a single truck and 96 $\mu\epsilon$ for two trucks side-by-side. The corresponding calculated strain for a single truck in a composite section is 139 $\mu\epsilon$ and for a non-composite section it is 249 $\mu\epsilon$. For two trucks side-by-side loading, the calculated strains are 172 $\mu\epsilon$ and 308 $\mu\epsilon$ for a composite section and non-composite section, respectively.

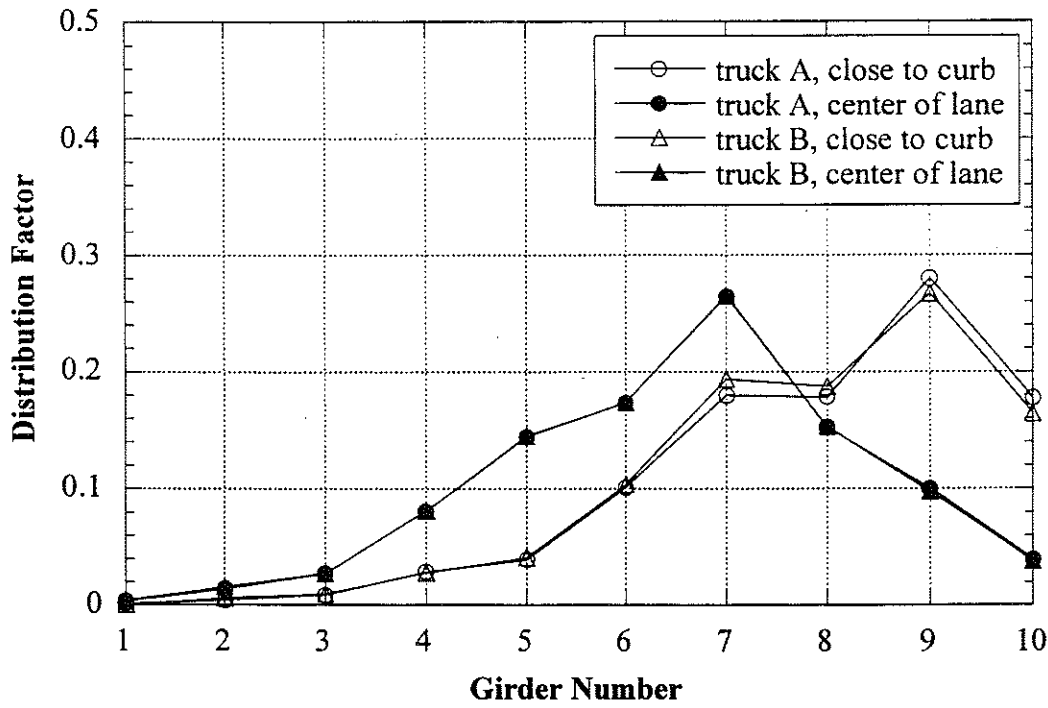
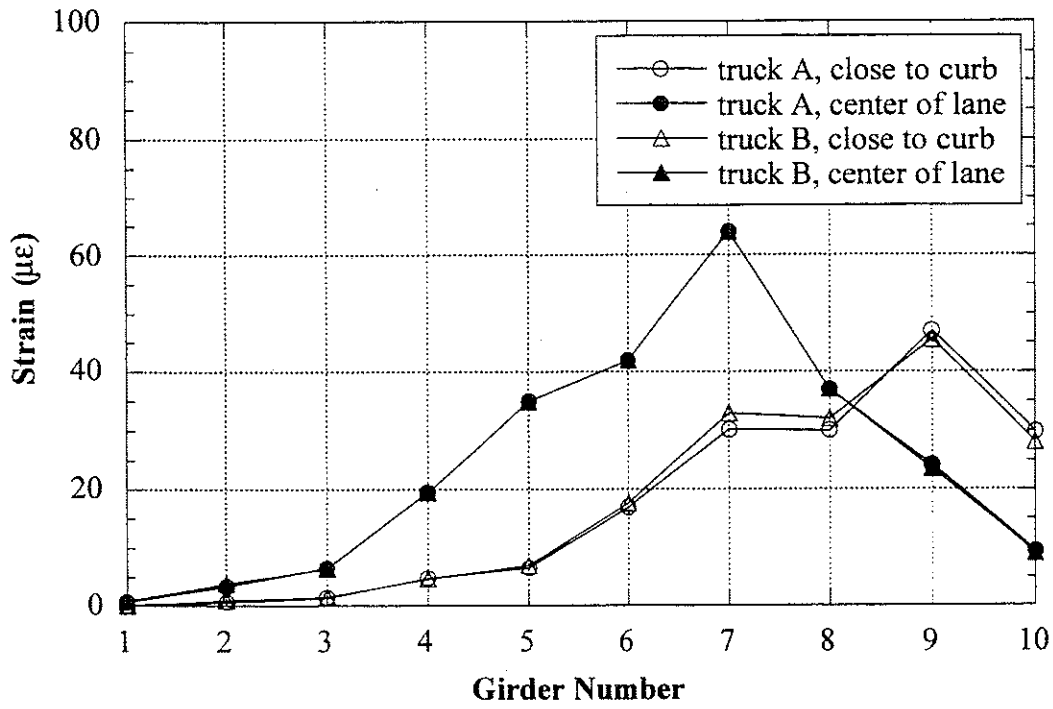


Figure 9.5 North Lane, Crawling Speed.

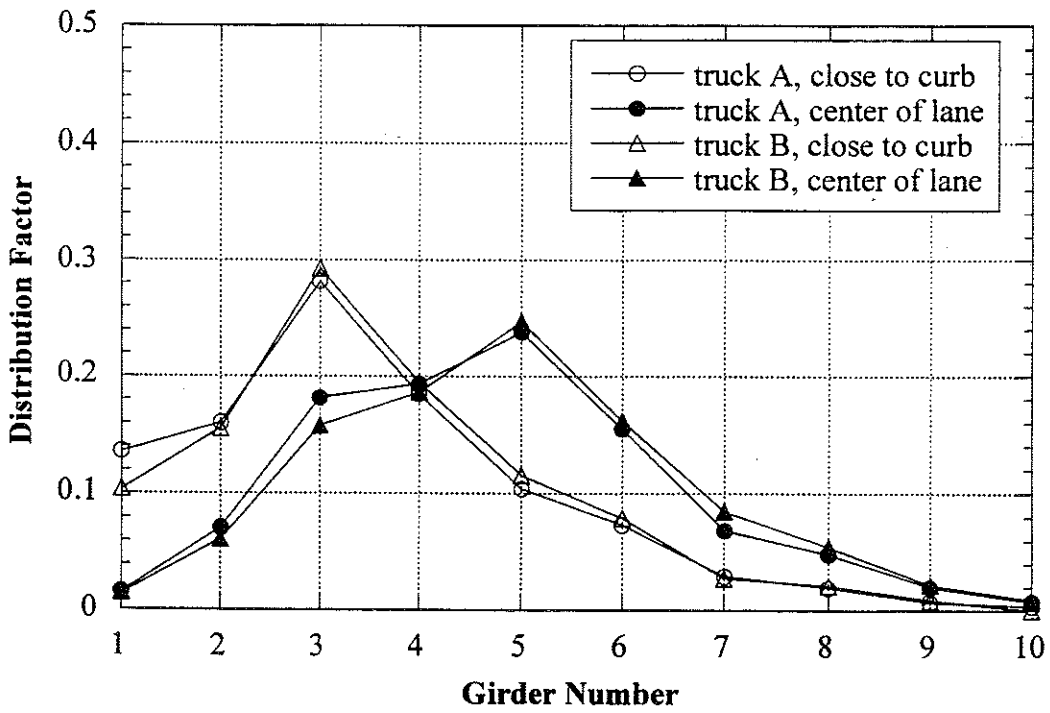
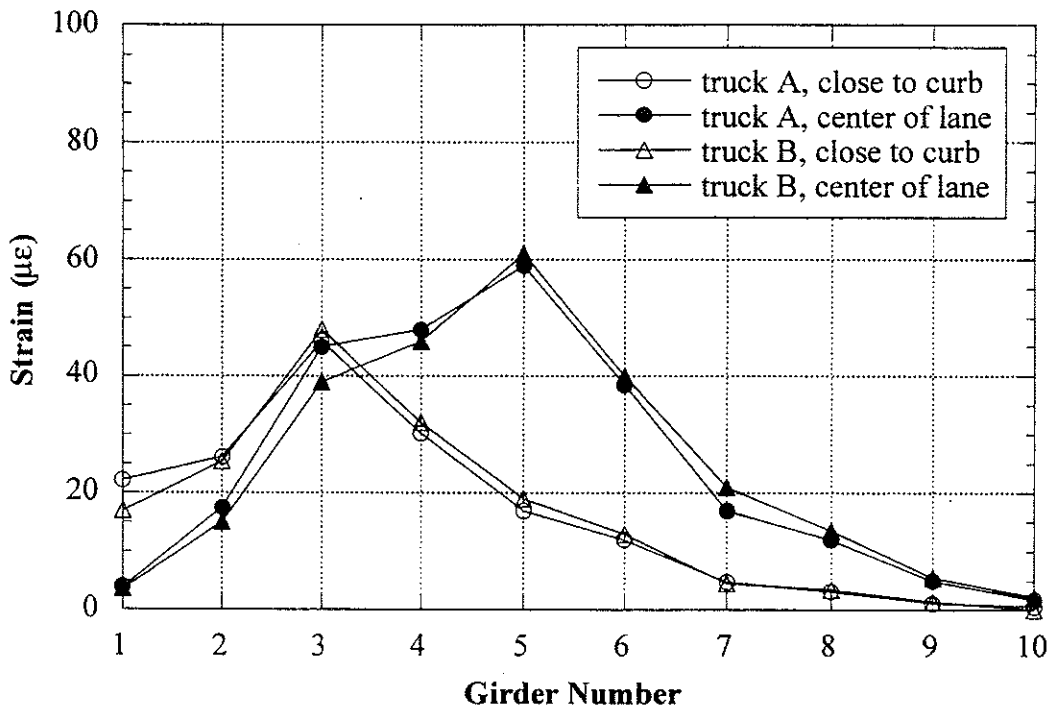


Figure 9.6 South Lane, Crawling Speed.

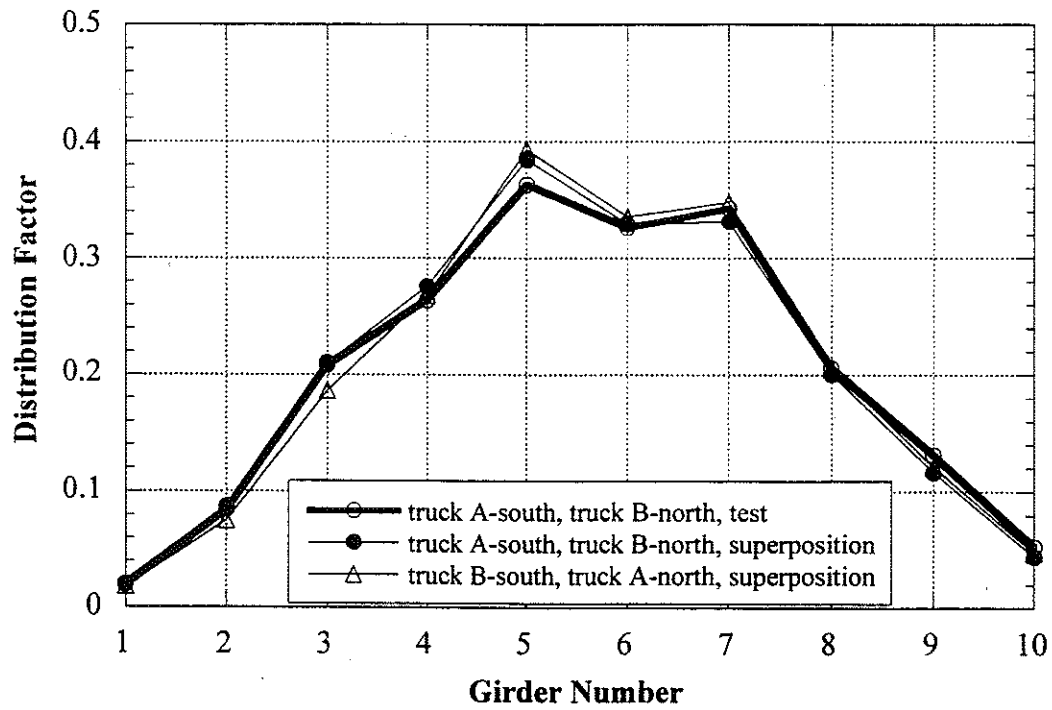
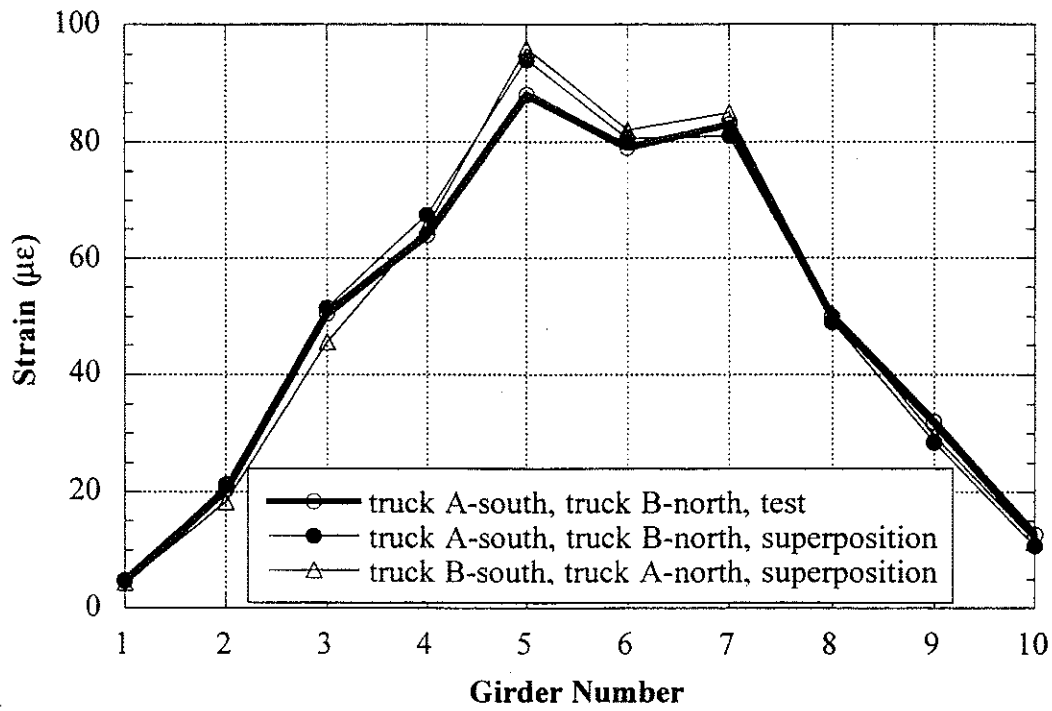


Figure 9.7 Side-by-Side Static Loading, Center of Lane.

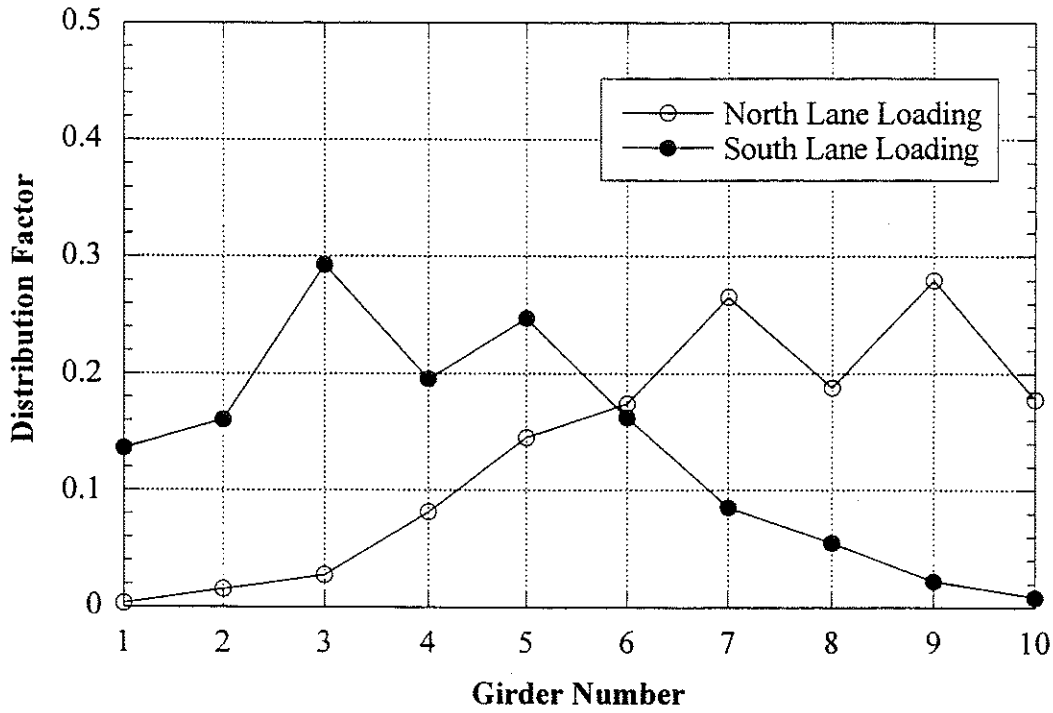


Figure 9.8 Envelope of Girder Distribution Factor For One Truck Static Loading, Crawling Speed.

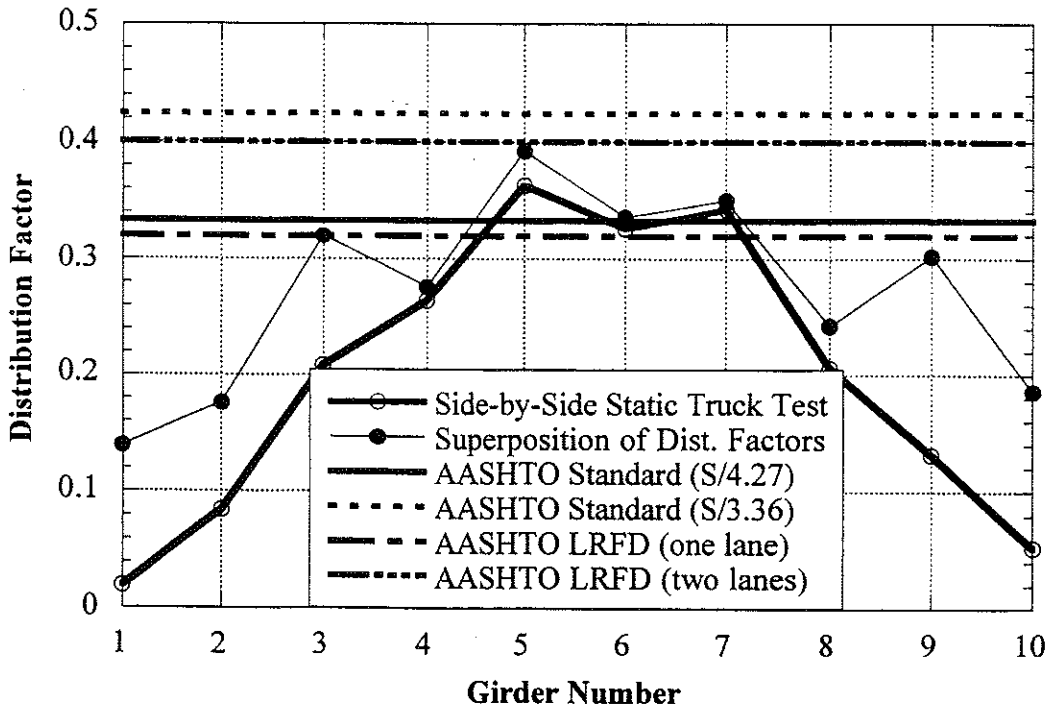


Figure 9.9 Comparison with Code Specified Distribution Factor, Crawling Speed.

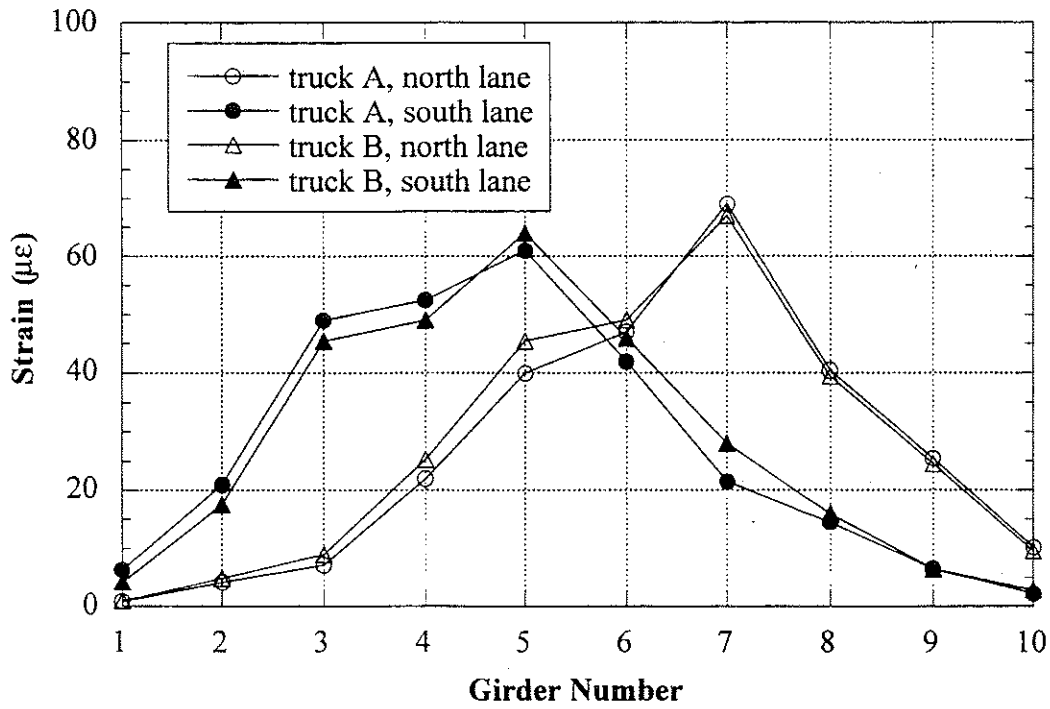


Figure 9.10 Strains under One Truck Loading at High Speed.

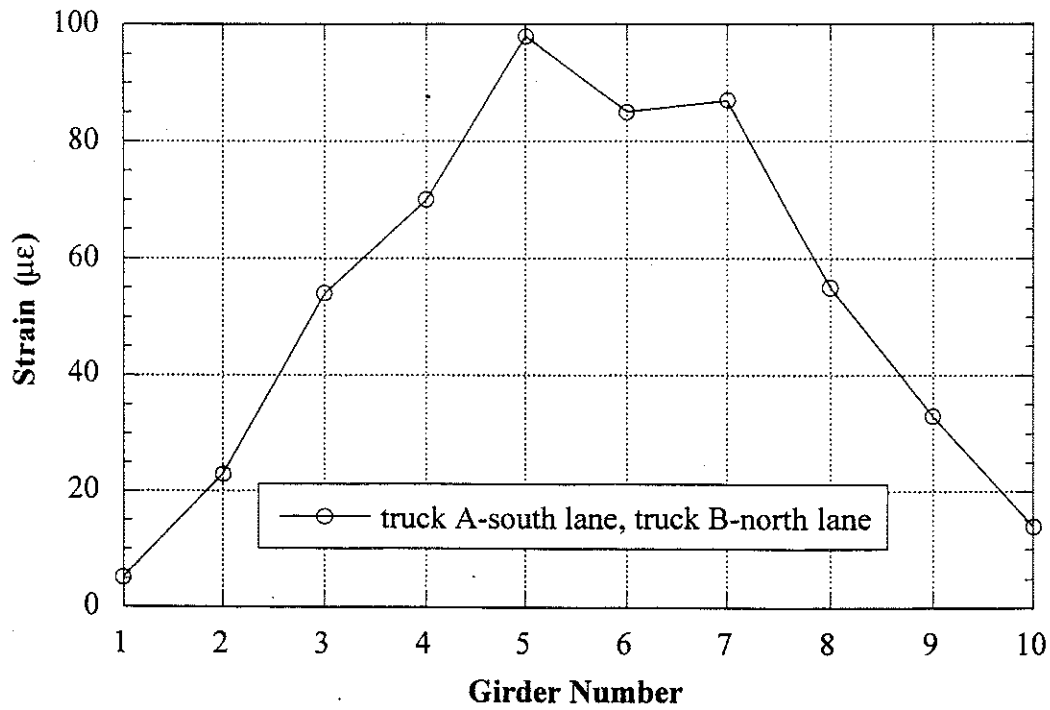


Figure 9.11 Strains under Side-by-Side Truck Loading at High Speed.

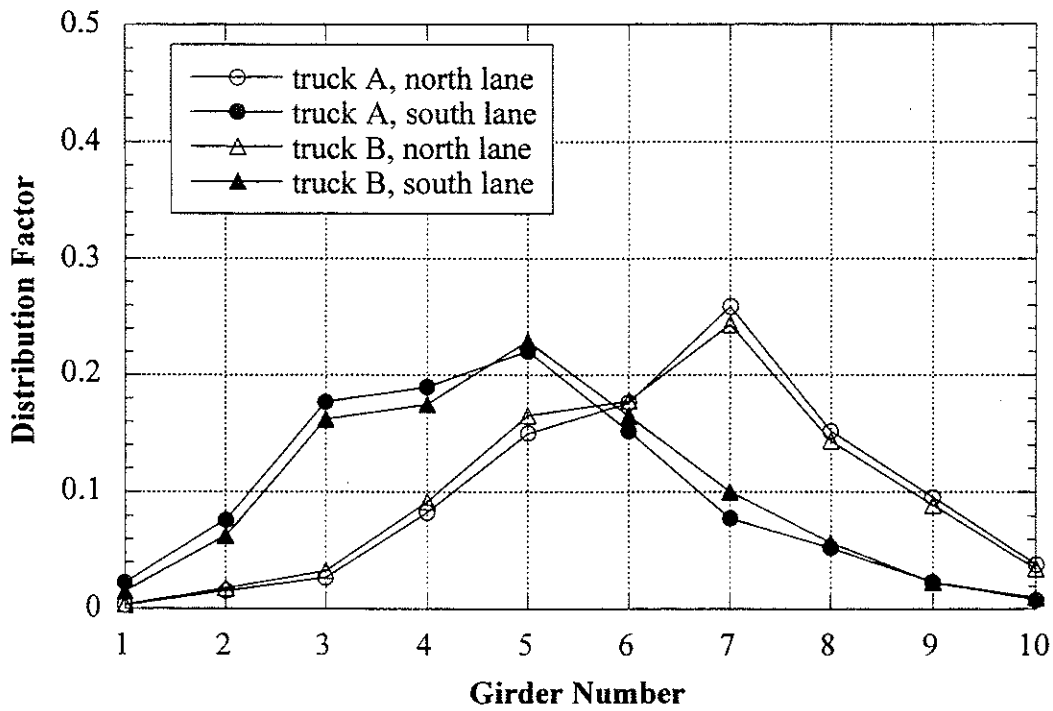


Figure 9.12 Distribution Factors for One Truck Loading at High Speed

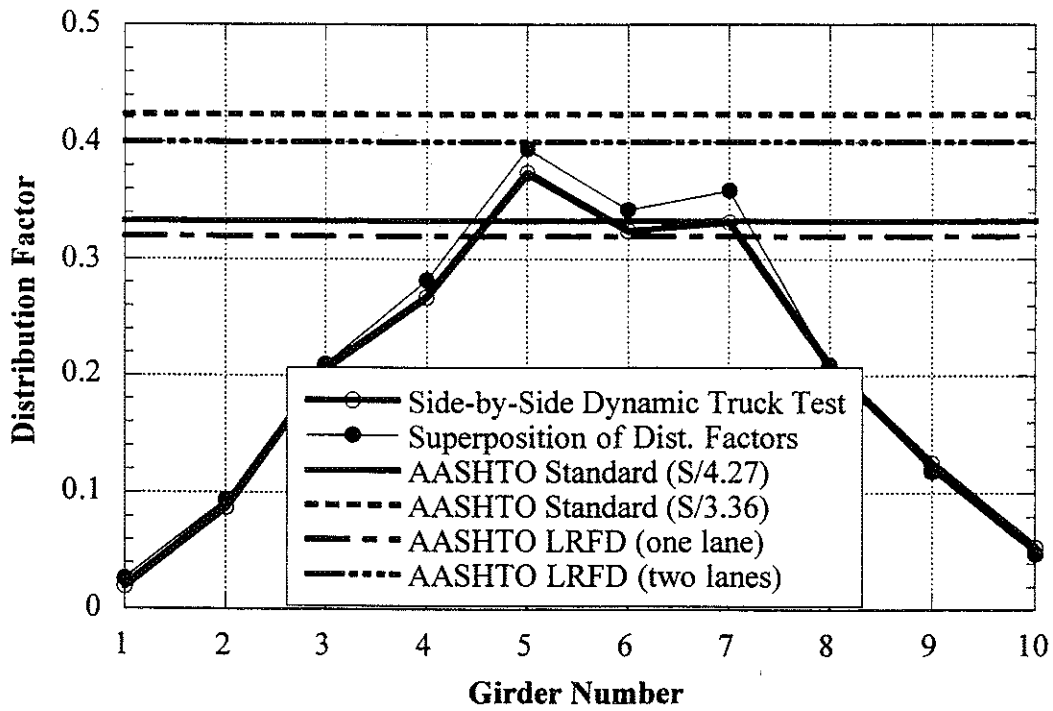


Figure 9.13 Comparison with Code Specified Distribution Factors at High Speed

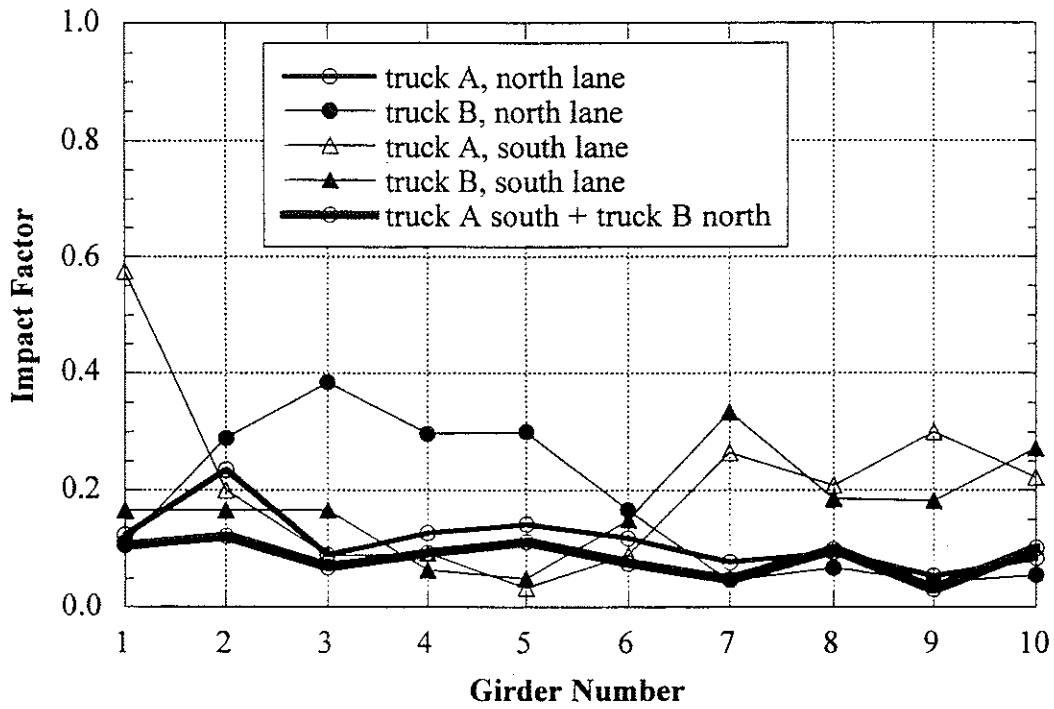


Figure 9.14 Impact Factors.

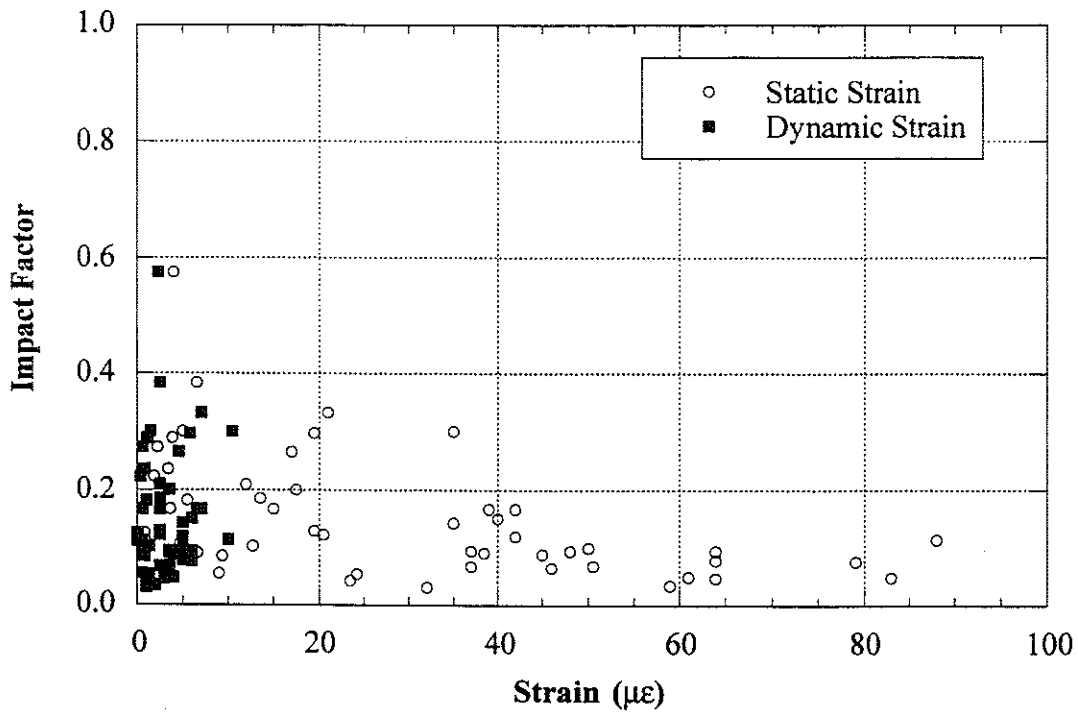


Figure 9.15 Strain versus Impact Factors.

Note:

Intentionally left blank

10. Summary and Conclusions

Five bridges were tested and the results are summarized as follows. Because all of the bridges tested are two lane bridges, traffic lanes are expressed in terms of left lane and right lane in figures 10.1-4. Specific lane orientations are shown in the figures.

Strains under a single truck are shown in Fig. 10.1 for vehicles moving at crawling speed in left lane, and in Fig. 10.2 for the right lane. The corresponding distribution factors are presented in Fig. 10.3 and 10.4. Strains caused by a single truck moving at high speed (40-60 km/h), are shown in Fig. 10.5. The corresponding distribution factors are plotted in Fig. 10.6. The envelopes of the distribution factors corresponding to a single truck are shown in Fig. 10.7.

For two trucks side-by-side at high speed (40-60 km/h), the strains are presented in Fig. 10.8. The measured strains due to two trucks at crawling speed are compared with the results of superposition of the effects of single trucks in Fig. 10.9. The distribution factors for two trucks are plotted in Fig. 10.10 for crawling speed and Fig. 10.11 for high speed. For comparison, the code specified distribution factors are also shown. The girder distribution factors for AASHTO (1996) are calculated as follows. In one lane steel girder and prestressed concrete girder bridges, GDF is:

$$GDF = \frac{S}{4.27} \quad (10-1)$$

and for multi lane steel and prestressed concrete girder bridges,

$$GDF = \frac{S}{3.36} \quad (10-2)$$

where S = girder spacing (m).

And for AASHTO LRFD (1994), the girder distribution factors are as follows. For moment in interior girders with multi-lane loading:

$$GDF = \left\{ 0.075 + \left(\frac{S}{2900} \right)^{0.6} \left(\frac{S}{L} \right)^{0.2} \left(\frac{K_g}{Lt_s^3} \right)^{0.1} \right\} \quad (10-3)$$

and with one lane loading:

$$GDF = \left\{ 0.06 + \left(\frac{S}{4300} \right)^{0.4} \left(\frac{S}{L} \right)^{0.3} \left(\frac{K_g}{Lt_s^3} \right)^{0.1} \right\} \quad (10-4)$$

where S = girder spacing (mm); L = span length (mm); $K_g = n(I + Ae_g^2)$; t_s = depth of concrete slab (mm); n = modular ratio between girder and slab materials; I = moment of inertia of the girder (mm^4); A = area of the girder (mm^2); e_g = distance between the center of gravity of the girder and slab (mm). Because the term $K_g / (Lt_s^3)$ implies more accuracy than exists for bridge evaluation, it is recommended that they be taken as 1.0. However, actual values of term $K_g / (Lt_s^3)$ are used to calculate girder distribution factors throughout this report.

Dynamic loads are also compared in Fig. 10.12. For two trucks side-by-side the dynamic load factor is shown as a thicker line. For exterior girders, the dynamic load factor is high, but it corresponds to a very low static load effect.

For comparison, the dynamic load factors are plotted vs. static strain in Fig. 10.13. It is clear that dynamic load factor decreases with increasing static load effect.

The measured maximum static strains are compared to calculated static strains in Table 10.1 for a single truck and in Table 10.2 for two trucks side-by-side. The calculated values are obtained using the maximum bending moment and the maximum GDF from the test results. Two cases are considered: (a) non-composite section, (b) composite section. Even assuming a composite action, the calculated strains are about twice larger than the maximum measured values. "Truck 1" indicates 11-axle truck or truck A for bridge B01-70041 and "Truck 2" indicates 10-axle truck or truck B for bridge B01-70041, respectively.

Table 10.1 Strains due to One Lane Loading

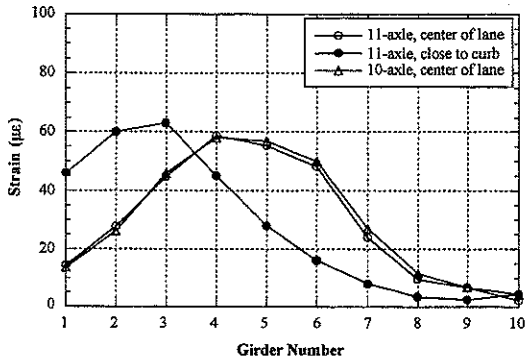
MDOT ID #	Maximum Strains from Test (10 ⁻⁶)	Calculated Maximum Strains (10 ⁻⁶)			
		Non-Composite Section		Composite Section	
		Truck 1	Truck 2	Truck 1	Truck 2
B02-46032	67.5	260.0	246.0	179.6	169.9
B05-46041	64.0	241.7	226.6	147.9	138.7
B02-12021	42.0	181.2	167.6	93.5	86.5
B02-38051	78.0	235.4	223.6	150.8	143.2
B01-70041	64.0	248.6	237.1	138.7	132.3
B02-12021(Proof Load)	72.0	302.5		156.2	

Table 10.2 Strains due to Two Lane Loading

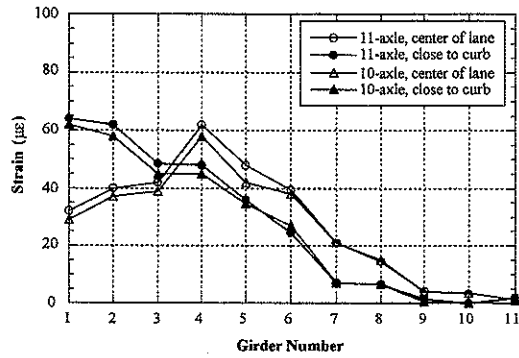
MDOT ID #	Maximum Strains from Test (10 ⁻⁶)	Calculated Maximum Strains (10 ⁻⁶)					
		Non-Composite Section			Composite Section		
		Truck 1 & Truck 1	Truck 2 & Truck 2	Truck 1 & Truck 2	Truck1 & Truck 1	Truck 2 & Truck 2	Truck 1 & Truck 2
B02-46032	102.4	378.8	358.4	368.6	261.7	247.6	254.6
B05-46041	87.0	328.2	307.7	317.9	200.9	188.3	194.6
B02-12021	71.0	240.0	220.0	230.0	123.9	114.6	119.3
B02-38051	111.5	369.1	350.6	359.9	236.4	224.6	230.5
B01-70041	96.0	308.6	294.3	301.5	172.2	164.2	168.2
B02-12021 (Proof Load)	137.0	504.2			260.3		

The most important conclusions are:

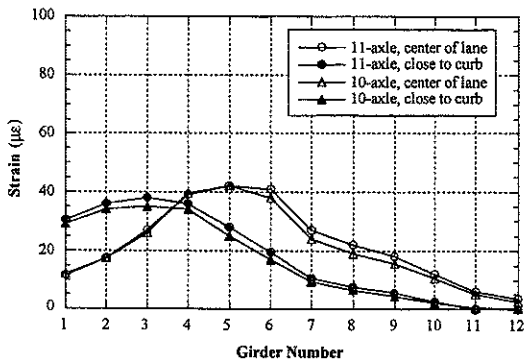
- (a) The observed response is linear, which is confirmed by superposition of truck effects. The comparison of strain values for a single truck indicates that for two trucks side-by-side tests, the results are equal to superposition of single truck results.
- (b) The absolute value of measured strains is lower than expected. For a single truck, the maximum observed strain is less than 80 microstrains. This corresponds to 16 Mpa. For two trucks side-by-side, the maximum strain is 111 microstrains, which corresponds to 23 Mpa. The main reasons for low strains are: unintended composite action, partial fixity of supports and increased actual stiffness due to sidewalks, parapets and railings.
- (c) Girder distribution factors observed in the tests are lower than AASHTO Standard (S/3.36) and LRFD (two lanes) GDF's. The maximum measured values for two trucks side-by-side tests were close to the specified values (S/3.36) in two bridges, and conservative for three bridges. However, the absolute values of stresses were rather low (less than 23 MPa).
- (d) Dynamic load is lower than specified value by AASHTO (1996). For two trucks side-by-side it is about 0.10. Dynamic load decreases with increasing static load effect.
- (e) Proof load test performed on Bridge US12/SC (B02-12021) confirmed that the bridge is adequate to carry the normal truck traffic. The measured deflections and strains were relatively low, and considerably lower than expected.



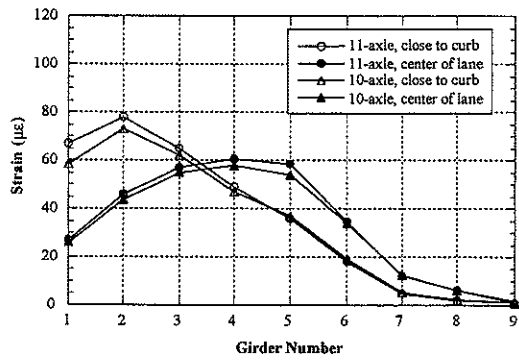
M156/SC, Morenci (B02-46032)



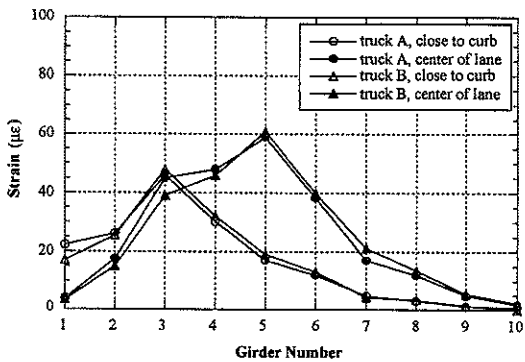
M34/RR, Adrian (B05-46041)



US12/SC, Bronson (B02-12021)



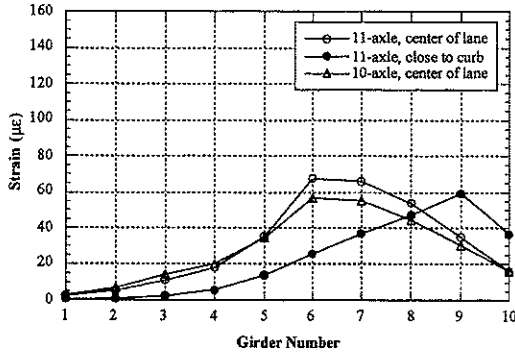
M106/PRD, Munith (B02-38051)



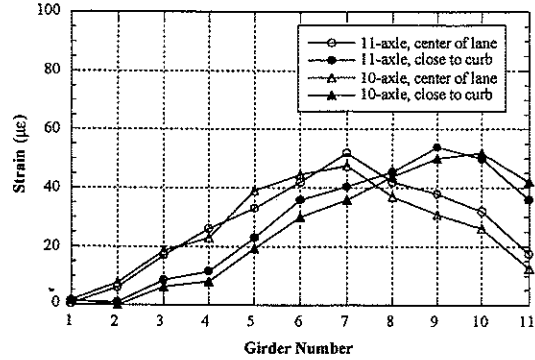
M45/BR, Grand Rapids (B01-70041)

Lane Orientations for Figure 10.1	
B02-46032	West Lane
B05-46041	North Lane
B02-12021	South Lane
B02-38051	South Lane
B01-70041	South Lane

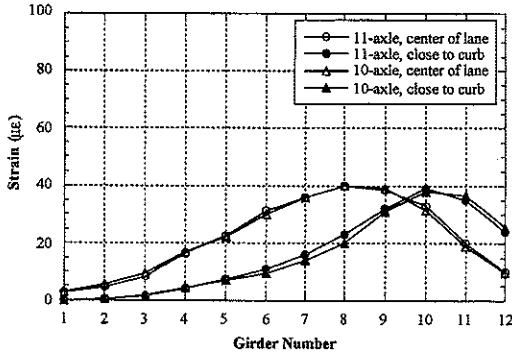
Figure 10.1 Strains under Left Lane Loading at Crawling Speed



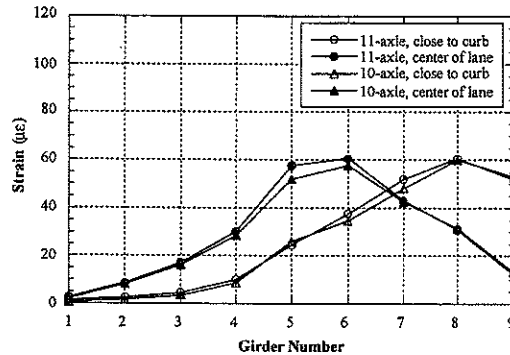
M156/SC, Morenci (B02-46032)



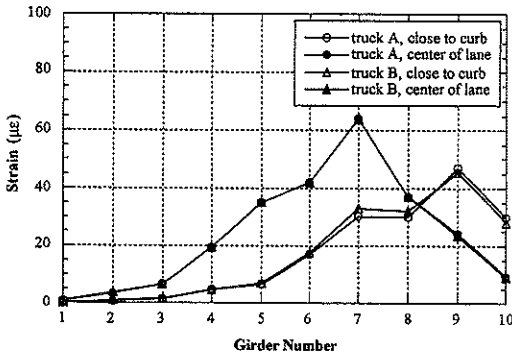
M34/RR, Adrian (B05-46041)



US12/SC, Bronson (B02-12021)



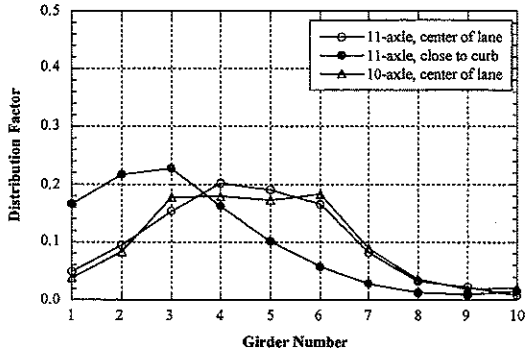
M106/PRD, Munith (B02-38051)



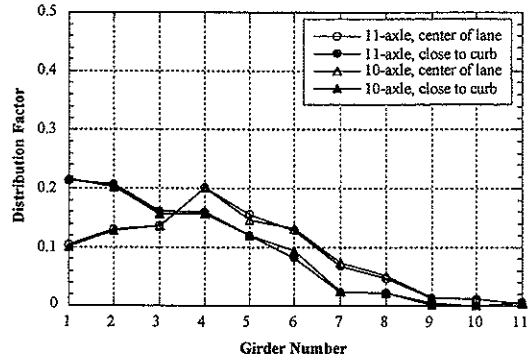
M45/BR, Grand Rapids (B01-70041)

Lane Orientations for Figure 10.2	
B02-46032	East Lane
B05-46041	South Lane
B02-12021	North Lane
B02-38051	North Lane
B01-70041	North Lane

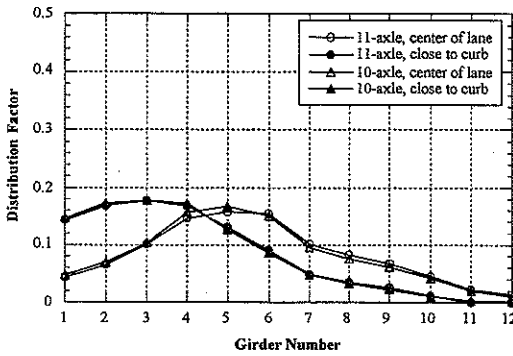
Figure 10.2 Strains under Right Lane Loading at Crawling Speed



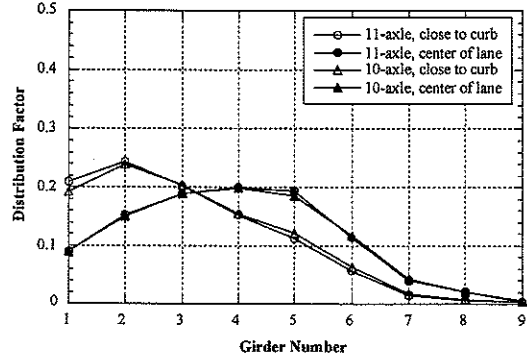
M156/SC, Morenci (B02-46032)



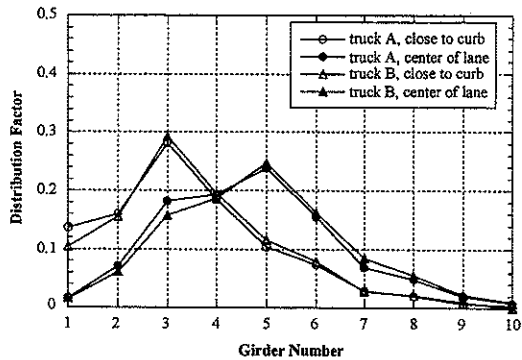
M34/RR, Adrian (B05-46041)



US12/SC, Bronson (B02-12021)



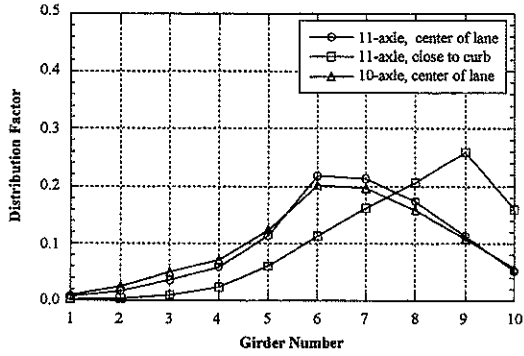
M106/PRD, Munith (B02-38051)



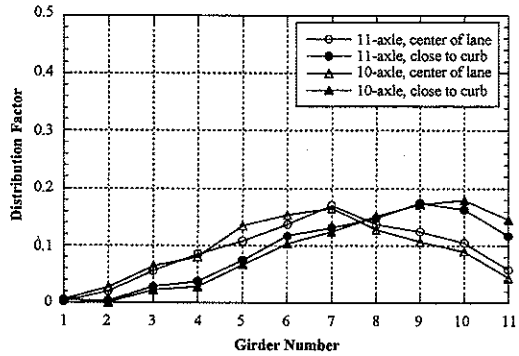
M45/BR, Grand Rapids (B01-70041)

Lane Orientations for Figure 10.3	
B02-46032	West Lane
B05-46041	North Lane
B02-12021	South Lane
B02-38051	South Lane
B01-70041	South Lane

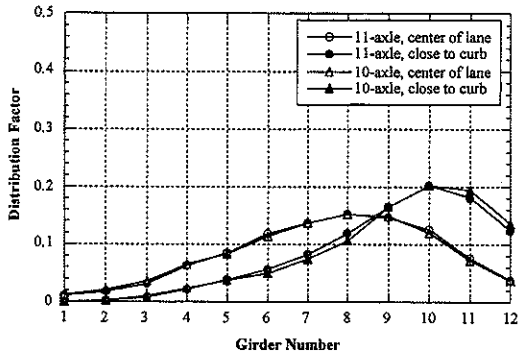
Figure 10.3 Distribution Factors under Left Lane Loading at Crawling Speed



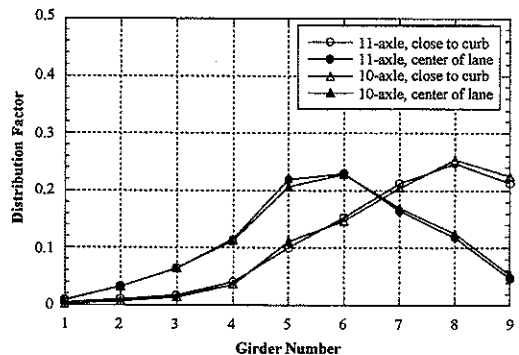
M156/SC, Morenci (B02-46032)



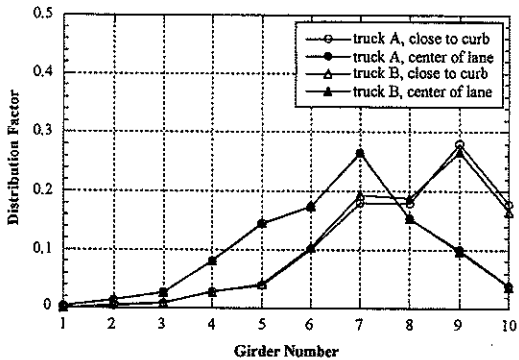
M34/RR, Adrian (B05-46041)



US12/SC, Bronson (B02-12021)



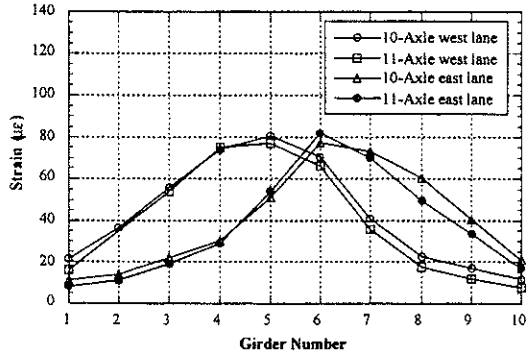
M106/PRD, Munith (B02-38051)



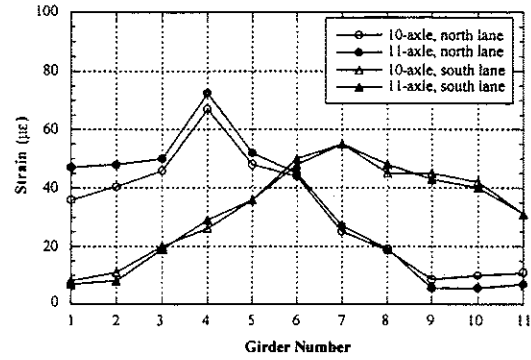
M45/BR, Grand Rapids (B01-70041)

Lane Orientations for Figure 10.4	
B02-46032	East Lane
B05-46041	South Lane
B02-12021	North Lane
B02-38051	North Lane
B01-70041	North Lane

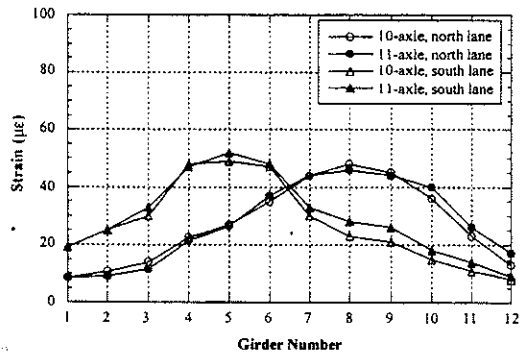
Figure 10.4 Distribution Factors under Right Lane Loading at Crawling Speed



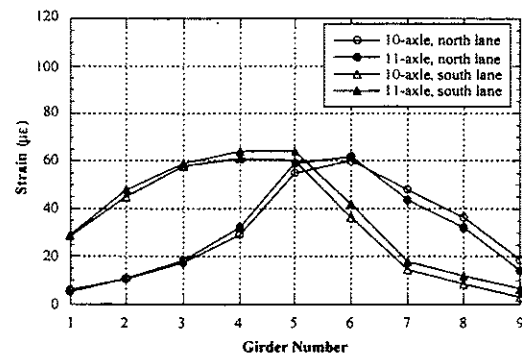
M156/SC, Morenci (B02-46032)



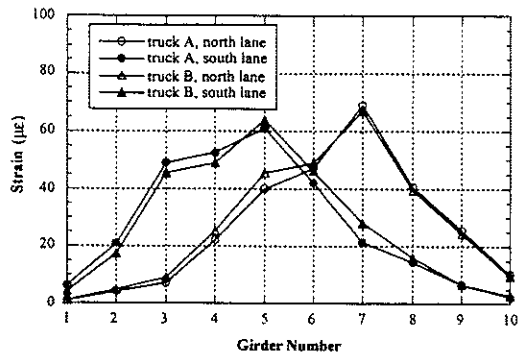
M34/RR, Adrian (B05-46041)



US12/SC, Bronson (B02-12021)

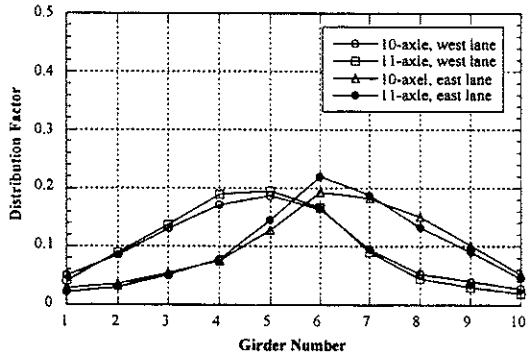


M106/PRD, Munith (B02-38051)

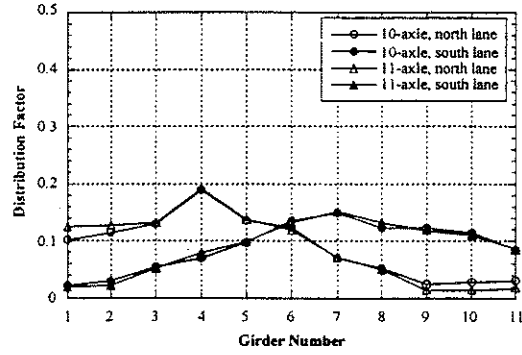


M45/BR, Grand Rapids (B01-70041)

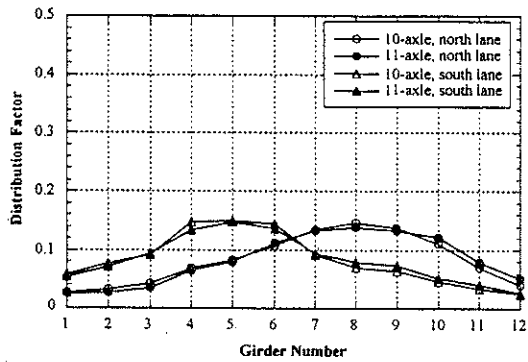
Figure 10.5 Strains under One Truck Loading at High Speed



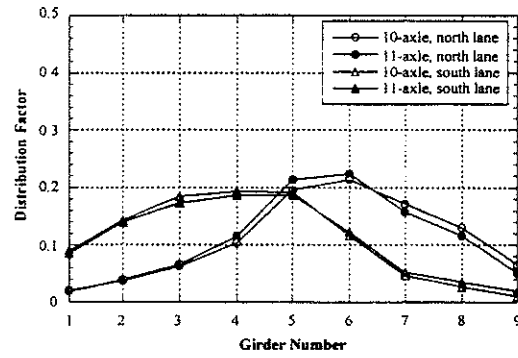
M156/SC, Morenci (B02-46032)



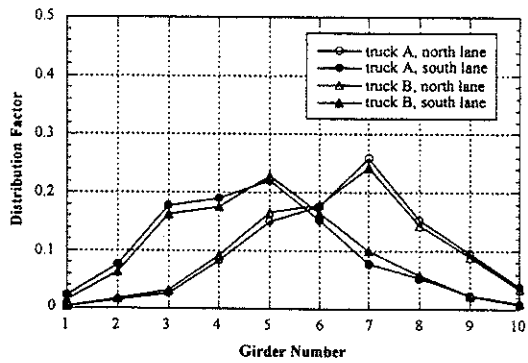
M34/RR, Adrian (B05-46041)



US12/SC, Bronson (B02-12021)

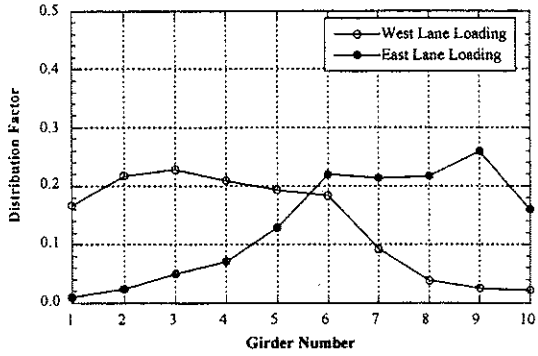


M106/PRD, Munith (B02-38051)

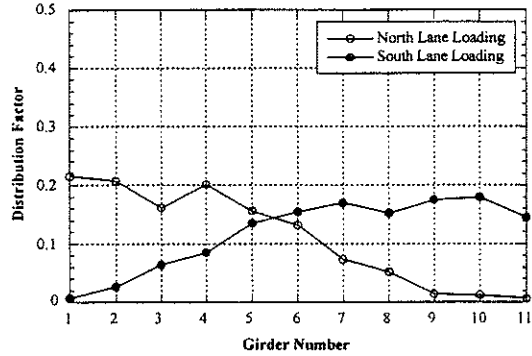


M45/BR, Grand Rapids (B01-70041)

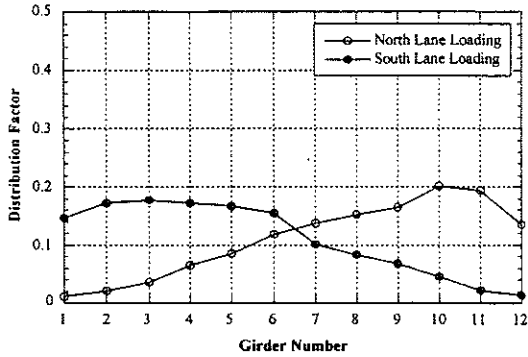
Figure 10.6 Distribution Factors under One Truck Loading at High Speed



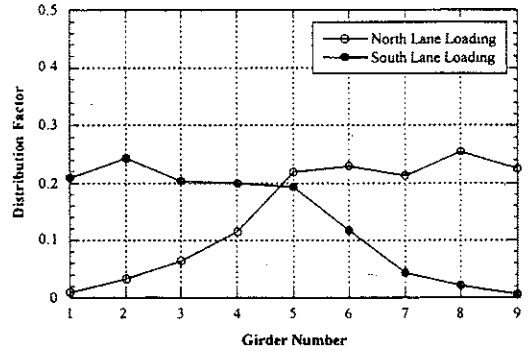
M156/SC, Morenci (B02-46032)



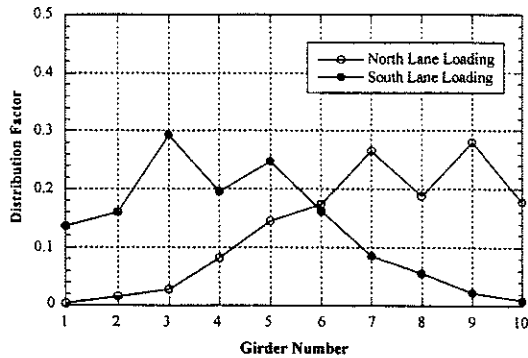
M34/RR, Adrian (B05-46041)



US12/SC, Bronson (B02-12021)

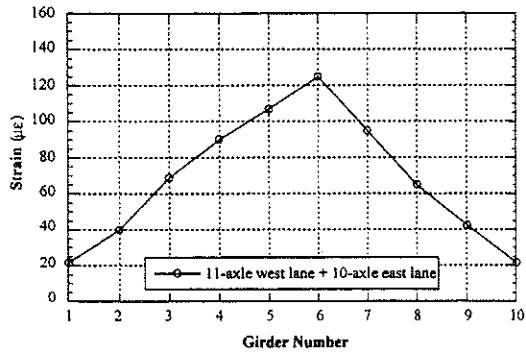


M106/PRD, Munith (B02-38051)

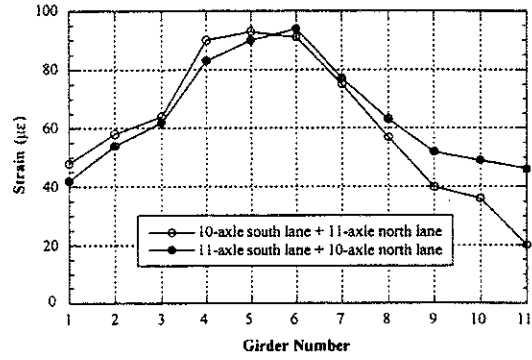


M45/BR, Grand Rapids (B01-70041)

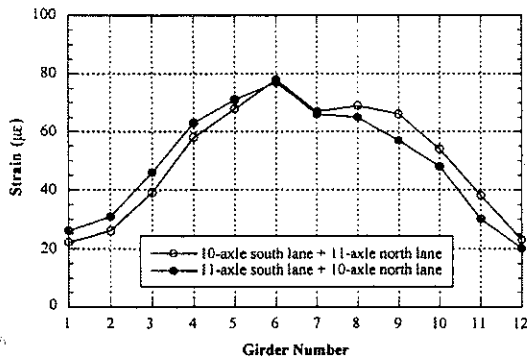
Figure 10.7 Envelopes of Girder Distribution Factors For One Truck Loading at Crawling Speed



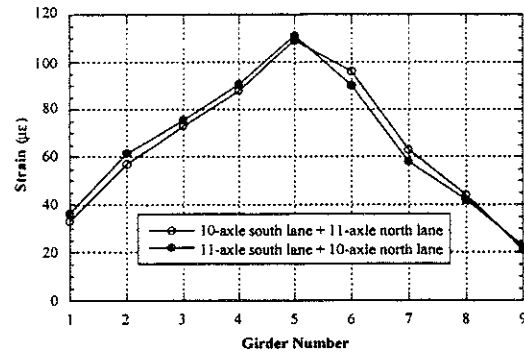
M156/SC, Morenci (B02-46032)



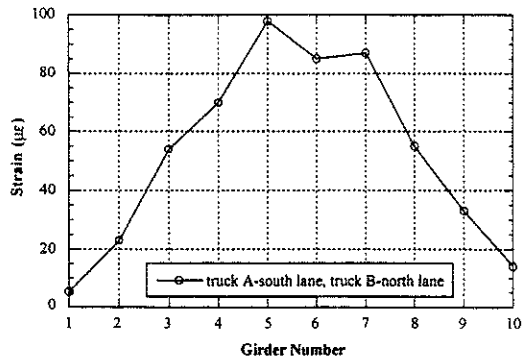
M34/RR, Adrian (B05-46041)



US12/SC, Bronson (B02-12021)

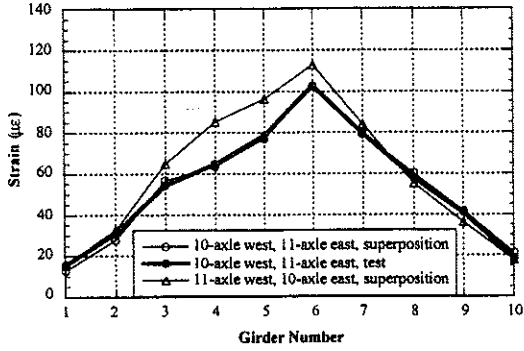


M106/PRD, Munith (B02-38051)

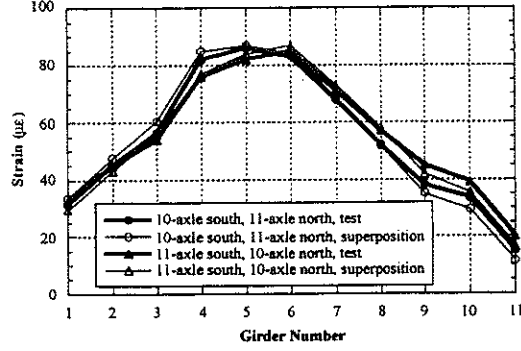


M45/BR, Grand Rapids (B01-70041)

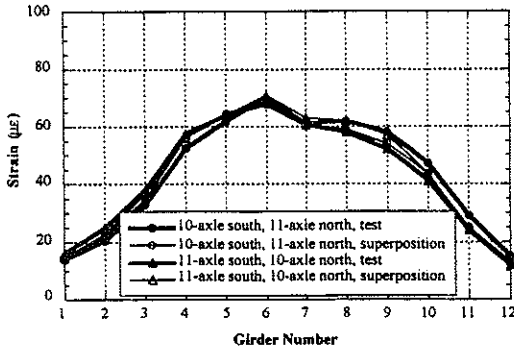
Figure 10.8 Strains under Side-by-Side Truck Loading at High Speed



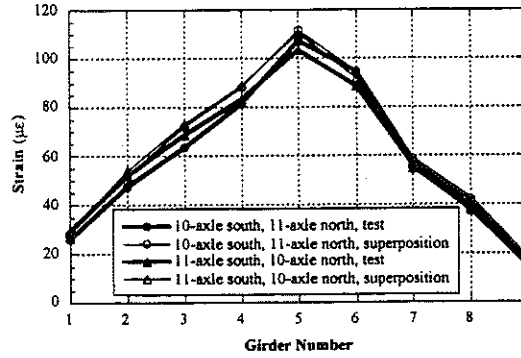
M156/SC, Morenci (B02-46032)



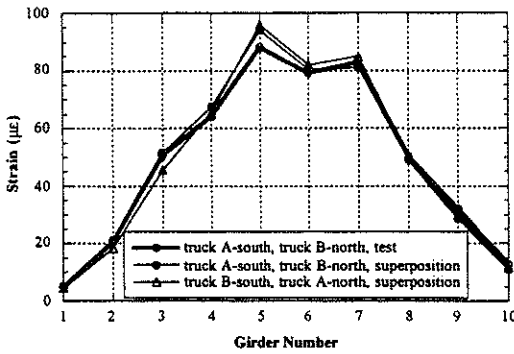
M34/RR, Adrian (B05-46041)



US12/SC, Bronson (B02-12021)

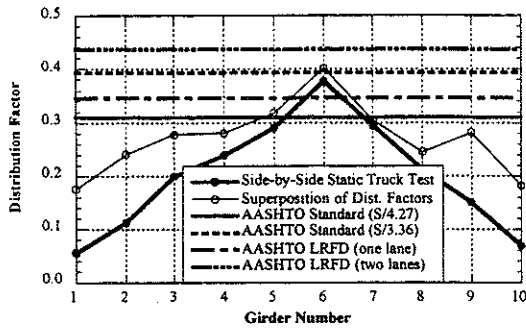


M106/PRD, Munith (B02-38051)

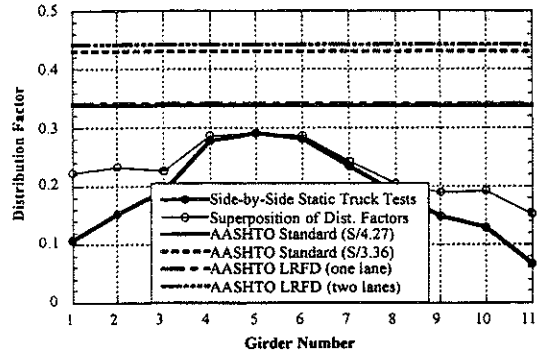


M45/BR, Grand Rapids (B01-70041)

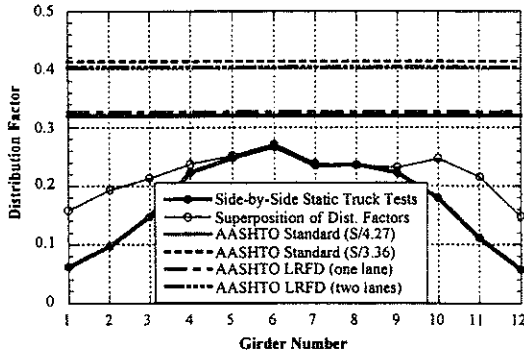
Figure 10.9 Strains under Side-by-Side Truck Loading at Crawling Speed



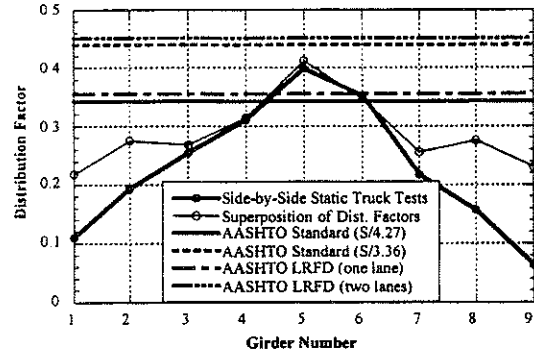
M156/SC, Morenci (B02-46032)



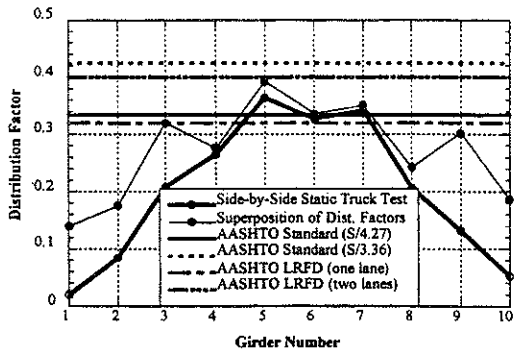
M34/RR, Adrian (B05-46041)



US12/SC, Bronson (B02-12021)

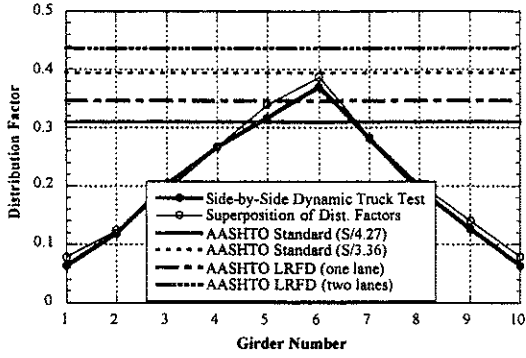


M106/PRD, Munith (B02-38051)

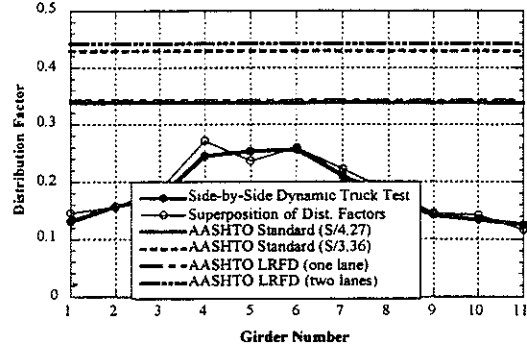


M45/BR, Grand Rapids (B01-70041)

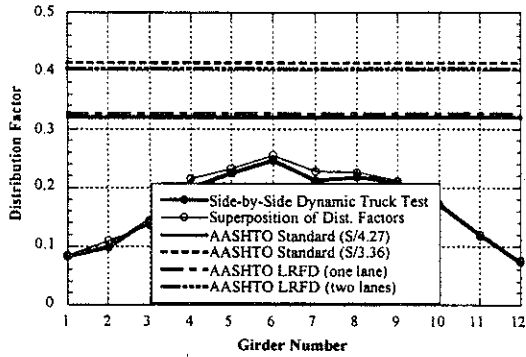
Figure 10.10 Comparison with Code Specified Distribution Factors at Crawling Speed



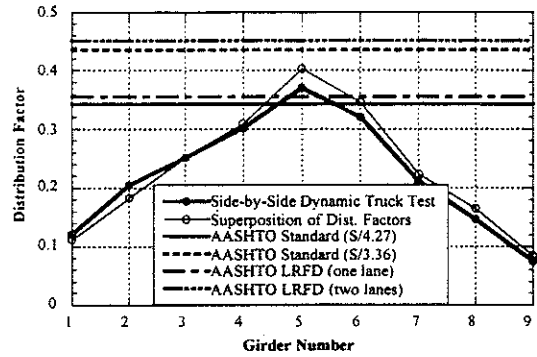
M156/SC, Morenci (B02-46032)



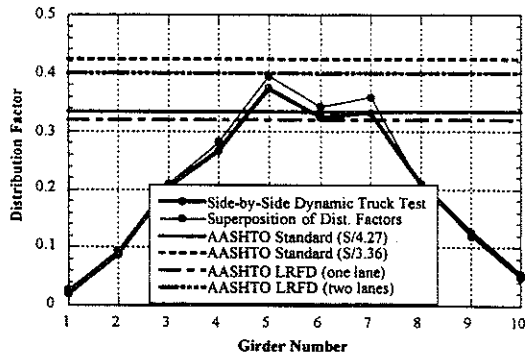
M34/RR, Adrian (B05-46041)



US12/SC, Bronson (B02-12021)

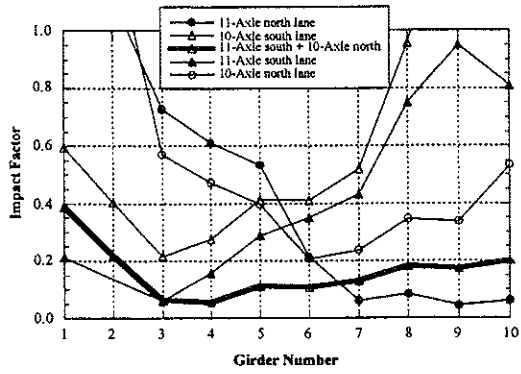


M106/PRD, Munith (B02-38051)

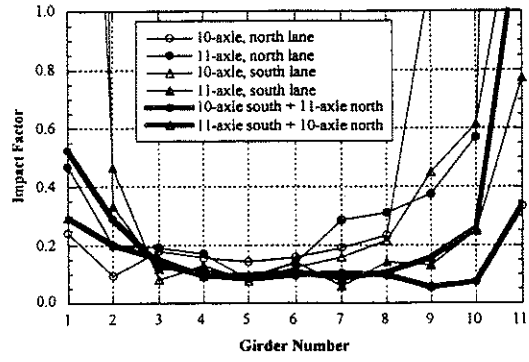


M45/BR, Grand Rapids (B01-70041)

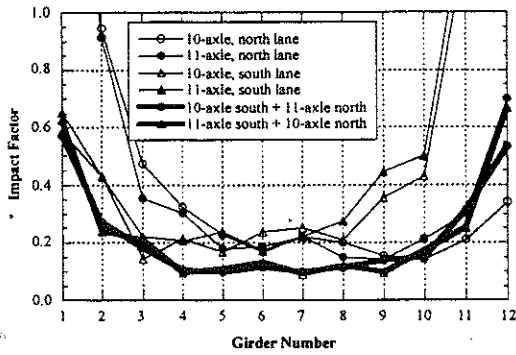
Figure 10.11 Comparison with Code Specified Distribution Factors at High Speed



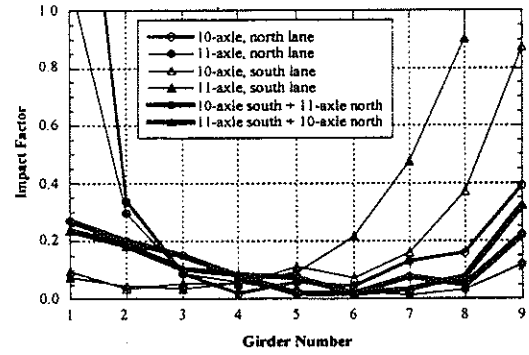
M156/SC, Morenci (B02-46032)



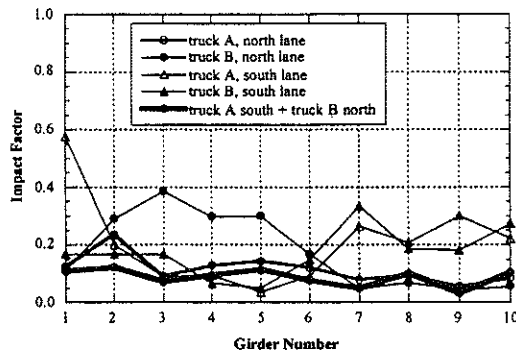
M34/RR, Adrian (B05-46041)



US12/SC, Bronson (B02-12021)

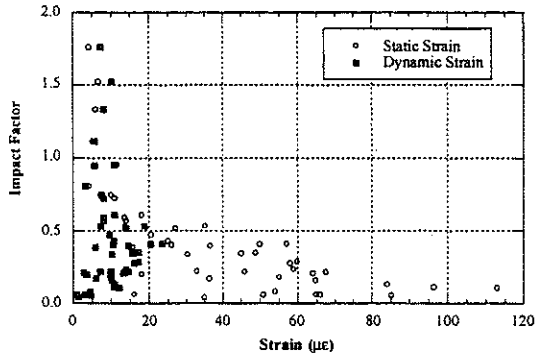


M106/PRD, Munith (B02-38051)

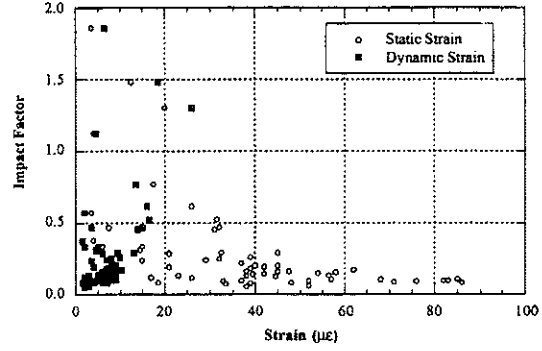


M45/BR, Grand Rapids (B01-70041)

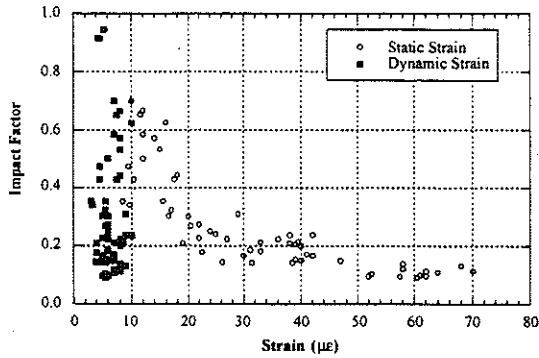
Figure 10.12 Impact Factors



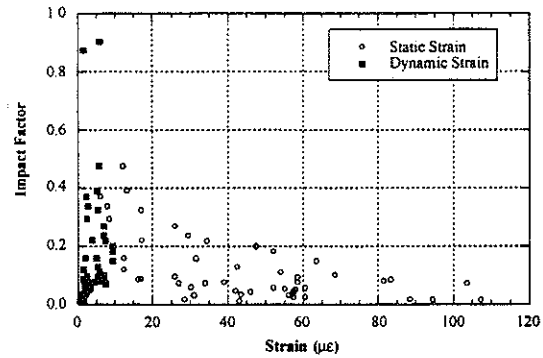
M156/SC, Morenci (B02-46032)



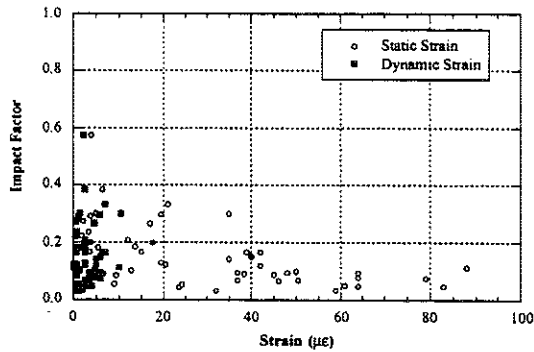
M34/RR, Adrian (B05-46041)



US12/SC, Bronson (B02-12021)



M106/PRD, Munith (B02-38051)



M45/BR, Grand Rapids (B01-70041)

Figure 10.13 Strains Versus Impact Factors

Note:

Intentionally left blank

11. References

1. *AASHTO Standard Specifications for Highway Bridges*, American Association of State and Transportation Officials, Washington, DC, 1996.
2. *AASHTO LRFD Bridge Design Specifications*. American Association of State Highway and Transportation Officials, Washington, D.C., 1994.
3. *AASHTO Guide Specifications for Distribution of Loads for Highway Bridges*, American Association of State Highway and Transportation Officials, Washington, D.C., 1994.
4. Bakht, B., and Pinjarkar, S.G., "Dynamic Testing of Highway Bridges- A Review." *Transportation Research Record 1223*, Transportation Research Board, National Research Council, Washington, D.C., pp. 93-100, 1989.
5. Ghosn, M., Moses, F., and Gobieski, J., "Evaluation of Steel Bridges Using In-Service Testing." *Transportation Research Record 1072*, Transportation Research Board, National Research Council, Washington, D.C., pp. 71-78, 1986.
6. Hwang, E.S., and Nowak, A.S., "Simulation of Dynamic Load for Bridges." *Journal of Structural Engineering*, ASCE, Vol. 117, No.5, pp.1413-1434, July, 1991.
7. Lichtenstein, A. G., *Bridge Rating Through Nondestructive Load Testing*, NCHRP Report 12-28(13) A, June 1993.
8. Nassif, H.H. and Nowak, A.S., "Dynamic Load Spectra for Girder Bridges." *Transportation Research Record 1476*, Transportation Research Board, National Research Council, Washington, D.C., pp. 69-83, 1995.

9. Nowak, A.S., Laman, J.A., and Nassif H., "Effect of Truck Loading on Bridges." Report UMCE 94-22. Department of Civil and Environmental Engineering, University of Michigan, Ann Arbor, 1994
10. Paultre, P., Chaallal, O., and Proulx, J., "Bridge Dynamics and Dynamic Amplification Factors-A Review of Analytical and Experimental Findings." Canadian Journal of Civil Engineering, Vol. 19, pp. 260-278, 1992.
11. Stallings, J.M., and Yoo, C.H., "Tests and Ratings of Short-Span Steel Bridges." Journal of Structural Engineering, ASCE, Vol. 119, No. 7, pp. 2150-2168, July, 1993.
12. Zokaie, T., Osterkamp, T.A., and Imbsen, R.A., *Distribution of Wheel Loads on Highway Bridges*, National Cooperative Highway Research Program Report 12-26, Transportation Research Board, Washington, D.C., 1991